esa SP-262

ERS-1
Wind and Wave Calibration Workshop

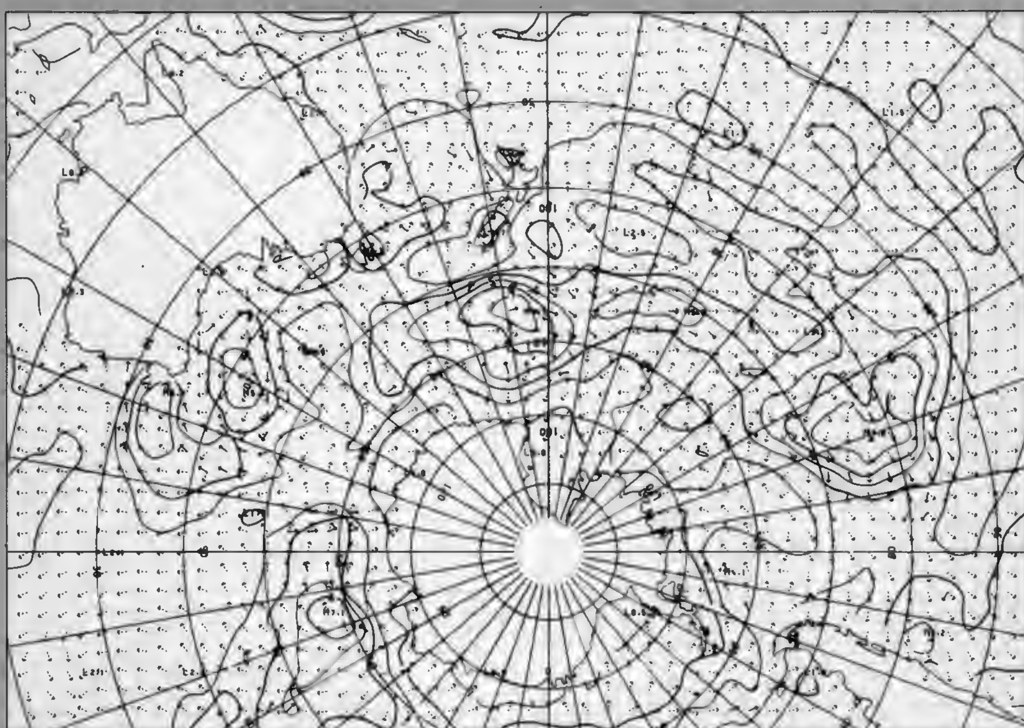

Proceedings of an ESA Workshop held at
Schliersee, Germany, 2–6 June, 1986

Sponsored by:
The European Space Agency

esa
european space agency

esa SP-262
September 1986

ERS-1
Wind and Wave Calibration Workshop

Proceedings of an ESA Workshop held at
Schliersee, Germany, 2–6 June, 1986

Sponsored by:
The European Space Agency

european space agency / agence spatiale européenne
8-10, rue Mario-Nikis, 75738 PARIS CEDEX 15, France

ESA SP-262

ERS-1 WIND AND WAVE CALIBRATION WORKSHOP

Schliersee, FR Germany, 2–6 June, 1986

MEMBERS OF THE STEERING COMMITTEE

E P W Attema	ERS-1 Project, ESTEC
A G Cavanié	IFREMER
C R Francis *(Secretary)*	ERS-1 Project, ESTEC
R Frassetto	CNR
T H Guymer	IOS
J Louet	ERS-1 Project, ESTEC
J C Morin	ERS-1 Project, ESTEC
W Rosenthal	GKSS (Institut für Physik)

Proceedings published by: ESA Publications Division, ESTEC, Noordwijk, The Netherlands

Edited by: J J Hunt

ISSN 079-6566 Price code E3

Printed in The Netherlands

Contents

Session 1
CLASSIFICATION OF MEASUREMENTS
Chairman: T H Guymer (IOS)

Session 2
CLASSICAL MEASUREMENTS
Chairman: W Rosenthal (GKSS) FRG

Session 3
DEDICATED MEASUREMENTS

Chairman: A Cavanie

Session 4
PLANNED/ONGOING PROGRAMMES
Chairman: R. Frassetto

PANEL REPORTS

Session 1

CLASSIFICATION OF MEASUREMENTS

Chairman: T Guymer (IOS)

ERS-1 MISSION CONSTRAINTS RELATED TO WIND AND WAVE CALIBRATION

J Louet

ESA/ESTEC (THE NETHERLANDS)

ABSTRACT

This paper outlines the approach taken for Validation and Calibration of the ERS-1 mission. A clear distinction is made between the Engineering and geophysical performances of the mission.

The pre- and post-launch activities required to calibrate the ERS-1 system and validate the geophysical performances are described within the framework of the adopted overall strategy. This paper assumes that the ERS-1 mission objectives and main characteristics, including payload description, are well known (see Ref 1 distributed to the participants at this Workshop.

1. INTRODUCTION

The overall approach taken by the Agency for the development and validation of the ERS-1 mission is based on the clear distinction between the **engineering** and **geophysical** performances of the mission.

The engineering performances are the basis of the contract between Industry and ESA. The derivation of engineering performances, from the original geophysical performances agreed for the mission, has been done with the support of Expert Teams selected by ESA to assist it from the outset of the project.

These engineering performances will be verified by pre- and post-launch activities, primarily conducted by ESA and the Contractor. These performances, verified sensor by sensor, are defined by engineering parameters such as geometric and radiometric resolutions, time delay measurement accuracy and measurement stability. Calibration of the engineering measurements will be carried out using both internal and external calibration loops.

The geophysical performances and algorithms that facilitate the conversion of calibrated backscatter and time delay measurements into wind field, wave spectrum, significant wave height and altitude estimates, are the responsibility of ESA and the scientific community supporting the Agency. They require a large number of pre- and post-launch activities which are briefly described hereafter.

The main activities from now until launch are concentrated on:

- A better understanding of the geophysical phenomena and models by processing/analysis of the already existing data sets (e.g. Seasat, SIR-A and B, Geosat) complemented by campaigns performed jointly by ESA and laboratories/institutes (e.g. airborne C-band scatterometer campaigns and radar altimeter campaigns);

- A review and confirmation, as far as possible before launch, of the algorithms to be used for each of the basic ERS-1 measurements;
- Identification and preparation of the measurement campaigns to be performed during ERS-1 commissioning phase, as well as the subsequent data processing and model/algorithm tuning process.

The post-launch activities will be composed of two phases:

- The ERS-1 commissioning phase of 3 months, during which the basic geophysical validation of the sensors will be conducted in parallel with their engineering calibration. At the end of this phase, the production and distribution to users of Fast Delivery (FD) products will be initiated on a routine basis.

- The exploitation phase, remaining part of the mission, during which fine tuning of the algorithms, taking into account such aspects as seasonal and regional dependence, coupling between phenomena (wind/wave inter-relations) will be performed. Naturally, the Agency will maintain the engineering calibration of the instruments during this phase.

2.1 The ERS-1 Primary Products and their Validation

In order to give a better insight to the approach followed, the relations between the ERS-1 instruments and the basic associated measurements are defined hereafter.

It must be noted that most of the basic measurements lead to an associated Fast Delivery product to be disseminated within three hours after the observation made by the sensor.

In this approach, each product is derived from a single instrument. A review of the status of these products will allow a better understanding of the activities required to validate these products.

SAR Image Mode

The primary product derived from the SAR is an image: there is no geophysical algorithm required to produce a SAR image. The processing algorithm is wellknown and based on the relative motion/attitude characteristics of the sensor and the observed scene, as well as the engineering characteristics of the instrument. The engineering calibration of the instrument is based on the use of instrument internal calibration loops, and also external calibration, by observation of point target responses of corner reflectors and transponders.

SAR Wave Mode

This mode, interleaved with the wind mode, will allow the sampling of the oceans at 200/300 km programmable intervals. Each sample will allow the SAR imaging of a 5 x 5 km area which will be converted into an image spectrum. Up to the image spectrum, the engineering calibration performed with the SAR image mode, is valid, since the same instrument is used.

The subsequent conversion of the image spectrum to the directional wave spectrum requires application of an algorithm describing the modulation transfer function of the SAR to the ocean waves.

The wave spectrum extraction is based on a radar signature model of the form:

$$\sigma^{\circ}(x,y) = \overline{\sigma}^{\circ}(1 + 2\mathrm{Re}[\int_{-\infty}^{+\infty} m(\vec{k})k\hat{\eta}(\vec{k})\exp(j\vec{k}.\vec{r})d\vec{k}])$$

where $\overline{\sigma}^{\circ}$ is the spatially averaged σ°

k is the complex wave number
r is the unit position vector
$\hat{\eta}$ is the directional wave spectrum
m(k) is the modulation transfer function.

Based on the above equation, the calibrated directional wave spectrum can be derived from the σ° map through two-dimensional spectral analysis. Unfortunately, the value of the modulation transfer function is not yet accurately known. It is also not universely agreed that the above linearised model is a satisfactory approximation of the real world.

Furthermore, experiments with SEASAT and SIR-B SAR's have demonstrated the limitations of the instrument in the case of azimuth travelling waves (waves travelling perpendicular to the SAR look direction).

Since this modelling problem is currently the subject of ongoing scientific research, it has been decided for the time being to commit to the production of image spectra rather than wave spectra, but to promote pre- and post-launch investigations of the possibilities and limitations of the extraction of the directional wave spectra.

AMI Wind Scatterometer Mode

The basic product obtained via this mode is the wind field over a 500 km wide swath.

The primary product to be delivered is a geophysical product: wind velocity and direction for 50 km x 50 km cells.

The processing algorithms to be used include two distinct parts:

- an engineering algorithm converting the raw measurements into normalised backscatter measurement triplets (3 observations, 45° apart), co-registered per cell;

- a geophysical algorithm converting the normalised backscatter triplets into wind vectors.

The engineering algorithm requires radiometric calibration of the instrument, which will be performed by internal and external calibrations, as well as application of all geometric corrections and filtering required to obtain the co-registered and normalised backscatter triplets. A rather complete engineering calibration plan has been elaborated, based on the use of a large homogeneous target (the Amazon Rain Forest), as well as use of active transponders.

The geophysical algorithm requires the availability of the C-band model describing the relation between the measured radar backscatter and the wind vectors, as a function of the incidence angle and direction of the C-band observation.

The status of this model is given later on, together with the performed and planned activities, to confirm this model.

The fitting of the backscatter measurement triplets to the C-band model does not give unfortunately one single solution, but up to four ranked solutions with an ambiguity of 180° in direction for the two most probable solutions; therefore an ambiguity removal algorithm has to be applied.

Several studies have been initiated to define ambiguity removal methods compatible with the fast delivery product delay requirements: objective methods based on continuity analysis of the wind field, complemented by use of some meteorological wind prediction data, seems to give a promising solution. The objective is clearly to disseminate non-ambiguous wind vector products.

Radar Altimeter

The radar altimeter FD products to be disseminated are derived from the on-board tracking loop estimates averaged over 1 second.

The significant wave height (SWH) information will be derived from the return echo slope estimate performed on-board.

The algorithm to be applied is the known relation between echo slope and SWH, as already used with several KU-band US radar altimeters flown so far.

For these reasons, the SWH product is considered as being an operational product.

The wind velocity at nadir is a foreseen product related to the backscatter strength measured by the calibrated on-board AGC. The calibration is rather stringent (.5dB absolute) and will require use of both internal loop calibration and external calibration with large corner reflectors or transponders.

Even if properly calibrated, an uncertainty remains concerning this product for high wind speeds, since the model (relation backscatter wind speed) is badly defined for wind speeds above 15 m/s where it seems to exhibit very small backscatter variation for large wind speed excursions. As a consequence, there is little hope to make a good estimate of high wind speeds with this instrument.

The time delay measurement is the basis of the altitude measurement. The time delay measurement will be calibrated as part of the commissioning phase using sea or reference corner reflector targets concurrent with undertracking by laser stations. Validation by comparison with PRARE is also foreseen.

A calibrated time delay measurement cannot be converted in an altitude without applying the ionospheric corrections as well as the atmospheric corrections. These corrections will be performed off-line, using in particular, the microwave sounder of the ATSR/M for correction of the contribution from the "wet" component of the refractive index of the atmosphere. This approach is justified by the fact that a precise altitude is not useable for derivation of geophysical products without a precise restituted orbit and this activity is also considered as a long-term task, offered at the moment in the German Processing Archiving Facility (PAF).

Nevertheless, a coarse RA altitude Fast Delivery (FD) product, with an accuracy in the order of 1 m. will be provided. The coarse ionospheric and atmospheric corrections to be applied are under study and will be provided via a predicted correction table. One use of this product already identified is the standard orbit restitution and prediction performed by the mission management and control centre. The quality of the standard restituted orbit, as well as the predicted orbits, used for programming of the satellite and FD processing, are greatly improved by the use of the altitude FD product.

ATSR/M

The ASTR/M will be processed, off-line, to derive the Sea Surface Temperature (SST). The calibration of the ATSR/M instrument will be performed under the leadership of the Rutherford Appleton Laboratory (RAL), the establishment in charge of this instrument development and of the processing performed off-line. This calibration will be done within the framework of the coordinated ERS-1 commissioning phase.

PRARE

For the PRARE, the calibration and all telemetry data are acquired direct by the Institute of Navigation, Stuttgart, (INS) the institute in charge of this instrument. The off-line processing will be performed in the German PAF. It is planned to have coordinated activities for the calibration of the Radar Altimeter and PRARE, the use of laser stations and the subsequent work on ERS-1 precise orbit restitution.

Summary of the Validation Approach

The above summary situation on the ERS-1 primary products highlights the need for engineering and geophysical validation/calibration.

The primary products are either calibrated engineering products or products requiring application of a geophysical algorithm following the engineering parameter extraction.

The engineering products (image, image spectra, backscatter triplets, return echo slope or time delay of the RA) are valuable calibrated intermediate products which we intend to store in the PAF's.

Whilst characterisation of the engineering performances can be performed on the instrument before launch at various levels of integration, the in-orbit calibration is mandatory, since it is the first time the total instrument is operated full scale in its environment. This activity will be performed within the first 3 months of the mission (commissioning phase) and should hopefully take less than 3 months. To speed up this task, a 3-day repeat cycle on a fixed phase orbit has been selected, allowing revisiting of the calibration sites at a maximum of 3-day intervals.

For the geophysical validation/calibration, pre-launch activities using campaign data, as well as relevant satellite data, are and will significantly enhance our understanding of the geophysical/algorithms; nevertheless, several new instrument concepts will be spaceborne "premières" on ERS-1 (in particular, C-band SAR/Wave Mode and Wind Scatterometer).

It is anticipated that, at the end of the commissioning phase, the level of confidence for engineering calibration will be different from that for geophysical calibration.

While the engineering calibration should be considered as completed, the geophysical validation should be at a stage where FD products can be disseminated, based upon a global tuning of algorithms and models.

A considerable amount of secondary phenomena will still remain to be analysed: proper tuning of the models to particular zones, seasons and parameter interdependence are likely to require years of research by the scientific community.

The focusing of the commissioning phase around the primary ERS-1 products will already be quite a challenge. If successful, it would allow, via the dissemination of FD products, their experimental/preoperational use in various potential applications and in particular, their assimilation in large models (meteorological or others).

A large number of off-line products, extending far beyond the primary products identified here, are foreseen to be produced on request in the PAF's.

The algorithms to be used are, in most cases, of a less defined nature than the primary product algorithms and are not dealt with in this document.

3. ENGINEERING CALIBRATION

The pre- and post-launch engineering calibration activities required for the AMI and the Radar Altimeter are summarised hereafter.

3.1 AMI Engineering Calibration

The pre-launch characterisation is based on a combination of tests, analyses and simulations.

Each of the ERS-1 components will be characterised separately, as well as after integration.

In particular, internal calibration loops, illustrated in Figure 1, allow on-ground as well as in-flight characterisation of most of the instrument chain, switching matrix and antennas excluded. This internal calibration is achieved by taking a delayed and attenuated sample of the transmit signal and feeding it into the receiver.

The antennas will be characterised separately on the ground. The potential coupling between the antennas, as well as alignment, will be performed by test plus analysis.

The overall AMI performances will be predicted by analysis, plus simulation, assimilating the measured technical parameters.

In particular, a rather sophisticated Scatterometer System Simulator is being built (Ref. 3).

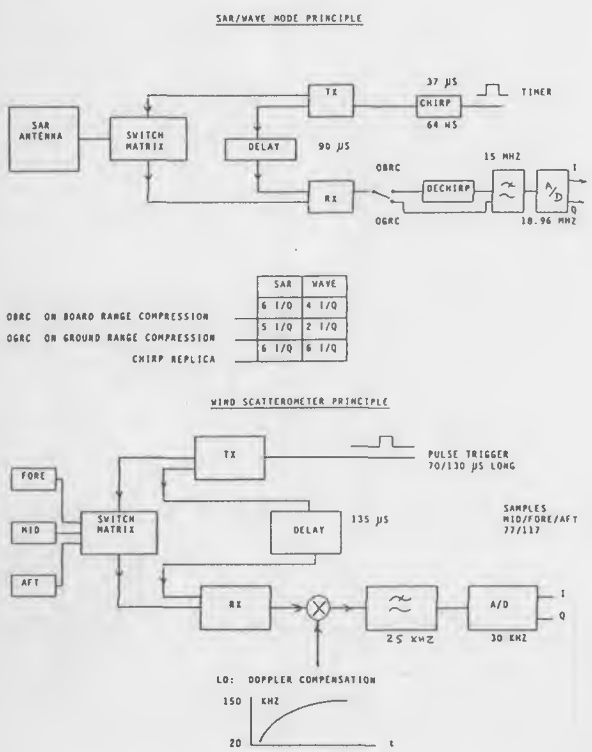

Figure 1. AMI Internal Calibration Loops

The In-flight Engineering Calibration of the instrument is based on internal and external loops.

The AMI measurement system is periodically calibrated to ensure that measurements of the radar scattering cross section of the earth's surface can be made to a known accuracy. Absolute calibration is achieved through the procedure of imaging external reference targets.

The SAR image and wave mode will be calibrated using reference point targets, corner reflectors and transponders.

The wind scatterometer mode will be calibrated using two methods: a set of 3 transponders and a natural homogeneous reference target.

For overflight of the 3 transponders, a special operation mode is used (as illustrated in Fig. 2). The 3 transponders are first illuminated by the forward beam for 120 seconds, then illuminated by the mid-beam (40 seconds) and by the aft-beam (last 120 seconds). These transponders retransmit the received signal with a frequency shift of 540 KHz, so that the transponder signal can be separated from the background echo of the illuminated and reflecting earth area. This frequency shift, as well as the operation sequence, define a special on-board mode, called the external calibration mode.

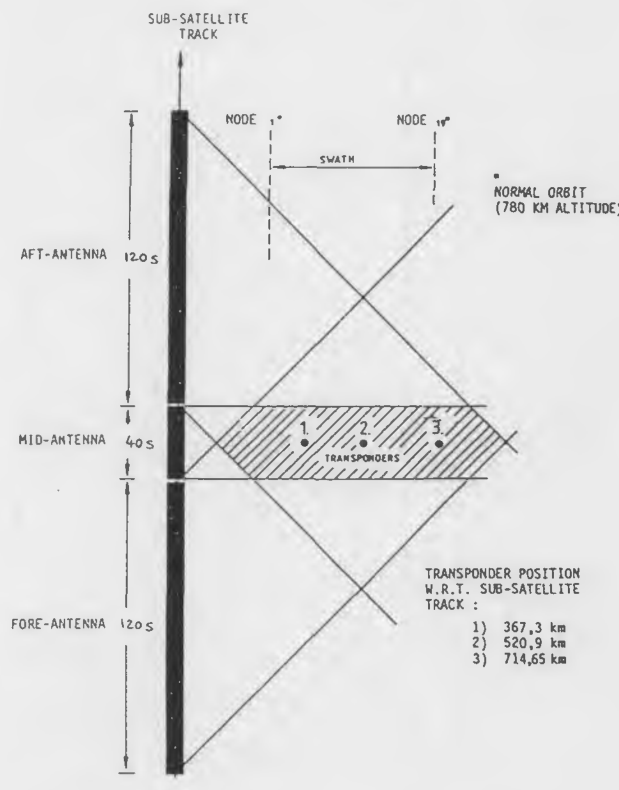

Figure 2. Wind Scatterometer External Engineering Calibration

To supplement the point target calibration procedure, it is envisaged imaging a large distributed target like the Brazilian Rain Forest. Based on previous satellite missions, it is expected that the stability over time and the spatial homogeneity of this target is adequate for this purpose. At C-band however, no experience exists. For this reason, an airborne scatterometer campaign is being carried out in September, 1986, to measure the radar signature of the rain forest.

Internal Calibration

A number of provisions are included within the AMI on-board instrument to ensure that relative measurement accuracy is maintained throughout the mission, between external calibrations. These relative calibrations are achieved by injecting known signals into the normal signal transmission path (same internal calibration loops as for pre-launch test).

Noise measurement of the receiver chain is performed for each of the AMI modes.

In the wind scatterometer mode, the gain and noise calibrations are performed with each measurement cycle of 32 pulses of the fore, mid and aft-beams.

In the SAR mode, the gain and noise calibrations are performed at the beginning and end of each operation period (operation period varying between 1 to 10 minutes maximum). In the wave mode, the same gain and noise calibrations are performed with each wave cell (5 x 5 km).

In both AMI imaging and wave on-ground recompression mode, the chirp replica is sampled (6 bits I, 6 bitsQ) and transmitted regularly within the auxiliary data field of the respective telemetry format.

AMI Operation Constraints

The AMI, operating in C-band, combines the functions of SAR imaging, wave and wind scatterometer modes. The instrument block diagram provided (Figure 3) demonstrates that the same transmitter and receiver are shared by the three instrument modes. For this reason, the SAR imaging mode is exclusive of the two other modes. The wind and wave modes can be operated in an interleaved wind/wave mode in which the wind scatterometer sequence is interrupted at 200 or 300 km preset interval for wave operation.

It must be understood that the wave cell position can be controlled only by the start of operation of the instrument. This operation is likely to be a severe constraint for the wave mode validation and it is suggested that the SAR imaging mode be used over the wave calibration/validation sites whenever possible. This is a valid approach since the AMI imaging and wave mode are totally identical except the bit truncation, performed after the Analog to Digital converter, in the wave mode. This truncation can be applied easily on the SAR imaging data before on-ground processing.

The transition from SAR imaging to wind/wave mode will take about 7.5 seconds (around 50 km along-track); this constraint has also to be taken into account in the calibration strategy and site selection.

Furthermore, for life-time reasons, the SAR imaging mode cannot be operated for less than 30 seconds and no more than 10 minutes accumulated time per orbit. The wind scatterometer cannot be operated for less than 180 seconds: there is no maximum operation limit except on-board energy balance; the 180-second constraint corresponds, roughly, to the interval between fore and aft-beam observation of wind cell at mid-swath.

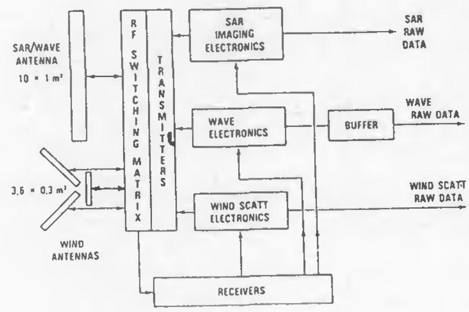

Figure 3. AMI Block Diagram

3.2 Radar Altimeter Engineering Calibration

Before the radar altimeter is launched, it will be possible to provide quite an extensive engineering calibration and validation, thanks to the development of some sophisticated test equipment. Following the launch, a combination of internal and external measurements will be used to extend the engineering calibration validation. These procedures are briefly described below.

For on-ground tests, a Return Signal Simulator (RSS) is being developed for the radar altimeter. This device will be attached in place of the antenna, and provides radar echo signals, with a realistic delay (corresponding to the altitude of ERS-1) and modulated to represent the return from an extended surface. The characteristics of modulation are controllable, so that most surfaces can be represented. During the development of the altimeter, the theoretical performance, based on part measurements, and the results from the RSS will be reconciled by extended analysis, until full confidence is obtained in the RSS technique. The RSS can then be used to determine the dynamic behaviour of the altimeter.

Pre-launch calibration will consist of detailed part measurement and analysis, and characterisation of the internal calibration loop. Since this process is carried out at one period in the satellite's life, it can be regarded as a "static" calibration: it does not calibrate temporal effects (with the exception of those associated with thermal testing).

Following the launch, internal open-loop calibration is performed every 4 minutes. This procedure is very fast (about 150ms), but must itself be calibrated by closed-loop calibration at regular intervals. The key item not covered by this scheme is the Ultra Stable Oscillator (USO) which provides the echo timing. This calibration is obtained by broadcasting the USO frequency on the X-band low bit rate telemetry channel to enable measurement on the ground. These elements of "dynamic" calibration are combined with the pre-launch results to obtain an engineering calibration, based on measurements within the satellite-ground station system.

To provide comparative measurements, which can be called calibration or validation, depending on relative confidence level, independent external measurements are required. The approach taken is to concentrate on the measured time delay and sigma-zero, since significant wave height (SWH) cannot be isolated as an engineering measurement: calibration and validation of this parameter is regarded as geophysical product, for which calibration/validation is to be performed at a later stage.

The time delay measurement is the basis of the altitude measurement. The time delay measurement will be calibrated as part of the commissioning phase using sea/ice or reference corner reflector targets when undertracking by laser stations. Potential use of active transponders is under study. Validation with PRARE is possible, but PRARE also needs to be validated during this period.

Studies are going on for the selection of the laser calibration sites: a potential candidate is DAKAR, with the laser station implemented on a peninsula; a second complementary concept is to use a laser transportable station (2 are available in Holland and Germany) possibly on the Greenland ice sheet. No firm decision has yet been taken but it is of paramount importance in the orbit phase selection.

3.3 Engineering Calibration Frequency

The internal calibration loops will be operated through the mission lifetime at their nominal built-in frequencies.

The external calibrations will be very intense during the commissioning phase, each calibration site being revisited at least once per three days.

During the following operation phase, ESA will maintain regular monitoring of the instrument calibration by instrument operation over the referenced natural targets and artificial stimuli (corner reflectors and transponders) at maximum intervals of one month: the frequency can be increased, if demonstrated/observed to be necessary.

4. GEOPHYSICAL VALIDATION/CALIBRATION

The geophysical validation of the primary products extracted from the AMI and Radar Altimeter are all related to wind and waves.

4.1 Pre-launch Activities

For the scatterometer, the surface wind field over the ocean has to be derived from the three images of the illuminated swath. The wind field extraction is based on a radar signature model of the form:

$$\sigma^\circ = A\, U^b\, [1 + C_1 \cos\phi + C_2 \cos\phi]$$

where U is the windspeed and ϕ is the angle between the radar look direction with respect to the wind direction (see Fig. 4). The development of this model at C-band and the determination of the model parameters A, B, C_1 and C_2 has been a major challenge of the ERS-1 Project.

In this baseline model, U is taken as neutral stability windspeed at 10 m. height.

Numerous campaigns were performed in 1984, 1985 and 1986, involving up to 4 different aircraft, equipped with airborne scatterometers, as well as deployment of ships, buoys and tower scatterometers (Ref. 4). Direct wind measurements at an altitude of 100 ft. have also been performed by several aircraft. From these campaign results, a C-band model has been elaborated, but confirmation is required in the satellite configuration (much larger instantaneous field of view in particular).

For the directional wave spectra extraction, much theoretical work has been performed but in addition, a Chili Campaign organised during the SIR B mission, provided a considerable amount of valuable information on the SAR wave spectrum capabilities and limitations, as well as on the capabilities of airborne instrumentation, to provide directional wave spectra.

In particular, a Surface Contour Radar (SCR) and a Radar Ocean Wave Spectrometer (ROWS), installed on-board a NASA-NRL P3, demonstrated very promising capabilities which should be used in the ERS-1 commissioning phase.

An airborne Radar Altimeter campaign, organised in the framework of MIZEX 84, has permitted acquisition of a valuable data set of return echoes over ocean, sea-ice and ice, to be used in our ERS-1 on-board tracker simulations, as well as to demonstrate the potential of corner reflectors in the Radar Altimeter calibration.

From now on, future ERS-1 campaigns will focus on rehearsal of the instrumentation to be developed and used in the dedicated campaigns of the satellite commissioning phase. In particular, new C-band airborne rotating beam scatterometers necessary for satellite under-flights, validation of new wind buoy development, joint use of surface and airborne wind and wave observations, and study of the potential and limits of colocation with satellite measurements acquired on a different spatial and temporal scale.

In all these activities, the Agency relies very much on the support of the member state institutes developing and deploying the surface and airborne measurement systems. Several non-ESA member states are also willing to contribute to these campaigns. This cooperation has so far been very successful and is the necessary basis of our future campaigns.

In parallel with these campaigns, numerous studies have been undertaken using either already existing satellite data (e.g. SEASAT) or simulating ERS-1 sensor data. The prospect of soon having access to the GEOSAT radar altimeter data is of great interest for confirmation of our radar altimeter algorithms, in particular, the wind speed algorithm already mentioned.

A significant effort will be put on the potential use of conventional surface data in our validation approach: this concerns not only GTS relayed data, but also numerous platform networks, operated by private or national entities, which collect very valuable wind and wave data. In this later case, the points of contact and links required for access to these data need to be investigated.

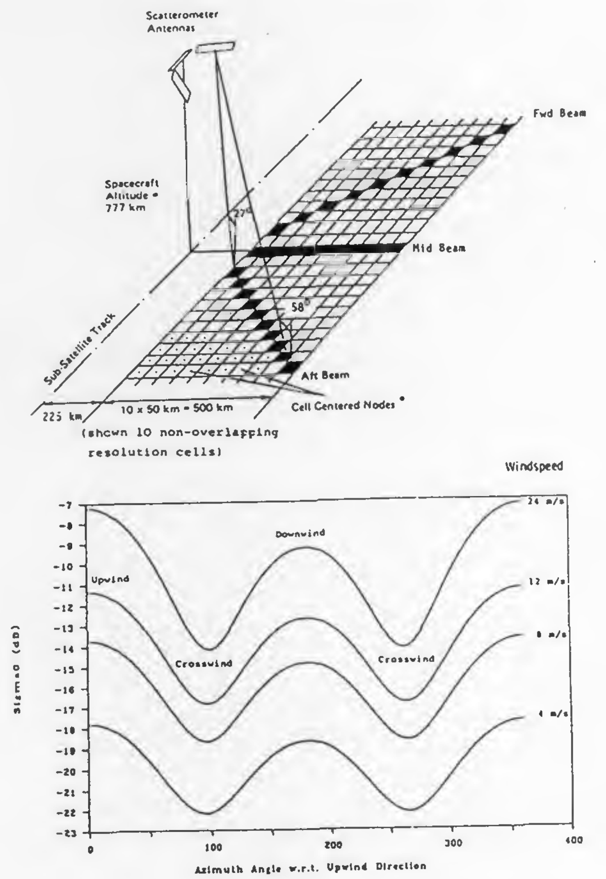

Figure 4. Wind Scatterometer Geometry and Radar Cross Section of the Sea as a Function of Wind Direction and Wind Speed

A systematic analysis of the way these in situ data can be used in our validation/calibration concept will also be undertaken. Basically, two approaches are possible: high quality data can be used for point to point colocation, the extent of the colocation being limited by the temporal/spatial variability of the measured parameters, or a second approach, based on the statistical analysis of a large data set, can be pursued. In this latter approach, the temporal/spatial scales to be used for statistical comparison of satellite and in situ need to be further analysed, the anticipated scales are weeks and oceanic regions.

A similar investigation will also be pursued with data assimilated in models. In this case, the statistical analysis would be carried out by comparison of wind/wave data from meteorological models compared with satellite data. The spatial/temporal scales of the statistical comparison, model versus satellite data, need to be analysed.

All these activities are pre-launch activities. The collection, retrieval and processing of the in situ/airborne data need to be organised prior to launch. The expected performances of the above-described method also need to be confirmed. The regularly collected in situ data, assimilated or not via models, could play a significant rôle in the mission validation, provided the error bars associated with the two approaches, colocation or statistical comparison, are demonstrated to be sufficiently small. The validity of this approach will be assessed during this workshop.

Whilst dedicated campaigns provide very precise measurements, colocated with satellite data, these measurements are limited in number, spatial coverage and duration of the campaign (basically 3 months for ERS-1). The use of conventional data, assimilated or not, would enhance significantly the dedicated campaign results by providing a world-wide data set, even if a majority of the measurements are taken in the northern hemisphere, and more importantly, measurements will be available continuously throughout the satellite mission.

4.2 Commissioning Phase

As stated already, during the 3-month commissioning phase, the engineering and geophysical calibration/validation will be performed in parallel.

The selection of a 3-day repeat orbit has also some benefit in the geophysical calibration, since it ensures a frequent revisiting of the dedicated calibration sites.

Dedicated campaigns and sites need to be defined for wind and wave calibration/validation and this is also a major objective of the workshop.

For wind calibration sites, conventional ship and buoy measurements, complemented by airborne wind instrumentation as already described, and in situ wave measurements are likely to be recommended.

For directional wave spectra measurements, the airborne instrumentation used in the already mentioned SIR-B experiment in Chile should be a major component. Complementary instrumentation shall be analysed during this workshop, in particular, potential availabilities in Europe.

The possible location of the sites in Northern and Southern hemisphere also needs to be addressed, as well as their relative merits with respect to the season of the commissioning phase.

Several national entities have also expressed their intentions to deploy dedicated in situ measurements in their zones of interest during the same period (Italy, Norway, India, New Zealand, Australia). Cooperation with USA, beyond the wave airborne instrumentation already mentioned, is also expected.

In parallel, the colocation and statistical methods based on exploitation of classical routine in situ measurements and models will be used within their domains of applicability.

To make this validation/calibration work possible, all satellite data, including auxiliary data and engineering calibration results, as well as the airborne and in situ measurements (including routine measurements), will be colocated at the PAF's. They will be accessible via a central catalogue and retrievable via a relational data base organisation, addressable in space and time. Those involved in the data validation/calibration will have the option of working either at the PAF's, or in their home institute, with privileged access to the PAF's data base.

As already mentioned, the 3-month commissioning phase will be a phase of high intensity data validation/calibration, which will be followed by a low intensity, but continuous through the mission lifetime, data collection and correlation of in situ and satellite data to reduce the residual error bars and uncertainties still existing after the commissioning phase, and to make a refined analysis of the geophysical parameters interdependence.

The major milestone, at the end of the commissioning phase is the start of distribution of the Fast Delivery primary products, based on the algorithms, tuned to the first three months of the mission.

It is recognised that this approach is very challenging, since the commissioning phase is short, but we believe these objectives can be reached if the preparation work (campaign rehearsal, data acquisition, retrieval and processing algorithms for data correlation, satellite versus in situ/airborne data) is well tested and validated before launch.

4.3 Exploitation Phase

The continuity of the effort of validation/calibration has already been stressed. In this phase, the PAF's will play a major rôle in providing the necessary data bases, their user friendly access and data retrieval.
It is also expected that significant support in this area will be provided by the scientific community, answering to the ERS-1 Announcement of Opportunity.

The community participating in the ERS-1 validation/calibration shall be organised such that the progress can be monitored and used in tuning of the algorithms, especially the routine Fast Delivery primary products.

5. CONCLUSION

This paper highlights the necessity of a rigorous approach both in the engineering calibration and geophysical calibration of the ERS-1 instruments which are two complementary activities. This need has been well understood and significant efforts in manpower and budgets have been, are and will be made to this aim.

The engineering calibration is the full responsibility of the Agency, supported by the industrial contracts and all necessary elements are well identified, most of them already being under development.

The preparation of the in-flight geophysical validation/calibration is of paramount importance. The quality analysis of the in situ/airborne measurements, their processing and assimilation/correlation with satellite data, as well as the data-base organisation and data retrieval, have to be organised and be ready before launch of the satellite. The same remarks apply to the development and deployment of the dedicated in situ/airborne measurement platforms.

For these tasks, the Agency rely heavily on the support of the ESA member state institutes, as well as commitments of the scientific community which should materialise in the expected answers to the ERS-1 Announcement of Opportunity. ESA will ensure the necessary lead and coordination of these activities, and also provide with the PAF's the necessary structure for data collection, processing and retrieval.

We believe that this very challenging approach is essential to fulfil the scientific and pre-operational demonstration objectives of the ERS-1 programme.

6. REFERENCES

1. Announcement of Opportunity for ERS-1 Technical Annex, 20 May 1986.

2. Overview and status of ERS-1 Programme: G. Duchossois - IGARSS 1986

3. The ERS-1 Scatterometer System Simulator and its relevance for Ground Processing Design: H. Munz, P. Hans - IGARSS, 1986

4. Results of the ESA Airborne C-band Scatterometer: E. Attema et al - IGARSS 1986.

THE INFLUENCE OF SPATIAL AND TEMPORAL SCALES ON CALIBRATION/VALIDATION

P G Challenor, T H Guymer & M A Srokosz

Institute of Oceanographic Sciences
Wormley, Godalming, Surrey, U.K.

ABSTRACT

In the calibration of the ERS-1 wind/wave sensors it will be necessary to include data not coincident with the sensor footprint. A knowledge of the space and time scales of the wind and wave fields is needed to decide whether to include or exclude data from the calibration. It is shown that the significant wave height variation, in both space and time, can be split into two signals - a low frequency scale, corresponding to depressions, and a high frequency 'noise' signal. Preliminary results for wind speed suggest a similar division of scales.

Keywords: Calibration, Space/time scales, Significant wave height, Wind speed, Remote sensing, ERS-1.

1. INTRODUCTION

When an instrument is to be calibrated in a laboratory, the procedure to be followed is well known. The new instrument is compared with a 'standard' at a number of fixed points. For example, if we are calibrating a temperature sensor a bath of water could be raised to a known temperature, as given by the 'standard' instrument (assumed more accurate than the new one), and the temperature measured by the new instrument. The measured temperatures are then compared with the standard and a calibration curve produced. This procedure, and some of the statistical problems arising from it, is described in ref. 1. Calibrating the 'wind-wave sensors' on ERS-1 does not fall into the 'classical' pattern. Nowhere in the world's oceans does there exist a laboratory where either the wind velocity or the wave parameters can be specified. Using our example of the temperature sensor, we can only measure the ambient temperature of the tank. Thus the range over which we can take measurements is limited to the range of conditions encountered. Since the wind and wave fields over the world's oceans are to a large extent stochastic we will be lucky if we encounter exactly the required conditions. Using our knowledge of meteorology and oceanography we can maximise the probabilities of finding these values, but we can never be certain. Therefore, in order to calibrate a sensor over the required range much more data is needed. For this reason it becomes impractical to use only data from dedicated experiments that are collocated with the satellite footprint in both space and time. We must also include other data, either collected routinely or especially for ERS-1, from buoys and ships deployed for other purposes which are some distance from the sensor footprint. This paper will look at the effects that the spatial and temporal scales in the wind and wave fields have upon calibration and then consider what we can learn about these scales from existing data.

A further problem arises in the calibration of ERS-1. This is caused by the lack of a 'standard'. There do not exist surface instruments that can give a much more accurate value of wind velocity or the wave parameters than the satellite sensors, indeed for significant wave height it seems likely that the altimeter may be more accurate than the conventional instrumentation (Ref. 2). We will not deal further with this problem except to note that a similar situation has been studied in a different context, ref. 3.

2. NON-COLLOCATED DATA AND CALIBRATION

If we are to include non-collocated data in the calibration there are two ways to proceed. We can either continue to perform a standard point-by-point calibration as if the data were taken from the same point (although possibly with some modification) or, alternatively, we could adopt a purely statistical approach and compare the 'climate' as measured by the satellite and conventional observations.

If we adopt the point-by-point approach we are immediately faced with a problem. We have extended the comparison set of surface observations to include not only those points that lie within the sensor footprint (in space and time) but also points that are 'near'. Our problem is to decide how close or far away can 'near' be. Obviously we would like to include as much data as possible, but we also have to guard against including data from positions where the wind velocity and/or wave parameters are different to that in the sensor footprint. Because of the different nature of satellite measurements and those taken on the surface, the former being an areal average whilst the latter is an average over time, any comparisons that are made are statistical. Thus our definition of 'near' must also be couched in statistical terms. In order for the expected (average) value to be the same we need the wind or wave field to be stationary over that distance. Measurements taken in this region of stationarity will have the same expectation but will differ from each other, possibly by quite a large amount, because of the random nature of the phenomena. Therefore if we want to consider pairs of data points (one from ERS-1 and one from the surface) that not only have the same expectation but also have values that are reasonably close to each other then we must go inside the region of stationarity and consider the region of high correlation.

If we include data at varying distances from the satellite footprint it is unreasonable to weight them all equally. It is obvious that data within the footprint should be given more credence than data farther away. A crude weighting would be to use simply the inverse of the distance from the footprint, however, if we have knowledge of the correlation scales we can utilise this to improve the weights. Indeed once the concept of weighting has been introduced other applications become apparent. For instance, we could weight different instruments according to their inherent accuracies, giving visual observations low weights, for example. However, to allow consistent results to be obtained it is important that weights are assigned according to some objective criteria rather than by the experimenter's prejudices!

If we use the second method of calibration, comparing averages in a space-time box, we still need to consider the space scales in the wind velocity and significant wave height fields. In particular we need to know over what areas and times they can be considered statistically stationary because this will dictate the size of the box to be used for the averaging. Before examining any data we can say that such boxes could be larger in the open ocean than in a shallow sea such as the Southern North Sea. In contrast to the point-by-point comparison here we want each data point to be independent of all the others and hence we are more interested in the stationary region that lies outside the area of high correlation. In order to achieve calibration to the required precision each box must also be large enough to contain sufficient data.

From this description of some of the effects that space time scales have upon calibration it can be seen that it is important to have a good understanding of these scales. In the next section we will consider some of the data and present some initial results.

3. SIGNIFICANT WAVE HEIGHT

In this section we will consider the dominant scales affecting significant wave height (Hs). In particular, we will look at the North East Atlantic. There are two reasons for this choice. Firstly it is an area of deep water, unlike the Southern North Sea for example where there are numerous sand banks which cause the variation of wave parameters on very short space and time scales (smaller than the satellite altimeter footprint); and secondly data from this region were available in IOS. Our data come from two instruments. To

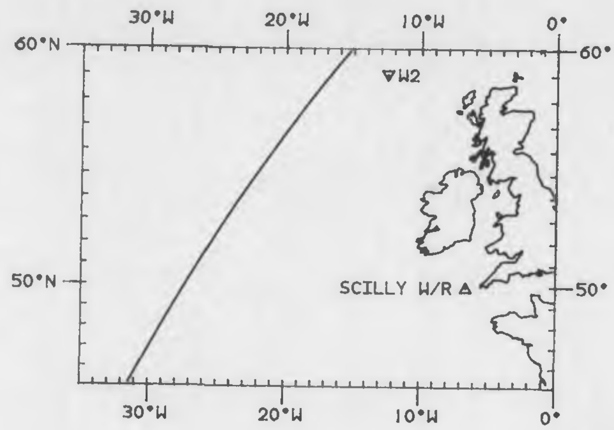

Figure 1. The Seasat altimeter track and the position of the Waverider and W2 buoys

look at the time variability we have considered data from a Waverider buoy deployed off the Scilly Isles (see figure 1 for a map). Sea surface elevation, derived from the vertical accelerations of the buoy, was recorded every half second for long periods of time during 1981 and 1982, and in a more conventional manner (Hs calculated from 1024s of elevation data every 3 or 1.5 h) from 1980 to 1983. The spatial scales have been studied using data from the Seasat altimeter during the three-day repeat period, the track used for the main part of the work is also shown in figure 1. In order to ensure consistency between the two instruments (the Waverider and the altimeter) it was decided to use data from the Waverider during the autumn (late August to early November), the same time of year as the three-day repeat for Seasat.

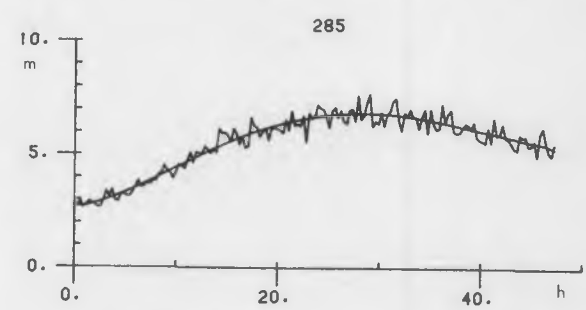

Figure 2. Hs data every 17 minutes starting day 285 and the cubic spline fitted to it.

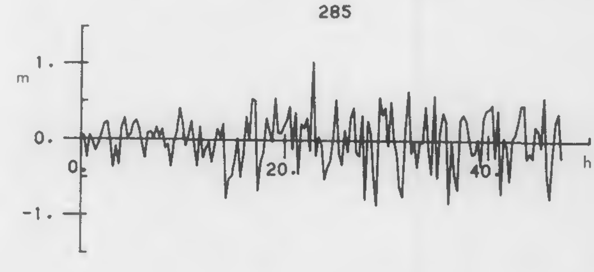

Figure 3. Residual variation in Hs after subtracting the cubic spline

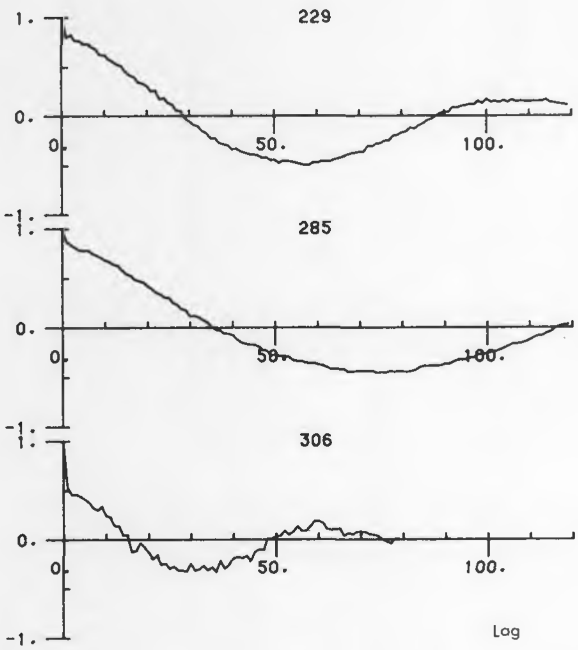

Figure 4. The ACF's of the residual 17 minute Hs values for day 229, 285, 306.

The stationarity of Hs along the Seasat track used here has been considered in an earlier paper (ref 4). There it was concluded that, in general, the data were statistically stationary, but that there were short distances over which the statistical properties changed quite rapidly. Because of this earlier study it was decided to concentrate here upon the correlation scales and ignore problems of stationarity. Ideally one would study both aspects simultaneously. It is proposed to look at this problem in future work.

Figure 2 shows data taken from the Waverider buoy. Significant wave height is calculated (via the spectrum) every 1024s from the 2Hz values of surface elevation. There seem to be two distinct scales present: a low frequency signal, corresponding to the passage of depressions, and a high frequency signal. This record is typical of those we have considered. In order to look at this high frequency component we applied a high pass filter by fitting a cubic spline (ref 5) and using the residuals. The spline fit is shown in figure 2. The residuals are shown in figure 3. This method should remove any non-stationarity in the mean. The autocorrelation function (ACF) is shown in figure 4. Also shown in this figure are the autocorrelation functions from two other records. One thing is immediately apparent. The three ACF's have quite different shapes. These vary from no sign of any scale, i.e. white noise (day 386), to clearly a highly organised signal (day 229). This could be caused by differences in the efficiency of the spline filter or by differing meteorological conditions. A growing sea may well have different scales present compared to a decaying one. These aspects merit further study. Returning to the ACF's even with the most highly organised signal the correlation after seventeen minutes is surprisingly low (about 0.8). Correlations at such short lags should be unaffected by the high pass filter. Therefore we can say that there is no region of high (> 0.9 say) correlation. This is due to the inherent variability in the wave field and, once more, illustrates the need to obtain as many comparisons as possible in order to calibrate to the required accuracy.

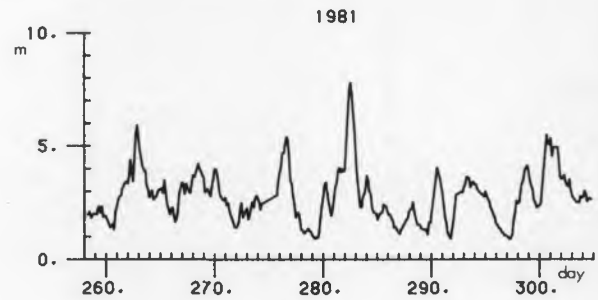

Figure 5. Hs variation during 1981

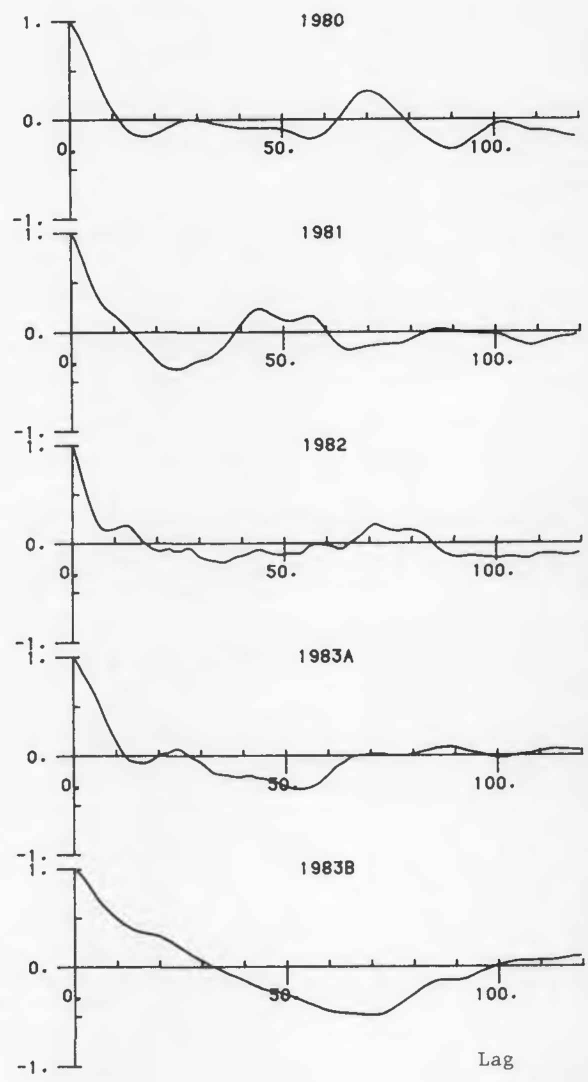

Figure 6. ACF's for Hs at 3 hrly intervals 1980-1983.

To look at the low frequency component we used data collected routinely at three hourly intervals from 1980 to 1981 and every one and a half hours in 1982 and 1983. An example of the data is shown in figure 5. The most important low frequency signal is the annual cycle. In our case we deliberately chose to look at data from a short period of the year (less than two months) and can therefore ignore any seasonal variation. For a study of these longer time scales see ref. 6. They have little relevance to calibration and we will not consider them further. The autocorrelation functions for the year 1980 to 1983 are shown in figure 6. There is a break in the data from 1983 and therefore two ACF's have been calculated, one for each half. Again there appears to be no consistency in the shapes. This is probably caused by the interannual variation in the wave field. However there appear to be moderately high correlations between 120 and 220 hours in all years except 1983. This corresponds to the time scale of the storms passing through the area. Both halves of the 1983 data are too short to have sufficient storms in them for this to show up. However for calibration purposes we are interested in scales of the order hours rather than days so the 'storm scale' is not particularly relevant.

Turning now to the spatial data figure 7 shows Hs

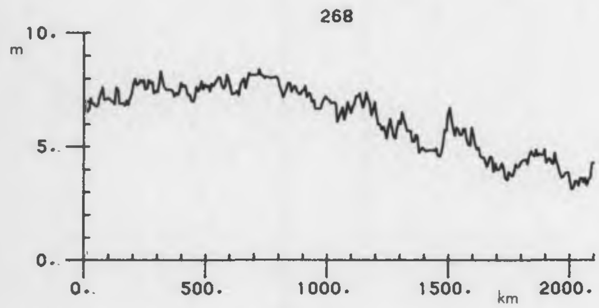

Figure 7. Hs variation along Seasat track on day 268

along an altimeter track (the satellite is travelling south). In ref. 4 it is shown that for a typical wave period (9s), 15 minutes in time is approximately equal to 7 km in space. Therefore we can consider the Seasat data and the 17 minute continuous Waverider data as equivalent. In a similar way to the Waverider data a cubic spline was used to extract the low frequency component. The splines used were identical to those in ref. 4. The ACF's of the residuals for the eight passes along this track are shown in figure 8. These are similar to the Waverider ACF's (figure 4). For large lags there is no definite shape but once again the correlations fall off rapidly.

Unfortunately for the spatial data we do not have the equivalent of the 3-hourly Waverider data and therefore cannot produce an ACF of the low frequency variation. A possible method for overcoming this difficulty will be given below.

In conclusion we can say that Hs variation consists of a low frequency component plus what appears to be high frequency noise. There is some evidence to suggest that, occasionally, there is some organisation in this noise.

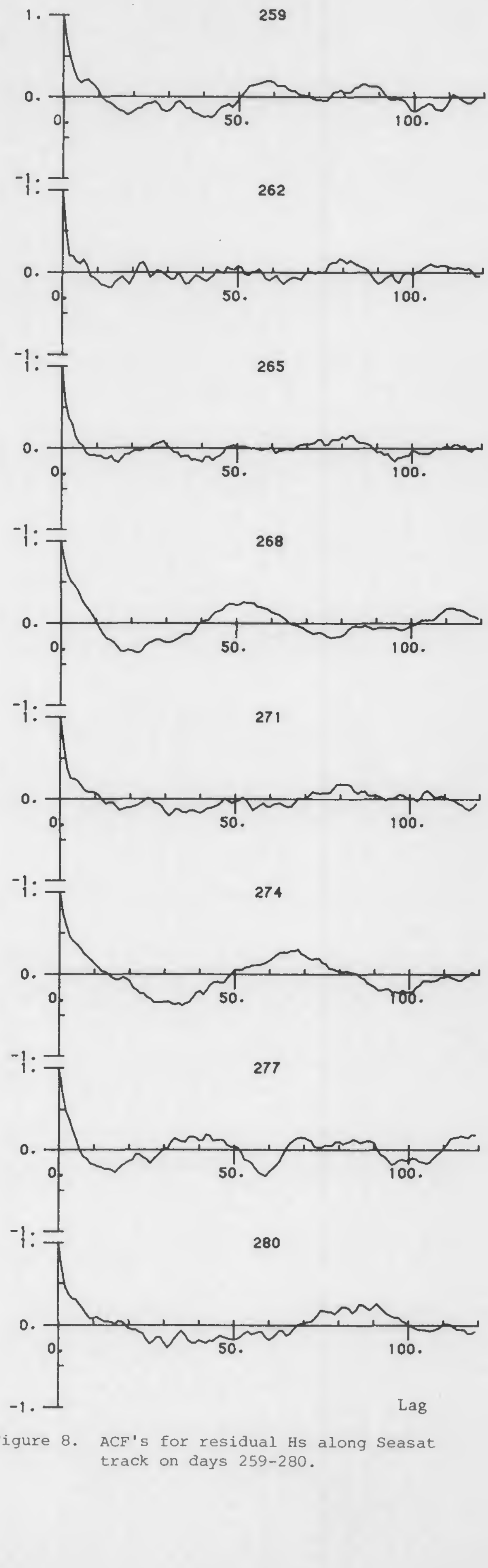

Figure 8. ACF's for residual Hs along Seasat track on days 259-280.

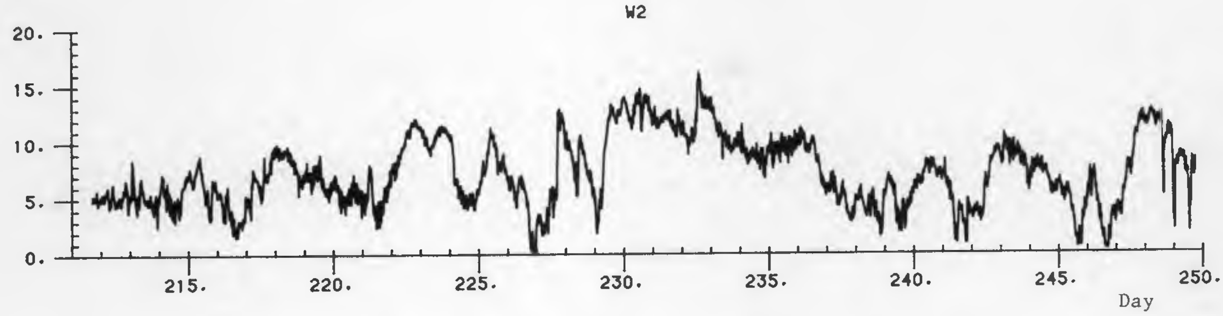

Figure 9. Wind speed recorded during JASIN by buoy W2

4. DIRECTIONAL WAVE SPECTRUM

Unfortunately it is impossible to repeat an analysis similar to the above for the directional wave spectrum. Instruments capable of measuring directional wave data routinely have been developed only recently. The data base for looking at temporal variability is therefore sparse. There is nothing comparable to the continuous Waverider data. For spatial variation there are no data whatsoever, the SAR data from Seasat being much too sparse. One could use the output from wave models. However, since there are no data with which to make comparisons, the scales present within the models have never been verified.

5. WIND SPEED

An analysis of wind speed data, similar to that of Hs, is at present underway at IOS, using JASIN (ref 7) and Seasat data. One problem with the Seasat data is the altimeter wind speed algorithm. The algorithm used to produce the wind speeds in the GDR's (geophysical data records) is known to underestimate at high wind speeds (ref 8). Therefore, before we can use altimeter wind speeds we must recalculate them with a better algorithm. Figure 9 shows the wind speeds from the buoy W2 during JASIN. The data appears to be similar to the significant wave heights discussed above. There is a series of 'storms' of between four and five days' duration with a high frequency 'noise' signal superimposed. The study is not sufficiently well advanced to allow any further results to be presented.

6. DISCUSSION

In the above sections we have discussed the effects of spatial and temporal scales on calibration/validation and given some preliminary results on the scales present in significant waveheight data. More work is needed on all aspects and in this section we will indicate the directions in which we think progress can be made.

Throughout this paper we have been concerned with the autocorrelation structure of the data. Autocorrelations are not easy to interpret, especially when we have separate autocorrelation functions for the high and low frequency variations. There are two possibilities for a more readily understood description of the scales present. One would be to fit an autoregressive model. These models are often used in statistics for forecasting, etc. (ref 9). Although they may give more insight than autocorrelations we do not believe them to be entirely appropriate in this context. The alternative is to look at the gradients present in the data. By

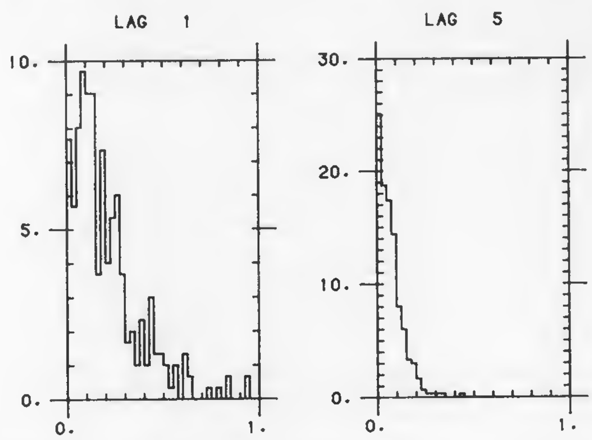

Figure 10. Histograms of the absolute value of Hs differences divided by lag and mean Hs along Seasat track at lags 1 (7 km) and 5 (35 km).

considering the statistical distributions of the change in Hs (say) over varying distances in time and space we may be able to produce statistics of more relevance to calibration than the ACF. An example of such a distribution is shown in figure 10.

All the Hs data considered above consisted of a smooth low frequency variation with a high frequency signal (possibly white noise) superimposed. There are occasions when this model does not hold. Figure 11 shows another altimeter track. Here Hs changes

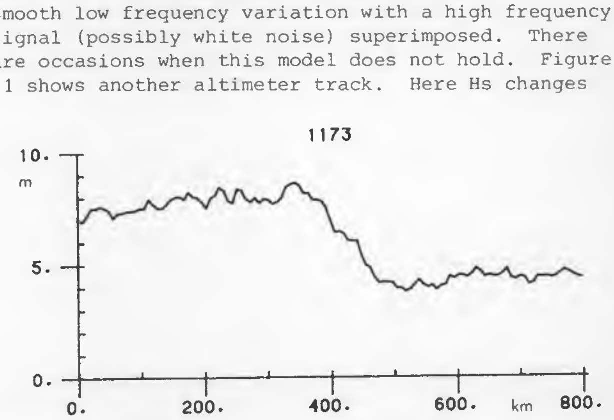

Figure 11. Hs along Seasat rev. no. 1173 showing 'Hs jump'

by 4 m over a distance of 125 km. Such jumps in Hs are by no means uncommon, thirteen are identified in the North Atlantic in ref 10. Obviously if an altimeter track were on one side of such a jump and a buoy on the other no useful data for calibration purposes could be obtained. Such data needs to be eliminated before performing the calibration. In ref 10 it is suggested that these jumps occur on the southern flank of depressions. Further work is needed on the identification of such jumps. One possibility is to use the altimeter data itself to identify them. Indeed it is possible to envisage a recursive scheme whereby ERS-1 data are used to identify the relevant scales which are then input to the calibration process! Care must be taken with such proposals however to stop them becoming too incestuous.

7. ACKNOWLEDGEMENT

We would like to thank Peter Thompson who performed the computations for this paper.

8. REFERENCES

1. Brown P J 1982, Multivariate Calibration, J Roy Statist Soc B, 44 (3), 287-321.

2. Fedor L S & Brown G S 1982, Waveheight and wind speed measurements from the Seasat radar altimeter, J Geophys Res, 87 (C5), 3254-3260.

3. Theobald C M & Mallinson J R 1978, Comparative calibration, linear structural relationships and congeneric measurements, Biometrics, 34, 39-45.

4. Challenor P G 1983, Spatial variation of significant wave-height, Satellite Microwave Remote Sensing, Ellis Horwood, 451-460.

5. Wold S 1974, Spline functions in data analysis, Technometrics, 16 (1), 1-11.

6. Jardine T P & Latham F R 1981, An analysis of wave height records for the N E Atlantic, Quart J R Met Soc, 107, 415-426.

7. Pollard R T, Guymer T H & Taylor P K 1983, Summary of the JASIN 1978 field experiment, Phil Trans R Soc Lond A, 308, 221-230.

8. Chelton D B & McCabe P J 1985, A review of satellite altimeter measurement of sea surface wind speed with a proposed new algorithm. J Geophys Res, 90 (C3), 4707-4720.

9. Box G E P & Jenkins G M 1976, Time series analysis: forecasting and control, Holden-Day.

10. Queffeulou P 1983, SEASAT wave height measurement: a comparison with sea-truth data and a wave forecasting model - application to the geographic distribution of strong sea states in storms. J Geophys Res, 88 (C3), 1779-1788.

NASA SCATTEROMETER DATA PROCESSING SYSTEM – FEATURES FOR VALIDATION

P S Callahan & J R Benada

Radar Science and Engineering Section
Jet Propulsion Laboratory
California Institute of Technology
Pasadena, California 91109 USA

ABSTRACT / RESUME

JPL is developing a scatterometer to be flown on the US Navy Remote Ocean Sensing System (N-ROSS) scheduled for launch in late 1990. JPL will develop and operate a data system for research users of scatterometer data. This system will have many features which will be used to support system calibration and validation efforts in the first year after launch. The overall design of the data system and the development of key processing algorithms is described. The data products and parts of the data system to be directly validated are listed. The main features of the Data Management Subsystem which will not only deliver data to science users but will also support system validation are outlined.

Key Words: Scatterometer, Data Processing, Algorithms, Remote Sensing, Validation

1. INTRODUCTION

The NASA scatterometer (NSCAT) will fly on the Navy Remote Ocean Sensing System (N-ROSS) which is scheduled for launch in September 1990 (Ref. 1, this volume). In additon to developing the space-borne instrument, JPL is developing an NSCAT Data System (NSDS) to process and make available to science users various data products from NSCAT. The requirements and preliminary design of the NSDS were discussed in Ref. 2. In this paper we will update the design description of the NSDS. We will cover progress on several of the key algorithms in the data processing -- data grouping, wind retrieval, and ambiguity removal.

The NSCAT project plans a one year calibration/validation effort following on-orbit checkout (Ref. 1). The first phase will emphasize system, and especially instrument, performance through the backscatter cross section level. The second phase will emphasize the geophysical performance (wind vectors). The NSDS has both elements which must be validated and features to assist the project with other aspects of calibration and validation. We will list the items which must be validated. We will discuss the features of the NSDS which will assist the project in validation activities. These features include algorithm development, early testing, and reserve capacity in the Data Processing Subsystem (DPS) of the NSDS and the extraction software and computing environment of the Data Management Subsystem (DMS). Finally, we will note some items which should be considered in planning for an overall succesful validation effort and for data exchange.

2. DATA SYSTEM FUNCTIONAL DESIGN

The NSDS consists of two major subsystems -- Data Processing (DPS) and Data Management (DMS). The DPS contains four major functions: (1) ingesting data and converting to engineering units, (2) producing sensor data records of Earth-located backscatter cross section (sigma-0), (3) producing geophysical data records of unique wind vectors, (4) checking data. Data products will be archived and will be available to data users at several levels through the DMS. The definitions of the data levels used in the NSDS and the daily volumes are shown in Table 1. We will not discuss processing from Level 2.5 to Level 3.0 as the Science Definition Team (SDT) is now developing the specification of the Level 3.0 map product.

2.1 Level 0 to Level 1.5 Processing

It is planned that the Navy's Fleet Numerical Oceanography Center will supply a data package to JPL to allow the NSDS to carry out its processing. The package will consist of

(1) time-ordered, nonredundant NSCAT raw data and N-ROSS orbit and attitude information,
(2) Special Sensor Microwave Imager (SSM/I) data processed to Earth-located brightness temperatures (Tb) from the same orbit as the NSCAT data,
(3) selected NSCAT data as processed by the Navy,

Proceedings of a Workshop on ERS-1 Wind and Wave Calibration, Schliersee, FRG, 2–6 June, 1986 (ESA SP-262, Sept. 1986)

(4) all available in situ wind data. The Navy-processed NSCAT data and the in situ winds will be used for monitoring of NSDS processing and checking of products.

The raw NSCAT data will be processed one frame (measurement of 25 sigma-0 cells from one attenna beam) at a time. The data will be converted to engineering units. The computations of the onboard digital signal processor will be duplicated in order to determine Doppler parameters for Earth location and bandwidths for sigma-0 computation. The coefficients for computing the normalized standard deviation (Kp) appropriate for the digital processor will also be computed. Geometric quantities for each cell such as Earth-location, cell area, slant range, etc. will be computed. Several points on each sigma-0 cell will be compared to a world map and an ice map in order to flag sigma-0 cells which are not over the ocean. From the measurements of signal-plus-noise and noise-only for each cell made by the onboard digital signal processor, the backscattered power and then the normalized radar cross section (sigma-0) will be determined.

The SSM/I Tb's will be used to determine a flag for atmospheric absorption caused by liquid water. The SSM/I data will be colocated with the NSCAT data by transforming both data types to a coordinate system with the subtrack as the equator (see Sec. 3.1). During Earth location the sigma-0 cells will have an index computed in this along-track cross-track grid for later grouping into wind vector cells. The same index will be computed for the SSM/I cells which will be interpolated from the orginal scans onto the sigma-0 grid. This will allow colocation with no explicit searching.

The geometric quantities, power measurements, sigma-0, interpolated SSM/I Tbs, plus additional housekeeping information will be written to the sensor data record (SDR, Level 1.5). The SDR is one of the primary outputs of the NSDS and should be used for detailed studies of backscatter and system performance. The large volume of this file should be noted.

2.2 Level 1.5 to Level 2.5 Processing

The sigma-0 data will be processed to wind vectors and a unique wind direction selected by the second major step in the DPS. The bin index in the subtrack coordinate system (see Sec. 3.1) will be used to group sigma-0s from the four beams on each side of the spacecraft into 50 km wind vector cells (WVC). This requires buffering at least 1.3 million bytes of data during the time that an outer WVC first collects a sigma-0 from a forward beam until the aft beam passes. Once a row of WVCs is completed -- nominally each WVC will have 16 sigma-0s (4 from each beam), but with a minimum of 6, at least 1 from each beam -- it is sent to wind retrieval.

Wind retrieval consists of finding the multiple speeds and directions which maximize the likelihood of the observed sigma-0s given the model function which relates wind speed and direction, incidence angle, polarization, and perhaps other geophysical quantities to backscatter (See Sec. 3.2). Typically, 2 to 4 wind ambiguities having nearly the same speed but different directions are found. The retrieval technique assigns not only errors to the speed and direction but also a relative likelihood to each solution. It is required that 90% of the time there be two main ambiguities approximately 180 degrees apart. The multiple wind solutions will be written to a file (Level 2.0), but will mainly be used for further processing.

The likelihood estimates are used in the next processing step which is called ambiguity removal (See Sec. 3.3). Several techniques have been shown to be successful at picking the correct direction at least 90% of the time given an "instrument skill" (highest likelihood retrieved vector is in direction of true wind) of 60-70%. Generally, the techniques use a minimum likelihood cutoff before creating a field from the highest likelihood vectors. The ambiguities are compared to the field, and those in agreement within a set tolerance are selected. The selected vectors are used to make a new field and the comparison repeated until a stable solution is reached.

The unique wind vectors with position information and some limited processing information will be output as the geophysical data record (GDR, Level 2.5). The SDT is considering whether to make the Level 2.0 and Level 2.5 records be physically the same file. In this case the Level 2.5 "record" would be an indication on the Level 2.0 record of the selected ambiguity. It is possible that the DMS would be set up to extract condensed Level 2.5 records from the Level 2.0 data to reduce data volumes for those users only interested in the unique vectors.

2.3 DPS Functions at All Levels to Assist Validation and Monitoring

The DPS design includes Master Catalog, Data Accountability, and Algorithm Performance Reports at each processing step. This information will assist the system users in monitoring the processing performance and in detecting incorrect setups or procedures, bad input data, and software problems.

The Master Catalog information will be used not only on the DPS but also by the data users on the DMS to determine the volume, state, and availability of data for any particular orbit. The catalog will be searchable on-line on the DMS.

Data Accoutability Reports will indicate the volume of data processed in different input and output categories. They will provide an indication of the quality of the incoming data.

Algorithm Performance Summaries will indicate the outcome of the processing at each level. They will provide running means and standard deviations of various parameters. They will show statistically the grouping of sigma-Os into WVCs, the number of ambiguities retrieved with their likelihoods, and the selection per centages of ambiguities during ambiguity removal. These data will give a crude indication of processed data quality.

Of the 25 sigma-0 cells in a beam, the innermost one at 10.5 degrees incidence angle will be used for system performance monitoring. Backscatter from the ocean is expected to be nearly independent of wind velocity at that incidence angle. A file of those data will be written and checked for trends. The checking for trends will be done within the DPS but not as part of the regular data processing stream.

While the Level 3.0 map product has not been defined by the SDT yet, it will be a useful tool for assessing coverage. It may also be possible to do some data quality assessment at high latitudes where swaths overlap frequently and thus there are good statistics on means and variations.

The DPS has several other design features which will assist the validation effort. These features should be common in any system produced with modern software engineering techniques. First, the DPS is designed to be a dedicated, self-sufficient system with 50% reserve computing power (estimated computing power (MIPS) divided by computing power purchased). This means that there should be little contention for resources. It will allow the DPS to met special processing requests during the validation phase while continuing routine production. It will also mean that no extraordinary measures, which might prove difficult to maintain or modify, will need to be taken in software implementation.

Second, as discussed in Section 3, the DPS software is preceded by an algorithm development effort which will test processing approaches and processing speed. The two main products of the algorithm development effort are detailed algorithm specifications and working prototype code. These two items will result in production software which is more efficient and more likely to be correct.

Third, the DPS is required to be ready for testing by the personnel who will use it for data production 6 months before launch. This testing will result in better trained system users and in the detection and correction of additonal system errors which may escape earlier testing by the software developers.

Fourth, data output by the DPS will be stamped with the version of the software and all tables used to produce it. This traceability will be very important during the validation period when there may be changes (not necessarily all correct) to the software or tables.

2.5 Data Management Subsystem Functions

The DMS will be the Project's interface with the data users. The DMS has a number of tasks to perform, several of them directly related to calibration and validation. The DMS tasks include
(1) provide access to required levels of processed NSCAT and in situ data for the science and engineering teams,
(2) provide access to Master Catalog and monitoring reports,
(3) provide computer resources for the validation efforts,
(4) provide computer resources for the mission operations team.

The percentage of on-line (available interactively, generally without operator intervention) data and its method of selection is indicated in Table 2. The menu system will use the software developed by the NASA Ocean Data System (NODS) at JPL. It allows the selection of data by geographical location and time. The software then finds data which fall in the location/time box from the swath-organized, indexed data. It is also possible that NSCAT will have NODS do the data management functions for the project. NODS will be performing these functions for TOPEX, so there could be significant benefits in having both wind and height data together.

It is planned to use optical media to store most of the data, especialy the voluminous Level 1.5 records. The Level 3.0 maps will be on magnetic disks. The raw input data will be copied from tape to off-line optical storage if there is sufficient time; otherwise, the tapes will be retained as the primary archive.

As noted in Table 2 a selected 5% of the Level 1.5 data for the most recent 6 months will be kept on-line. The 5% will be in 3 to 4 regions of the world (Gulf of Mexico, North American coasts, etc.) determined by the SDT. It is planned that the validation sites will be included in this 5%. For ease of data transfer, it would be desirable that the NSCAT and ERS-1 projects consult on these areas. If possible, this 5% data extraction will be done in the DPS; otherwise, it will use the regular extraction software of the DMS, perhaps in batch mode.

3. ALGORITHM DEVELOPMENT

Algorithm development for the DPS is being carried out in an Algorithm Testbed (ATB). When completed, the ATB will contain most of the steps that will be in the final processing stream. It also uses the level records as they are currently defined. The ATB will not have all the reports and other features needed to make an operational software system, but it does allow testing of processing approaches and speed. We will not discuss all the algorithms in the ATB but will touch on several which are novel or very important to the success of the final data processing.

The ATB software is being maintained with a Change and Configuration Control (Trademark of Softool Corporation) system in order to insure orderly development and to gain experience with such systems. Automated procedures have been built around this system to update the ATB daily. It is planned to use a similar system during DPS development.

3.1 Level 1.0 to Level 1.5 Algorithms

As noted in Section 2.1, the NSCAT data are processed frame by frame in time order. Generally, each of the 25 sigma-0s in a frame will belong to a different 50 km WVC. In order to ease the grouping process for wind retrieval, it was decided to do a transformation from the geographic coordinates which are computed for each cell (and written to the Level 1.5 record) to a coordinate system with the satellite subtrack as the equator. The coordinate strip from one ascending node to the next is defined to contain 1600 along-track rows (thus, very slighly more than 25 km along track) and 64 across-track 25 km columns. The transformation of the cell coordinates produces a new "longitude" and "latitude" which are reduced to integers to determine the bin indices. The computation requires iteration on the longitude for elliptical orbits and/or an oblate Earth, but it converges in only 2 or 3 steps and is not a significant computational load. The indices are stored on the Level 1.5 record for use in the grouping step which precedes wind retrieval.

The SSM/I data are collected in a semicircular scan which covers a swath nearly as wide as that of the NSCAT. The brightness temperatures will be received with Earth locations already computed. A convenient way to treat these data is to perform the same transformation on them as is done to the sigma-0s. Then, items with like bin indices can be associated with no file searching or rereading of data. The SSM/I data will be interpolated to the NSCAT grid using equal area circle approximations to both the beams and grid cells. The use of circles allows a fairly straightforward formula to give area weighting. Unfortunately, the computational speed of this approach has not been tested yet.

The NSCAT instrument uses an onboard digital signal processor to define the sigma-0 cells in the along-beam direction by Doppler filtering. The performance of the digital signal processor is analyzed in Reference 3. During ground processing in the DPS, it is necessary to duplicate the onboard computations which produced the Doppler frequencies. The intersections these frequencies with the antenna pattern on the Earth determine the cell location. It is also necessary to determine the cell bandwidths and windowing in order to produce the coefficients needed in the computation of the normalized standard deviation (Kp) of sigma-0. Both the Doppler binning and the Kp coefficient calculations are running in the ATB. The computation of the Kp coefficients needs to be speeded up by a factor of at least 10 from its current implementation, which uses the full analysis (Ref. 3) in a straightforward way, in order to meet the processing time budget.

3.2 Level 1.5 to Level 2.0 Algorithms

The bin indices calculated in the location processing and written to the Level 1.5 record are used to group the data for wind retrieval. "Rotating buffers" 32 rows along track by 32 bins across (50 x 50 km) are set up for all the quantities desired in the Level 2.0 data. As the Level 1.5 data are read in frame by frame, each sigma-0 is put in a bin based on its indices. The along-track indices are reduced to a "span" number (integer part of row number divided by 64) and a reduced row number (remainder from row number divided by 64). When an attempt is made to add a sigma-0 with a new span number to a buffer row containing data with an old span number, the filled row is sent to wind retrieval.

Wind retrieval is done with a combination of the SASS sum-of-squares (SOS) technique (Ref. 4) and a maximum likelihood estimator (MLE). The intial search for solutions is done with the SOS as it provides a closed form solution for the wind speed given the direction as is done in the search. Around each of the initial solutions, an interpolation using the MLE objective function is carried out. Several techniques for finding the final solution around the initial estimates have been tried. The interpolation technique is the fastest and also provides error estimates. From the residuals of the solutions, relative likelihoods for the solutions are determined.

Although the retrieval has been speeded up by nearly a factor of 3, it is still running a factor of 3 slower than the initial processing budget. Numerous methods of speeding it up, including using the SOS technique exclusiviely as was done for SASS, have been tried. The SOS technique resulted in only about a 30% speed up. Most of the retrieval time is spent in doing the initial search of directions. It may be necessary to start most solutions from estimates based on neighboring cells. It is also likely that the processing budget will have to be changed.

3.3 Level 2.0 to Level 2.5 Algorithm

From the multiple wind vectors output by the wind retrieval, a unique vector (direction) must be selected. Very strict requirements have been placed on the DPS for this processing:
(1) no external data may be used,
(2) the overall success rate is to be better than 96%,
(3) no 12 x 12 area may have less than 85% correct solutions.

Initially, a wind field algorithm patterned after one proposed by the University of Wisconsin for testing for the NOSS scatterometer (Ref. 5) was tried. The algorithm nearly met the success criteria, but it deteriorated rapidly with decreasing instrument skill and required forced choices for about 5% of the vectors. The algorithm very seldom chose large patches in error (typically reversed) as some of the other algorithms tested for NOSS did.

The ATB now uses the median filter algorithm described in Reference 6. The median filter is a technique for removing noise and enhancing edges in image processing. This algorithm has been tested on the same 5 swaths as the previous algorithm and has equal or better performance in all cases. Statistics within the swaths suggest that it is less sensitive to instrument skill than the previous algorithm. The tests to date suggest that it can bring data with only approximately 40% instrument skill up to approximately 90% correct selections. The median filter, like all objective algorithms, has the most difficulty at the edges of swaths and, in the end, requires reasonable instrument skill (generally, >~ 50%) in order to succeed. With an instrument skill of 60 - 70% the median filter makes correct choices in approximately 90 - 97% of the cases (There is not necessarily a one to one correspondence between instrument and algorithm skill.).

The ambiguity removal algorithm operates on only one side of the swath at a time. It is most efficient when it has a long stretch of data over which to move its 7 x 7 cell window. First, the algorithm selects highest likelihood vectors for which the likelihood is above a predetermined value. Using the median filter as an interpolator, it fills in the missing data. The vectors are then median filtered as components, and the components reassembled into vectors. For each WVC, the ambiguities are compared to the filtered field. If one of the ambiguities agrees with the field to within a predetermined value, it is selected; otherwise, the cell is marked as missing data. The algorithm then returns to the interpolation and filtering steps. It is a property of median filters that they reach a stable point; thus, after a few iterations, typically 3 to 4, every WVC has a selection made.

Testing of the ambiguity removal capability on SASS dual polarization data has started. Reference 7 has shown that these data have an instrument skill of approximately 45% which should be sufficient for the median filter to correctly select vectors. One problem with the SASS data is that in order to get good wind retrievals 100 km WVCs must be used. The swath is then only 5 cells wide so that essentially all cells are edges where the algorithm has the most difficulty. Testing with more simulated data is also planned. These tests will concentrate on difficult situations such as fronts.

4. DATA SYSTEM INPUTS AND OUTPUTS TO BE VALIDATED AND MONITORED

A number of NSDS items will need to be verified once NSCAT is on orbit, in addition to the geophysical validation of the overall NSCAT system performance. The N-ROSS operational plan calls for the spacecraft contractor to check the spacecraft and instrument functions once the operational orbit is achieved and then turn the system over to the Navy operations team 30 to 60 days after launch. This is called IOC -- Initial Operations Capability.

Within 6 months of IOC the NSCAT project plans to complete system calibration and validation through the Sensor Data Reord. This part of validation will emphasize the instrument performance. Within one year of IOC the geophysical validation of wind products will be completed (Ref. 1, this volume).

4.1 Instrument Parameters

The NSCAT antennas will be aligned optically when they are mated with the spacecraft. On orbit the antennas will be deployed to fixed angles; a deployment signal may be present in the telemetry. Part of the initial instrument verification will be to determine that the antennas are pointing as they were designed. In addition, the antenna gain tables, which will be from antenna range measurements and calculations, must be validated/calibrated.

During calibration, and perhaps throughout the mission, ground receivers will be used to measure the transmitted power and antenna gain. These data will be combined with several regular NSDS products to complete the calibration and validation of the antenna pointing, antenna gain, and transmit power monitor. The NSDS will use land edges, especially areas with multiple edges closely spaced, to help determine pointing. Data from rain forests, especially the Amazon, and deserts will be used to intercalibrate the antennas. This should result in essentially no bias among the antenna beams on each side of the spacecraft. Data from these calibration areas will be monitored throughout the mission as a data quality check. The reduction of interbeam bias is extremely important for ambiguity removal. Accurate knowledge of antenna pointing and gain will allow measurement of the transmitted power from ground receivers and thus calibration of the onboard power monitor.

As noted previously, NSCAT uses a digital signal processor to determine along-beam Doppler cells. The parameters for the onboard computation of cell center frequencies and bandwidths can be reloaded from the ground. The processing to Level 1.5 is dependent upon these tables being the same in the spacecraft and the NSDS. An early part of the validation activities will be to insure that the procedures for defining, uploading, and passing to the NSDS (and to the Navy processing system) these tables function as planned. The frequency of table reloading depends upon the orbit eccentricity. In the nominal orbit, the parameters will be reloaded approximately once per month. If the N-ROSS plan of having a 19 day repeat orbit is carried out, it may not be necessary to reload the parameters at all.

4.2 Sensor Data Record Outputs

The instrument gain will be monitored on orbit by calibration frames which will occupy 1 out of every 128 antenna cycles (sequence of 8 beams). Thus, approximately every 8 minutes there will be a set of 8 calibration frames during which the receiver will view a high and low temperature noise source instead of received signal. These data will be processed routinely in the NSDS to determine the system gain for use in computing sigma-0. The data will be output to a separate file for statistical analysis.

As noted in Sec. 2.1 one of the 25 cells in each beam is at an incidence angle of 10.5 degrees where the backscatter from the ocean is insensitive to the wind velocity. These cells will be processed to Level 1.5 along with the other cells. The data will also be output to a separate file for statistical analysis.

There will be at least three tools for monitoring the performance of the NSCAT system on orbit:

(1) the constancy of scattering from rain forests and deserts,

(2) the constancy of system gain from the calibration frames,

(3) the constancy of scattering from the monitor cells.

These data will all be produced routinely by the DPS in processing to Level 1.5. The data will be available on the Level 1.5 record but will also be output to a separate files. Statistical processing of these files will take place in the DPS separately from the main level processing. Additional analysis of these data may be carried out in the DMS in order not to interfere with production on the DPS.

During the validation period, aircraft underflight data will be collected to validate/calibrate the sigma-0 data produced by the NSCAT system. While there will be questions of spatial scale between the NSCAT 25 km cells and the typical aircraft scatterometer beams of 100 m, it is planned directly validate the NSCAT system measurement of backscatter.

4.3 Geophysical Data Record Outputs

The principal scientific output of the NSDS is wind vectors, in particular unique vectors, for each wind vector cell. The winds will be the subject of the geophysical phase of the validation. The plans for validation are discussed in Ref. 3 (this volume).

During routine processing, the wind products will be monitored by comparison with Navy-processed NSCAT winds and Navy-collected in situ winds. Statistical processing of these data will be handled in the DPS. It is also planned to have Data Product Analysts who will check the DPS output winds for "reasonableness" -- large areas of extremely high or low speeds, single directions, etc. As experience is gained with these functions, it is likely that software can be implemented to carry out many of them.

5. VALIDATION CONSIDERATIONS AND APPROACHES

In addition to planning of validation field experiments, it is necessary to plan for the processing of the data from these experiments (usually carried out by the investigators themselves) and then the merging and comparison of the experiment data with the regular scatterometer products. If intercomparisons between the ERS-1 scatterometer and NSCAT data are to be carried out, planning of these activities is also needed. In both cases, it would be highly desirable if intercomparisons were considered in the early design phases of the data systems so that support of such activities was as straightforward as possible.

5.1 Use of DPS

The DPS will not allow access by general users or investigators. This will allow all the DPS power to be concentrated on level conversion and statistical analysis of data. There will be a minimum of multiuser or other special operating system features. However, the DPS software will be flexible enough to allow for special processing (25 km resolution winds, processing of small areas) of data during the validation period. As noted in Sec. 2.4, the reserve computing capacity of the DPS will allow multiple processing of at least some data during the validation period. Multiple processing will be necessary in case of instrument parameter changes, problems with the ground data transmission system, or DPS software or procedure errors.

While model function refinement will be an important element of the geophysical calibration, it is not planned to routinely reprocess data. Reprocessing of the first years's data may be undertaken on a best efforts basis if there are significant changes in the DPS software or in the model function.

It will be desirable to have a second copy of the DPS software in which the project team can make changes that are not under formal change control as the production software will be. The use of a system like the Change and Configuration Control (CCC) system now used on the ATB will make it easy to have a "second copy" which can be clearly related to the production software. Once the changes are tested in the development configuration, CCC will make it easy to update the production software when a change is formally approved. Scheduling of DPS time will be required to minimize conflicts between production and validation processing. All data produced by the NSDS will be stamped with the time and version of the software.

The above discussion makes it clear that statistics and data sets which are needed for calibration, validation, or intercomparison should be designed into the DPS. It will be difficult in a production environment to allow extra processing runs or to make major structural changes to software or procedures to produce needed data.

5.2 Use of DMS

The DMS will be crucial to the validation effort for several reasons. It will provide the computing enviroment for most of the project analysis of validation experiment data. The data extraction capability will be used to produce small, easily accessed data files of the validation regions. The DMS may also be used to extract the 5% of Level 1.5 data (which will probably cover the validation areas) which will be kept on-line. The DMS will contain a catalog of all validation and comparison data and will host some of these data sets.

The computing environment for validation will include standard languages, mathematical and graphics libraries, and the data display capabilities developed by NODS. This environment will generally only be available to the JPL project teams.

The data extraction function of the DMS allows the selection of data by geographical coordinates and time. This will be very convenient for finding all NSCAT data which fall in the validation experiment areas. Because the NSCAT data for the validation regions will be used frequently, it will desirable to store it in special files. Data for intercomparison with ERS-1 can be extracted as required. It would be useful if the regions desired, the data types and volumes could be defined ahead of time so that operational procedures for the extraction could be developed.

The NODS system includes several levels of catalog information. For data produced by the DPS, the main catalog will be that output by the DPS as data are processed. The catalog will include information on the NSCAT data from each orbit such as
(1) time and location of beginning of orbit,
(2) status of processing of each level,
(3) volume of data at each level,
(4) indicators of data quality and system performance.

The catalog will list other data related to the validation effort. Many of these data sets will be available on the DMS. The catalog for these data sets will contain information on the content and format of the data.

Along with the data needed to process the NSCAT data, the NSDS will receive in situ wind data and FNOC-processed NSCAT data from FNOC. After these data are used for product checking on the DPS, the in situ data will be transferred to the DMS for investigator use. At least during the validation period, buoy data will be requested by the project from the agencies who normally collect such data. These data will be stored on the DMS. The aircraft data which are collected to validate the sigma-Os will be retained in files on the DMS, although they may not be generally available.

The Science Defintion will attempt to identify investigator-produced data which would be of interest to more than one group of investigators. If these data are of wide enough interest and a suitable format can be developed, the data sets will be supported on the DMS. Intercomparison data received from ERS-1 will be stored on the DMS. If it is appropriate, the data may be available for extraction thorugh the NODS software.

The availability of numerous analysis tools and convenient access to NSCAT, validation, and other comparison data on the DMS will make the validation task much easier than if these capabilties were on separate systems. As noted previously, NSCAT may use NODS for the data management function. In this case, the TOPEX data would be available so that analysis involving winds and currents would have a common data source. Planning for validation data processing and storage and for exchange of data between ERS-1 and NSCAT will further enhance the validation efforts of both projects.

6. REFERENCES

1. Martin, B D, Freilich, M H, Li, F K, Callahan, P S 1986, An overview of the NSCAT/N-ROSS Program, ESA Wind and Waves Calibration Workshop Report, this volume.

2. Callahan, P S, Benada, J R, Noon, E L, Leach, G E, Brown, J W, Pihos, G, McCabe, P J, Lame, D B 1984, NASA Scatterometer research data processing system -- requirements and design, ESA SP-215, Proceedings of IGARRS'84 Symposium, Strasbourg 27 - 30 August 1984, 771-5.

3. Chi, C Y, Long, D G, Li, F K 1986, Radar backscatter measurement accuracy using digital Doppler processor in spaceborne scatterometer, IEEE Journal of Geoscience and Remote Sensing, GE-24, 421-437.

4. Boggs, D H 1982, Seasat geophysical data record users handbook -- Scatterometer, JPL D-129.

5. Schroeder, L C, Grantham, W L, Bracalente, E M, Britt, C L, Shanmugam, K S, Wentz, F J, Wylie, D P, Hinton, B B 1983, A study of ambiguous wind direction results for a Ku-band scatterometer using measurements at three azimuth angles, IEEE 83CH1837-4, Digest of IGARRS'83, San Francisco August 31 - September 2, paper FP3-6.

6. Schultz, H J 1985, Median filter ambiguity removal technique, IEEE Proceedings of IGARRS'85 Symposium, Amherst 7-10 September 1985.

7. Woiceshyn, P M, Wurtele, M G, Boggs, D H, McGoldrick, L F, Petherych, S 1986, The necessity for a new parametrication of an empirical modle for wind/ocean scatterometery, J. Geophys. Res., 91, 2273-88.

We would like to thank the other members of the NSCAT Data System Team for their assistance with the overall design and their work in algorithm and software development.

The work described in this paper was carried out by the Jet Propulsion Laboratory, California Institute of Technology under contract with the National Aeronautics and Space Administration.

TABLE 1: DATA LEVEL DEFINITION AND DAILY DATA VOLUMES

LEVEL	DESCRIPTION	VOLUME (UNITS)	VOLUME (MBytes)
0	RAW DATA -- FRAME SYNCHRONIZED, TIME-ORDERED AND NON-REDUNDANT	188,000 Frames*	30
1	DECOMMUTATED DATA IN ENGINEERING UNITS	188,000 Frames	40
1.5	SENSOR DATA RECORD (EARTH-LOCATED, CALIBRATED σ_0 WITH RAIN FLAG)	188,000 Frames	506
2	WIND VECTORS IN 50 km CELLS WITH MULTIPLE DIRECTIONAL AMBIGUITIES	188,000 WVC+	17
2.5	GEOPHYSICAL DATA RECORD (WIND VECTORS WITH DIRECTION SELECTED)	188,000 WVC	4
3	MAP OF 2-DAY WIND VECTORS	33,800 CELLS	1

* DATA FROM 1 ANTENNA BEAM
\+ WIND VECTOR CELLS, 50 x 50 km

TABLE 2: ON-LINE DATA AND ACCESS

LEVEL	ON-LINE VOLUME	SELECTION METHOD
1.5	5%, 6 MONTHS	REV NO., START/STOP TIME. 5% - REGION, TIME
2.0	0	REV NO., START/STOP TIME
2.5	100%, MISSION	LAT/LONG/TIME-MENU DRIVEN
3.0	100%, MISSION	LAT/LONG/TIME-MENU DRIVEN

GATHERING AND PROCESSING A COMPARATIVE DATA SET FOR THE CALIBRATION AND VALIDATION OF ERS-1 DATA PRODUCTS; PREPARATORY WORK AT THE UK-ERS-DC

R J Powell

Rutherford Appleton Laboratory, Didcot, Oxon, UK.

ABSTRACT

It is suggested that the main European effort to validate the wind and wave data products of ERS-1 should be concentrated in the North-East Atlantic and Norwegian sea. Also, that conventional oceanographic data gathering techniques using ships and buoys should be augmented with permanently deployed and well validated "master stations" and airborne instrumentation. The need to site such stations and altimeter transponders on the ground track argues strongly for the early selection of the location of the ground tracks associated with the initial three-day repeat orbit and for ensuring that any higher repeat cycle is a multiple of three. A brief description is given of some of the early work on this subject at the UK-ERS-DC.

1. THE CONCEPT OF MID-OCEAN WIND VELOCITY AND WAVE HEIGHT

When beginning to think about calibration and validation of satellite-based, mid-ocean, wind and wave height measurements we should keep in mind the background of these concepts. It may be helpful to begin by considering the more clear-cut case of a satellite-based geodetic measurement of a permanent terrestrial baseline. Here, our concept of the distance between the ends of the baseline is firmly established to a level of precision and accuracy which is thought, at least initially, to be an order of magnitude better than that expected to be achieved by the satellite-based measurement. The baseline is fixed throughout the satellite life, it can be remeasured as required and the measurements related back through a series of transfer standards to an International Bureau of Standards. In these circumstances it is acceptable to concentrate all effort on the definition of satellite sensor outputs, atmospheric corrections and associated algorithms and judge them to be wrong if they do not agree with the ground-based measurement.

For satellite-based oceanographic measurements the situation is different. Mid-ocean winds and waves are essentially ephemeral so that truly repeated measurements are impossible. Our concept of , for example, wind velocity at ten metres above the sea surface is much less firmly based than that of baseline length. The link between measurements made at sea and any internationally agreed standard is seldom made rigorously for a wide range of conditions to an accuracy much better than that predicted for the ERS-1 sensors. Indeed one aim of any calibration effort would be to provide a surface data set for which that link is rigorously maintained.

Also, for oceanographic parameters, satellite and ground-based measurements are not wholly independent. The lack of a complete and rigorous description of the physics relating wind velocity and wave height to sensor outputs means that, at the time of launch the satellite sensor algorithm will have been "tuned" to match the relationship between past sensors and a previous data set. This process necessarily involves a great deal of averaging. Properly controlled the overall approach is inherently superior to that of making surface measurements with individual instruments. After the tuning is complete individual satellite-based measurements from different geographic locations will effectively be compared via the satellite sensor algorithm to the mean of an historic data set, they are then potentially inter-comparable with an accuracy which is limited only by the stability and noise level of the sensor and the system sampling statistics. If the data set used in the initial tuning was sufficiently accurate, sufficiently large and thoroughly representative of all seasons and global locations and if all the necessary geophysical parameters are represented in the algorithm then it will only be necessary to make a few measurements after launch to check the performance of the new sensor and then procede to the more protracted process of validation. In fact, we know that previous surface data sets used for instrument tuning have been deficient in all respects and we suspect that the current algorithms do not involve all of the required geophysical parameters. Therefore, a more substantial effort is required.

We must gather an initial set of high-quality surface data which is related in a well-understood manner to common standards and can provide an improved tuning of the sensor algorithms. A further independent data set will be required to demonstrate the validity of that improved tuning.

2. LEVELS OF SENSOR ALGORITHM TUNING

It is also valuable to define clearly the level of tuning and validation that is being sought. Three target levels can be envisaged:

a) to demonstrate that the proposed specification for the sensors has been met,

Proceedings of a Workshop on ERS-1 Wind and Wave Calibration, Schliersee, FRG, 2–6 June, 1986 (ESA SP-262, Sept. 1986)

b) while achieving a) to provide an improved surface data set which will enable the identification of missing parameters in the algorithms and tuning to a level better than that required to meet the specification,

c) to provide sufficient high quality surface data to permit a complete and rigorous definition of the physics relating wind velocity at 10 meters and wave-height to sensor outputs.

The target for ERS-1 calibration and validation is very definitely a). Adequate preparation to achieve a) may allow some progress towards target b). However, the achievement of target c) would probably require the collection of very long sets of high quality surface data, an activity beyond the scope of ERS-1 calibration and validation. Even so, it is worth bearing in mind that when c) is achieved we will be able to define the surface parameters in terms of satellite sensor outputs and be much less dependent on expensive surface-based measurements.

3. CLASSES OF DATA GATHERING AND USE AS INDICATED BY THE PROPOSED WORKING GROUP TITLES

The working groups identified for this workshop suggest the possibility of the following types of data contributing to ERS-1 calibration and validation:

a) the outputs from atmospheric and ocean models,

b) statistical analyses of routinely available data ,

c) data from existing platforms which may be specially prepared,

d) data from dedicated ERS-1 data gathering campaigns,

e) data from coincident campaigns designed to address other scientific problems.

Work at the UK-ERS-DC has so far concerned mainly activities of the type c) and d).

4. SOME PARTICULAR PROBLEMS

The following paragraphs will identify some of the problems to be addressed in gathering a suitable surface data set.

4.1 Quality of the Comparative Data Set

Data will probably be gathered wherever it is available but there are clear advantages in identifying a class of high quality data gathering facilities which can provide long series of satellite-coincident, co-located measurements made with the same set of calibrated instrumentation, at sites where a wide dynamic range of surface activity is likely to occur. The benefits of this approach are clearly illustrated by some work on SEASAT significant wave height validation (Ref.1). Specially processed data from the Ocean Station Papa waverider buoy and the standard output data from three NOAA buoys were compared with the SEASAT altimeter significant wave height measurements. Data collected at Ocean Station Papa shows near perfect agreement with SEASAT (an rms difference of 10cm), for one other buoy the agreement was also good (16cm rms), but data from the remaining two buoys showed distinct trends resulting in rms differences of 26 and 29cm. The comparison of the four separate data sets with SEASAT demonstrated that there were distinct error trends in the buoy calibrations. Fedor concluded that the altimeter provided significant wave height measurements that were more reliable than those obtained from routine buoy measurements and that in future the altimeter should be used to calibrate new or refurbished buoys.

It is suspected that a similar situation obtains for wind measurement. The problems of making wind measurements from all types of platforms are well documented (Ref.3) and it is clear that none are perfect. Data from ships is corrupted by effects due to the ship's superstructure which change as the ship's direction with respect to the wind changes, mid-ocean towers and oil rigs with a complex structure have similar problems, data from buoys is corrupted by wave-induced motion and data measured on land is corrupted due to differences of surface height, roughness and temperature.

Smith et al and the Bedford Oceanographic Institute (Ref.4) have sought to deal with all of these difficulties by providing an exceptionally stable buoy 50km off the coast of Nova Scotia. It was used for a programme of measurements lasting about 21 months and collected what is possibly the best set of wind data in existence. As no such platform is likely to be available for the ERS-1 post-launch period, probably the best approach is to select a platform for which the problems seem to be tractable and to mount a performance definition study well before the ERS-1 launch. One candidate location for a "master station" might be the lighthouse on Monarch Islands off the west coast of South Uist. The building is about 20km from an airport 15km from the main island on the seaward edge of an islet which is nowhere greater than 18 metres in altitude. The constraints suggested for negligible wind measurement corruption, a height to fetch ratio of greater than 1:10 and an instrument to tower distance of more than twice the tower diameter, would be readily achievable. Measurements could be made at a range of altitudes and related to ocean surface measurements prior to ERS-1 launch. Some encouraging work of a similar nature has already been completed in this region (Ref.2). However, we must also remember that the highest data quality may not be required if we seek only to demonstrate that sensor specifications are met.

4.2 COINCIDENCE AND SAMPLING

Given that very accurate measurements of waves and winds can be made at a few "master station" locations there is a further requirement to relate that data set to measurements made at remote sites. This is necessary in order to provide a comparative surface data set sampled on the same spatial scale as ERS-1 measurements which contains sufficient co-located coincident measurements of very high wind and wave conditions. The best way to achieve this is by using airborne instruments which are first calibrated in the master station area and then deployed to regions where standard

meteorological information suggests that ERS-1 will observe high wind and wave conditions.
At an altitude of 10km most of the discomforts of the violent weather will be avoided and only photographic records will be seriously degraded. The microwave instruments required to measure significant wave height, directional ocean wave spectra and sea-surface wind to an accuracy greater than that required by the ERS-1 specification are for the most part available in Europe, but some of them have yet to be fully validated. Further airborne instrumentation is planned which will enable wind measurements to be made at 5 and 14 GHz and the measurement of sea-surface temperature using the same infra-red channels as are used in ATSR.

4.3 RANGE OF MEASUREMENT CONDITIONS

In general it is the high wind and wave states for which it is most difficult to collect sufficient comparative surface data. A data gathering programme should therefore be concentrated in an area where most opportunities for such measurements occur. This is a matter of both local climate and the closeness of sequential ERS-1 ground tracks. In both respects the North East Atlantic and Norwegian Sea are very suitable regions. The Antarctic oceans have frequent high sea states but ice-free ocean exists only to latitudes of about 60 degrees in winter and 70 degrees in summer. At these latitudes sequential ERS-1 tracks are widely spaced. Also, the selection of airports and logistic considerations in general are comparatively discouraging in the Antarctic region. In the Norwegian Sea region sequential ground tracks are sufficiently close that wind measurements will be collected at the same location by the altimeter and scatterometer within about 1.5 hrs. During periods when the area north of Spitsbergen is ice-free the same will be true there for significant wave height and wave spectra measurements. The closeness of tracks and the large selection of airports in Scotland, Iceland, Greenland, Spitsbergen and Norway. Will make this a very convenient area for European experimenters to work in.

5. ORBIT PHASE SELECTION

The need to prepare "master stations" on the ERS-1 ground track emphasises the importance of an early agreement on the location of three-day repeat ground tracks. Potential master station sites, laser station locations,the locations of existing fixed platforms and data coverage requirements should all be taken into account when selecting track locations. A decision should be made by the spring of 1987 in order that pre-launch studies can be properly planned. The other repeat cycles used should be multiples of three so that a subset of the new tracks coincide sufficiently well with the original tracks to allow continued use of the fixed calibrating instalations and altimeter transponders. The use of transponders with the altimeter shows promise of being an excellent technique for calibrating the altimeter range measurement and for making many oceanographic and seismic studies. Transponders need to be positioned within about 4 km of the satellite ground track. If many are deployed during the commissioning phase it would be desirable to be able to use them during later phases.
This sort of preparation and data gathering can ensure that the ERS-1 wind and wave products are validated and provide a set of facilities which could be used for the validation of lower priority products.

6. PREPARATIONS AT THE UK-ERS-DC

Within the UK-ERS-DC an activity has begun to identify the manner in which all of the UK products from ERS-1 will be calibrated and validated.

6.1 Global Databases

Databases containing details of all of the institutes and organisations likely to be involved in the activity, the major facilities available to support it and the major data gathering campaigns that might produce pertinent data are being produced and will be made available to the UK science community.

6.2 Orbit Phase Selection for Commissioning

A software package is being prepared which will support discussion on the selection of orbit phasing and the selection of a set of "prime" existing platforms. The package takes in information from the above databases, primarily locations of facilities. For each type of facility a rational for establishing a quality factor is provided which takes into account the closeness of the facility to an ERS-1 ground track. The proposed ERS-1 orbit is generated with a particular longitudinal phasing and these quality factors are applied to each available facility. An overall quality factor for that particular choice of phasing is calculated. The process is repeated with incremental changes of longitudinal phase so that overall "quality" can be plotted against longitudinal phase. For prefered values of longitudinal phase the orbit and facilities can be plotted onto a high resolution world map and printed versions produced which are about 1 metre wide as long as required and multi-coloured.

6.3 Preparation for UK Data Gathering and Processing Activities

Because of the quasi-operational objectives of the ERS-1 mission it will be necessary to determine the quality of the data being produced within three or four months of launch. This is a difficult and demanding tasks which will require very careful and thorough preparation.

As part of our preparations we will identify the preferred contribution that will be made by the UK to the calibration and validation of ERS-1 and those areas where there will be a need for international collaboration. On the basis of this information and the activities in 6.1 & 2 it will be possible to identify a set of instrumentation and data sources. Each source must then be defined with respect to data type, format, quantity, quality, supply route etc.

It is anticipated that the proposed surface data set will be used to identify a sub-set of colocated satellite data, that both sets of data will be collected and brought rapidly to the UK-ERS-DC where they will be tested for quality before being merged onto a single composite cal/val record. That record will be analysed very rapidly using algorithms which have been carefully prepared for the purpose. On the basis of that analysis a report will be issued relating the satellite data to coincident surface data and recommending any algorithm tuning that has been shown to be required. The composite satellite-surface data record would then be made available for more thorough scientific analysis by individual institutes.

It is appreciated that this aproach to data gathering and analysis is very different from that normally adopted in scientific studies, however it does have the following advantages:

> It leads to efficient use of the scientific manpower available. The restricted number of scientists available to work on ERS-1 data will be a major limitation on our ability to benefit from the satellite.
>
> A complete set of satellite and surface validation data is available in a single convenient data package.
>
> Several institutes may work on a single data set during the same period.
>
> Each institute has easy access to the whole data set.
>
> Multiple cross-checking is simplified.
>
> Multi-instrument studies of complex regions are more convenient.
>
> Smaller groups and institutes can more readilly contribute to the data analysis.
>
> The discipline required to generate the centralised algorithms will encourage an adequate preparedness of all the groups involved to process the data in the short time allowed.
>
> There will be an automatic, central check on preparedness and central responsibility for producing the output statement of satellite data product quality to schedule.

There will be a need to demonstrate the capability to merge the two types of data and produce a satisfactory output with the appropriate speed. It is clearly difficult to do this completely without satellite data being available, however, it is suggested that most of the required capabilities can be demonstrated during pre-launch data gathering exercises by merging surface and aircraft data on the same time scale.

7. REFERENCES

1. Fedor L S and Brown G S 1982, Waveheight and windspeed measurements from the SEASAT radar altimeter, Journal of Geophysical Research, Vol 87 No. C5, April 30th 82.

2. Ewing J A 1980, Observations of wind-waves and swell at an exposed coastal location, Esturine and Coastal Marine Science, 1980, 10, 543-544.

3. Blanc T V 1983, A Practical Approach to Flux Measurements of Long Duration in the Marine Atmosphere Surface Layer, Journal of Climate and Applied Meteorology, Vol. 22, June 83, pp 1093-1110.

4. Smith D S 1980, Wind Stress and Heat Flux over the Ocean in Gale Force Winds, Journal of Physical Oceanography, Vol. 10, May 1980, pp 709-726.

VALIDATION OF WIND SPEED AND SIGNIFICANT WAVE HEIGHT FROM GEOSAT

J Wilkerson

National Environmental Satellite, Data, and Information Service, NOAA
Washington, D.C., U.S.A.

ABSTRACT/RESUME

Geosat ground tracks come within 150 km or less of NOAA moored buoys on the average of 25 times each 3 months. Of these, about 10 are within 50 km or less. If only ground tracks within 50 km of buoys are used for validation comparison, the network yields in one year about 1600 data pairs for wind speed and 1400 comparison pairs for wave height evaluation. These numbers increase to 4400 and 4000 if the range is extended to 150 km. Error budgets are estimated to account for uncertainties in both Geosat and in situ measurements due to time and space variability, instrument measurement accuracies, and averaging times for buoy measurements, particularly for winds. Processing of first year wind and wave retrievals from Geosat data will be completed in September with validation completed by the end of the year.
Keywords: Geosat, Wind Speed, Significant Wave Height, Validation Error Budget

1. INTRODUCTION

The National Oceanic and Atmospheric Administration (NOAA) will use wind and wave data from Geosat to increase significantly data currently needed for operational warnings and forecasts. At present these data, which are comprised of widely scattered reports from ships and buoys, total between 2000-4000 reports per day. Geosat will add 60,000 satellite-derived wind speed and wave height observations each day to this total. The availability of this additional data from Geosat will produce the following benefits for NOAA.

- Improved tropical and extra tropical storm analyses with increased warning time for hurricanes and winter storms.
- Improved initial surface analyses for regional, hemispheric, and global numerical models resulting in improved accuracies of weather forecasts out to 5 days.
- Provision of a coherent global data set of wind and wave data for improved seasonal and interannual variations for climate research.
- Provision of significant wind data to derive wind-driven currents within time frames needed to produce yield predictions for fisheries management and for increased fish catches.

In order to establish the measurement accuracies of the Geosat wind and wave observations, for the National Centers, Forecast Office and the Ocean Service Centers of NOAA, the National Environmental Satellite, Data, and Information Service (NESDIS) was tasked to conduct a validation of these measurements in parallel, and in cooperation with, the effort ongoing at the Naval Research Laboratory.

The NOAA-funded wind and waves validation effort is composed of the following:

- Comparison of near-simultaneous observations from Geosat with observations from 43 moored ocean buoys of NOAA's National Data Buoy Center (NDBC), to provide accuracy of measurement statistics. Included is the establishment of error bars associated with these statements of accuracy due to the uncertainties in the wind speed and wave height algorithms, the measured backscatter from the altimeter, the buoy wind and wave measure time and space variability of the wind and wave fields, and the statistical averaging.

2. WIND SPEED ALGORITHMS

The algorithms of Refs. 1-3 are being evaluated in this effort. The basis for wind speed estimates from satellite altimetry is that the measured average radar echo power backscattered from the sea surface ($\sigma°$) at nadir is proportional to surface roughness and therefore to surface wind speed.

The algorithm in Ref. 1 was developed using the GEOS-3 satellite radar altimeter data and 184 near-overflights of NOAA moored buoys. It encompasses a wind speed range of 1-18 m/s. During the Seasat post-mission evaluation, this algorithm was found to be flawed. Discontinuities in the slope of the model function produced a bimodel distribution of wind speeds, as shown in Figures 1 and 2.

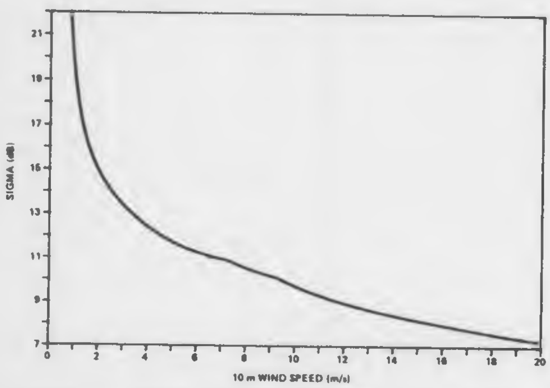

Figure 1. Wind speed model function of Ref. 1

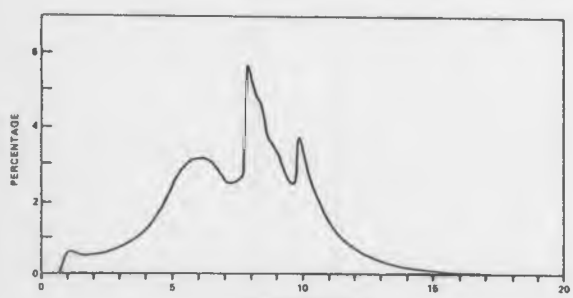

Figure 2. Histogram of wind speeds at 19.5 m height computed by Ref. 2 using wind speed algorithm of Ref. 1 and approximately 3 million values of σ^o obtained during the Seasat mission

Ref. 2 proposed an alternate model function derived from time and space averages of the Seasat Scatterometer off-nadir winds. Using spatial averages of 2° of latitude and 6° of longitude over the 96 days of Seasat, a model function was derived from the averages of σ^o from the Seasat altimeter and the Scatterometer off-nadir winds. The limitation of this model function is the accuracy of the Scatterometer wind speed estimates which have been shown to be deficient under certain conditions.

The Ref. 3 model function is simply a smoothed version of the three-branch algorithm of Ref. 1 derived from a best fit fifth order polynomial.

3. WAVE HEIGHT ALGORITHM

The technique of significant wave height determination from radar altimetry is based on the slope of the leading edge of the return waveform. The principal effect of ocean waves on the radar altimeter transmitted pulse is to stretch the leading edge of the return waveform. Hence the slope of the leading edge is inversely proportional to the height of the waves. The physical mechanism for this is illustrated in Figure 3.

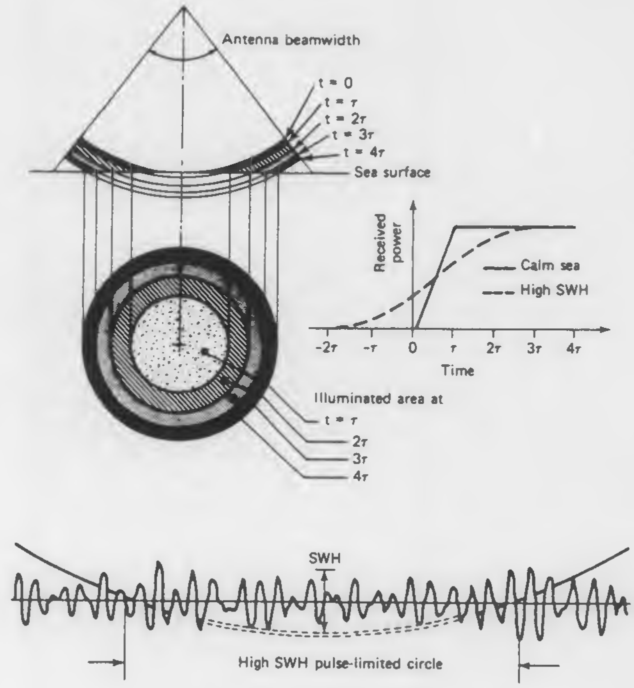

Figure 3. Pulse limited geometry

This algorithm together with the three wind speed algorithms mentioned above will be tested against wind and wave observations from the network of moored ocean buoys of the National Data Buoy Center (NDBC).

4. THE NDBC BUOY NETWORK

The 66 reporting stations in the NDBC buoy network cover the North Pacific, North Atlantic, Great Lakes, Gulf of Mexico, and Hawaiian Islands. Most are in coastal regions, but 16 are located in the open ocean. Because of land effects on coastal waters and the nature of the wind fields in coastal zones, coastal stations will not be used in the validation of Geosat. However, moored buoys in coastal regions and in the deep ocean constitute the majority of stations (43) in the network and will provide sufficient data for comparison over the full range of wind speeds and wave heights.

All buoys in the network measure wind speed and direction, atmospheric pressure, air temperature, and sea surface temperature each hour. A subset of these buoys also makes hourly measurements of significant wave height, significant wave period and in some cases wave spectra. However, within the hour, the times of measurement and the periods of integration differ for these measurements. For coastal and deep ocean buoys, the wave data are acquired at 29 min. after the hour for a period of 20 min. Winds are averaged for 8.5 min. starting at 40 min. after the hour.

Since the overflight of Geosat rarely coincides with either the buoy measurement times or their locations, there almost always exist temporal and spatial separations between paired Geosat and buoy measurements. Because buoys report every hour, time separations are never greater than 30 minutes. As for spatial separations, the validation strategy limits these to a maximum of 150 km. Typical histograms of these time and space separations for winds at a given buoy over a 3-month period are shown in Figures 4 and 5. Figure 6 shows the typical pattern of ground tracks laid down by Geosat within a 150 km radius of a buoy over that same time period. The magnitude of the uncertainties due to these temporal and spatial separations are discussed in Section 5.

As can be seen from the histograms of Figures 4 and 5, there are relatively few coincident satellite and buoy measurements over a 90-day period. Ideally, comparisons should be made using only those sets that are closest in time and space. The total number of Geosat passes within 150 km radius of buoy 44005 for the period April through June is 23. This number is typical for most buoys. Those located at higher latitudes in the Pacific have slightly larger numbers of intersections with the Geosat ground track. Buoys in the Gulf of Mexico somewhat fewer. Quarterly and yearly summaries of the total number of potential wind and wave comparison data sets for all locations in the network are shown in Tables 1 and 2. If only comparison data within 50 km of the Geosat observations are used, the total number of wind observation pairs available for performance evaluation is about 1600 for the year. If all observations within 150 km of each buoy are used then the total increases to about 4400. Assuming some reduction in these numbers due to the editing of questionable data, the total sample size for the year, none the less, will be large enough for completing the evaluation.

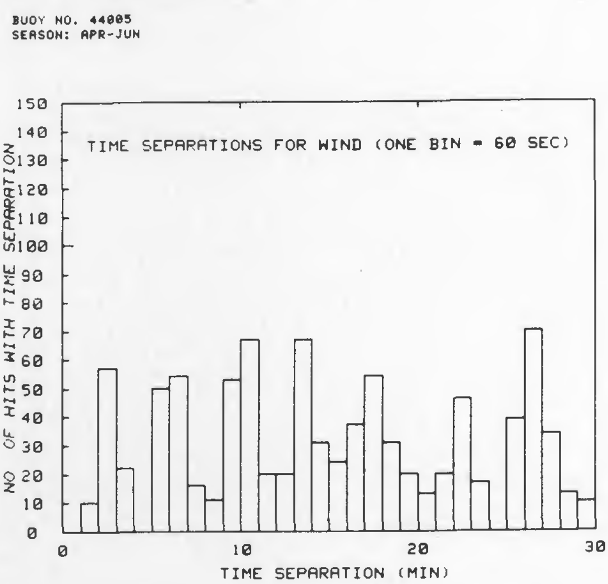

Figure 4. Histogram of wind hits as a function of time separation at a given buoy when paired with Geosat observations

5. ERROR BUDGETS

Since the Geosat and buoy measurements are not coincident, it is necessary to estimate the expected differences in the two measurements due to temporal and spatial variability in the wind fields over the ocean. There are also other uncertainties that will contribute to the error budget of the comparisons. One is related to the time vs space averaging. The buoy measurement is a time series average of 8.5 min. at a point,

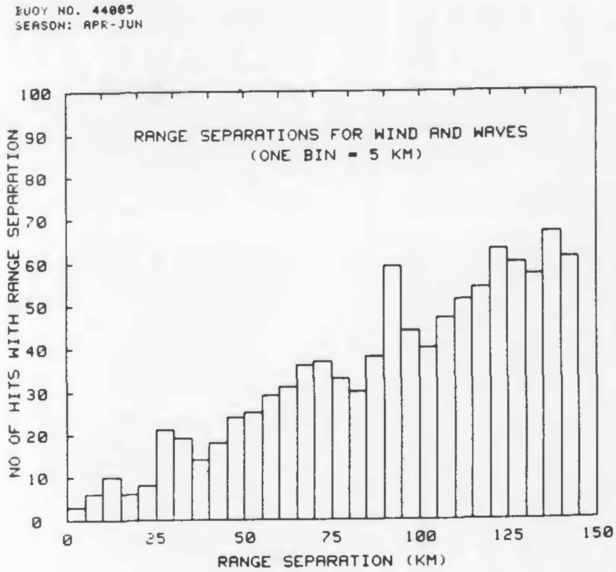

Figure 5. Histogram of wind and wave hits as a function of range separation at the buoy in Figure 4 when paired with Geosat observations

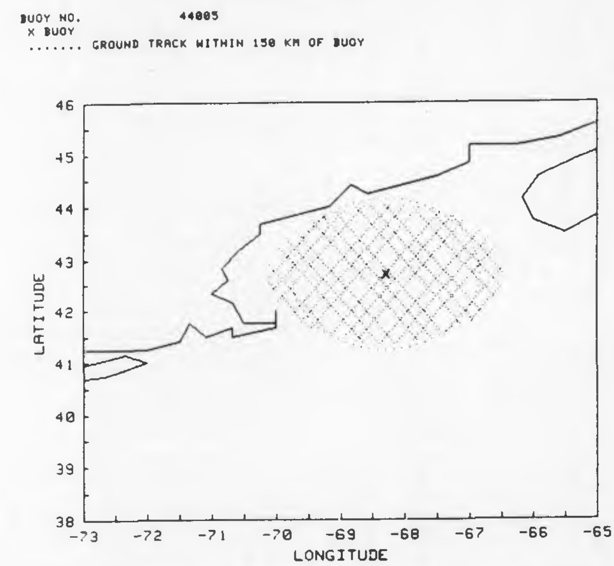

Figure 6. Typical pattern of ground tracks for Geosat within 150 km radius for the same buoy and time period shown in Figures 4 and 5

while the altimeter estimate is an area integration over an instant of time. Since several altimeter footprints must be averaged to get a stable estimate of the radar backscatter cross section, the spatial extent of the altimeter footprint is mesoscale. Therefore, the 8.5 min. average from the buoy is insufficiently long to filter out the variability at this scale and an uncertainty is introduced because the quantities are not equivalent.

Other contributions to the error budget come from uncertainties in the measurement of the buoy due to its calibration and to physical effects of the measurement such as buoy motion. Likewise, uncertainties exist in the altimeter measurement that relate to the radar cross section accuracy obtainable from the instrument and from the wind speed algorithm itself.

Table 1. Total All Buoys, Wind Data, April - June

Region	No. of Buoys/ Platforms	Points of Closest Approach <150 km	Points of Closest Approach <50 km
N. Pacific	19	515	178
N. Atlantic	10	250	87
Gt. Lakes	7	192	72
Gulf of Mex.	6	139	48
Hawaiian Islands	1	53	17
Totals (3 mos.)	43	1149	401
Totals (1 yr. projected)	43	4436	1604

Table 2. Total All Buoys, Wave Data, April - June

Region	No. of Buoys/ Platforms	Points of Closest Approach <150 km	Points of Closest Approach <50 km
N. Pacific	19	515	178
N. Atlantic	8	142	69
Gt. Lakes	7	192	72
Gulf of Mex.	6	139	48
Totals (3 mos.)	40	988	367
Totals (1 yr. projected)	40	3952	1468

In order to understand the results of the comparisons of the buoy and altimeter measurements, it will be necessary to estimate the magnitudes of these uncertainties and account for them in the validation process.

5.1 Temporal variability

Because the buoy reports hourly, time separation between measurements of the buoy and altimeter will never be greater than 30 minutes. To estimate the uncertainty due to changes in the averages of the wind with time, an analysis was performed on the hourly time series of buoy measurements to produce the expected wind speed difference as a function of time separation.

The result is shown in Figure 7. As can be seen, the difference for separations of up to 30 min is about 0.4 m/s.

5.2 Spatial variability

To estimate the effect of spatial separations between measurements of wind speed, Seasat altimeter wind speed data for days 263-271 were analyzed. The expected difference in wind speed as a function of separation distance to 150 km is shown in Figure 8. These results show that differences of 1 m/s and greater can be expected for separation distances greater than about 40 km.

5.3 Time vs. Area Averaging

Because the altimeter measurement will be an average over a number of individual resolution cells, the effective footprint will have an along-track dimension of about 50 km. The equivalent time series measurement for moderate to low winds for this area average should be 60 min. or more. Since the buoy average is only 8.5 min., the uncertainty due to this mismatch must be estimated. The difference to be expected may be characterized by the standard deviation of the 8.5 min. average relative to a 60 min. synoptic scale average. Ref. 4 has calculated theoretical values of standard deviations of differences between mean wind speeds for various averaging times relative to a 60 min. average as a function of stability and wind speed at 10 m. His calculations show that for a mean wind of 10 m/s, standard deviations between 0.42-0.57 m/s can be expected for an 8.5 min. average relative to a 60 min. average over the range of stable to unstable conditions.

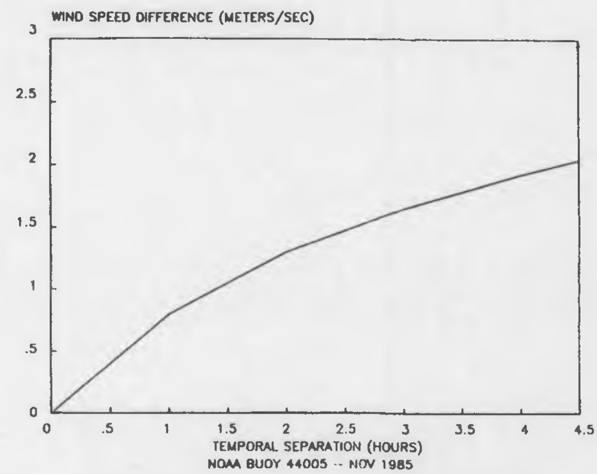

Figure 7. Expected wind speed differences as a function of time separations

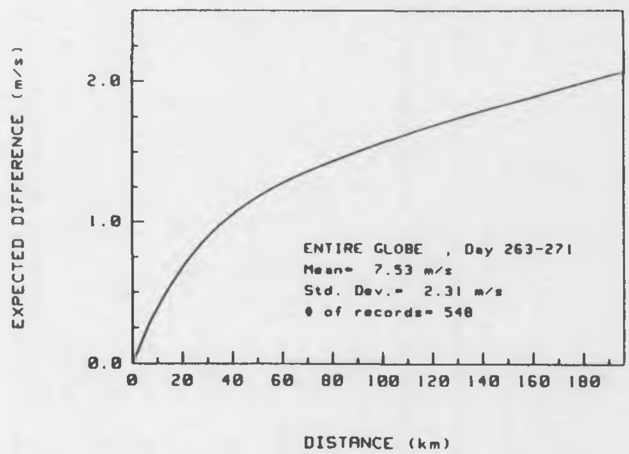

Figure 8. Expected wind speed difference as a function of separation distance to 150 km

5.4 Buoy measurement errors

The uncertainties in the buoy measurement of the wind are related to the instrument calibration, the effects of buoy motion, and the processing and transmission of the recorded data to shore.

Ref. 5 states that NDBC calibrates each anemometer before deployment by obtaining outputs at 15 wind speeds ranging from 2 to 60 m/s. The relationship between these outputs is linear and a calibration coefficient for the slope is determined. Speeds are then calculated using this slope and compared to measured speeds. If the measured speed differs from the computed speed by more than 0.5 m/s or 5%, the anemometer is rejected. Typical calibration errors for five anemometers are shown in Table 3. The data show that calibration errors in wind speed are of the order of 0.25 m/s.

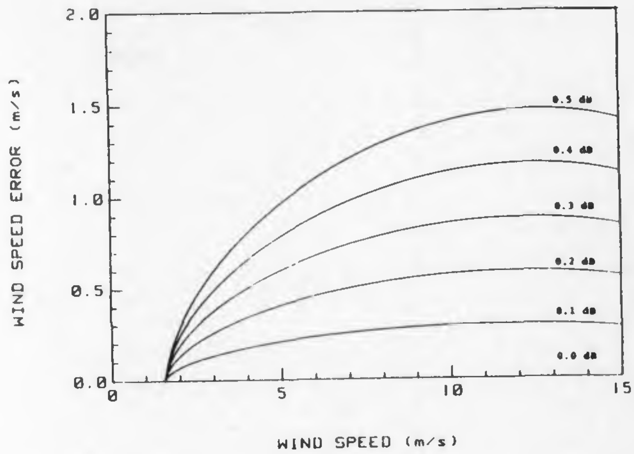

Figure 9. Uncertainty in altimeter measurement of wind speed expressed in terms of ^{o} accuracy measurements

Table 3. Wind Speed Errors for Five Anemometers as Determined by Calibration Before and After Deployment.*

Anemometer Serial No.	Before Deployment XBAR	Before Deployment SD	After Deployment XBAR	After Deployment SD
054	0.38	0.11	0.14	0.20
035	-0.02	0.24	-0.08	0.13
016	0.04	0.25	0.35	0.52
082	0.05	0.20	-0.03	0.27
069	-0.22	0.36	0.08	0.21
Overall	0.05	0.23	0.09	0.27

*The mean errors, XBAR, and the standard deviations, SD, are given in meters/second.

With regard to buoy motion, average pitch responses have been calculated for each buoy to estimate its effect. All hull types were found to have similar pitch responses and model runs show that pitch angles remain below 10 degrees for significant wave heights under 11 meters. Studies cited by Ref. 5 have shown that pitch angles of up to 10 degrees produce negligible effects on the measurement of the wind.

The NDBC-published overall system accuracy figures for buoy measured winds is $\pm$ 1.0 m/s or 10% in speed. In actual practice, however, every attempt is made to insure accuracies of $\pm$ 0.5 m/s or 5%. The true system accuracy lies somewhere in between.

5.5 Altimeter measurement errors

The uncertainty in the altimeter measurement of the wind speed is determined by the accuracy to which σ° can be measured and to the validity of the model function relating σ° to wind speed. The radar backscatter cross section measurements from the Geosat altimeter can be made to within 0.5db. A 0.5db uncertainty in the determination of σ° translates to an uncertainty of 1.2 m/s in wind speed at 7 m/s. At higher wind speeds the error reaches 1.5 m/s. See Figure 9.

The uncertainty in the model function remains to be estimated. Since its derivation was based on backscatter cross sections from GEOS-3 and measurements of wind speed from data buoys where separations of up to 110 km in distance and 1.5 hours in time were accepted, there is a significant but unknown uncertainty in retrievals associated with it.

5.6 Measurement Errors for Winds

Table 4 summarizes the expected difference in buoy and altimeter measured winds. For the worst case, the combined errors in measurement can amount to 1.8 m/s. The total uncertainty in comparison differences, when the effects of the model function are included probably exceeds 2 m/s. This is the accuracy specification of the wind speed to be verified.

Similar errors exist for the differences in significant wave height comparison. These estimates are currently being derived.

Table 4. Expected Differences in Buoy and Altimeter Measured Winds (m/s)

Non-altimeter	High	Low
Temporal Proximity	0.4	0.2
Spatial Proximity	0.9	0.5
Point/Area Averaging	0.4	0.4
Buoy Accuracy	0.7	0.5
Subtotal	1.3	0.8
Altimeter		
Cross Section Accuracy	1.2	0.8
Algorithm	?	?
Subtotal	1.2	0.8
Total	1.8	1.1

6. RESULTS

The processing of Geosat data for the wind speed and wave height retrievals is ongoing under a classified military program. Unfortunately, clearance from the Department of Defense for release of the analysis results of this NOAA program could not be obtained in time for inclusion in this report. When release is obtained, the author will make results available to interested workshop members.

7. CONCLUSIONS

The validation of wind speed and wave height measurements from Geosat, using the moored buoy network of the NDBC, provides a unique opportunity to study the problems to be faced in validating the wind and wave data from ERS-1. The errors introduced by temporal and spatial variability and uncertainties in the in situ measurements used for comparison need to be systematically examined and better understood. The illustrations of time and spatial variability presented here are preliminary estimates derived from selected data that may not be totally representative, but none the less these examples indicate the levels of error to be expected. The work of Ref. 6 will add considerably to the understanding of this problem.

The processing of one year of Geophysical Data Records (GDR) from Geosat for the wind and wave retrievals for this analysis will be finished in September. The validation of data for this period will be completed by the end of the year.

The processing of GDRs for analysis under the NOAA program will continue through the first year of the extended mission. At that time, sufficient numbers of stable cross section measurements with negligible time and space separations will be available for use in deriving an improved model function.

8. REFERENCES

1. Brown G 1979, Estimation of surface wind speeds using satellite-borne radar measurements at normal incidence, J Geophys Res 84(88), 3974-3978.

2. Chelton D & McCabe P 1985, A review of satellite altimeter measurement of sea surface wind speed: with a proposed new algorithm, J Geophys Res 90(C3), 4707-4720.

3. Goldhirsh J & Dobson E 1985, A recommended algorithm for the determination of ocean surfaces wind speed using a satellite-borne radar altimeter, John Hopkins University Applied Physics Laboratory SIR-85-U005, 23 pp.

4. Pierson W 1983, The measurement of the synoptic scale wind over the ocean, J Geophys Res 88(C3), 1663-1708.

5. Gillhausen D 1986, An accuracy statement for meteorological measurements obtained from NDBC moored buoys, Proceedings Marine Data Systems Symposium, New Orleans, La., 198-204.

6. Esraty R, Queffeulou P & Champagne M 1985, The Toscane-T campaign illustration of wind field time and space statistics, pub Institut Francais de Recherche pour l'Exploitation de la Mar, Centre de Brest, 3 pp.

REQUIREMENTS AND CONSTRAINTS IN THE CALIBRATION AND VALIDATION OF ERS-1 WIND AND WAVE PARAMETERS

T H Guymer

Institute of Oceanographic Sciences,
Wormley, Godalming, Surrey, U.K.

ABSTRACT

Some of the issues relating to the calibration and validation of ERS-1 wind and wave parameters are discussed using the experience of other oceanographic satellite missions and material from earlier papers in these proceedings is incorporated where appropriate. Major limitations of past efforts appear to be: the limited number of comparisons with near-coincident in-situ platforms, the small dynamic ranges encountered, and the introduction of regional biases by calibrations that were heavily weighted to mid-latitude , summertime conditions. On the basis of a preliminary study of climatological statistics suitable locations for measuring high wind and wave conditions are suggested.

Keywords: calibration, in-situ, wind speed, significant waveheight, climatology, ERS-1

1. INTRODUCTION

The majority of the wind and wave parameters to be extracted from ERS-1 data rely on a high degree of empiricism in the geophysical model functions used. This arises in part from the lack of a complete understanding of the interaction of microwave radiation with a roughened sea surface and with the intervening atmosphere. Another reason, which has plagued previous satellite remote sensing sensors, is poor pre-flight calibration and unexplained shifts and biases in the sensor data itself. Examples of this are the change in brightness temperatures of the 18Ghz channel of the Seasat Scanning Multichannel Microwave Radiometer (SMMR), more widespread problems with the NIMBUS-7 SMMR, and the apparent 1.6 dB discrepancy in Seasat altimeter σ^o's. Only significant waveheight can be obtained without external calibration and as such is the best understood and best validated measurement that microwave remote sensing can provide at present. For the rest careful calibration of sensor outputs against high-quality conventional data is required.

Once calibrated values are available there is a need to evaluate the accuracy and usefulness of the resulting data. For this purpose an in-situ comparison data set independent of that used for calibration is required.The main difference is that ancillary measurements of quantities involved in the retrieval algorithms e.g. sea-state dependence of σ^o , may not be needed. Since potential end users may have no knowledge or interest in what the satellite sensor is actually measuring it is important that, in the course of validation the satellite-derived geophysical parameter is related to measurements that are readily understood by him e.g. Waverider determinations of Hs, even if, in a fundamental sense this is not the most meaningful method of validating the measurement.
There are several lessons to be drawn together from the calibration and validation aspects of other satellite missions and a preliminary attempt is given here in the context of the particular requirements and constraints of ERS-1. Of particular importance is the climatology of winds and waves. Taken together consideration of these elements provides a basis for a coherent calibration/validation programme.

2. PARAMETER CHARACTERISTICS

The primary wind and wave parameters requiring calibration/validation are the equivalent neutral stability wind vector at 10m, V_{n10}, significant waveheight, H_s, defined as $4\sqrt{m_0}$ (m_0 being the variance of the sea surface elevation) and the directional wave spectrum. V_{n10} has been selected because 10m height is between the levels at which most buoy and ship anemometers are situated and is also the height recommended as a standard in a recent WMO report(Dobson, ref. 1). Neutral stability is assumed since there is no way at present of determining the near surface temperature profile from space. Therefore all in-situ measurements of wind must be corrected for height and stability which will require a knowledge of sensor height and air and SST (for the highest accuracy the relative humidity of the air is also needed). A common, agreed scheme for this height correction should be adopted to avoid biases between comparisons.

Specifications for the accuracy of the above parameters have been drawn up by ESA for Fast Delivery (FD) products only (see Table 1). Also shown are the dynamic ranges over which these specifications must be met. Generally, the figures are similar to those proposed for Seasat and reflect the requirements of operational users (e.g. meteorological forecasting agencies). They are also similar to the accuracies achieved in validation of Seasat. However, there is an important section of the user community which will use Off-Line Precision products which are to be processed by national resources coordinated by ESA. In some cases the requirement is for spatial and temporal means, which allow random errors to be significantly reduced. However, stringent demands for absolute accuracy highlight the need for systematic errors to be kept smaller than for FD products. As a particular example we can cite that of winds for climate research. In order to achieve a goal of 0.01 Nm^{-2} error in surface stress, averaged over 1 month and 500km x 500km, wind speeds need to be accurate to ±0.5 ms^{-1} and $\pm5^o$ at 10 ms^{-1}. The calibration/validation of values obtained from individual footprints should therefore be consistent with these higher-level requirements.

These considerations have implications for the accuracy of in-situ measurements. It is desirable that data to be used for comparisons should have errors which are significantly smaller than the target accuracies of the satellite sensors. Thus for FD products in-situ wind speeds should be made to better than 1.0 ms^{-1} (which would contribute ~15% of the total uncertainty).

3. LESSONS FROM OTHER SATELLITE MISSIONS

3.1 Brief review of GEOS-3 and Seasat

In a comparison of GEOS-3 waveheights with conventional data the standard deviation of the differences was within 0.75m for H_S<4.0m and within 0.50m for 4.1<H_S<8.0m (Fedor et al.,ref 2). The wind speed algorithm required substantial modification to bring agreement within specification and since the limited in-situ data were used in the tuning process no independent validation was possible. Several evaluations of wind and wave algorithms used for routine production of Seasat altimeter data have been made. For H_S Webb (ref. 3) compared estimates with pitch-roll buoy measurements in the JASIN experiment and found a slight underestimate of 0.04±0.12 m on the eight occasions. The variance in nearly all of the cases was consistent with spatial variations in the wave field and other known sources of error. However, comparisons were limited by the small range of waveheights (0.8 to 2.3 m). Subsequently, Fedor and Brown (ref. 4) carried out a more comprehensive validation against NOAA buoys and a Waverider deployed at Ocean Weather Station P giving a total of 51 comparisons. Overall, a mean difference (altimeter-buoy) of 0.07±0.29 m over the range 0.5<H_S<5.5 m was found. When the statistics were calculated separately for each platform some showed much poorer performance than others, with the Waverider showing best agreement (0.07±0.10 m, which is similar to the JASIN results).

For wind speed the GEOS-3 algorithm was applied after removal of an unexplained 1.6 dB discrepancy in σ^o between Seasat and GEOS-3 at near-coincidences of their footprints. Fedor & Brown (ref. 4) analysed 87 near-overpasses of 18 NOAA buoys and observed a mean difference of 0.25 ms^{-1} and a standard deviation of 1.58 ms^{-1}. However, the range of wind speeds in their study was restricted to 2-12 ms^{-1}. At higher winds it has been demonstrated that the algorithm underestimates significantly (Guymer et al.,ref. 5, Chelton & McCabe,ref. 6). Retrievals are particularly sensitive to errors in σ^o at winds greater than 10 ms^{-1} and this implies that effects of mispointing and atmospheric attenuation must be allowed for in the calibration of ERS-1 altimeter winds. When wind and wave data from the Geosat altimeter are available (Wilkerson, these proceedings), they may resolve some of the problems associated with high winds. It is also expected that validation of sea states with H_S > 8m will be possible.

Although wind algorithms proposed for the Seasat scatterometer at launch were based on extensive prelaunch campaigns it was still found necessary to modify these in the light of comparisons with measurements made in the Gulf Of Alaska Seasat Experiment (GOASEX). For independent evaluation appeal was made to ship and buoy winds obtained in the JASIN experiment. These had been carefully intercalibrated to produce a data set which was internally consistent to 0.7 ms^{-1} and 0.5^o. Two algorithms met the ±2 ms^{-1} and $\pm5^o$ specification over the range of 3-16 ms^- and for most incidence angles (Jones et al.,ref. 7). For production of the entire geophysical data set a new algorithm called SASS-1 was produced which brought slightly closer agreement with JASIN winds. One source of uncertainty, which is of general relevance, was the absolute accuracy of JASIN winds (Weller et al., ref. 8). There is no way of knowing which of the many sensors used was the most accurate. It is possible that buoy W2 which was used as the JASIN standard overestimated by 7% ,although there is some dispute about this. Even if true this does not imply that all the scatterometer wind speeds are also too high by this amount. A more serious drawback is that the data are heavily weighted to mid-latitudes and there is some evidence that tropical winds are biased, possibly because of SST effects on radar backscatter.

In their comprehensive review of SAR imagery of the ocean surface Vesecky & Stewart (ref. 9) reported that for wavelengths longer than 100m Seasat could measure dominant wavelength to ±12% and dominant direction to $\pm15^o$. However, ocean waves are not always visible in SAR images and when they travel approximately parallel to the satellite track they may suffer severe distortion. Thomas (ref. 10) used the variation of image intensity couples with dominant wavelength estimates and assumptions about the shape of the waves to estimate H_S from SAR; two comparisons with buoys were made and these exhibited agreement within 0.8 m. The number of directional wave measurements made during SEASAT was rather small but studies such as those of Beal et al. (ref. 11) suggest that the SAR is often capable of revealing spatial vatiations in wavenumber and direction which are qualitatively consistent with the history of weather systems responsible for the generation of the waves and also with hydrographic and bathymetric features.

3.2 Summary of lessons for ERS-1

Several points emerge from the above (and other studies not cited):
(i) very few near overflights of in-situ platforms occur unless they are specifically dedicated to satellite calibration. Use of non-coincident data would increase the size of the comparison data base.
(ii) the location and duration of the Seasat comparison measurements severely limited the range of wind and wave conditions sampled. Stormier conditions could only have been obtained in the southern hemisphere at that time of year. Preferred locations for calibration campaigns should be assessed in relation to the wind and wave climatology.
(iii)the altimeter and scatterometer wind algorithms are based almost entirely on calibration against mid-latitude surface measurements. This leads to biases in the retrievals for other regions due most probably to incomplete modelling of all the parameters affecting radar backscatter,e.g. SST.
(iv) the accuracy of the altimeter σ^0 measurements is questionable and the correction scheme adopted for Seasat is strictly valid over only a part of the range of interest. In GOASEX biases between scatterometer antennae were discovered. Engineering calibration should receive careful attention in the ERS-1 commissioning phase but it is possible that some discrepancies will emerge only as a result of geophysical validation.
(v) the latest altimeter wind algorithm ignores the dependence of σ^0 at nadir on the mean square slope of the surface.
(vi) rain can distort comparisons and such occasions need to be identified and eliminated from calibrations. In general attenuation will result leading to an underestimate in scatterometer winds and an overestimate for the altimeter. Under some circumstances precipitation increases the backscatter.
(vii) proper comparison requires averaging of satellite and in-situ data. The appropriate periods and areas for this depend ,in part, on the characteristic time and space scales of wind and wave fields.
(viii) some of the scatter in comparisons is due to errors in the in-situ data. Problems were observed in the calibration of wind and wave sensors and on ships flow distortion can be very troublesome unless care is taken (Taylor, these proceedings).

Sections 4 and 5 consider two of the above issues in more detail.

4. SPATIAL AND TEMPORAL VARIABLITY

Satellites and in-situ instruments provide very different views of the sea-surface. The latter provide time series at a point which can be averaged over appropriate periods while the former give spatial averages (for an altimeter over a few tens of km^2, for a scatterometer a few thousands of km^2) which, because of the high spacecraft velocity, are essentially snapshots. It then becomes necessary to determine the appropriate averaging of both data sets to achieve the most meaningful comparisons. For the scatterometer in-situ winds were averaged over 1 h to be compatible with the ~50km length scale of the footprint. It is not clear what averaging Fedor and Brown used in their altimeter winds comparisons. Such temporal averaging assumes Taylor's hypothesis and neglects any cross-flow variations which will affect an areal mean but not that calculated from a fixed platform. For waveheight, Fedor and Brown averaged 50 km sections of altimeter data and Webb adopted 150 km. These are much longer scales than would be implied by group velocity considerations.
The space-time variability also implies that non-coincidence of satellite and surface measurements may lead to scatter in comparisons, the magnitude of which will depend on the degree of inhomogeneity in the wind and wave fields. In general, imposing a condition of exact coincidence is unrealistic because it gives too small a data set; this is particularly severe for altimeter estimates where the footprint is small. Webb allowed separations up to 170 km while Fedor and Brown employed a tolerance of 80 km and 1$^1/_2$ h. The question of how large a separation in time and space can be allowed for useful comparisons still to be made has been addressed by Challenor et al. (these proceedings). Their preliminary analyses, which are restricted to the N.E. Atlantic, indicate that for both waveheight and windspeed there are two correlation scales. The larger one is associated with the passage of atmospheric depressions (days,hundreds of km) and superimposed on this is high frequency variability which suggests that unless measurements are made within $^1/_4$ h and 10 km of the satellite overpass statistical techniques will have to be employed to eliminate the additional uncertainties. If these effects are not truly random (e.g. bathymetric effects on waveheight) then the problem becomes even more difficult. Fig. 1 summarises some analyses of H_S changes as suggested by Challenor et al. For intervals longer than 7 $^1/_2$ h H_S changes exceed 0.5 m for more than 50% of the time; most of the variation is contained within the first few hours. Thus, increasing the space-time windows will increase the size of the comparison data set

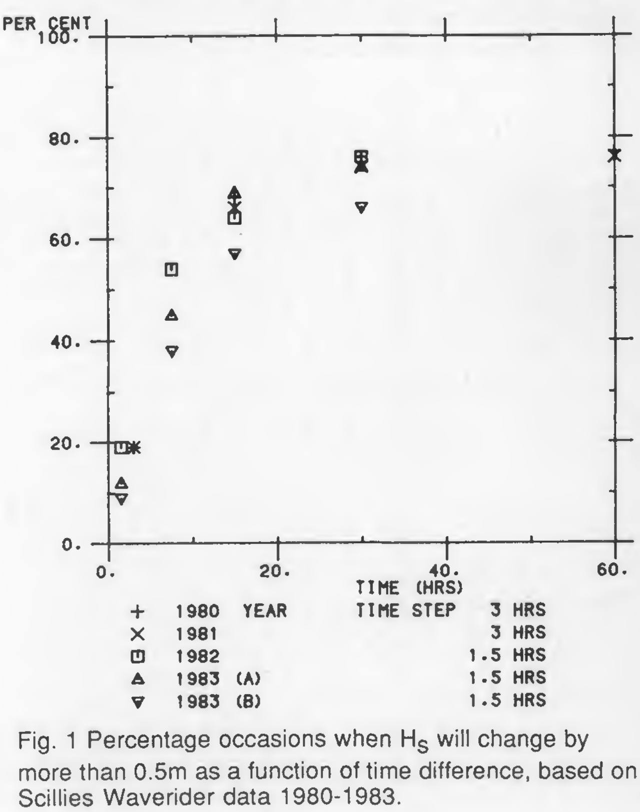

Fig. 1 Percentage occasions when H_S will change by more than 0.5m as a function of time difference, based on Scillies Waverider data 1980-1983.

but will result in significantly increased scatter, which may be difficult to interpret.

5. LOCATION AND TIMING

The range of conditions which can be sampled during the ERS-1 calibration/validation phase will depend on geographical location, time of year and the duration of any in-situ measurement campaign. A survey of conditions in the Atlantic and Pacific Oceans has been conducted for the months of January, April, July and October using the U.S. Navy Climatic Atlas of the World. Waveheights are based on visual estimates of sea-state. Here only the results for the North Atlantic are shown,The main conclusions were:
(i) most of the observations are made in mid-latitudes in the N. Hemisphere, with the highest concentration along major shipping routes (Fig. 2). In the Southern Hemisphere south of 50°S the data in winter are very sparse indeed.

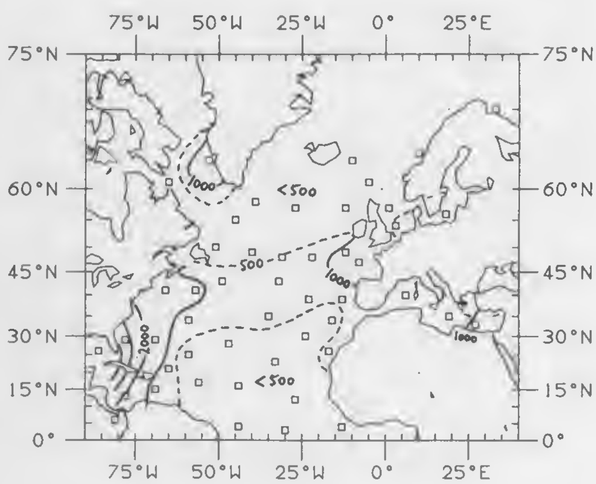

Fig. 2 No. of January wind observations per 1° box used to compile U.S. Navy Climatic Atlas. Boxes used denoted by squares.

(ii)The windiest and roughest areas lie in latitudes 40-60° during winter, with little difference between the hemispheres or oceans either in terms of mean wind speed, % frequency of gales or frequency of H_S>6m (Figs. 3-5). A different picture emerges in summer, however, for there is much less seasonal variation at mid-latitudes in the Southern Ocean and winds are significantly stronger than in the N. Hemisphere for the same season (Fig. 6). Thus, <u>for a calibration phase near January the northern N. Atlantic should provide a sufficient number of high-wind and high-wave occasions. If it were to be held in July a southern hemisphere site would be needed.</u>

(iii)As well as locating in-situ measurements in stormy regions some will need to be placed in areas of more moderate conditions. Of these the statistics show that there is a wide variation in the frequency with which light winds (<7kt) are observed and this may influence the choice of site. Given similar mean speeds a site which

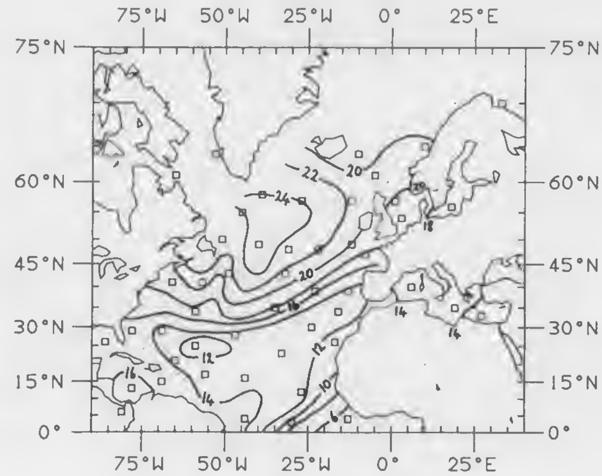

Fig. 3 Mean wind speed distribution in January (kt).

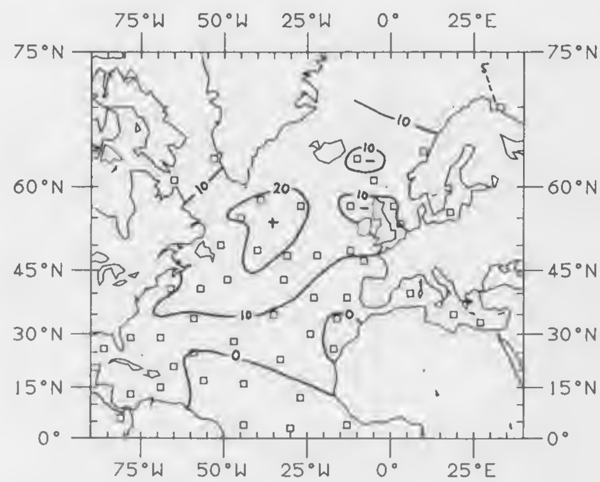

Fig. 4 Percentage occasions with wind speed > 34kt (Beaufort Force 8), January.

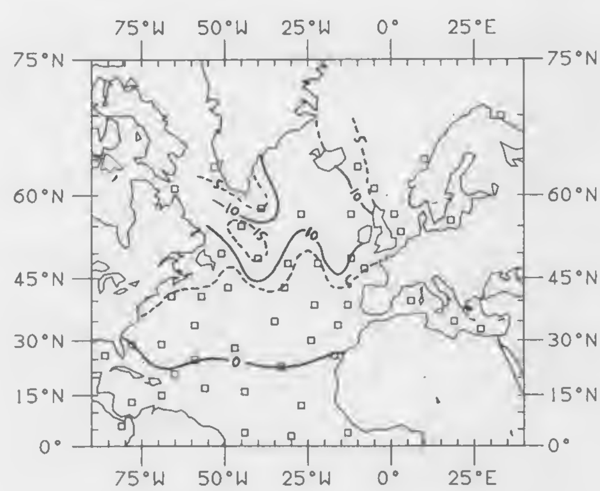

Fig. 5 Percentage occasions with H_S > 6m.

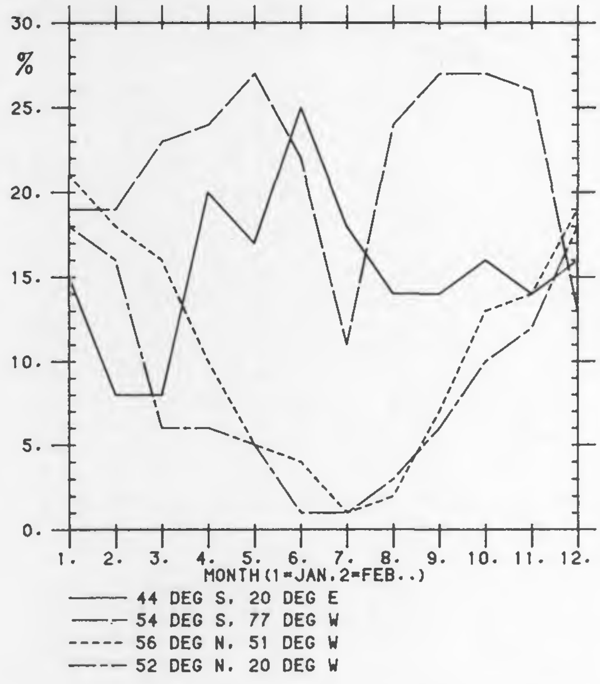

Fig. 6 Seasonal variation of percentage occurrence of winds > 34kt for selected Northern and Southern Hemisphere sites.

has steady moderate winds may be preferable to one which has a high percentage of light winds. The Atlantic is more likely to have light winds in winter than the Pacific. Apart from the tropics eastern sides of basins are more likely to have light winds. In summer the frequency of light winds is higher than winter nearly everywhere and there is more zonal banding in the distribution due to the effect of the sub-tropical highs (light winds) and the slightly increased strength of the Trades. In some cases the summer Trades produce the strongest winds within a basin e.g. the Caribbean. Thus, for a summertime calibration, latitudes 30-40^{o} should be avoided; 10-20^{o} would however be suitable. In winter, eastern portions of oceans should be avoided. At all times $\pm$ 10^{o} of the equator is unreliable.

It is apparent that the areas of strongest winds and highest waves are not the most densely observed. As well as casting some doubt on the statistics it also implies that during the commissioning phase there may be insufficient, routinely-observed high wind data. This is particularly true of the Southern Hemisphere. Consideration should be given to increasing the number of ships which make meteorological reports along ship-tracks in "stormy" areas. These could also be priority areas for measurement campaigns dedicated to ERS-1. A particular source of concern is that in the Southern Ocean the maximum winds are not far from the ice-edge, which probably explains the lack of data and which may create problems for special measurement programmes.

Some useful data to supplement these statistics may be obtainable from remotely-sensed winds, though only for a few years. The GEOS-3 altimeter provided wind speeds for 3$^{1}/_{2}$ years but not globally; the NIMBUS-7 SMMR has produced ~7 years of brightness temperatures from which wind speeds can be retrieved but there are calibration problems.

The previous discussion assumed that the only parameters affecting the choice of site and time are wind speed and waveheight. However, it is likely that the relationship of measured backscatter to wind is affected by SST and precipitation. It is therefore desirable that the intercomparisons cover a wide range of SST and that contamination by precipitation be kept to a minimum. (Precipitation at sea is difficult to estimate quantitatively; otherwise a correction scheme could be devised, based on the intercomparison data set. Some progress towards this may be made if ATSR/M liquid water estimates are of sufficient reliability).

SST decreases from a maximum near the equator towards the poles. In the N. Hemisphere there are pronounced east-west differences at latitudes greater than 20^{o}N with warmer water lying to the east. These gradients are much less marked in the S. Pacific and S. Atlantic. Within the high wind speed regions identified above there is only a small variation in SST, typically 5-12^{o}C. Measurements in the Trades, e.g. the Caribbean or the Mediterranean in summer would allow reasonably strong winds to be measured with SST >25^{o}C.

A preliminary analysis of precipitation statistics shows that mid-latitudes in winter and the Tropics throughout the year have the greatest chance of rainfall (~30%). The western North Atlantic is worse than the east and the Trades and Mediterranean have a low probability of rain. No analysis of precipitation intensity have been made and because heavy rain, to which the ERS-1 altimeter will be vulnerable, is of short duration the statistics may not give a reliable picture. Nevertheless, until a fuller study is made, these results should prove useful. A further complication is that in many regions rainfall and wind speed may be correlated so that the chances of obtaining winds >34kt with little or no rain may be extremely small.

On the basis of the wind ,SST and precipitation statistics examined certain locations suggest themselves as fulfilling many of the requirements, either individually or in combination. They are summarised in Table 2. Where there is little difference the Atlantic has been chosen in preference to the Pacific and the N. Hemisphere in preference to the southern, e.g. in winter the N. Atlantic is capable of providing as full a range of conditions as the other three basins.

6. ADDITIONAL COMMENTS

The calibration of Seasat data and their subsequent evaluation has taken several years. ERS-1 is a pre-operational satellite system and during its commissioning phase in-situ data will be required as rapidly as possible so that calibration and validation can be completed before routine processing and dissemination takes place. A potential source of delay is the time taken for in-situ data to be available. Data from oceanographic cruises are often not processed for several months, delays being due to shipment of data from ports-of-call, mooring recovery schedules and calibration and editing of data. Some wind and wave data are transmitted in near real-time from Voluntary Observing Ships via GTS but for the majority of cases access to ships' log-books is the only way of obtaining the data. The problem would be alleviated if automatic data transmission techniques were used and if relevant subsets of in-situ data could be processed (in full consultation with owners of data) and merged with the satellite data at a single data centre.

In addition to ERS-1 a U.S. satellite, NROSS, equipped with wind and wave sensors is planned to be launched. Depending on launch dates it may be possible to jointly calibrate both satellites thus making more efficient use of resources. Plans for the N-SCAT Data System, which will include validation, are described by Callahan & Benada (these proceedings).

The ERS-1 orbit pattern will exert a considerable constraint on the location of calibration campaigns. Although the repeat period for this phase has been decided (3 days) the longitudes of the tracks have not. Given that there are many competing demands and that compromises will be inevitable it is important that a proper study be made of tradeoffs involved. and that the tracks should be fixed within the next few months. Early knowledge of the location of ERS-1 ground tracks will provide adequate time for long-term facilities to be installed, will greatly facilitate the planning of surface data-gathering campaigns (such as those discussed by Powell, these proceedings). It will also allow prospective measurement sites to be studied with respect to possible data corruption and logistic support. For wind and wave calibration there may be some advantage in positioning tracks to be near a long-term wind/wave buoy (e.g. DB2). Fig. 7 shows tracks which do this and which would also provide altimeter tracks in the middle of the North Sea.

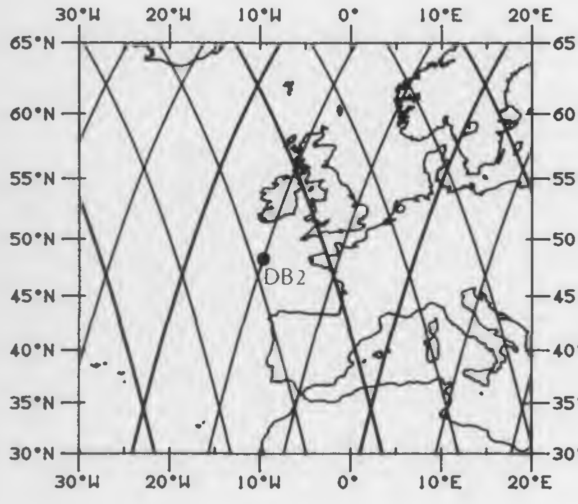

Fig. 7 ERS-1 sub-satellite tracks during the calibration phase (i.e. 3-day repeat) constrained to pass through the long-term wind-wave buoy DB2.

The coverage of the AMI wind and wave modes may be less satisfactory. Indeed, it is understood that, because of a requirement to operate the AMI imaging mode extensively over Europe in the commissioning phase, it may not be possible to operate the wind-scatterometer frequently in coastal areas. The use of routine measurements in coastal waters should not be neglected, however. For SIR-B IOS, acting as Principal Investigators, coordinated the operation and data gathering of a number of platforms in UK waters, including oil rigs and HF radar. Unfortunately the Shuttle radar malfunctioned but the in-situ programme was very successful. Finally, it should be noted that sites can be selected which are viewed by both the scatterometer and altimeter within a few hours of each other.This may help to ensure consistency between winds from the two sensors and also enable wave effects on wind retrievals to be studied.

ACKNOWLEDGEMENT

The support of the UK ERS-1 Product Support Team in part of this work is gratefully acknowledged.

Table 1 Fast Delivery Product specifications

PARAMETER	ACCURACY	RANGE
Wind speed	$\pm 2ms^{-1}$ or 10% (whichever greater)	$4\text{-}24ms^{-1}$
wind direction	$\pm 20^{\circ}$	$0\text{-}360^{\circ}$
H_S	±0.5m or 10% (whichever greater)	1-20m
wave direction	$\pm 15^{\circ}$	$0\text{-}360^{\circ}$
wavelength	±20%	50-1000m

Table 2 Wind/wave statistics at possible locations for cal/val

SITE	U(KT)	%<7KT	%>34KT	SST(^{O}C)	% PPN	% H_S>6M
JANUARY						
55-60N 20-30W	24	3	20	10	25	13
40-60S 20W	21	10	15	11	25	9
W.MED.	16	16	6	14	6	2
CARIBBEAN	18	1	2	27	4	0
JULY						
40-60S 10E	22	10	15	10	?	?
W.MED	10	40	1	23	2	0
CARIBBEAN	18	3	1	28	3	0

7. REFERENCES

1. Dobson F.W. 1983 Review of reference height for and averaging time of surface wind measurements at sea, Marine Meteorology and Related Oceanographic Activities Report No. 3, WMO, 50pp.

2. Fedor L.S., Godbey T.W., Gower J.F.R., Guptill R., Hayne G.S., Rufenach C.L. & Walsh E.J. 1979 Satellite altimeter measurements of sea-state - an algorithm comparison J. Geophys. Res., 84(B8), 3991-4002.

3. Webb D.J. 1981 A comparison of Seasat-1 altimeter measurements of waveheight with measurements made by a pitch-roll buoy, J.Geophys. Res., 86(C7), 6394-6398.

4. Fedor L.S. & Brown G.S. 1982 Waveheight and wind speed measurements from the Seasat radar altimeter J.Geophys. Res., 87(C5), 3254-3260.

5. Guymer T.H., Challenor P.G., Srokosz M.A., Rapley C.G., Queffeulou P., Carter D.J.T., Griffiths H.D., McIntyre N.F., Scott R.F. & Tabor A.R. 1985 Institute of Oceanographic Sciences Report No. 220., 268pp.

6. Chelton D.B. & McCabe P.J. 1985 A review of satellite altimeter measurements of sea surface wind speed with a proposed new algorithm, J. Geophys. Res., 90(C3),4707-4720.

7. Jones W.L., Schroeder L.C., Boggs D.H., Bracalente E.M., Brown R.A., Dome G.J., Pierson W.J. & Wentz F.J. 1982 The Seasat-A Satellite Scatterometer: the geophysical evaluation of remotely sensed wind vector over the ocean, J. Geophys. Res., 87(C5), 3297-3317.

8. Weller R.A., Large W.G., Payne R.E. & Zenk W. 1983 Wind measurements from oceanographic moorings, J. Geophys. Res., 88(C14), 9689-9705.

9.Vesecky J.F. & Stewart R.H. 1982 The observation of ocean surface phenomena using imagery from the Seasat synthetic aperture radar: an assessment, J Geophys. Res., 87(C5), 3397-3430.

10. Thomas M.H.B. 1982 The estimation of waveheight from digitally processed SAR imagery, International J. Rem. Sensing., 3, 63-68.

11. Beal R.C., Gerling T.W., Irvine D.E., Monaldo F.M. & Tilley D.G. 1986 Spatial variations of ocean wave directional spectra from the Seasat synthetic aperture radar, J. Geophys. Res., 91(C2), 2433-2449.

Session 2

CLASSICAL MEASUREMENTS

Chairman: W Rosenthal (GKSS)

EVALUATION OF THE DIFFERENT PARAMETERS IN LONG'S C-BAND MODEL

A Cavanié, J Demurger & P Lecomte

Antenne CREO, Centre IFREMER, B.P.337, BREST 29273 CEDEX

ABSTRACT

Because ERS-1 is yaw-steered :

1) In the space of σo values of the three, respectively forward, rear, and central, antennae (S1, S2, S3), the surface of solutions is symmetric with respect to the plan S1 = S2.

2) The ratios S1/S2 or S2/S1 reach two distinct maxima for a given wind speed. These remarks lead to two independent methods of calibration of parameters in the C-Band model, using only the wind speed furnished by meteorological fields.

Such methods could be applied to pretune the scatterometer in its first months of flight, investigate regional variations and monitor possible evolutions in the instrument's behaviour.

Keywords : ERS-1, AMI-Wind, Calibration, Scatterometer, Yaw-Steering.

1. INTRODUCTION

ESA-led C-band scatterometer measurements over the ocean (PROMESS, TOSCANE-T) have been analyzed and A. Long has presented a model for sigma-zero (here often designed by the letter "S") as a function of wind speed "V", wind direction relative to the beam direction "Φ" and incidence angle, "I", which is of the following form :

$$S = A\ (1 + B \cos \Phi + C \cos 2\Phi)$$

where A, B and C are wind speed and incidence angle dependent. A detailed description of these parameters is given in Ref. 1 ; we will only use the information that A varies roughly as the wind speed, and that B and C take values which vary between -0.1 and 0.6. (see figures 1.a, 1.b, 1.c, relative to Long's model). The objective of this paper is to evaluate how well A, B and C may be estimated using meteorological surface-wind fields jointly with ERS-1 scatterometer data.

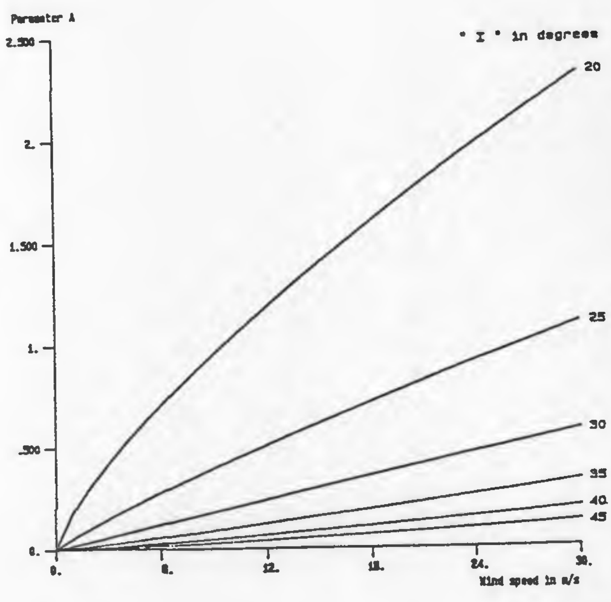

Figure 1.a

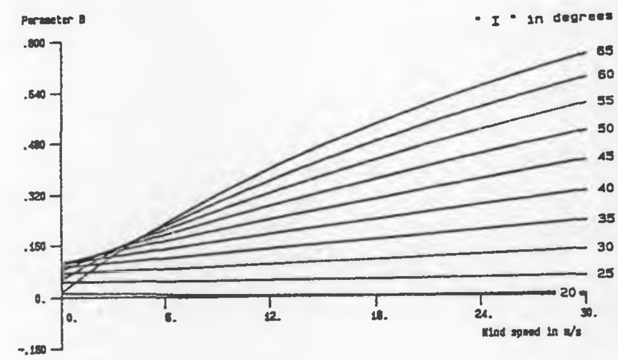

Figure 1.b

Proceedings of a Workshop on ERS-1 Wind and Wave Calibration, Schliersee, FRG, 2–6 June, 1986 (ESA SP-262, Sept. 1986)

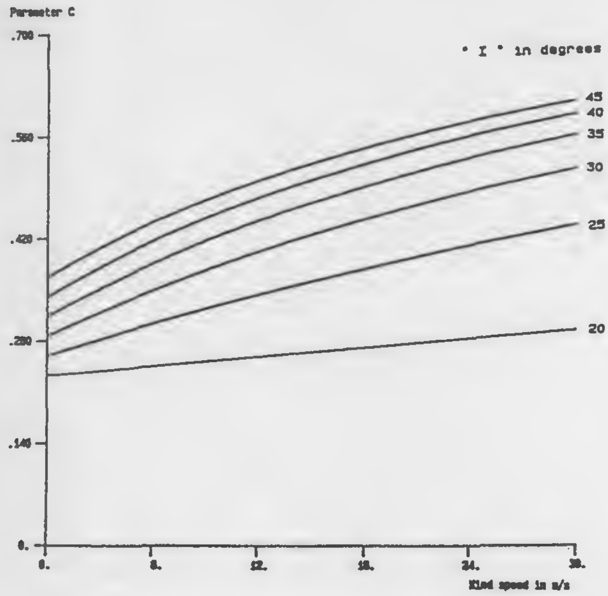

Figure 1.c

A crucial simplification in what follows is linked to the fact that ERS-1 is yaw-steered so that the forward and rear antenna beams, respectively pointed 45° and 135° to the right of the effective ground-track, observe a given point of the ocean at practically equal incidence angles. Figure 2 shows the absolute difference in angle between the two beams as a function of latitude of the satellite and distance from the satellite sub-track.

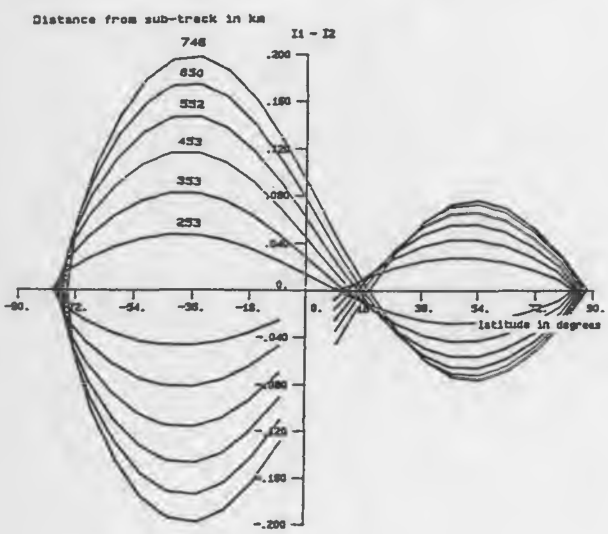

Figure 2.

These results were obtained using Klinkrad's program (Ref. 2) describing ERS-1's three-day orbit associated to a GEM6 geoid ; maximum absolute differences of 0.2° occur in the southern hemisphere at mid-latitudes, corresponding to a relative difference of about 0.003 in "I".

Substituting such a perturbation in Long's C-band model, should, and does, lead to differences in "S" which are negligeable.

The equation for the sigma-zero values of the forward, rear and central antennae (S1, S2 and S3, respectively) now take the form :

$$S1=A1\ [1+B1\ \cos(\Phi-45)+C1\ \cos2(\Phi-45)] \quad (1.a)$$
$$S2=A1\ [1+B1\ \cos(\Phi+45)+C2\ \cos2(\Phi+45)] \quad (1.b)$$
$$S3=A3\ [1+B3\ \cos(\Phi)+C3\ \cos(2\ \Phi)] \quad (1.c)$$

At a given position on the earth surface, these three equations determine a surface of solutions in the (S1, S2, S3) space, surface which is symmetric with respect to the plane : S1 = S2, and described by the two parameters (V, Φ).
The surface of solutions in S-space is described schematically in Figure 3. It varies of course with model parameters and therefore with geographical position of points considered : but since altitude variations of ERS-1 are not large, the general representation remains valid, as detailed studies, using Long's model parameters, show.

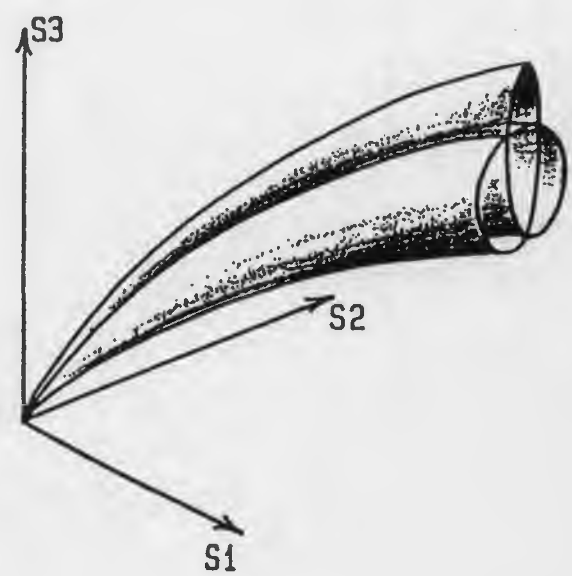

Figure 3.

It is from these very simple and general considerations that two procedures, hereafter described, have been developped to determine the values of the coefficients A, B and C in the "S" model equation.

1.2 Evaluation of parameters using maxima of the ratio S1/S2 or S2/S1

1.2.1 Determination of B and C in wind speed bins. Consider now the ratio S1/S2, which is only function of B1, C1 and Φ :

$$\frac{S1}{S2} = \frac{1 + B1\cos(\Phi-45) + C1\cos(2\Phi-90)}{1 + B1\cos(\Phi+45) + C1\cos(2\Phi-90)} \quad (2)$$

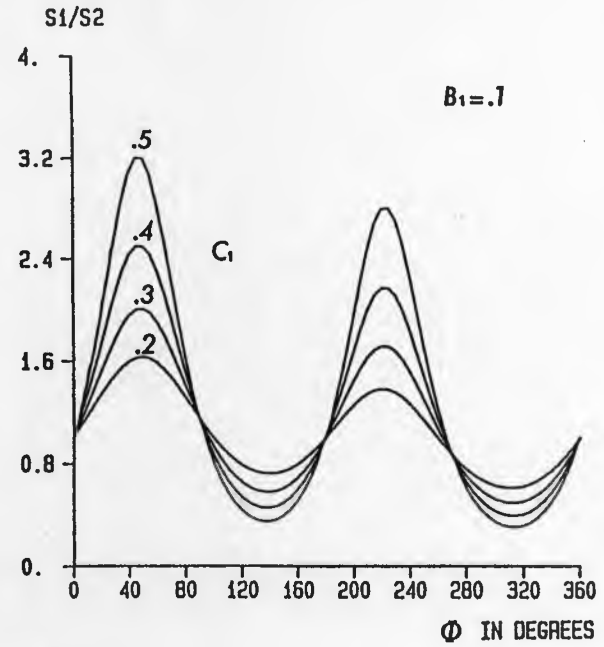

Figure 4.

As Figure 4 shows, this ratio reaches two maxima as a function of Φ ; the curves have been computed for reasonable values of B1 and C1. To find the extrema of S1/S2, as a function of Φ, its first derivative is taken and set to zero which leads to the condition :

$$S2\left(\frac{dS1}{d\Phi}\right) - S1\left(\frac{dS2}{d\Phi}\right) = \sqrt{2}\,BC(\cos\Phi) + 4C(\cos\Phi) + \frac{B}{\sqrt{2}}\cos\Phi + \frac{B^2-4C}{2}$$

$$=0$$

This is a third order equation in "cos Φ" whose different solutions (Ref. 3) are given by the following equations :

$$\cos\Phi = 2\sqrt{Q}\cos\left(\frac{a}{3}\right) - K \quad (4.a)$$

$$\cos\Phi = 2\sqrt{Q}\cos\left(\frac{a-360}{3}\right) - K \quad (4.b)$$

$$\cos\Phi = 2\sqrt{Q}\cos\left(\frac{a+360}{3}\right) - K \quad (4.c)$$

where :

$$K = 2\frac{\sqrt{2}}{3B}$$

$$Q = 2\frac{4}{9B^2} - \frac{1}{6C}$$

$$R = \frac{\sqrt{2}}{6\,BC} - \frac{B^2-4C}{4\sqrt{2}\,BC} - \frac{16\sqrt{2}}{27\,B}$$

$$a = \frac{R}{\sqrt{Q}}$$

Knowing the values of Φ, the values of the two maxima of S1/S2, namely M1 and M2, are computed for different values of B1 and C1. This being done, the graph of Figure 5 can be drawn, the abscissa and ordinate being defined as :

$$S = \frac{M1 + M2}{2} \quad (5.a)$$

$$D = \frac{M1 - M2}{2} \quad (5.b)$$

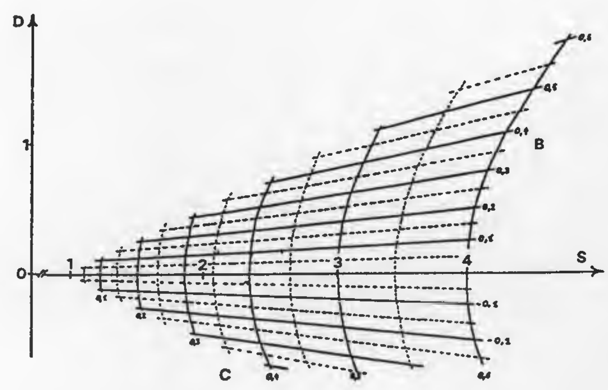

Figure 5.

If the ratio S1/S2 obtained from the scatterometer is followed at a given incidence angle over several days, it will be possible to evaluate M1 and M2, which correspond roughly to upwind and downwind directions of the forward beam. In view of symmetry, the ratio S2/S1 will also be followed and its maxima evaluated ; both distributions should lead to the same type of information. Once separated into different wind speed bands (say V = (4+n4) m/s, (n = 1, 2, 3..), mean values of S and D will give an estimate (Figure 4) of the parameters B1 and C1.

1.2.2 Evaluation of the error in this estimation of B and C. An estimate of the error introduced by this method can be obtained as follows.

Let Var(S) be the variance of one measurement of Si(i = 1,2); by definition, we shall suppose that :

$$\mathrm{Var}(S_i) = Kp_i^2\, S_i^2$$

where Kp may vary with incidence angle, but is, hopefully, less than 1. Moreover

$$\mathrm{Var}(S) = \mathrm{Var}(D) = \frac{\mathrm{Var}(M1) + \mathrm{Var}(M2)}{4} \qquad (6)$$

To estimate the variance of Mi, which in pratice will be determined experimentally, let us assume that fluctuation, ei Si, about the mean values, Si, of Si, are small. Then :

$$\mathrm{Var}\left(\frac{S1}{S2}\right) = \mathrm{Var}\left[\frac{S1(1+e1)}{S2(1+e2)}\right]$$

$$\approx \frac{S1^2}{S2^2}\,\mathrm{Var}(1+e1-e2) = (Kp1^2+Kp2^2)\,\frac{S1^2}{S2^2} \qquad (7)$$

Then, from Eq. 6,

$$\mathrm{Var}(S) = \mathrm{Var}(D) \approx (Kp1^2+Kp2^2)\,\frac{M1^2+M2^2}{4} \qquad (8)$$

As Figure 4 shows, the evolution of B with D is roughly four times that of C with S. Since Var(D) = Var(S), the absolute error in the estimation of B will therefore be four times that the error in the estimation of C ; and the relative error of B, when B is close to zero, will be very, very large. These are limitations which can, to some extent, be alleviated by increasing the number, n, of points in the estimate, the standard error decreasing as $1/\sqrt{n}$. But, there will always be a region close to the S axis, where B will be determined with very poor relative precision.

As an example, consider the case where B = 0.1 and C = 0.4 ; then S = 2.34 and D = 0.18 ; from Eqs. 5.a and 5.b, M1 = 2.52 and M2 = 2.16. If Kp1 = Kp2 = 0.1 the standard deviation of S will be :

s.d.(S) = s.d.(D) = 0.23

Values of C at [S + 1 s.d.(S)] will be 0.35 and 0.44, and those of B at [D + 1 s.d.(S)] will be -0.04 and 0.24.

To reduce these errors to reasonable values, a few points (≈ 10) will suffice for the estimate of C, but fifty will be required to estimate B to 20%.

1.2.3 Evaluation of A, having determined B and C. Having evaluated B and C, the values of Φ at the maxima are determined ; in all reasonable cases, they will correspond to directions nearly upwind or downwind relative to the forward or rear antenna (45° or 225° for S1/S2 and 135°, 315° for S2/S1).

Therefore, using Eq. 1.a or 1.b, the value of A can be determined, in a wind speed bin, using the estimations of B, C and from these, Φ, as well as the measured values of S1. But since fluctuations of these parameters (determined from scatterometer measurements and the meteorological wind field) are not independent, only simulations with models approaching reality will furnish precise evaluations of the variance of A, thus determined.

2. DETERMINATION OF MODEL PARAMETERS FROM MEASUREMENTS OF THE CENTRAL ANTENNA

2.1 Formulation of the problem and solutions

Consider the three curves formed by the intersection of the plane S1 = S2 with the surface of possible solutions ; from Eqs. 1.a and 1.b, these curves correspond to the directions Φ = 0, Φ = 180° and $\Phi i = + \arccos[-B1/(2\sqrt{2}\,C1)]$.

If we take the range of values of B and C given by Long's model as indicative, Φi ranges from 90 to 111 degrees. As a first estimate, which might be refined later on, let us estimate Φi by the parameter : Φie = 100°.

From selection of scatterometer data such that S1 = S2, and evaluation of the wind speed corresponding to each point of measurement selected from the meteorological wind field, the evolution of V along the three curves described can be determined, and the curves (at a given incidence angle of the central beam) will take the form :

$$S3=F1(V)=A3\,(1+B3+C3) \qquad (9.a)$$
$$S3=F2(V)=A3\,(1-B3+C3) \qquad (9.b)$$
$$S3=F3(V)=A3\,(1+B3\cos\Phi i + C3\cos 2\Phi i) \qquad (9.c)$$

Reformulating these equations, using Φie previously defined, gives :

$$S = \frac{F1 + F2}{2} = A3\,(1 + C3) \qquad (10.a)$$

$$D = \frac{F1 - F2}{2} = A3 \times B3 \qquad (10.b)$$

$$E = F3 - D\cos(\Phi ie) - S\cos(2\,\Phi ie)$$
$$= A3\,[1 - \cos 2\Phi ie + B3\,(\cos\Phi i-\cos\Phi ie) + C3\,(\cos 2\Phi i-\cos 2\Phi ie)\,] \qquad (10.c)$$

Therefore

$$\frac{E}{1 - \cos 2\,\Phi ie} = A3\,(1 + e)$$ where

$$e=\frac{B3(\cos\Phi i-\cos\Phi ie)+C3(\cos 2\Phi i-\cos 2\Phi ie)}{1 - \cos 2\,\Phi ie} \qquad (11)$$

If the values of B3 and C3 are taken from Long's model, the term "e" is smaller than 0.05 and more like 0.01 over the range of wind speeds and incidence angles ; it is therefore reasonable to neglect it and evaluate directly A3 by the approximation:

$$A3 \approx \frac{E}{1 - \cos 2\Phi ie} \qquad (12)$$

Having evaluated A3, then B3 and C3 are evaluated using Eqs. 10.b and 10.a :

$$B3 \approx \frac{D}{A3} \qquad (13)$$

$$C3 \approx \frac{S}{A3} - 1 \qquad (14)$$

2.2 Evaluation of the error in this estimation of A, B and C

The variance of the functions F1, F2 and F3 will depend both on the variance of S3, measured by the scatterometer and also on that of the wind speed extracted from the meteorological wind field. We shall assume here that these variances are majored by

$$\mathrm{Var}\ F1(V) \leq K^2/n\ A3^2 \qquad (15)$$

where n is the number of independent evaluations used; K may reach values around 0.4, depending on the quality of the meteorological wind field used. The variance of different terms are then given directly by

$$\mathrm{Var}\ (S) = \mathrm{Var}\ (D) \leq \frac{K^2}{n}\ \frac{A3^2}{2} \qquad (16)$$

$$\mathrm{Var}\ (E) \leq 2\ K^2/n\ \ A3^2 \qquad (17)$$

$$\mathrm{Var}\ \left(\frac{E}{1 - \cos 2\ \Phi ie}\right) \approx K^2/n\ \ A3^2 \qquad (18)$$

which, according to Eq. 12, determine the variance of the estimate of A3.

Evaluation of the variance of the estimations of B3 and C3 are not readily made, because of correlation of the different estimates in their evaluations. Once again, this will have to be done by simulation, once a good approximation of model parameters is obtained.

3. CONCLUSIONS

The method of paragraph 1 determines all parameters, but can give directly an estimate of the error in the estimation only for B and C. That of paragraph 2 can also determine all parameters, but can give directly an estimate of the error in the estimation only for the parameter A. Moreover, if the first method requires the data of the forward and rear antennae, the second requires only that of the central antenna (plus the marginal information that S1 = S2). All this to say that they appear complementary.

The major advantage of these methods is to use available wind speeds from meteorological fields ; but it is also recognized that these fields are noisy (≈ 2 or perhaps 3 m/s at times) which may lead to require a large number (≈ 100) of points of measurement.

The presentation of these methods is made at the ESA-Workshop in the hope that they be criticized and if possible improved on, by the different participants having a long experience of meteorological wind fields and their limitations.

4. REFERENCES

1. A.E. Long 1985, Towards a C-Band Radar Sea Echo Model for the ERS-1 Scatterometer, Proc. First Int. Coll. on Spectral Signatures of Objects in Remote Sensing, 1974.ESA, Les Arcs.

2. H. Klinkrad 1985, Algorithms for Orbit Prediction and for the Determination of Related Static and Dynamic Altitude and Ground trace Quantities, ESA/ESTEC/ORM doc N° ER-RP-ESA-SY.00001.

3. M.R. Spiegel 1974, Mathematical Handbook of Formulas and Tables, Mc Graw-Hill Inc. N.Y.

THE USE OF NUMERICAL WIND AND WAVE MODELS TO PROVIDE AREAL AND TEMPORAL EXTENSION TO INSTRUMENT CALIBRATION AND VALIDATION OF REMOTELY SENSED DATA

P E Francis

Meteorological Office, Bracknell, United Kingdom

ABSTRACT

Satellite derived ocean surface data will have a large impact on many environmental sciences. A scheme to use these data most efficiently is outlined. The scheme involves three component comparisons, between satellite data and ground based measurements, between ground based measurements and numerical models, between numerical models and satellite data. Each comparison yield vital information eg primary retrieval algorithms, model validation, extension of satellite data validation beyond the regions of surface based networks. Examples are given of the performance characteristics and output products of the Meteorological Office global atmospheric and sea state models.

Keywords: Data calibration and validation, numerical models of atmosphere and oceans.

1. INTRODUCTION

The launch of ERS-1 and other earth observing satellites at the end of this decade will result in large increases in both data volume and data coverage with respect to ocean surface parameters such as winds and waves. These increases in data will have a marked impact on many associated scientific disciplines, especially in the area of the southern oceans where data coverage has always been relatively sparse. At national meteorological and oceanographic centres these data will give added insight to dynamical processes, expand and enhance climatological data bases, and provide extra input to numerical models of atmosphere and ocean fields. The largest impact will probably be in the field of ocean wave modelling since at present so few measurements of sea state are made, and reported in real time, that the calculation of an 'analysis' (or starting field) for a sea state forecast is performed purely by using reconstructed wind fields as forcing functions. Large numbers of consistent and reliable measurements of sea state will make the inclusion of such data in a model a worth while and constructive process. To make optimum use of large amounts of these new data it is essential that a system be devised to assess the validity of the data over a wide range of geographical locations and meteorological conditions. Such a scheme is outlined in this presentation.

The 'classical' validation technique for remotely sensed data, ie comparing them with data obtained from more conventional surface based instruments, is an essential procedure that gives useful insight into possible ways to construct retrieval algorithms, and some indication as to the eventual accuracy of the retrieved data. However such a technique will use only a small fraction of the available satellite based data even if extensive (and expensive!) surface instrument development campaigns are carried out. Other problems also arise from the comparison of the satellite data, which are essential spatially averaged, with data from a variety of site specific instruments on the surface.

Numerical models of surface wind and wave parameters can provide an invaluable extension to this classical approach. The models provide matrices of physically representative and coherent data against which both surface based and remotely sensed measurements can be assessed. Models also have the added advantages of a wide geographical extent, possible extreme conditions somewhere in the modelled domain, and the grid point values represent areal averages rather than spot values.

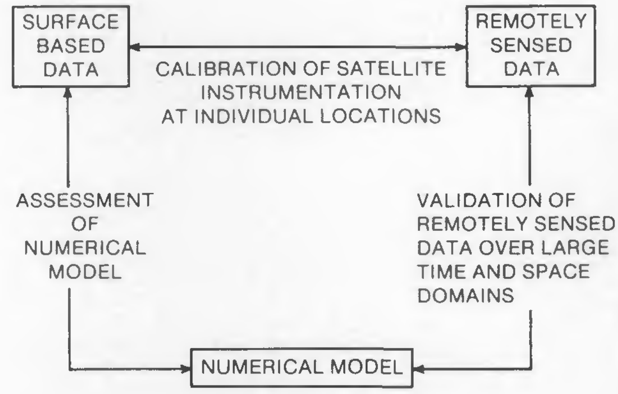

Figure 1. Complete comparison system

2. THE SYSTEM

The proposed evaluation systems would consist of a three-way comparison procedure, as illustrated in Figure 1.

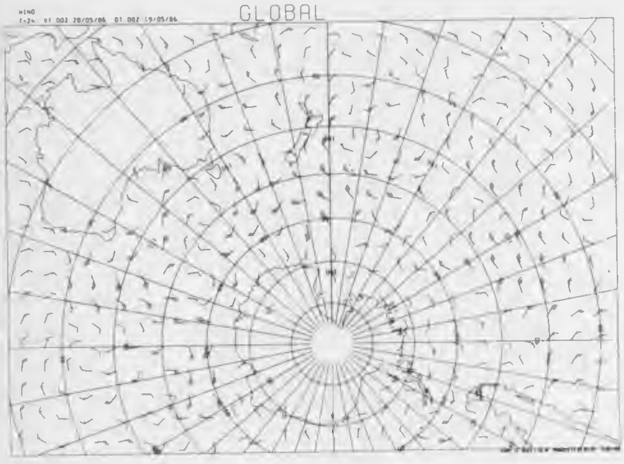

Figure 2. Example surface wind output

All the possible field comparisons shown in the figure are used in the proposed system. The comparison of surface based and remotely sensed data is the classical approach already described, giving the primary instrument - instrument relationship. In order to work, such an approach requires a planned and dedicated surface network, ideally with the real time return of all network data to collecting centres for immediate use. Development of primary algorithms will take place at this stage with some question marks over spatial averaging effects, and the use of more than one kind of surface based measuring system.

The comparison of surface based data and co-located model values will serve to validate and calibrate the models being used. In this way model characteristics are determined which can be extended to apply in geographic areas devoid of surface measured data. If well established operational models are used for this purpose then much validation will already have been performed, leading to improved and acceptable levels of model performance by means of feed-back of information to model developers. Such operational validation would however have been carried out using a comparatively restricted supply of measured data. A well planned observing experiment would yield a better test bed against which to calibrate the models, and perhaps also reveal any biases between different kinds of surface based instruments.

The third comparison, of model data and remotely sensed data, will serve to extend the size and coverage of the possible usable data sample from the satellite. Knowing the relationship between model values, surface measurements and satellite measurements at co-located points, the extension into areas devoid of surface measurements becomes a possibility. Care has to be taken however to ascertain the possible variation of model behaviour in different geographical locations. Regions such as the southern oceans, where relatively little meteorological information is presently available near the surface, may not be so well modelled as the North Atlantic for instance, from where many ship reports are routinely available, and the data fed into the atmospheric model analysis.

The system outlined here may also be of importance in the design of any surface based network that is envisaged as part of the overall ERS-1 program. Specifically, the use of models should enable

a) A variety of surface based instruments to be used, providing a consistent background against which to compare instrument performance. This is particularly important if considering the use of such different sources of data as anemometers, conventional wave recorders/buoys and radar/microwave sensors.

b) A more widely spaced network to be established, relying on the models to give detail and structure at higher spatial resolution. Many networks, in different oceanic areas, can be united into a single framework.

c) A solution to the problem of areal average versus site specific measurement, by means of a consistent framework in which to assess variability in time and space.

3. THE PROCEDURE

Of the three component comparisons mentioned above, only the third, ie comparison of satellite data with model data, will be discussed in detail here. It is assumed that the derivation of primary algorithms (comparison 1) and the definitions of model 'error' characteristics (comparison 2) are well defined tasks which can be discussed elsewhere. A sufficient illustration of the degree to which numerical models presently fit surface wind and wave observations is given in Table 1 and Table 2.

Both examples show how the models compare with the measurements, without the influence of the measurements in the model. In the case of the wave results this is a straight forward exercise since as yet wave measurements are not used in sea-state models. For the wind comparisons the effect is achieved by comparing the measurements with a 6-hour forecast, thus to some extent freeing the model from the previous set of input data.

Table 1.

Latitude extent	No of data	Mean Speed error	RMS Speed error	Mean Vector error	RMS Vector error
90 -20N	27664	1.2	3.6	4.4	5.2
20N-20S	7983	0.6	2.8	3.6	4.2
20 -90S	4444	0.9	4.1	5.1	6.1

Comparison of surface wind data from the Bracknell global model, 6 hour forecast, with measurements during April 1986. Units are ms^{-1}.

Table 2.

Area	No of data	Mean Height Error(m)	Standard Deviation(m)
East Pacific	2769	0.1	0.8
Gulf of Mexico & West Atlantic	4004	0.1	0.5
N. E. Atlantic	2468	0.2	1.1

Comparison of significant wave height data from the Bracknell N. Oceans model hindcast with measurements during 1985.

The detailed procedure for comparing satellite based surface wind and wave measurements with modelled data would involve several distinct steps. Since initially the remotely sensed data should be assessed against model fields that are not themselves influenced by these data, it would be acceptable to use model analyses, rather than short period forecasts, as the numerical framework. This has the added advantage that conventional surface wind measurements are fitted to a better degree than that demonstrated in Table 1. Gross quality control of the satellite based surface wind measurements, calculated using retrieval algorithms derived from relationships between the satellite data and ground station measurements, could then be performed. Making some allowance for the possible degradation of wind modelling performance away from areas of relatively frequent conventional data input, it should be possible to assess whether the algorithms in use are valid for a wider range of conditions than may be available at the time of derivation, and also whether the performance of the whole measurement/retrieval scheme is constant over many orbits, making use of much more data than was used in the derivation of the algorithms.

A suitably designed impact study could then demonstrate the advantages of the more usual semi-iterative procedure by which the data are actually quality controlled against a short term (say 6 hour) forecast and then assimilated into the model as useful input data, ready for the next forecast.

A similar sequence can be employed for the satellite derived wave information, although the details are slightly different. The present conventional wave 'analysis' (ie a hindcast) would be used as the first guess field for assessing the remotely sensed data. These data of course being derived using algorithms obtained from comparisons between remotely sensed and surface based data series. Again, making allowance for variations in model performance, it should be possible, using much more data, to assess the performance of the algorithms and the satellite/retrieval scheme in a meaningful way.

The necessary impact study would need to be in two stages, first to repeat the above process, this time using 'improved' winds for the hindcast generation. Where 'improved' means having assimilated satellite derived winds into the atmospheric model. Secondly to attempt to assimilate the quality controlled satellite derived wave data into the wave model. These separate steps would allow an assessment of the impact of winds alone, and winds and wave combined, to be performed.

Finally the whole question of a more complex retrieval process could then be addressed. When wind and wave data are being seperately retrieved and assimilated the quality control against model fields should show up regions where the seperate univariate retrieval schemes may be failing. If this is the case then an iterative scheme, using short period wind and wave forecasts as input data, could be devised, whereby a multivariate retrieval mechanism could be examined. A model framework would appear to be the only one possible where such an iterative scheme could adequately be derived and made to function.

4. THE MODELS

Atmospheric and surface wave predictions models are to be found at many operational meteorological forecast centres. The degree of sophistication of the models being primarily a function of the available computing resources. It is safe to say that the kind of schemes outlined here require global scale models in order to function to the most efficient level, but regional models would fulfil a useful function if carefully used in conjunction with the global programme. The Meteorological Office presently operates global and regional versions of atmospheric and surface wave prediction models, using many years of experience, and keeping abreast of modern developments in the field. Examples of forecast products from these models are given as illustrations in Figures 2 and 3, depicting coverage of the South Pacific. Some validation of model wave products in this area is still required, but the wind products would appear to be adequate for use, as shown in Table 1. Such models would provide an ideal framework for the approach to data calibration outlined above, especially in the environment of a large operational forecast centre with extensive computing and telecommunications facilities.

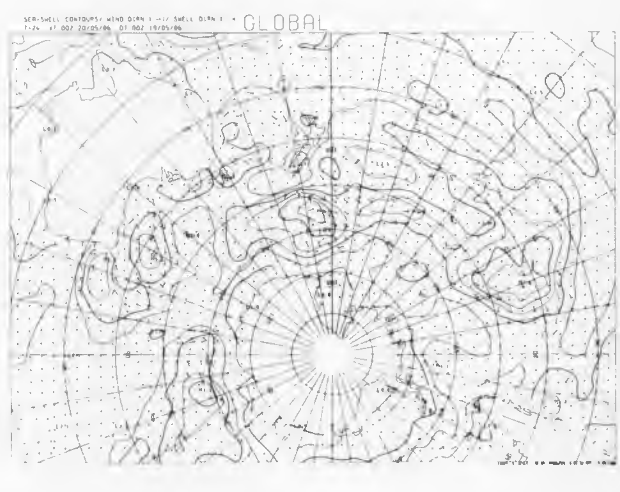

Figure 3. Example surface wave output

SATELLITE SCATTEROMETER COMPARISONS WITH SURFACE MEASUREMENTS: TECHNIQUES AND SEASAT RESULTS

M H Freilich

NASA Scatterometer Project
Jet Propulsion Laboratory
California Institute of Technology
Pasadena, CA 91109

ABSTRACT/RESUME

This paper addresses some statistical techniques for comparing satellite scatterometer vector wind measurements with conventional, point surface observations. Proper comparisons can be used to evaluate the overall performance of the scatterometer, as well as to gain insight into dependences of scatterometer measurements on other geophysical variables such as sea-surface temperature. Techniques are illustrated and results are discussed in the context of a careful analysis of Seasat SASS-buoy comparisons, using a large set of heretofore unexamined surface data.

1. INTRODUCTION

Existing operational meteorological buoy systems can be used for validating satellite measurements of near-surface winds. Buoy measurements are taken and reported frequently (typically every one or three hours), thereby affording many opportunities for comparison with co-located satellite data. Buoys and their instrumentation are designed and calibrated to yield accurate measurements, when compared with those from voluntary observing ships. Most existing buoy systems acquire data on air and sea temperatures, near-surface humidity, and surface wave conditions. The buoy data can be input to a boundary layer model, to allow calculation of neutral stability wind velocity as measured by scatterometers.

Proper comparisons between buoy and satellite wind measurements can thus be used to evaluate the overall performance of the satellite instruments. In addition, the non-wind variables measured by the buoy can be used to elucidate possible systematic dependencies in the satellite winds.

However, satellite and buoy wind measurements cannot be compared directly. Satellite observations are essentially instantaneous spatial averages over a fixed area, while buoy observations are fixed-length temporal averages at a single location. The turbulent nature of surface winds, with motion on a variety of spatial and temporal scales, accentuates the differences between the two types of measurements. Even perfectly accurate satellite and buoy measurements will differ, simply because of the differing averaging involved.

In this paper, we present a method by which satellite and surface measurements can be compared in order to validate satellite wind observations. The regression method, described in Section 2, requires knowledge of the expected differences (due to atmospheric variability and differing averaging) between perfect satellite and perfect buoy measurements. A model for estimating these differences is described in Section 3. In Section 4, the regression method is applied to comparisons between Seasat Scatterometer (SASS) and U.S. National Data Buoy Office (NDBO) buoy data. Further comparisons indicating a dependence of SASS accuracy on sea-surface temperature are described in Section 5.

2. REGRESSION WITH ERRORS

Scatter plots and linear regression techniques have historically been used to compare scatterometer data with co-located (in space and time) conventional observations from buoys and ships. In theory, simple linear regression of satellite data on compatible observations of the "true" (spatially averaged) wind could be used to estimate bias and gain errors, as well as the magnitude of the random scatter in the satellite data. Further analyses of the deviations between satellite measurements and the regression line can be used to indicate fundamental inaccuracies in the satellite system. Details of the regression techniques for the case of compatible "true" wind observations are discussed in many elementary texts (e.g., Refs. 1 and 2).

However, the regression problem becomes statistically ill-posed (Ref. 3) when the buoy measurements (the independent variable in the regression) contain errors are incompatible with the satellite data. Approximate methods (Refs. 2-4) must then be used to estimate the "true" regression coefficients and the random error attributable to the satellite data.

Following Ref. 2, let w_i denote the "true" wind speed compatible with the i^{th} satellite obser-

Proceedings of a Workshop on ERS-1 Wind and Wave Calibration, Schliersee, FRG, 2–6 June, 1986 (ESA SP-262, Sept. 1986)

vation, y_i. The linear regression model involves estimating A, B, and $\langle e^2 \rangle$, where

$$y_i = A + Bw_i + e_i, \quad (1)$$

and $\langle e \rangle = 0$.

In general, however, measurements of ξ_i are not available. Assuming that the buoys are perfectly calibrated and linear, the i^{th} buoy measurement, x_i, is related to w_i by

$$x_i = w_i + d_i, \quad (2)$$

where d_i is random error in the buoy measurement ($\langle d \rangle = 0$).

Regression of y on x yields the model

$$y_i = A + Bw_i + (e_i - Bd_i). \quad (3)$$

The explicit appearance of B in the last term of Eq. 3 emphasizes the fundamental differences between Eqs. 1 and 3 (cf. Refs. 2-4). Reference 2 shows that if B is the estimate of $\hat{B}$ calculated by regressing y directly on x,

$$E(\hat{B}) \approx B(s_w^2 + s_{wd})/(s_w^2 + s_d^2 + 2sw_d), \quad (4)$$

where s_w^2, s_d^2 are the sample variances of w and d, respectively, and s_{wd} is the covariance between w and d. If $s_{wd} < s_d^2$, and $s_d^2 << s_w^2$, then $E(\hat{B}) \lesssim B$.

In practice, then, the regression coefficients calculated from direct regression of y on x can be modified to yield estimates of the true coefficients A and B, if s_{wd}, s_w^2, and s_d^2 are known. Once (corrected) estimates of A and B have been obtained, estimation of $\langle e^2 \rangle$, the random mean square error due to the satellite measurement, is straightforward.

3. ERRORS IN BUOY MEASUREMENTS

In the previous section, it was shown that regression coefficients and the random error attributable to the dependent variable (satellite measurements) can be estimated even when the independent variable (the "true" compatible wind speed) is observed with error, when the error in the independent variable is small relative to its observed range. This section outlines a model for the magnitudes of "errors" in buoy measurements of wind speed.

There are three major sources of discrepancies between buoy wind speed measurements and the "true" wind (spatially averaged, compatible with satellite data). The first source is due to instrumental error in the buoy itself. Reference 5 discusses these errors. Wind tunnel tests by the U.S. National Data Buoy Center yield an approximate rms magnitude of (the greater of) 1 m/s or 10% for these errors. In the following, we will assume that the buoy instruments are perfectly calibrated, so that this "instrumental" error is purely random.

The second source of error is due to the incompatibility between the fixed spatial averaging of the satellite and the fixed temporal averaging of the buoy. Even if Taylor's hypothesis ("frozen turbulence") is assumed to be valid for mesoscale atmospheric motions, fixed sampling parameters for both the satellite and the buoy lead to discrepancies that are functions of the "true mean" wind speed.

We assume for simplicity that the satellite measurements correspond always to a "synoptic" time scale on the order of 1 hour. Buoy measurements, on the other hand, are 8.5 minute averages obtained once every one or three hours. A simple model is proposed in Ref. 6 for estimating the variability of this 8.5 minute average with respect to the 1 hour synoptic wind. Based on historical data, Ref. 6 assumes that the frequency spectrum of winds (for periods of about a minute to an hour) falls off like 1/frequency. The total variance in this frequency band is further a function of the synoptic wind speed. Figure 1 shows the standard deviation of the 8.5 minute average as a function of the synoptic neutral stability wind speed at 10m height.

A third discrepancy between satellite and buoy winds arises from the fact that the observations are not perfectly co-located in either space or time. This error source, discussed in Ref. 7, is not considered in the present work.

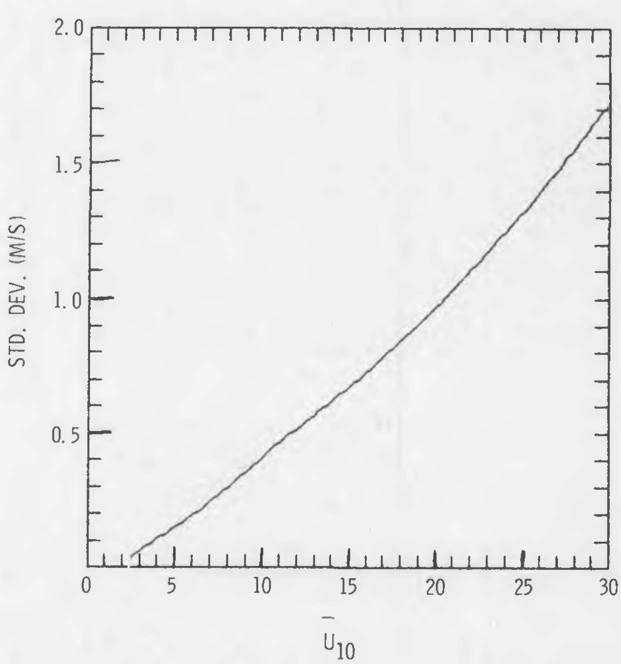

Figure 1. Standard deviation of 8.5 minute average speed as a function of the "true" synoptic neutral stability wind measured at 10 m height.

4. BUOY-SASS SPEED COMPARISONS

In this section we apply the regression technique of Section 2 to a point-by-point comparison between wind measurements from 19 NDBO buoys around the coasts of N. America, and similar measurements from SASS.

The SASS measurements are thought to correspond to U19.5N, the equivalent neutral stability wind speed at a height of 19.5m. The boundary layer model of Ref. 8 was used to calculate U19.5N from buoy measurements of wind speed, air and sea-surface temperatures, and humidity. It was necessary to perform these calculations using "raw" buoy data as inputs, since several errors have been discovered in available processed/reduced buoy data sets from the Seasat period (see also Ref. 9).

The SASS data have been processed, tuned, and re-processed several times in the years since the Seasat mission. We consider only two of these processed data sets. Both are based on σ_o measurements reduced by the Atmospheric Environment Service (AES) of Canada. In each data set, winds were retrieved by binning σ_o measurements falling within 100 km squares on the earth's surface. Both sets span the entire Seasat mission.

The "GSFC" (Goddard Space Flight Center) data set contains winds retrieved using the SASS-I model function (cf. Ref. 10) and the sum-of-squares (SOS) algorithm (Ref. 9). Both h-pol and v-pol σ_o's were used in the wind retrieval. Unique vector winds were determined by assimilating the ambiguous data into the GSFC 5° x 5° at atmospheric general circulation model.

The "Wentz" data set was produced by F. Wentz of Remote Sensing Systems, using the "SASS-II" model function and an alternate retrieval algorithm (Ref. 11). Separate wind retrievals were made for h-pol and v-pol. Unique vector winds were determined at JPL by choosing, on a point-by-point basis, the Wentz ambiguity closest to the unique vector selected by the GSFC scheme.

SASS data was co-located with buoy measurements, edited, and averaged. SASS measurements falling within 1 hour and 100 km of a buoy observation were individually compared with U19.5N as derived from buoy data. Data associated with buoy U19.5N speeds of less than 2 m/s were not considered in this study. If the SASS wind speed differed from the buoy speed by more than 5 m/s, the SASS observation was discarded. (Only a very small number of SASS observations were deleted based on this criterion.) As a final step, all remaining co-located SASS speeds were averaged. This process resulted in about 1000 independent h-pol, and about 1200 independent v-pol/all-pol comparisons with buoy data.

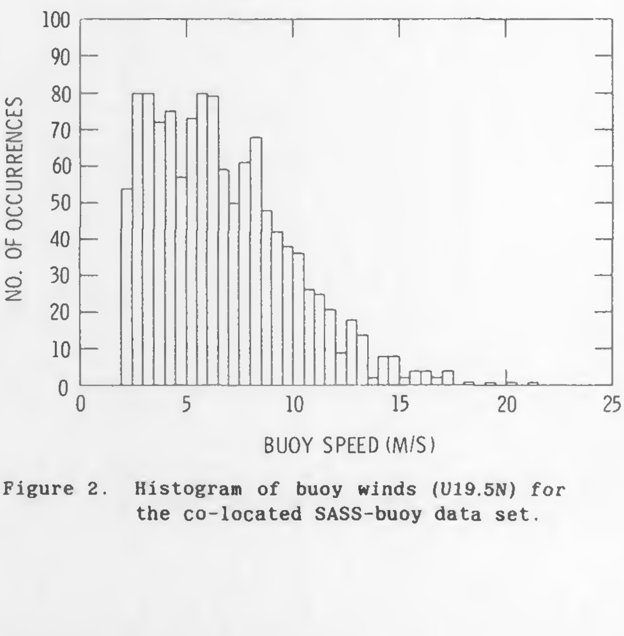

Figure 2. Histogram of buoy winds (U19.5N) for the co-located SASS-buoy data set.

Figure 2 shows the histogram (for all-pol) of buoy U19.5N winds in the comparison data set. The distribution of speeds is approximately Rayleigh (as suggested by Ref. 11), and there are few observations with speeds greater than 15 m/s.

Figures 3-5 show the results of the regression analysis for the GSFC, Wentz-v-pol, and Wentz-h-pol data sets, respectively. Although the regressions were performed on all SASS-buoy co-located pairs, the results are presented by averaging all data in each 0.5 m/s buoy wind speed band. Error bars shown represent ±1 standard deviation from both the buoy and SASS averages.

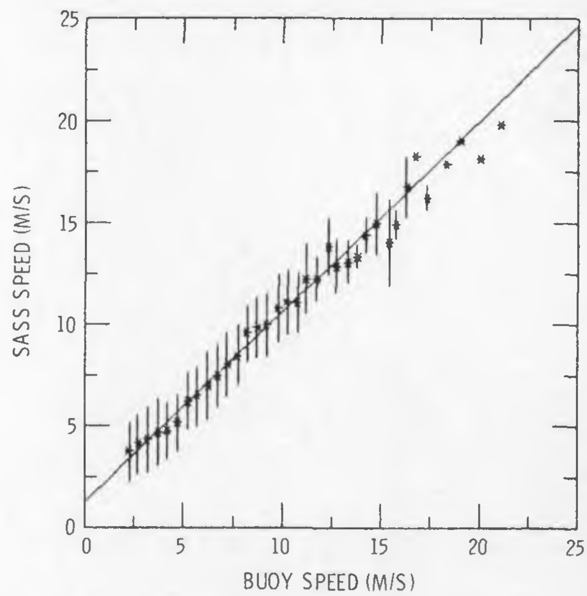

Figure 3. Scatter plot of SASS speeds vs. buoy speeds (both U19.5N) for the GSFC data set. For clarity, observations have been averaged within 0.5 m/s bins based on buoy speed. Error bars are 1 standard deviation for the averages. Regression line is shown.

Regression coefficients corrected for buoy "errors" (due to atmospheric turbulence and short buoy averaging times) are given in Table 1. In all cases, the slopes of the regression line (B of Eq. 1) are close to, but less than, 1. The SASS-I/SOS (GSFC) model (Fig. 3) has an intercept of 1.3 m/s, indicating that the SASS measurements are biased high. This possibility was first suggested by Ref. 12, and may be the

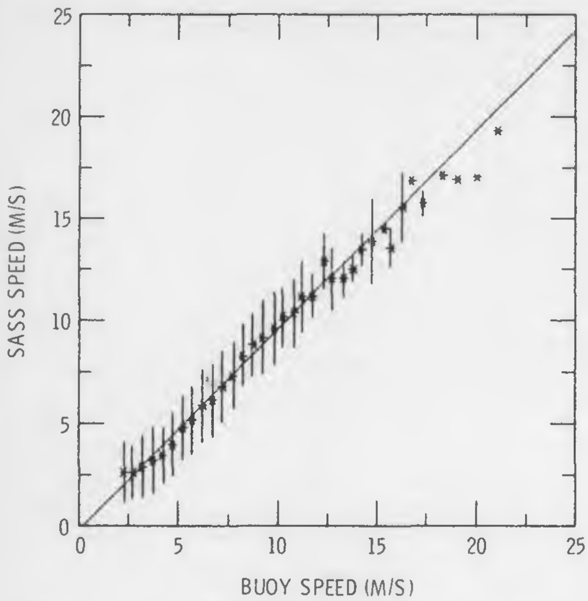

Figure 4. As in Fig. 3, but for the Wentz v-pol data set.

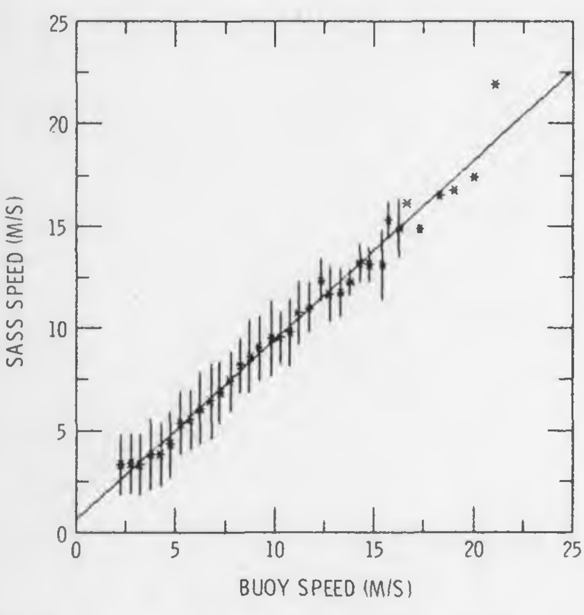

Figure 5. As in Fig. 3, but for the Wentz h-pol data set.

Table 1

Regression Coefficients for SASS-Buoy Comparisons

Data Set	A (m/s)	B	rms deviation (m/s)
GSFC (all-pol)	1.3	0.94	1.5
Wentz (v-pol)	-0.2	0.98	1.6
Wentz (h-pol)	0.7	0.88	1.6

result of a mis-calibration of a crucial JASIN data buoy used to tune the model function. The Wentz model function was not tuned using conventional measurements, and Table 1 shows that the biases for these data sets are considerably smaller (almost negligible for the v-pol data).

Figures 3-5 also show systematic deviations of SASS data as a function of buoy speed. The SASS data appear almost insensitive to buoy speed for buoy speeds less than about 4 m/s. This effect, consistent with the results of Ref. 9, may be due to flaws in the SOS-type retrieval algorithms used. Finally, although the data is sparse, there appears to be a slight underprediction by SASS at high wind speeds.

5. DEPENDENCIES ON SEA-SURFACE TEMPERATURE

The effects of other geophysical processes (besides wind velocity) on SASS measurements can be elucidated by examining deviations between SASS speeds and the (corrected) regression line, as functions of the other variables. Although dependences on long-wave height and stability were also examined, in this work we present only the results for sea-surface temperature (SST).

Figure 6 shows the distribution of SST, as measured by the buoys, for the co-located data sets. Because of the varied geographical locations of the NDBO buoys, a range of nearly 25°C is spanned by the data.

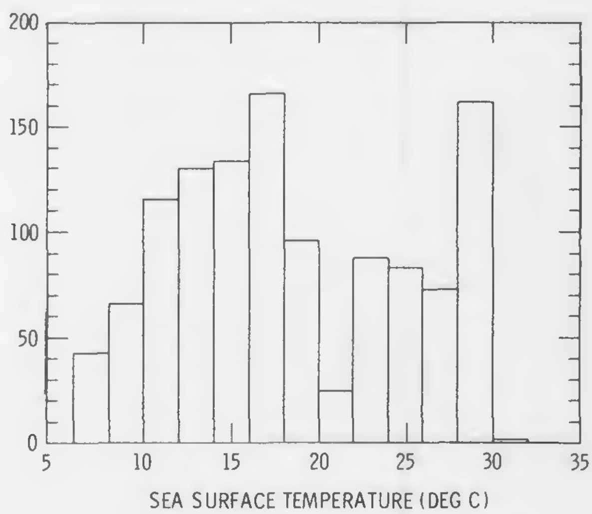

Figure 6. Histogram of SST, as measured by the buoys, for the co-located SASS-buoy data set.

Residuals, defined as $y_i - A - Bx_i$, are plotted against SST in Fig. 7. Data are averaged, as in Figs. 3-5, in 2° bins, and the error bars in Fig. 7 represent ±1 standard deviation in each variable. Mean residuals are positive (i.e., SASS is biased high) for low SST. The mean residuals fall rapidly with increasing SST for values less than about 15°. At larger SST, the mean residual is approximately constant and small. These results compare favorably with those of Ref. 13, both qualitatively and quanti-

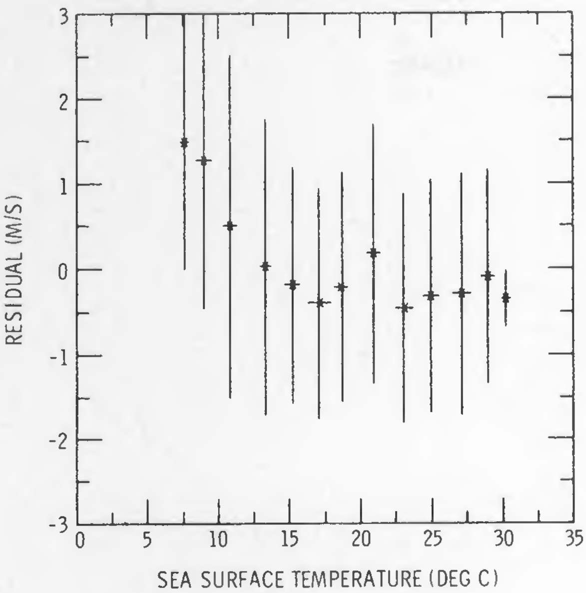

Figure 7. Residuals ($y_i - A - Bx_i$) vs. SST. For clarity observations have been averaged within 2°C bins. Error bars are as in Fig. 3.

tatively (after subtraction of the 1.3 m/s bias from the data presented in Ref 13). Although no attempt has been made in this analysis to decorrelate SST from buoy wind speed effects, a plot of buoy speed vs. SST, as in Fig. 8, strongly indicates that the results of Fig. 7 are truly due to SST, and are not due to the systematic wind speed errors in the SASS data discussed in Section 4 above.

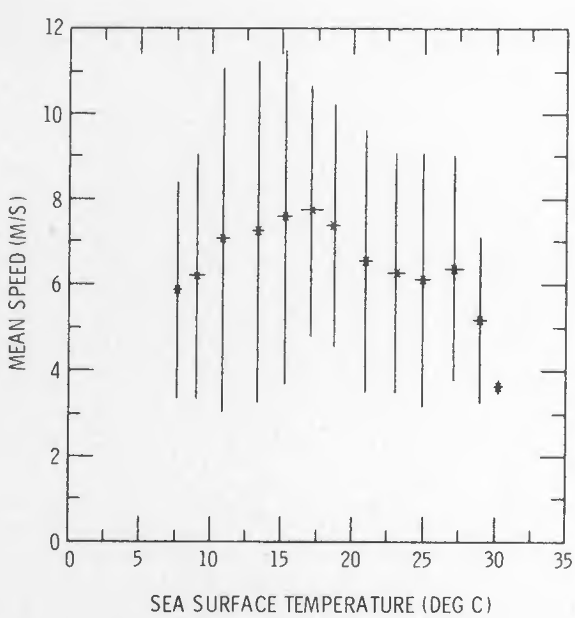

Figure 8. As in Fig. 7, but buoy speed (U19.5N) vs. SST.

6. CONCLUSIONS

Data from meteorological buoy systems can be used to quantitatively validate satellite scatterometer wind measurements over a wide range of conditions. A modification of classic linear regression techniques must be used in order to take into account errors and incompatibilities associated with the buoy measurements. While the modification presented yields only an approximation to the "true" regression coefficients (i.e., the coefficients that would have been obtained if the satellite measurements were regressed against perfect, compatible buoy observations), it is quantitatively accurate when the range of buoy observations is large compared with the expected "errors" in the observations.

A model for errors/discrepancies due to short buoy averaging times and atmospheric variability was used to estimate the errors in the buoy observations. Two sets of data from SASS, corresponding to different model functions, were then co-located with buoy measurements, and the regression analysis was performed. Examination of the corrected regression coefficients shows that slopes for all data were near 1. However, data retrieved using SASS-I/SOS were biased high by 1.3 m/s, while the SASS-II model did not exhibit such large biases. Both data sets exhibited an insensitivity of SASS to buoy winds at speeds less than about 4 m/s. Finally, plots of the mean residuals (SASS-regression line) against sea-surface temperature show a positive bias for low SST, quantitatively similar to earlier results by others based on completely independent (ship) data.

7. ACKNOWLEDGMENTS

Greg Pihos contributed significantly to the processing of the SASS and buoy data. This work was carried out at the Jet Propulsion Laboratory, California Institute of Technology, under contract with the National Aeronautics and Space Administration.

8. REFERENCES

1. Jenkins G M & Watts D G 1968, Spectral Analysis and its Applications, San Francisco, Holden-Day, 105-115.

2. Draper N & Smith H 1981, Applied Regression Analysis (2nd Ed.), New York, John Wiley & Sons, 122-125.

3. Madansky A 1959, The fitting of straight lines when both variables are subject to error, J Am Statis Assoc vol 54, 173-205.

4. Hodges S D & Moore G P 1972, Data uncertainties and least squares regression, App Stat vol 21, 185-195.

5. Wilkerson J 1986, (this volume).

6. Pierson W J 1983, The measurement of the synoptic scale wind over the ocean, J Geophys Res vol 88(C3), 1683-1708.

7. Challenor P G et al 1986, (this volume).

8. Liu W T & Blanc T V 1984, The Liu, Katsaros, and Businger (1979) Bulk Atmospheric Flux Computational Iteration Program in FORTRAN and BASIC, NRL Memorandum Report 5291.

9. Woiceshyn P M et al 1986, The necessity for a new parameterization of an empirical model for wind/ocean scatterometry, J Geophys Res vol 91(C2), 2273-2288.

10. Shroeder L C et al 1982, The relationship between wind vector and normalized radar cross-section used to derive Seasat-A satellite scatterometer winds, J Geophys Res vol 87, 3313-3336.

11. Wentz, F. J et al 1984, A model function for ocean radar cross sections at 14.6 GHz, J Geophys Res vol 89(c3), 3689-3704.

12. Weller R A et al 1983, Wind measurements from an array of oceanographic moorings and from F/S Meteor during JASIN 1978, J Geophys Res vol 88, 9689-9705.

13. Liu W T 1984, The effects of the variations in sea surface temperature and atmospheric stability in the estimation of average wind speed by Seasat-SASS, J Phys Oceanog vol 14, 392-401.

COMPARISON CONCEPT OF SATELLITE DERIVED WIND AND WAVE DATA WITH GROUND TRUTH

W Koch

Forschungszentrum Geesthacht
FR Germany

R Ramseier

Ice Research and Development
Ottawa/Canada

ABSTRACT

To demonstrate the capabilities of todays numerical models for the calibration of satellite derived pressure-, wind-, and wave-fields some results from numerical simulations are shown and compared to measurements and SMMR-data from NIMBUS 7. The proposed calibration procedure relies on numerical simulation models which themselves are quantitatively calibrated with regionally representative measurements.

1. INTRODUCTION

This contribution demonstrates the use of conventionally achieved pressure-, wind- and surface wave parameter fields for calibration of satellite information on wind and wave parameters. It also shows the use of satellite information to generate wind and pressure fields over the ocean.

The calibration philosophy is to construct the spatial and temporal parameter field for an oceanic area. This field will be calibrated by single-point measurements at suitable fixed locations over an extended period in time. The bias of the model can be brought to zero by this calibration, and the standard deviation can be determined to the desired accuracy.

The satellite calibration is done with the fields generated by the numerical model. Since bias and standard deviation for the model data are known these parameters can also be derived for the satellite data. The proposed method provides a much larger data set for calibration in comparison with ships of opportunity or single specially equipped platforms. The quality of the calibration is given by the standard deviation and bias in the same way as for single-station comparison.

Satellite-provided data fields can be

1. wave height from the altimeter
2. peak frequency of the surface-wave spectrum from the wave scatterometer
3. peak direction of the surface-wave spectrum from the wave scatterometer
4. surface-wind field in U_1U_2 components or in wind speed V and direction Θ from the wind scatterometer and partly from the altimeter
5. surface pressure differences

In the following it is demonstrated with wind speeds derived from SMMR data, how a calibration can be done. An impression is also given on the state of the art for modelling the other parameters mentioned above. Section 5 contains a short review on the derivation of surface pressure fields from satellite wind data.

2. MODEL DATA ON SURFACE PRESSURE, SURFACE WIND AND OCEAN WAVES CALIBRATED AGAINST SINGLE LOCATIONS

2.1 Pressure and Wind Data

At the ECMWF and the national weather services, global and regional fields of analyzed pressure and wind are available. They are generated by the use of previous and present observations and objective or subjective analysis methods. In order to give an impression of the quality of this information over the open ocean, fig. 1 and fig. 2 show a few comparisons between measured and objectively analysed wind fields at Atlantic weather ships for several months. Fig. 3 shows locations in the North Atlantic where the comparison data for wind and waves have been taken.

Fig. 1 and fig. 2 also show wave data comparisons at the weather ships, derived with the modelled wind fields. An evident conclusion from this comparison is that the quality of a wave model should always be considered in connection with the quality of the associated wind model, since the errors of both fields are strongly correlated.

It should be recognized that objective analysis methods have been strongly improved since the results of figs. 1, 2 were achieved. Nevertheless we propose to use subjectively analysed wind fields for the calibration of ERS-1 wind fields

Proceedings of a Workshop on ERS-1 Wind and Wave Calibration, Schliersee, FRG, 2–6 June, 1986 (ESA SP-262, Sept. 1986)

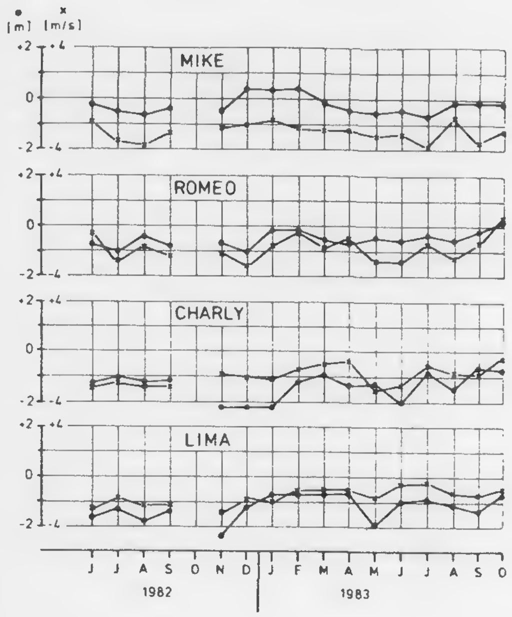

Fig. 1: Monthly averages of 6 h and 12 h-forecasts for significant wave height (• left scale) and wind speed (x right scale) at some weather ships

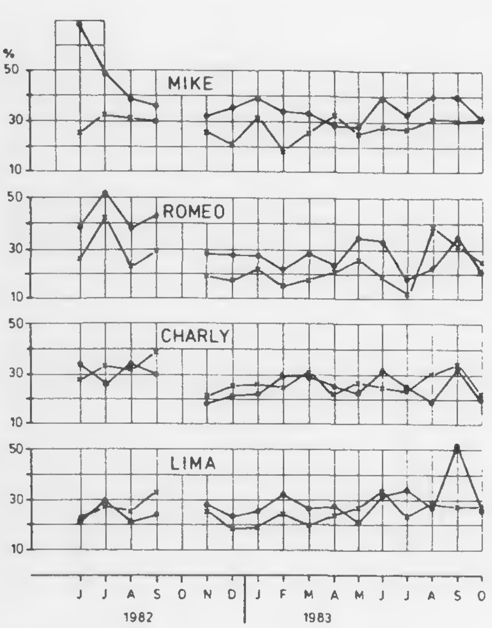

Fig. 2: Scatter-index (ratio of rms error and mean value) of 6 h and 12 h forecasts for significant wave height • and wind speed * at some weather ships.

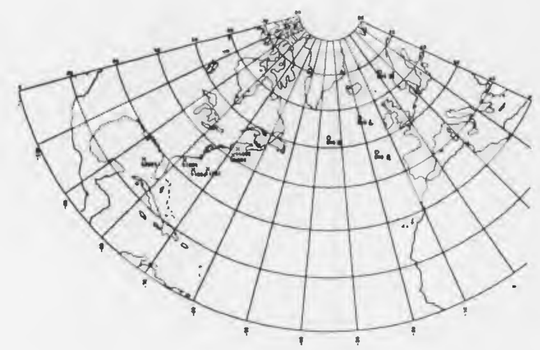

Fig. 3: North Atlantic weather ship positions and NOAA-data-buoys that have been used for comparison with wind and wave model results.

For this contribution we took as a source the subjective analysis of the surface pressure from the German weather service (Seewetteramt Hamburg). This information is available on routine working charts at intervals of six hours. The isobars of the charts have been digitized and the first and second derivatives were calculated

$$G = \left\{ \frac{\partial p}{\partial x_1}, \frac{\partial p}{\partial x_2}, \frac{\partial^2 p}{\partial x_1 , \partial x_2}, \frac{\partial^2 p}{\partial x_1{}^2}, \frac{\partial^2 p}{\partial x_2{}^2}, \frac{\partial^2 p}{\partial x_1\ \partial t}, \frac{\partial^2 p}{\partial x_2\ \partial t} \right\} \qquad (1)$$

With a linear transformation A, the row matrix G is transformed into a surface wind vector $\vec{U} = (U_1, U_2)$ at a nominal height of 10 m:

$$\vec{U} = A \cdot G \qquad (2)$$

The coefficients of the matrix A are valid for oceanic conditions and depend on the air-sea temperature difference.

An example of a wind field derived in this manner is shown in fig. 4. Here G is calculated from pressure values on a spatial grid of 55 km.

In order to demonstrate the importance of the pressure grid to be sufficiently small, fig. 5 shows a wind field derived from the same pressure field resolved on a 385 km grid and afterwards interpolated to the 55 km grid. It is obvious that the errors introduced are very large. The vector differences of both fields are shown in fig. 6.

A verification of this surface wind model has been done with wind measurements from the German research platform 70 km NW of Helgoland. Ten-minute averages of wind measurements at a height of 40 m were scaled to a nominal height of 10 m and compared with the model wind at the associated grid point.

The result is given in the table 1 for 1983. Such a comparison for the purpose of calibrating satellite data should be improved in several respects. For instance, it should be distinguished between several

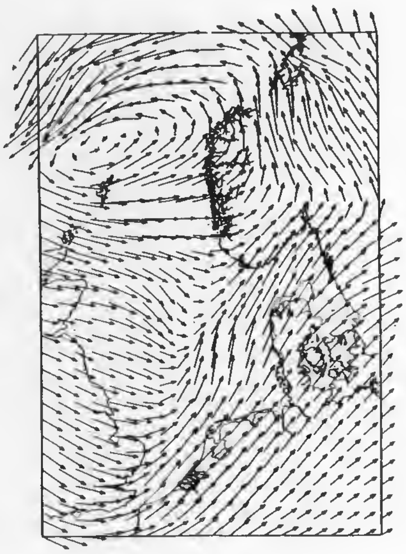

Fig. 4: Wind field, calculated from a pressure field, given on a grid spacing of 55 km. The arrow length of 1 grid length corresponds to 10 m/s wind speed.

classes of weather situations, stability conditions and wind directions. The 10-min average should be replaced by a longer averaging period. Presumably a two or three-hour time averaging of the measured wind would be more appropriate to compare with a model wind representing a spatial average over an area of 50 km x 50 km.

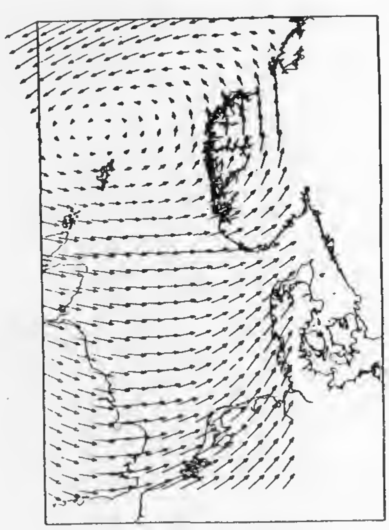

Fig. 5: Wind field, calculated from the same pressure field as in fig. 4. For the calculation of the pressure differences each seventh grid point is used, corresponding to a grid spacing of 385 km. The intermediate points in the wind field are interpolated.

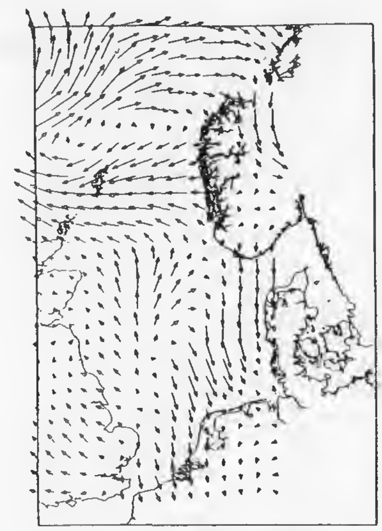

Fig. 6: The vector difference of the wind fields in figs. 4 and 5

Table 1: Differences in wind speed and wind direction (model-measurement) for January-November 1983.

Wind Speed

Month	Number	Av.Obs	Av.err	RMS	Minus	Plus	Scatter Index
1/83	124	13.00	1.86	3.31	40	84	25.43
2/83	106	8.57	-.45	3.32	64	42	38.72
3/83	106	8.91	.80	3.86	39	67	43.28
4/83	119	7.61	-1.02	2.97	77	42	38.97
5/83	121	7.01	-1.10	3.43	85	34	48.93
6/83	118	7.40	-.74	2.30	81	37	31.07
7/83	124	6.45	-.63	2.90	79	45	44.96
8/83	115	6.78	-1.40	2.88	81	34	42.40
9/83	120	10.17	-1.08	3.00	83	37	29.55
10/83	122	11.61	-.22	3.11	66	55	26.76
11/83	88	7.58	-.34	3.01	46	42	39.65
12/83	0	0.00	0.00	0.00	0	0	0.00

Wind Direction

Month	Number	Av.err	RMS	Left	Right
1/83	124	-.45	17.30	66	58
2/83	106	4.11	42.08	52	54
3/83	106	2.47	35.93	40	66
4/83	119	7.36	42.92	50	69
5/83	121	1.91	57.22	45	75
6/83	118	-2.51	38.16	68	50
7/83	124	-14.27	50.92	88	36
8/83	115	-8.27	50.77	75	40
9/83	120	-7.11	27.78	81	39
10/83	122	-10.88	25.68	90	32
11/83	88	-6.98	56.98	52	36
12/83	0	0.00	0.00	0	0

Wave data

Ocean wave models are driven with the model winds to produce output fields of wave spectra. It is normally not possible to verify the two-dimensional spectral output because there are no commercially available instruments for routine measurement. The wave data output is, therefore, reduced to directional or frequency integrated quantities that are available from routine buoy measurements. Normally even more reduced information is compared, such as significant wave height, mean period, mean direction. Fig. 7 shows wave height isolines of a wave field modelled for the North Sea and the Dutch station K 13 equipped with a wave rider. A typical time series of wave height for station K 13 is given in fig. 8. Table 2 provides an example of a verification statistic for wave models at K 13 (reference 1)

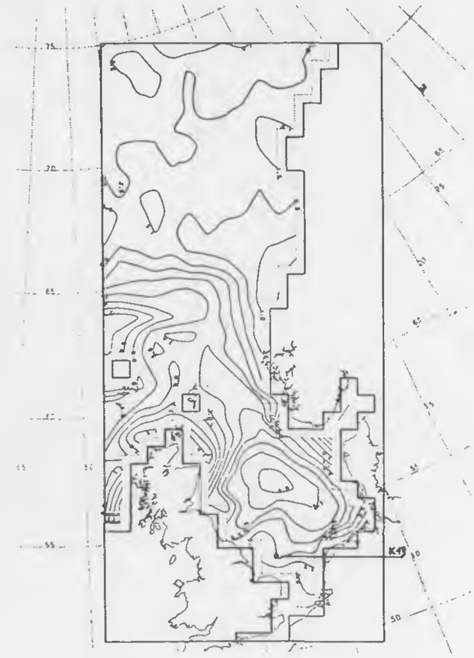

Fig. 7: Isolines of significant wave height and location K 13.

Table 2: Statistical parameters for April 1980 concerning the numerical wave models GONO and HYPAS at three North Sea stations (K 13 from the text is the same as Pennzoil)

Station	average error HYPAS	GONO	RMS HYPAS	GONO	scatter HYPAS	GONO
	cm	cm	cm	cm	%	%
Euro	10	-6	34	40	28	33
Ijmuiden	11	-5	39	46	28	34
Pennzoil	9	2	44	49	29	33

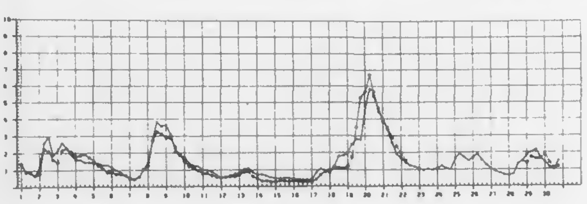

Fig. 8: Time series of significant wave height at location K 13.

3. THE SATELLITE WIND FIELD

The satellite wind field is derived by Ph. D. Associates from Microwave data (SMMR) of the NIMBUS 7 satellite. The algorithm is based on a measured linear increase of microwave radiation in the 18 GHz and 37 GHz band with increasing wind speed. The wind direction is not detected by this measurement. The approximate distance between adjacent measurements is 30 km. The satellite data we were using in this work are given in fig. 9. The overflight was on 16.1.1982 at 10 h UTC. In the figure the length of the bars indicate the wind speed. The distance between neighbouring grid points corresponds to 25 m/sec. The modelled wind is depicted by white bars. The corresponding satellite wind is given by the hatched bars.

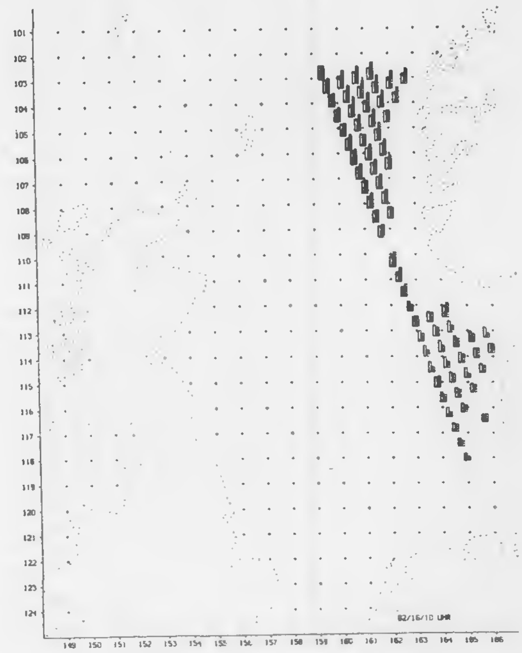

Fig. 9: Satellite measurements of wind speed (hatched buoys) compared with model derived wind speeds. The bar length is proportional to the wind speed. 1 grid distance corresponds to 25 m/s.

4. COMPARISON OF SATELLITE DERIVED AND CONVENTIONAL DATA

Since the satellite data normally are available at times which do not coincide with the six hour schedule of the meteorological weather charts (0 h, 16 h, 12 h, 18 h), the model data must the interpolated in space and time. Because the change of the local pressure during 6 hours is mainly due to propagation of the spatial pressure pattern, it seems inappropriate to interpolate in time at a fixed location. We try to incorporate the propagation effect by Fourier-transforming the pressure field in space at time T_1 and $T_2 = T_1 + 6$ h:

$$p(\vec{x}, T_1) = \sum_{\vec{k}} \alpha(\vec{k}, T_1) \exp(i \vec{k} \vec{x}) \qquad (3)$$

For an intermediate time $T_1 < t < T_2$ we interpolate the phase and amplitude of the complex $\alpha_{\vec{k}}$ linearly:

$$\text{phase } \alpha_{\vec{k}}(t) = \text{phase } \alpha_{\vec{k}}(T_1) + \frac{t - T_1}{T_2 - T_1} (\text{phase } \alpha_{\vec{k}}(T_2) - \text{phase } \alpha_k(T_1)) \qquad (4)$$

$$|\alpha(\vec{k},t)| = |\alpha(\vec{k},T_1)| + \frac{t - T_1}{T_2 - T_1} (|\alpha(\vec{k},T_2)| - |\alpha(\vec{k},T_1)|) \qquad (5)$$

The pressure field at t is then Fourier-synthesized:

$$p(\vec{x},t) = \sum_{\vec{k}} \alpha_{\vec{k}}(t) \exp(i \vec{k} x) \qquad (6)$$

After the derivation of the windfields with the algorithm described in section 2 we get table 3 for the error statistics between model- and satellite-derived wind.

Table 3: Statistical differences between satellite derived and analyzed pressure at 16 January 1982

mean difference:	1.28 hecto pascal
r.m.s error :	3.78 hecto pascal

5. THE CONVERSION OF SATELLITE DERIVED SURFACE WINDS INTO SURFACE PRESSURE

The knowledge of the transformation matrix A in the previously mentioned relation

$$\vec{U} = A \cdot G \qquad (7)$$

enables us to derive an inverse transformation matrix B that converts surface winds into surface pressure. As G contains first and second derivatives (thus using slope, curvature and advection information of the pressure field) we can start with quantities similar to the surface wind

$$H = \left(U_1, U_2, \frac{\partial U_1}{\partial x_2}, \frac{\partial U_2}{\partial x_1}, \frac{\partial U_1}{\partial x_1}, \frac{\partial U_2}{\partial x_2}, \frac{\partial U_1}{\partial t}, \frac{\partial U_2}{\partial t}\right) \qquad (8)$$

and derive a relation

$$\vec{\nabla} p = \left(\frac{\partial p}{\partial x_1}, \frac{\partial p}{\partial x_2}\right) = B \cdot H \qquad (9)$$

For the present purpose of demonstration we omit, however, all derivatives in H.

As pointed out to us by T. Guymer the method is similar to the technique proposed by Endlich et al. (reference 2). Our transformation into pressure is, however, not the pure geostrophic relation but in contrast to ref. 2, takes into account friction effects of the boundary layer. The wind direction is of course taken from the modelled wind field since it is not provided by the SMMR data.

The motivation to derive the pressure gradient field is manifold:

1. From the gradient field the pressure field can be derived (for an integration constant, the surface pressure at one location must be known) and directly compared with isobar charts of the usual kind.

2. Numerical atmospheric models that are forced to assimilate surface wind data may react by modifying the boundary layer without effect on the upper layers. The assimilation of pressure data derived from the surface wind is assumed to give a stronger effect on the numerical three dimensional fields in numerical atmospheric models.

3. Errors and ambiguities in the surface wind field will be mapped by relation (2) into errors and ambiguities of $\vec{\nabla} p$. Those deficiencies may be corrected by using the mathematical identity for the gradient of a function of x,y:

$$\vec{\nabla} \times \vec{\nabla} p(x,y) = 0 \qquad (10)$$

which holds for any closed integration path.

4. Pressure data are less sensitive than wind data to the sensor position in the neighbourhood of buildings. There is no danger of shadowing effects as there is in the case of wind measurements. For calibration and comparison, therefore, data from coastal stations, oil rigs and ships of opportunity may be useful. The wind data from such stations are, however, not always reliable.

Fig. 10 shows the analyzed pressure data and fig. 11 the satellite derived pressure fields. They are generated by integrating the pressure gradients in space. The integration starts at arbitrary points where the pressure is taken from the analyzed fields. Fig. 12 gives the differences of the two fields. The SMMR-data are influenced by heavy rain and are not applicable in the vicinity of land-sea-boundaries. In fig. 12 this seems to result in fairly constant pressure differences in areas more than 100 km from land boundaries and increasing differences in some areas within this distance from land. From the exact positions in fig. 9 of the satellite data it can be deduced, that our procedure works well for the actual pass of the satellite and becomes erroneous in areas where spatial extrapolation of the pressure gradient is involved.

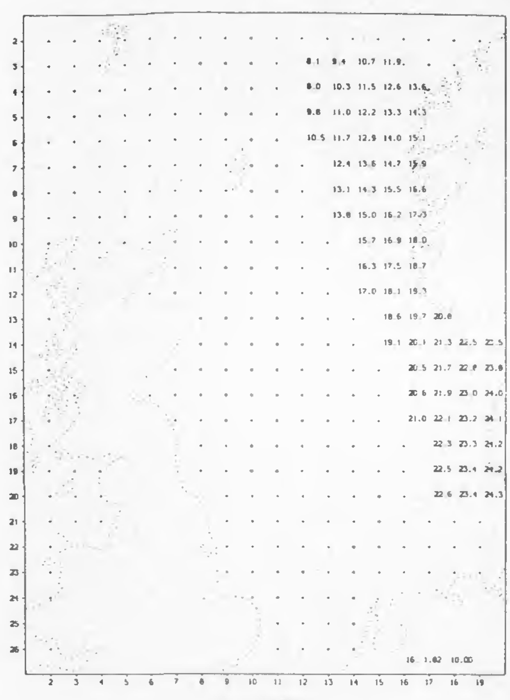

Fig. 10: Pressure from the meteorological analysis interpolated to the satellite pass.

6. SUMMARY OF A CALIBRATION STRATEGY FOR SATELLITE PARAMETERS

a. As an example we take the two components of the wind field for an oceanic region and prepare the analysed surface wind field.

   In that region one or several locations with reliable wind measurements should be available.

b. At that locations monthly the U_1, U_2 components from measured data and from analysed data have to be compared.

In order to improve the analysed data we calculate the linear transformation Ω

$$(U_1, U_2)_n = \Omega * (U_1, U_2)_a \qquad (11)$$

that minimizes the squared difference:

$$< \left|(U_1, U_2)_m - (U_1, U_2)_n\right|^2 >. \qquad (12)$$

The averaging is over all suitably conditioned U_1, U_2 (for instance selected in groups with special wind direction).

The $(U_1, U_2)_n$ field is considered the best available wind field at the points where satellite data are available in the considered region and can, therefore, be used to calibrate the satellite data.

It is suggested that this calibration is not being done in quasi real time using the fast delivery products. The model input should be carefully prepared which causes the calibration result to be available with a delay of at least 3 weeks after the products from the satellite are ready for use.

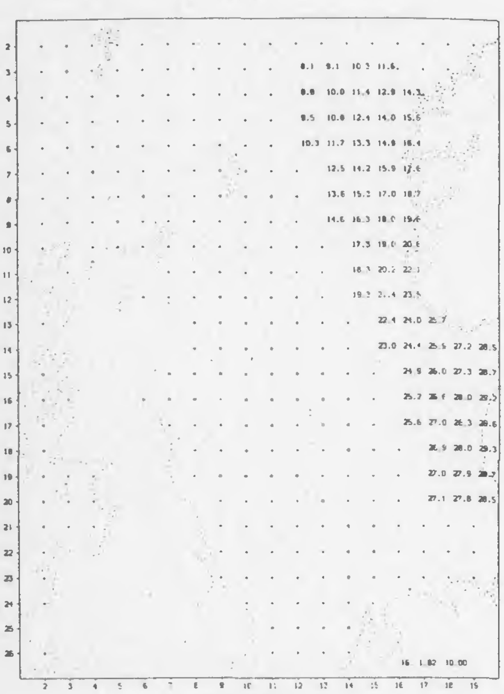

Fig. 11: Satellite derived pressure

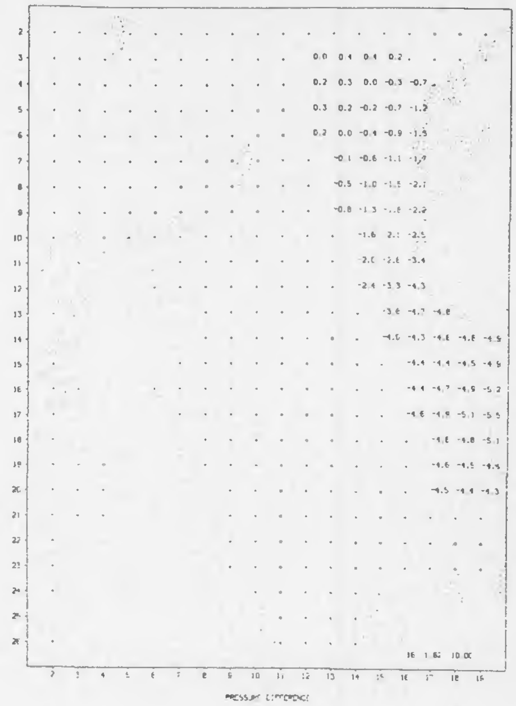

Fig. 12: Difference between satellite derived pressure and pressure analysis.

REFERENCES

1. Günther H, Komen G., Rosenthal W., "A Semi-Operational Comparison of Two Parametrical Wave Prediction Models", Dtsch. Hydrogr. Z. 37, p. 89-106, 1984.

2. Endlich Roy M., Wolf Daniel E., Carlson Christopher T., Maresca Joseph W. jr., "Oceanic Wind and Balanced Pressure-Height Fields Derived from Satellite Measurements" Monthly weather review, 109, 2009-2016, 1981.

VALIDATION OF ERS-1 WIND DATA USING OBSERVATIONS FROM RESEARCH AND VOLUNTARY OBSERVING SHIPS

P K Taylor

Institute of Oceanographic Sciences, Wormley, GODALMING, Surrey, UK.

ABSTRACT

A method for validation of ERS-1 wind measurements using observations from the Voluntary Observing Ships (VOS) is proposed. These data are available from most ocean regions allowing validation over a wide range of conditions. Although the observations are individually of poor quality, data from the North Sea is used to demonstrated that, where sufficient observations exist, a mean value averaged over one month and a few hundred kilometres should be accurate to 1m/s or better. For absolute calibration a subset of the VOS would be used. For these ships, the wind errors due to poor anemometer exposure must be determined. Results obtained by mounting a high mast in ships' bows are encouraging. However action is needed well before the launch of ERS-1.

Keywords: Voluntary Observing Ships, validation, winds, ERS-1.

1. INTRODUCTION

This paper will propose that observations from the Voluntary Observing Ships (VOS) of the World Weather Watch be used for validation of the ERS-1 wind measurements. Such a scheme would be in addition to the use of specially obtained observations from research ships or buoys. Although the latter method can provide high quality data there are limitations, particularly with regard to the number of satellite in situ coincidences and the range of conditions sampled. For example, algorithm development and validation of the wind measurements from the Seasat satellite made extensive use of observations from the Joint Air-Sea Interaction Experiment, JASIN (summarized by Guymer, ref. 1) . This 2 month experiment involved some 14 ships and 3 aircraft. However only a limited range of conditions was sampled and wind speed comparisons were restricted to the range 4 to 16 m/s. The cost of using even one or two research ships is high, and it will not be practicable to mount many campaigns specially for ERS-1.

Buoy deployments are less expensive and therefore allow sampling of larger and more varied ocean areas. Buoys present little airflow disturbance and have often been considered to give the best quality data. This is not necessarily the case. For example, Weller et al. (ref. 2) discuss accuracy problems for the JASIN buoy measurements used in Seasat validation. Careful attention to sensor exposure, calibration, and maintenance is necessary. Buoys can then be used to obtain accurate measurements (Ezraty, ref. 3).

Within the World Weather Watch VOS scheme there are over 7500 ships which make observations upto 4 times daily. The VOS observations were used, for example, by Liu (ref. 4) to extend the Seasat validation over a wider range of atmospheric stability and sea surface temperature than was experienced during JASIN. However there has not been extensive use of the VOS data for satellite validation because of doubts as to its inherent accuracy. For example, Guymer et al. (ref. 5) found that, whereas the scatter of Seasat SASS winds compared to JASIN observations was about $\pm$1.5m/s, comparison with North Sea VOS observations gave about $\pm$4m/s scatter. At first study, detailed discussions of the errors in VOS observations presented by Blanc (refs. 6 - 8), apparently demonstrate that the VOS data are not of useful quality.

It must, however, be stressed that the use of VOS data proposed in this paper is fundamentally different from the point by point comparisons used, for example, for Seasat/JASIN validation. Rather than compare individual ship observations with particular satellite passes, each type of data will be used to calculate a mean value for a given area and over a chosen period. Thus there will be no requirement for simultaneous satellite and in situ observations. The aim will be to perform the satellite validation using mean values which, despite being derived from a large number of individually inaccurate estimates, are themselves accurately calibrated. It will also be assumed that it will be basic quantities such as windspeed that will be validated. This avoids the uncertainties involved in using the bulk formulae to calculate fluxes (e.g. Blanc, ref.7).

By validation of ERS-1 measurements using, in effect, the whole VOS fleet, far more data will be available for comparison than if a limited number of high quality measurements were used directly. However, accurate measurements will be required for calibration of the VOS observations. It will be suggested that carefully quality controlled and calibrated anemometer wind measurements from a subset of the VOS could provide these reference measurements. The calibration of the VOS fleet could begin immediately, and need not await the launch of ERS-1.

This paper will consider the likely success of such a technique if, for illustration, mean values over a one month period, and an area of order one to two hundred km square, were to be used. However, first the characteristics of the VOS data set must be reviewed.

2. THE VOS DATA SET

2.1 Data distribution

Over 4000 observations are obtained from the VOS on a global basis each day. In one month there are about 40000 observations from the North Atlantic alone. The observations are not evenly distributed but are concentrated in the shipping lanes. For validation purposes this is an advantage. It is possible to identify ocean regions in both hemispheres where more than 150 observations are received each month from each 5 degree square area. Such observational densities occur over much of the north Atlantic and north Pacific, and in southern hemisphere shipping lanes such as that from Cape Verde, Senegal, to the Cape of Good Hope.

2.2 Observation method

The declared method of wind measurement for each VOS is listed in the WMO List of Selected Ships ("WMO47", ref. 9). The winds are either read from an anemometer or estimated subjectively using the Beaufort Scale. Table 1 shows the percentage of ships using each estimation technique for the entire VOS fleet and for the six largest national fleets (1984 figures). The actual percentage of observations made using each method may be somewhat different and will vary significantly from one area to another.

Country	Beaufort	Anemo	Hand anemo
USSR	100	0	0
USA	63	37	0
Japan	0	97	3
F.R.Germany	97	3	0
UK	~100	<1	0
Canada	22	75	3
All VOS	66	22	11

Table 1. Percentage of VOS using Beaufort estimates, fixed or hand held anemometers.

2.2.1 Anemometer readings An increasing number of ships use anemometers supplied either by the Meteorological Agency recruiting the VOS, or by the shipping company for use during docking etc. Anemometers might be expected to give good data for satellite validation. However there are a number of problems. Siting, calibration and maintenance of anemometers on ships is not easy and the accuracy of anemometer derived winds is questionable (see section 4.2 below). Often only instantaneous dial readouts are provided and the observer is instructed to average the values by eye over two minutes. This is both impracticable and, because it provides only a short sample of a rapidly varying quantity, inadequate (e.g. Pierson, ref. 10). In those cases where hand-held anemometers are provided, in rough weather it is unlikely that the observer would either wish, or be able, to stand in a suitably exposed position.

2.2.2 Beaufort Scale estimates The majority of ships report, as wind observations, subjective estimates of the Beaufort wind force by the ship's officers. These are based on visual observation of the sea state, with factors such as the handling of the ship also contributing, particularly at night. That such data might be of use for satellite validation may seem unlikely. However the method does have a number of advantages over the use of anemometers. Because the observed sea state is determined by the integrated effects of the wind over perhaps the previous hour, the Beaufort estimate includes a degree of averaging on scales similar to a satellite sensor footprint. The observation height is effectively the sea surface; and the problems of obtaining adequate anemometer exposure are avoided.

There have been several recent studies of the accuracy of the Beaufort technique (e.g. refs. 11 - 13) Individual wind estimates are subject to large scatter, for example ± 5 m/s at 20m/s (ref 11). However where a large number of observations are available during a particular averaging period it is only the magnitude of any systematic errors that is important. The problem then reduces to the accuracy of the scale used in converting the Beaufort estimates into wind speed values. Since 1970 the scale recommended for scientific use has been different from that used by the ships' officers when making the observations. However, even following correction for this, uncertainty still exists at about the 10% level (Taylor, ref. 14). It is possible that this uncertainty will vary regionally due to different sea conditions, a varying mix of ship types, and similar factors.

3. QUALITY OF VOS OBSERVATIONS

3.1 Method of Assessment

Given that errors exist in both anemometer and Beaufort estimates, will the VOS observations be of any use for ERS-1 calibration? A preliminary investigation has been made using VOS data (for the months of February, March and April 1984) from the North Sea. This region was chosen because it contains a number of fixed platforms which provide regular weather observations. These include meteorological buoys and towers, light vessels, and oil rigs.

The quality of the data will vary from one platform to another, and may or may not be better than that achieved by the VOS. However each platform should provide a consistent series of data for comparison with the VOS observations. Within the area surrounding the platform there will be a constantly changing subset of VOS. The comparison results will therefore show the degree of consistency between different VOS, and between the VOS and the platforms. It will not be possible to determine the absolute accuracy since an independent high quality standard is not available.

The comparison results are also of interest because it has been suggested that ERS-1 winds should be validated using wind observations from such fixed platforms as oil rigs, light-houses etc. One problem of this approach is the impossiblity of bringing the reference sites together for intercomparison. This study will show whether the VOS could be used as transfer standards between the reference sites.

3.2 Platform Characteristics

Of the different available platforms, four were selected as representative, these being a meteorological buoy, a meteorological platform, a

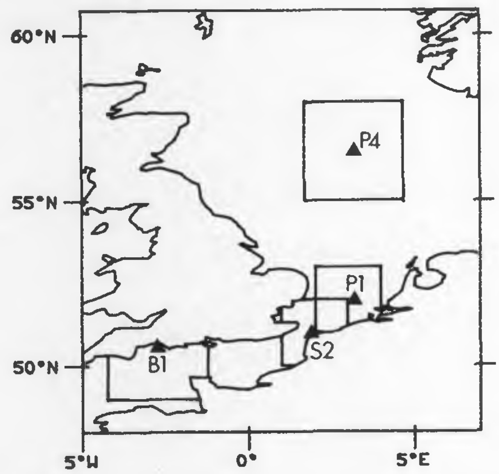

Figure 1. Positions of the chosen fixed platforms and the surrounding VOS areas.

light vessel, and an oil rig. For ease of reference they have been given the labels shown below. Table 2 gives their positions and these are illustrated in figure 1.

3.2.1 Meteorological Buoy - "B1" situated 10 km from the coast in Lyme Bay in the English Channel. Since the Offshore Data Aquisition System (ODAS) buoys are directly maintained by the Meteorological Office, "B1" should be a source of high quality data. Observations are normally obtained every 3 hours, about 200 reports were available during each study month.

3.2.2 Meteorological Platform - "P1" This and the nearby "P2" (Goeree light tower) and "P3" (Meetpost Noordwijk) are platforms in the Dutch North Sea meteorological observing network. The platforms are larger and present more flow distortion than a buoy. However the sensors are well exposed and high quality data should be expected. A complete set of 3 hourly observations was available from each platform.

3.2.3 The Dunkerque light vessel - "S2" In the same region reports are also available from "S1" (the Bassurelle light vessel) and "S3" (the Sandettie Light Vessel). These are a reliable data source giving on average about 160 observation each month. However meteorological observations are not their primary purpose.

3.2.4 Oil Platform - "P4" The Ekofisk Oil Platform Complex was chosen. It provides about 200 reports each month. Other nearby oil platforms are "P5" (Fulmar) and "P6" (Auk) providing 230 and 130 obs. per month respectively. An advantage of the oil platforms is that they are far from the coast. However it is extremely difficult to ensure good anemometer exposure on such large constructions.

3.3 VOS observations

The areas for which the VOS observations were selected are shown in table 2 and figure 1. In order to examine the worst case, the data used were the original ship reports as received over the WWW Global Telecommunications System. Thus the quality control procedures normally used by Meteorological Agencies had not been applied. No

Reference Platform	Other	Platforms	VOS Area Lat -degs- Long
"B1" 50.6N 2.7W			49-51N 4.2-1.2W
"S2" 51.0N 1.9E	"S1" 50.5N 0.9E	"S3" 51.1N 1.7E	50-52N 1.0-3.0E
"P1" 50.9N 3.2E	"P2" 51.9N 3.6E	"P3" 52.2N 4.2E	51-53N 2.0-4.0E
"P4" 56.5N 3.2E	"P5" 56.5N 2.1E	"P6" 56.4N 2.0E	55-58N 1.7-4.7E

Table 2. Position of the fixed platforms and the areas from which VOS observations were chosen.

distinction was made between anemometer and Beaufort winds. It was, therefore, neither possible to correct the Beaufort winds to the "scientific scale" nor to adjust the anemometer winds for the height of observation. Thus the scatter demonstrated by the VOS observations in this study should represent a worst case limit to that achievable.

In order not to bias the statistics, care was taken to reject observations from any ship which remained in the area for several days. This was a particular problem in the "P4" oil platform region. The average number of observations accepted each month was about 170 at "S2", 200 at "P4", and 285 at "B1" and "P1". Of the ships included, over 70% provided only one or two reports from the chosen area during a month. At "B1" where ships were on passage along the Channel, 90% of some 170 different ships each month reported at most twice. In total for the whole study 2813 observations were obtained from 676 different ships.

3.4 Comparison results

3.4.1 Monthly mean values Figure 2a shows the mean windspeed during each of the three months, as

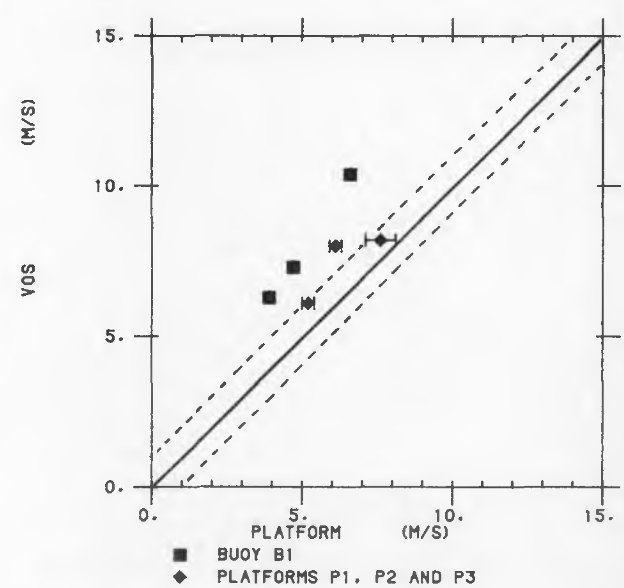

Figure 2a. Comparison of the monthly mean windspeed values for the "meteorological platforms" and the VOS. The error bars indicate the scatter for platforms P1, P2 and P3.

measured on the meteorological platforms (buoy "B1", and platforms "P1", "P2", and "P3"), plotted against the VOS values. For comparison the line of equality and $\pm$1m/s difference range is marked. In every case the VOS observed higher windspeeds than the platforms. This was particularly marked at "B1" which each month reported lower windspeeds than any other platform or any of the VOS data sets.

The comparison for the light vessels ("S2", "S1" and "S3") and oil platforms ("P4", "P5", and "P6") is shown in figure 2b. The agreement between these observations and the VOS values is generally within

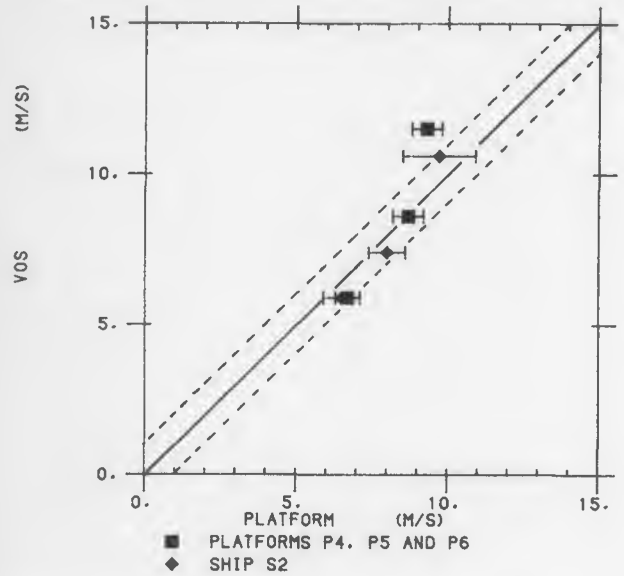

Figure 2b. As figure 2a but for the light vessels and oil rigs.

1m/s. However there is possibly a trend toward relatively higher VOS values at higher windspeeds.

3.4.2 Three-month windspeed distributions The characteristics of the three month data sets from

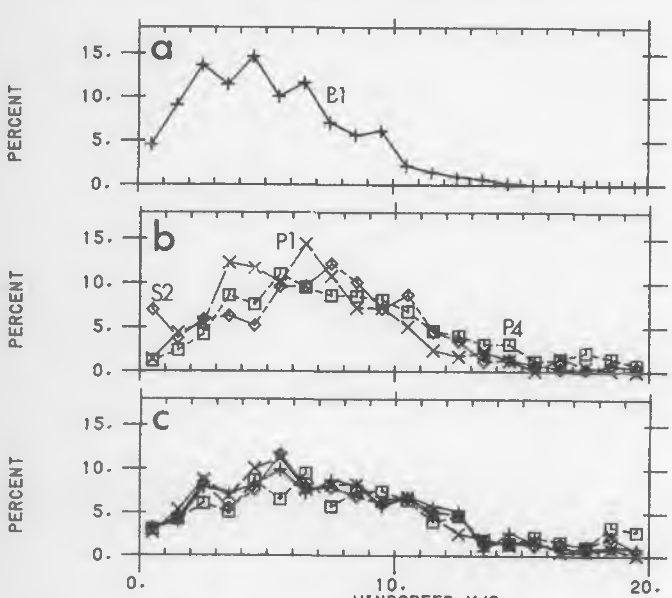

Figure 3. Histogram of wind speed values for the three month data-set: a) buoy "B1"; b) platforms "P1", "P4", and "S2" c) the four VOS areas.

each of the reference platforms is shown in figure 3a-b, the corresponding VOS values are shown in figure 3c. All the histograms have essentially similar shape except that for buoy "B1" (fig. 3a) which peaks at much lower values. Possible reasons are: an instrument calibration problem; the sheltering effect of waves at high sea states; or the inshore location of the buoy. The latter effects might be expected to vary depending on whether the wind was on- or off-shore, however no such effect could be detected.

The VOS histograms show less difference from site to site than do the reference platforms. However they do show more values at higher windspeeds, a tendancy which could possibly be detected in the mean values (figure 2b) and which is evident in individual reports.

3.4.3 Individual windspeed reports Figure 4a shows the time series of reports from "P1" for March with

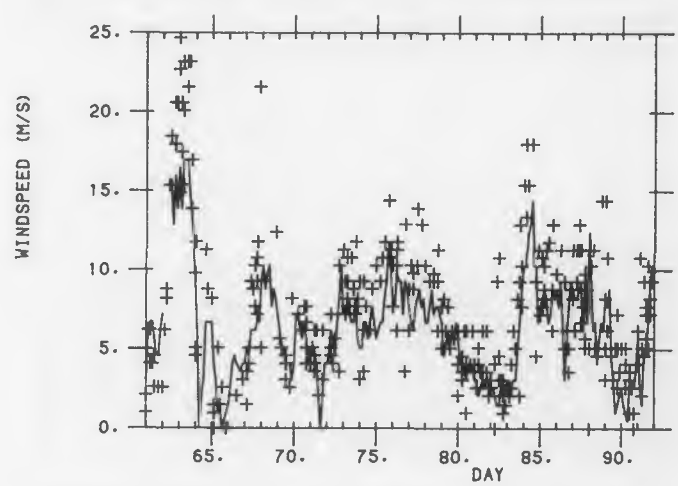

Figure 4a. Time series of windspeed at "P1" for March 1984 (solid line) and corresponding VOS reports (+).

the corresponding VOS reports. Data for other platforms and months were essentially similar. The tendency for the VOS to report higher values for higher wind speeds is evident both in this plot and

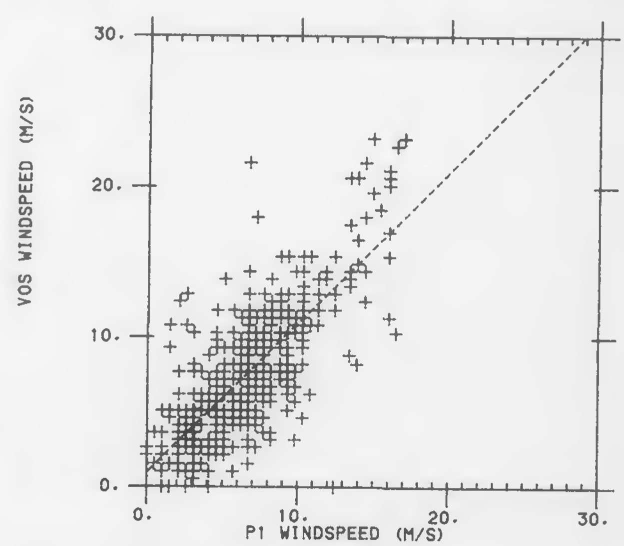

Figure 4b. Three month data-set of windspeed measurements at P1 compared to VOS reports

the associated scatter diagram (figure 4b). Some but not all of this trend would be removed if the ship reports based on Beaufort estimates were adjusted to the "scientific scale".

3.5 Discussion

The VOS data sets, consisting of observations from many different ships, give mean values which are in general consistent with those from the fixed platforms. The only exception, the meteorological buoy "B1", seems to have been due to anomalous platform values rather than the VOS data. Indeed, there is some evidence that the VOS set may be internally more self-consistent than those from the platforms.

The quality of the VOS data set is therefore encouraging, particularly since a "worst case" approach has been used (section 3.3). However before the VOS data is used for satellite validation, features such as the higher values reported in the upper windspeed ranges must be understood. It will also be necessary to calibrate the values against an absolute standard. The next section will consider ways in which the VOS data set might be improved both in terms of decreased random errors and absolute calibration.

4. CALIBRATION OF THE VOS OBSERVATIONS

4.1 Method

There is clearly an outstanding requirement for a set of reference measurements by which the rest of the VOS could be calibrated. Following the discussions presented by Blanc (ref 6) one might conclude that the best type of calibration site is a high mast on a small island. Unfortunately, suitable islands are few, and the site, with its special mast and equipment, would be expensive and difficult to maintain. If such sites could be established then they would form a valuable part of the calibration data set. However intercalibration of such sites would be difficult, and the site will need to be properly maintained over a decade or more if continuity of calibration between ERS-1 and successor satellites is to be achieved. Such continuity is vital for the full exploitation of ERS-1 for climate studies.

Those VOS ships which have anemometers in well exposed masthead positions represent a ready made island/mast combination. Since they move around, intercalibration is feasible. The problem to be considered is whether the necessary accuracy can be achieved.

4.2 Accuracy of anemometer winds

The effects of windflow disturbance by the ship have been discussed by Dobson (ref. 15), Blanc (ref. 6) and others. Investigations for anemometers on research ships are summarized in table 3.For relative winds within $\pm 45^{\circ}$ of the bow an accuracy of $\pm 5\%$ seems a good estimate. For other directions the errors are often larger and less predictable.

Merchant ships are larger and offer worse anemometer sites so even greater errors might be expected. However there is a possibility that some of the errors shown in table 3 were in reality caused by airflow disturbance at the reference anemometer site. This is particularly likely where a bow boom mounting was used. In any case the past results are often contradictory, and further investigation of errors in anemometer measurements on ships is therefore an urgent need.

Ref.	Standard Used	Wind Speed m/s	Relative wind direction On bow $\pm 45^{\circ}$	On beam	Astern 115°-255°
16	Met buoy	<8	<+3%	~0	
		~10	~-8%	-6%<x<+21%	
17	Buoys	<10	~0	-4%	
18	Bow boom	~8	-3%<x<+5%	-45%<x<-11%	
19	Bow boom	<10	-6%<x<-2%	-1%<x<+8%	-30<x<-65%

Table 3. Error of anemometer winds measured on research ships (adapted from Taylor, ref. 20).

We have constructed a 10m mast which can be mounted far forward in a ship's bow. It is designed so that, using a fast response anemometer, the surface stress can be determined using the inertial dissipation technique. Such data will be used for direct scatterometer validation. However the mast can also be used for calibration of ships wind observations. At the mast top, the anemometer is in the region were the flow disturbance by the ship is likely to be minimum, probably well under 10% for winds forward of the beam (e.g. Kahma and Lepparanta, ref. 21). Cases where the relative wind is from astern can be investigated either by relocating the mast or by steaming the ship in a pattern such that a undisturbed wind reading is periodically obtained. The latter will be difficult on a merchant ship so for a preliminary evaluation we are using measurements from research ships.

Results which have been obtained using this technique suggest that for many ships the major errors in the anemometer readings are due to nearby obstructions to the flow rather than by the general flow distortion around the ship. This can also be shown by using potential flow theory (e.g. Ref. 22) to calculate the windspeed error for an anemometer at different distances from a circular mast. Ships' masts are often of a size such that it is difficult for a mast mounted anemometer to be positioned at more than a few mast diameters distant. For a position 1 mast diameter from the mast face the wind speed is in error by over 10% even when the anemometer is upwind of the mast (figure 5). For this case, and in the large wake region, the wind

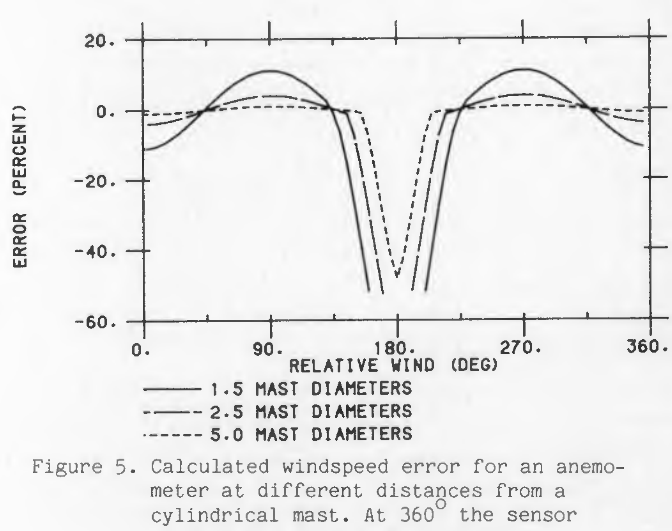

Figure 5. Calculated windspeed error for an anemometer at different distances from a cylindrical mast. At 360° the sensor is directly upwind of the mast.

is underestimated. When the relative wind is such that the mast is to one side an overestimate results.

Figure 5 shows that, with increasing separation between anemometer and mast, most of the errors decrease rapidly, becoming less than 2% at 5 (and well under 1% at 10) mast diameters. However the wake region persists for a considerable distance. Errors of order 20% still occur at 30 mast diameters although only for a narrow range of relative wind directions. This is illustrated in figure 6 which shows the windspeed error for an anemometer on the research ship RRS Discovery plotted against relative wind direction. The

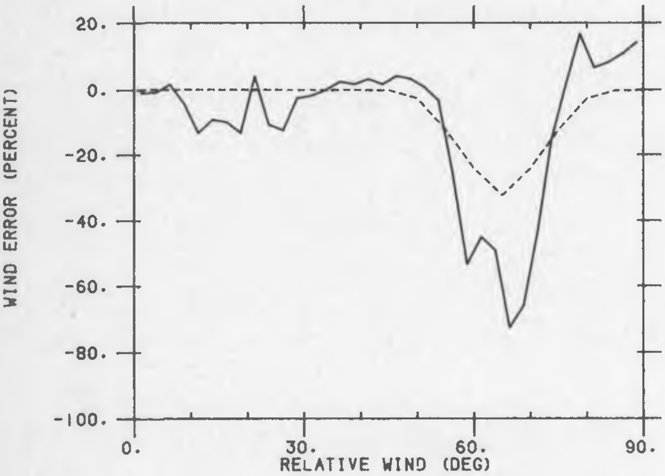

Figure 6. Measured anemometer error on RRS Discovery for different relative winds (solid line) compared to the calculated value (dashed line).

results were obtained while the ship repeatedly steamed round a triangular survey pattern. The wake caused by the foremast extension is evident and the angular region affected is well predicted by calculation. Wind errors within the wake depend on the turbulence and are hard to predict. Errors for other wind directions are also not well predicted, presumably because of the complex shape of the mast and ship compared to that assumed. Since this will generally be the case, it is probable that accurate calibration of anemometer winds will be by field measurements and wind tunnel studies rather than by calculation. However the degree of consistency from ship to ship is likely to be such that it will only be necessary to calibrate one ship of a given class.

With good exposure and careful calibration, ship-borne anemometers have been shown to give good results. For the JASIN ships Macklin and Guymer (ref. 23) found differences of ±0.75m/s or less. In the present studies, in a case where an anemometer was sited at the mainmast top, errors of less than ±1 m/s and ±2 degrees were found for almost all relative wind directions.

4.3 Discussion

The preliminary studies reported here suggest that anemometer measured winds from ships could be of adequate quality to be used to calibrate the VOS fleet and hence for ERS-1 validation. However several actions need to be taken:

i. Further research is needed into the errors of anemometer winds on ships.

ii. A suitable subset of the VOS must be selected taking into account anemometer type, exposure, calibration, and maintenance; routes plied, and other factors.

iii. For each of the chosen ships or ship classes the anemometer errors must be determined as a function of relative wind.

iv. Arrangements must be made to ensure that observations from the chosen ships are available in a form such that anemometer corrections can be applied.

The last point is important since at present the ships do not report the relative wind direction at the time of observation. Only the true wind and the ship's average course and speed over the preceeding three hours is available and this may not always be sufficient. It is unlikely that the extra information could be incorporated into the radio message but it could be recorded in the ship's meteorological log book for later recovery.

It has also been assumed that properly averaged winds are available from the chosen ships. On research ships this is usually achieved by computer. On merchant ships, manual observation of a dial will not be adequate and electronic averaging must be provided.

5. SUMMARY

It is proposed that observations from the fleet of Voluntary Observing Ships be used for validation of the ERS-1 measurements. Such validation would be based on area and time means, a period of one month and dimensions of a few 100 km has been proposed. The technique exploits the concentration of the VOS observations within the shipping lanes, a factor which limits their usefulness for climate research. However an important property of satellite observations is the uniform global coverage. Thus the strengths of both types of observations would be employed.

The VOS observations have been compared with data from fixed platforms, including a meteorological buoy and towers, light vessels and oil rigs. The monthly mean VOS values appeared to be consistent with the platform measurements to about +1m/s. However the VOS tended to report higher wind speeds above about 10m/s. Histograms of the entire three month data set studied suggested that the VOS data was internally more consistent than the platform data. One platform, the meteorological buoy, appeared to consistently underestimate the windspeed. The performance of the VOS data could be improved by further quality control, by distinguishing between Beaufort and anemometer winds, and by applying the appropriate corrections to each type.

However there is still a need for an absolute calibration standard. It is suggested that a carefully chosen subset of the VOS be used for this purpose. Such ships would have carefully calibrated anemometers in well exposed positions. Even so, for some relative wind directions the data quality would be poor and the data would be rejected. Such quality control can be partly based on theoretical calculations and wind tunnel modelling, however field calibrations will also be needed. For this purpose we are using a 10m mast which can be mounted in the ship's bow.

It is suggested that the validation of ERS-1 using VOS observations appears to be a viable technique. Indeed, no single validation method is likely to be sufficient, and the limitations of other methods are such that the use of VOS data will probably also be a necessary technique. However a number of measures have been identified (section 4.3) which must be implemented if successful validation is to be achieved. These include further research, selection of the calibration subset of the VOS, and changes to the method of data reporting. Since these actions would result in improvements to the VOS system they are in accord with WMO resolutions. However the requirements of satellite validation may go beyond those for weather forecasting. Therefore extra funding may initially be necessary to ensure implementation. Considering the large source of free validation data which would then be available, the amounts involved would be modest. Implementation of these measures needs to begin now in order to be ready for the launch of ERS-1.

6. ACKNOWLEDGEMENTS

The VOS data used in this study were provided by the U.K. Meteorological Office. P.W.Larkin prepared the data and wrote programs used in the analysis.

7. REFERENCES

1. Guymer T H 1983 Validation and applications of SASS over JASIN, in Satellite Microwave Remote Sensing, Allan T.D. (Ed), Chichester, Ellis Horwood Ltd., 87 - 104.

2. Weller R A, Payne R E, Large W G, & Zenk W, 1983 Wind Measurements From an Array of Oceanographic Moorings and From F/S Meteor During JASIN 1978, J Geophys Res 88, 9689 - 9705.

3 Ezraty R, 1986 Using Buoy and ships to calibrate ERS-1's Altimeter and Scatterometer (this volume)

4. Liu W T 1984 The Effects of the Variations in Sea Surface Temperature and Atmospheric Stability in the Estimation of Average Wind Speed by Seasat-SASS, J Phys Oceanog 14, 392 - 401.

5. Guymer T H, Challenor P G, & Zecchetto S, 1986 An evaluation of Altimeter and Scatterometer Winds in European Waters, (submitted to Earsel/ESA Symp on Europe from Space, Lyngby, Denmark, 25 - 28 June 1986).

6. Blanc T V 1983 A Practical Approach to Flux Measurements of Long Duration in the Marine Atmospheric Surface Layer, J Clim Appl Meteorol 22, 1093 - 1110.

7. Blanc T V 1985 Variation of Bulk-Derived Surface Flux, Stability, and Roughness Results Due to the Use of Different Transfer Coefficient Schemes, J Phys Oceanog 15, 650 - 669.

8. Blanc T V 1986 The Effect of Inaccuracies in Weather-Ship Data on Bulk-Derived Estimates of Flux, Stability and Sea-Surface Roughness, J Atmos Ocean Tech 3, 12 - 26.

9. WMO 1984 International List of Selected, Supplementary, and Auxiliary Ships, WMO-47, World Meteorological Organization, Geneva.

10. Pierson W J 1983 The Measurements of the Synoptic Scale Wind Over The Ocean, J Geophys Res 88, 1683 - 1708.

11. Graham A E 1982 Winds estimated by the Voluntary Observing Fleet compared with instrument measurements at fixed positions, Met Mag 111, 312 - 327.

12. Kaufeld L 1981 The development of a new Beaufort equivalent scale, Meteorol Rundsch 34, 17-23.

13. Quayle R G 1980 Climatic comparisons of estimated and measured winds from ships, J Appl Meteorol 19, 142 - 156.

14. Taylor P K 1984 The determination of surface fluxes of heat and water by satellite microwave radiometry and in situ measurements, in Large-Scale Oceanographic Experiments and Satellites, Gautier & Fieux (Eds), D.Reidel, 223 - 246.

15. Dobson F W 1981 Review of reference height for and averaging time of surface wind measurements at sea, Marine Meteorol & Related Oceanog Activities Rep 3, WMO, Geneva.

16. Augstein E, Hoeber H, & Krugermeyer L 1974 Errors of Temperature, humidity, and wind speed measurements on ships in tropical latitudes, Meteor Forsch Reihe B, 9, 1 - 10.

17. Large W G and Pond S 1982 Sensible and Latent Heat Flux Measurements over the Ocean, J Phys Oceanog, 12, 464 - 482.

18. Ching J K S 1976 Ships influence on wind measurements determined from Bomex mast and boom data, J Appl Meteorol, 15 102 - 106.

19. Kidwell K B & Seguin W R 1978 Comparison of mast and boom wind speed and direction measurements on U.S. GATE B-scale ships, NOAA Tech Rep EDS28

20. Taylor P K 1985 TOGA surface fluxes of sensible and latent heat by in situ measurement and microwave radiometry, in Rep Third Session JSC/CCCO TOGA Scientific Steering Group, WMO/TD 81, WMO, Geneva.

21. Kahma K K & Lepparanta M 1981 On errors in wind-speed observations on R/V Aranda, Geophysica 17, 155 - 165.

22. Kondo J & Naito G 1972 Disturbed Wind Fields around the Obstacle in Sheared Flow near the Ground Surface, J Meteorol Soc Japan, 50, 346 - 354.

23. Macklin S A & Guymer T H 1980 Inter-platform comparisons of JASIN WMO observations, JASIN News 15, 5 - 9 (Unpub. manuscript - available from IOS, Wormley, Godalming, Surrey, UK).

ACCURACY ESTIMATES OF WIND AND WAVE OBSERVATIONS FROM SHIPS OF OPPORTUNITY IN THE WMO VOLUNTARY OBSERVING SHIP PROGRAM

J Wilkerson

National Environmental Satellite, Data, and Information Service, NOAA
Washington, D.C., U.S.A.

ABSTRACT/RESUME

Wind and wave reports from ships of opportunity are compared with each other and with reports from 47 moored buoys when the ships were within 100 km of the buoys or each other at the same reporting times. Analyses were performed on more than 113,000 paired reports dating from 1973-1983. In general, standard deviations of differences for winds are of the order of 5-8 knots and 40°-50° with means of 2-4 knots and 10°. Poor agreement is the result of systematic errors shown to be in part the preference for reporting speed in multiples of 5 knots and directions near eight points of the compass. Differences in significant wave heights reported by ships and buoys have a mean of about 0.5 m with standard deviations of 1.5-2.5 m.

Keywords: Wind Speed, Wind Direction, Significant Wave Height, Ships, Buoys, Measurement Error

1. INTRODUCTION

This paper presents results of two studies funded by the National Environmental Satellite, Data, and Information Service, NOAA, to produce quantitative estimates of the accuracy of marine environmental reports from ships in the WMO Voluntary Observing Ship Program. This assessment was necessary to determine the roll of ships of opportunity in the validation planning of satellite oceanic measurements, since ships in the WMO voluntary program provide a large source of potential comparison data for such work.

The studies were conducted by Refs. 1 and 2. Both investigations produced statistical analyses of comparisons between marine observations from ships and buoys using the measurements from moored NOAA buoys as a standard. Table 1 provides information about the buoy measurements and states the estimated system accuracies. All available ship observations taken within 100 km of a buoy were used. Ref. 1 examined data collected during 1980-1983, compiling statistics for ship/buoy differences for all common parameters at 47 buoy stations. These parameters were wind speed, wind direction, atmospheric pressure, air temperatures, sea surface temperature, wave height and wave period.

The data base in Ref. 1 consisted of 62,898 pairs of reports. Statistics were calculated for many categories including station location, year, season and region (Atlantic, Pacific, Gulf of Mexico, etc.). Also, statistics were calculated for ranges separating ship and buoy at each station. The data base in Ref. 2, on the other hand, consisted of ship and buoy reports taken during the time period 1973-1979 and their analysis was of winds only. In addition to ship/buoy comparisons, ship/ship comparisons were also made. The data base in Ref. 2 consisted of 50,864 pairs of reports. All data were obtained from the National Climatic Data Center (NCDC), Asheville, N.C.

The conclusions in both of these studies are that reports of winds (both measured and observed) from ships of opportunity differ substantially from buoy measurements made at the same time when ships were within 100 km of the buoy. Typically,

Table 1. Buoy Measurement Information and Estimated Total System Accuracy

Measurement	Reporting Range	Sampling Interval	Averaging Period	Total System Accuracy (1σ)
Wind speed	0 to 155 knots	1 s	8.5 min	$\pm$1.9 knots or 10%
Wind direction	0 to 360°	1 s	8.5 min	$\pm$10°
Air temperature	-15° to 50°C	90 s	90 s	$\pm$1°C
Sea level pressure	900 mb to 1100 mb	4 s	8.5 min	$\pm$1 mb
Sig. wave height	0 to 20 meters	0.67 s	20 min	$\pm$0.5 meter
Wave period	2 to 30 s	0.67 s	20 min	$\pm$1 s
Surface water temp.	-15°C to 50°C	1 s	1 s	$\pm$1°C

mean differences were 2-4 knots with ships reporting higher winds than buoys over the full range of wind speeds. Standard deviations of differences were of the order of 5-8 knots, with no correlation of this variation with distance from the buoy, with its location in the network, or with season or year. Direction biases were usually within 10° with standard deviations of 40°-50°. As with wind speed, there was no correlation of these differences in direction with the various analysis categories. An unexpected conclusion was that measured wind speeds from ships equipped with anemometers were not significantly better than observed wind speeds reported from ships without anemometers, even when the measured winds were corrected for the differences in anemometer heights.

The data for differences in significant wave height were analyzed several ways because these observations are reported from the ships as sea and swell. The results for differences in significant wave height showed a bias between -0.5 m to +0.4 m with standard deviations ranging from 1.5 m to 2.4 m depending on the method of analysis used. (See Analysis Section).

The initial data consisted of magnetic tapes containing ship observations and buoy measurements. The ship observation data base contained several million reports with each report consisting of time, ship call sign, location, and the various observed and measured parameters. The initial buoy data base contained more than one million reports. Most ship reports were made at the synoptic times 0000 GMT, 0600 GMT, 1200 GMT, 1800 GMT, while most of the buoy reports were made hourly.

The ship data bases were decreased by removing observations for ships which were further than 100 km from buoy stations (or each other, in Ref. 2) and by retaining only the parameters common to the buoy measurements or those needed to adjust winds for anemometer elevations. The buoy data base was reduced by retaining only those measurements at synoptic reporting times for which ship observations were available. The reduced data bases were sorted and placed in chronological order. The sorted ship and buoy data bases were searched for pairs of simultaneous reports and difference statistics were calculated for pairs of common parameters.

Some screening of the data was performed at this stage to weed out obvious recording and transcribing errors and to remove pairs with missing data. Ref. 2 also rejected data pairs where either one or both of the wind reports exceeded 50 knots, because this value was greater than the size of their analysis matrix.

Errors that were not screened by these processes are: 1) incorrectly coded latitude and longitude in the 10's value that could place a ship that was actually somewhere else within 100 km of a buoy; and 2) the transposition of integers in the wind report that could, for example, result in a 13 knot wind being transposed to 31 knots and paired with another report of 10 knots. Similar transposition in wind directions would also be undetectable.

Some of the outliers in the data analyzed may be the result of these sources of errors. The possibility for these errors coupled with the results of these two studies indicate that great care is required in evaluating the results of any studies based on archived ship reports.

2. ANALYSIS

In Ref. 1, statistics were calculated for the parameters listed in Table 2. The symbols used are those in the listings in the complete report and in Table 3.

Table 2. Parameters for which statistics were calculated in Ref. 1

- Wind speed (knots)

  SPD(1) all ships (with and without anemometers)
  SPD(2) ships without anemometers
  SPD(3) ships with anemometers

- Wind direction (degrees)

  DIR(1) all ships (with and without anemometers)
  DIR(2) ships without anemometers
  DIR(3) ships with anemometers

- Atmospheric pressure (mb), PRES

- Air temperature (°C), T(A)

- Sea surface temperature (°C), T(S)

- Wave period (seconds)

  P(1) ship sea observations
  P(2) periods corresponding to the higher of ship sea or swell height observations

- Wave height (meters)

  H(1) ship sea observations
  H(2) the higher of ship sea or swell height observations
  H(3) the square root of the sum of the squares squares of ship sea and well observation

The definitions for P(2) and H(2) are those used in oceanographic atlases. Buoy wave heights are significant wave heights obtained from the total variance in wave spectra which the buoys transmit to shore. Buoy wave periods are zero-crossing periods obtained from moments of the spectra.

Analyses were performed using the units of the parameters as stored on the archival tapes i.e., wind speed in knots, wave height in meters, etc. To examine the possible correlation of accuracy with category, the difference statistics in Ref. 1 were grouped in the following joint categories:

Individual buoy stations (47)
Year (1980, 1981, 1982, 1983)
Quarter (Jan-Mar, Apr-Jun, Jul-Sep, Oct-Dec)
Range of ships from buoy (0-25 km, 25-50 km, 50-100 km)

Table 3. Example of Statistical Output (All Ships Within 100 km of All Buoys)

BUOY: ALL BUOYS YEAR: 80-83 QUARTER: 1-4 RANGE (KM): 0-100

	SPD(1)	DIR(1)	SPD(2)	DIR(2)	PRES	T(A)	T(S)	P(1)	H(1)	P(2)	H(2)	H(3)
MEAN	3.5	6.	2.5	8.	-.5	1.1	.1	-.5	-.5	-.2	.1	.4
STD. DEV.	7.7	47.	8.0	46.	4.2	4.3	3.5	2.8	1.5	2.4	2.2	2.2
NUM. OBS.	62898	60798	24221	23257	44477	61625	54172	35429	47273	22005	25566	25566

BUOY: ALL BUOYS YEAR: 80-83 QUARTER: 1-4 RANGE (KM): 0-25

	SPD(1)	DIR(1)	SPD(2)	DIR(2)	PRES	T(A)	T(S)	P(1)	H(1)	P(2)	H(2)	H(3)
MEAN	4.3	4.	2.4	6.	-.3	.9	-.3	.4	-.4	-.4	.0	.3
STD. DEV.	7.3	42.	7.4	40.	3.5	5.8	3.6	3.1	1.2	2.3	2.4	2.5
NUM. OBS.	11215	10791	3610	3442	4731	10904	9481	5515	8501	1997	2258	2258

BUOY: ALL BUOYS YEAR: 80-83 QUARTER: 1-4 RANGE (KM): 25-50

	SPD(1)	DIR(1)	SPD(2)	DIR(2)	PRES	T(A)	T(S)	P(1)	H(1)	P(2)	H(2)	H(3)
MEAN	4.2	5.	3.2	5.	-.6	1.1	.0	-.5	-.3	-.1	.1	.5
STD. DEV.	6.6	45.	7.6	44.	4.1	2.7	3.9	2.4	1.3	2.5	2.4	2.5
NUM. OBS.	21447	20755	5967	5745	9432	20113	17500	9322	15785	4669	5391	5391

BUOY: ALL BUOYS YEAR: 80-83 QUARTER: 1-4 RANGE (KM): 50-100

	SPD(1)	DIR(1)	SPD(2)	DIR(2)	PRES	T(A)	T(S)	P(1)	H(1)	P(2)	H(2)	H(3)
MEAN	2.7	8.	2.3	9.	-.5	1.1	.3	-.8	-.7	-.2	.1	.4
STD. DEV.	8.4	50.	8.3	48.	4.3	4.6	3.1	2.9	1.7	2.4	2.0	2.1
NUM. OBS.	30236	29252	14644	14070	30314	30608	27191	20592	22987	15339	17917	17917

Results were combined for the above detailed categories to provide statistics for the following regions:

Atlantic
Pacific
Gulf of Mexico
Great Lakes

Also, the years were combined to provide results for the four year period and ranges were combined to give results for the total range 0-100 km.

Wind speed and direction were analyzed in more detail than the other parameters. For the first pass through the data in Ref. 1, wind speed and direction statistics were calculated for all ship/buoy pairs. For the second pass, only ships without anemometers paired with buoys were selected and the wind speed and direction differences were recalculated. A third pass through the data was made to pair buoys with ships with anemometers with buoys at five buoy stations. The analysis was repeated for these ship/buoy pairs after adjustments were made to correct for differences in the anemometer heights. This reanalysis provided information on the effects of adjusting the ships' wind speed measurements to the elevations of the buoy measurements (5 m and 10 m) before comparisons. For the calculations, an atmospheric model developed by Ref. 3 was used. Also wind speed and direction differences as a function of wind speed categories were calculated.

In the Ref. 2 study, only one portion of the analysis (involving 6% of the data) dealt with paired ship and buoy reports and these were for winds only in Marsden Square 116. For the purposes of this analysis, ships were grouped into three categories, those with and those without anemometers, and a third group composed of ships whose call signs were not among those registered with the WMO. The ship reporting code states whether winds are measured or observed so this third category could have been separated and combined with the first two groups but this was not done.

Ref. 2 concentrated on paired ship difference of winds measured or observed within 100 km of each other in Marsden Squares 116, 120, 121, and 158. Ships with anemometers were paired with ships without anemometers and also with ships from the third group. Also examined were paired differences in all possible combinations including pairing ships in the same category. These analyses gave insight as to why reports from ships in the Voluntary Observing Program are in such disagreement with reports from moored buoys when measurements are taken at the same time and the platforms are in close proximity to one another.

3. RESULTS

The volume of results and detailed explanation from these studies cannot be properly presented in this paper. The complete findings of the numerous stratification of the data are left to the reader who may obtain copies of Refs. 1 and 2 by writing to the authors. A summary of the findings from these two studies follows.

Table 3 presents an example of the output of analyzed data from the Ref. 1 study. The first of the four groups of data presents a summary of the means and standard deviations of differences for all of the common parameters for the total data set. This presentation includes all buoy locations, all years, and all ranges out to 100 km. The numbers of observation pairs in each of the calculations is also indicated. The remaining three sets of data present the results after stratifying the data according to the distance of the ship from the buoy in range groups of 0-25 km, 25-50 km, 50-100 km.

Figures 1 and 2 illustrate the mean differences and standard deviations of the differences for wind speed and direction, as a function of buoy station, for the total ship data base in the Ref. 1 study. These results are plotted in approximate geographical order from Hawaii to Alaska and the Pacific Coast, through the Gulf of Mexico to the Atlantic Coast and the Great Lakes. These figures illustrate the findings of the more detailed analyses, i.e., that roughly similar differences occur for all buoys and that there is no clear geographical dependence. Large mean differences at a few buoy stations are usually due to a small number of comparisons which in some cases may be affected by poor quality control. The results for the five buoy stations, where ship measured winds were corrected for anemometer elevations, are displayed on Figures 1 and 2 for comparison.

Figures 3 and 4 show wind speed and direction differences as a function of wind speed categories as measured by the buoys, both for the total ship data base and for ships with anemometers near the five selected buoys. Substantial speed differences occur for all wind speed ranges. There is a significant decrease in direction differences away from low wind speeds where wind directions are often variable. The results for high speed categories for the individual buoys contain statistical uncertainties due to small sample sizes. The increasing positive bias (ship speeds higher than buoy speeds) as wind speeds decrease may be due largely to the fact that speeds are non-negative. An inherent scatter or random error in ship observations would cause a positive bias as zero wind speed is approached.

Figures 5 and 6 illustrate the mean differences and standard deviations of the differences for significant wave height and wave period as a function of buoy station, for the total data base. These figures present the results of the analysis of H(2) and P(2) in Table 2.

As previously mentioned, in the Ref. 2 study only a small portion of the analysis dealt with paired ship and buoy reports. The investigation focused on paired ship reports and on reasons for the large differences in the reported winds. In the analysis of 5,422 pairs of ship and buoy reports in Marsden Square 116, however, mean differences in wind speed were -3.4 to -0.4 knots with standard deviations of 6.5 to 7.6 knots. Direction means were -2° to 4° with standard deviations of 31° to 44°. These results are in agreement with the findings in Ref. 1.

In the examination of paired ship reports from a group containing both ships with and ships without anemometers, it was found that more than 51% of the wind speeds were evenly divisible by 5. The apparent reasons are that anemometer readouts are numbered in increments of 5 and if observations are made quickly rather than carefully, these types of display could lead observers to make gross estimates. The Beaufort scale also provides opportunities for reporting in multiples of 5 since Beaufort numbers 2 to 7 contain multiples of 5 and Beaufort 8 contains both 35 and 40 knots.

This finding is illustrated in Figure 7. To accentuate the reports that were evenly divisible by 5, values from each pair, if divisible by 5, were plotted on the vertical. This treatment produced a rose trellis effect. Shown also for each row are the totals, the mean, the variance, and standard deviation of differences for each value of wind speed on the vertical. This treatment highlights another finding, i.e., some ships have difficulty measuring light winds. When the ship speed on the vertical was reported to be calm, the second ship reported winds from calm to 45 knots.

Direction differences are shown in Figure 8. As in Figure 7, the rows show the variation in reports from the second ship when the first ship reported a value on the vertical axis. For ships without anemometers, Ref. 2 found that reports of direction tend to be near eight points of the compass. In treatment of data in Marsden Square 116, composed of 2,845 paired ships without anemometers, 47% of the directions clustered about these headings.

They also attributed differences in reported values of wind speed to be due in part to rounding errors in reporting winds measured in m/s and converted to knots. They showed that an error results from double rounding in the conversion. If the value in m/s is rounded to the nearest m/s and then converted to knots and rounded to the nearest knot, the result yields a doubly rounded value that can produce an uncertainty of ±1 knot.

4. CONCLUSIONS

The most important conclusion to be drawn from these studies for this meeting is that the systematic and random errors in the reports from ships in the Voluntary Observing Program make these data unsuitable for use in the calibration and validation of satellite remotely sensed wind and waves.

In all cases, the variability in the reported values exceeds the design specification for accuracy of measurement of the space sensors for the ERS-1, i.e., ±2 m/s or 10% for wind speed, ±20° for wind direction, and ±0.5 m or 10% for significant wave height. As noted, possible reasons for these random and systematic errors are that ship wind sensors may not be carefully calibrated or read; ship speed and direction may be incorrectly accounted for aboard ship in the vector calculation to change the relative wind to the true wind; and the measurements may be relatively instantaneous measurements which reflect natural wind variability and, consequently, are not equivalent to the longer 8.5 min. averages of winds from the buoys. Other systematic errors in wind reports result from the air flow around and over the ships for various wind directions, ship speeds and headings, and anemometer locations. Other systematic errors include rounding errors in converting from m/s to knots and a reporting preference for wind speeds in multiples of 5 and directions to eight points of the compass. For ships with anemometers, the correction for the speed and direction of the ship was found not to be done well. Reported wind speeds from ships with anemometers contained a mix of values with an exceptionally large proportion of speeds evenly divisible by 5 and with frequent errors in direction of close to 180°.

A surprising finding was that most of the ships in the Voluntary Program are undocumented by WMO. About 60% of the ship call signs in these studies could not be located on the data tape provided by WMO.

5. REFERENCES

1. Earle M 1985, Statistical comparison of ship and buoy marine observations, MEC Systems Corporation report MEC-85-8, 291 pp.

2. Dischel R & Pierson W 1986, Comparison of wind reports by ships and data buoys, in preparation.

3. Liu W & Blank T 1984, The Liu, Katsaros, and Businger (1979) bulk atmospheric flux computational iteration program in FORTRAN and BASIC, Naval Research Laboratory Memorandum Report 5291, 16 pp.

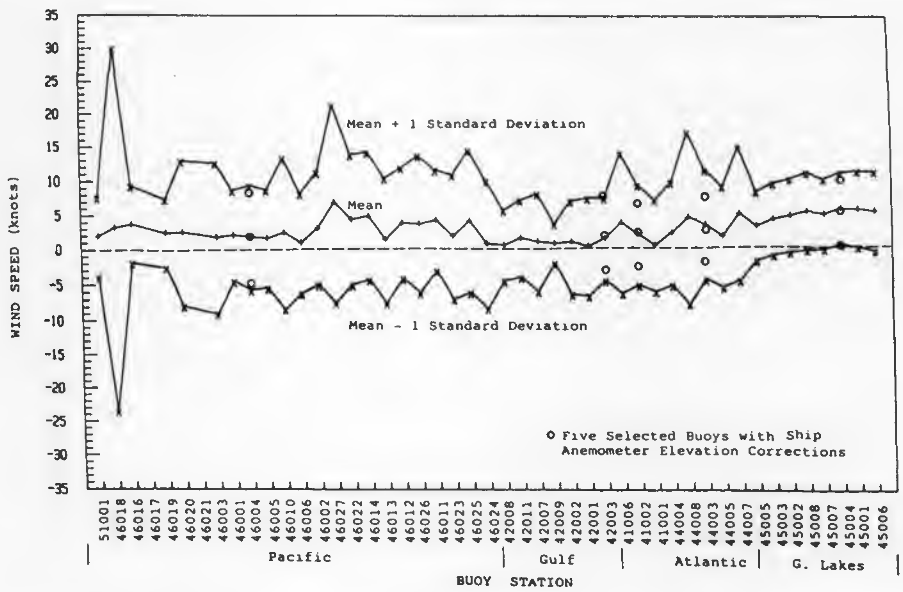

Figure 1. Wind speed differences as a function ofbuoy station (all ships)

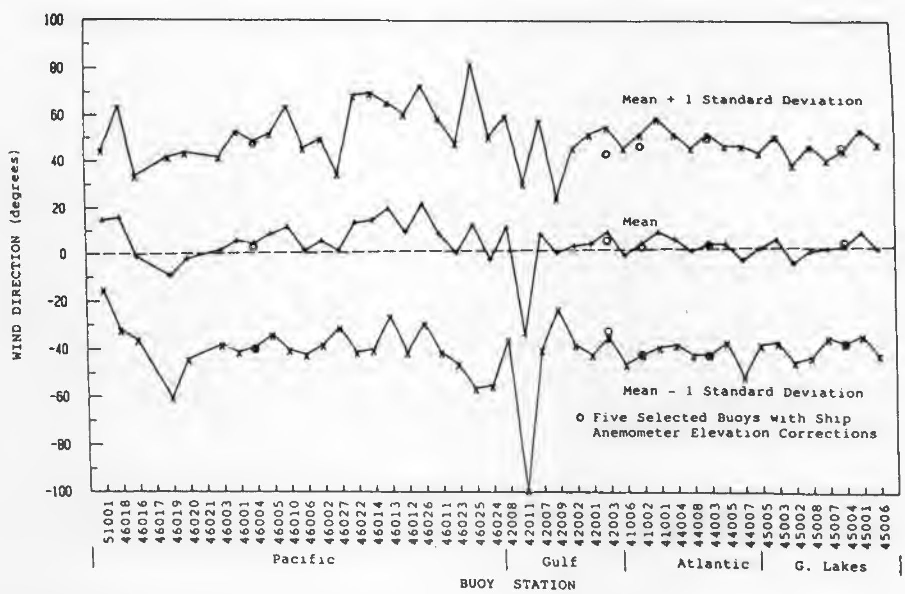

Figure 2. Wind direction differences as a function of buoy station (all ships)

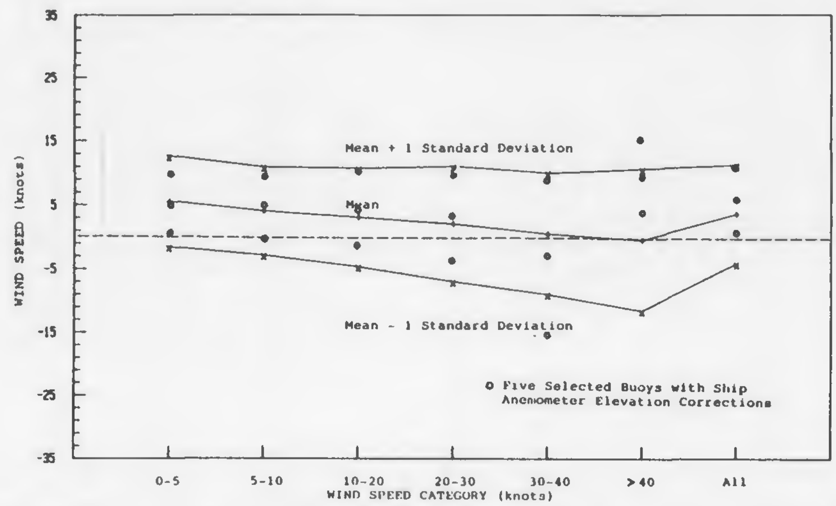

Figure 3. Wind speed differences as a function of wind speed category (all ships)

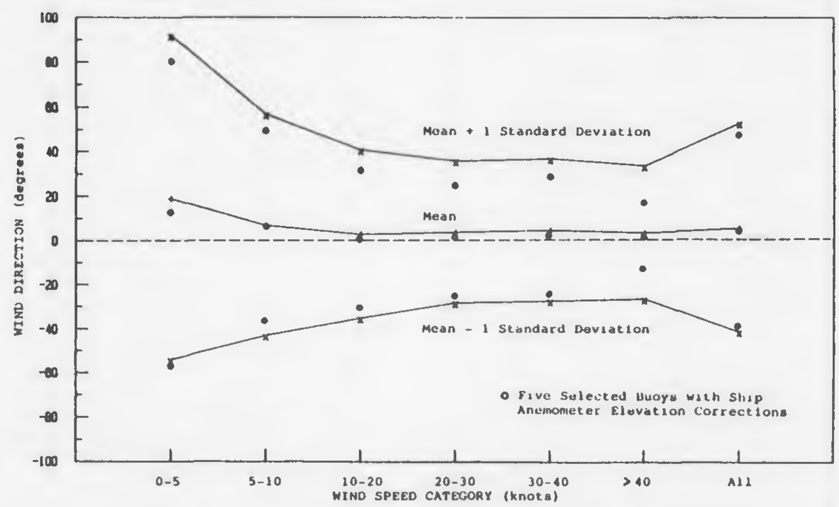

Figure 4. Wind direction differences as a function of wind speed category (all ships)

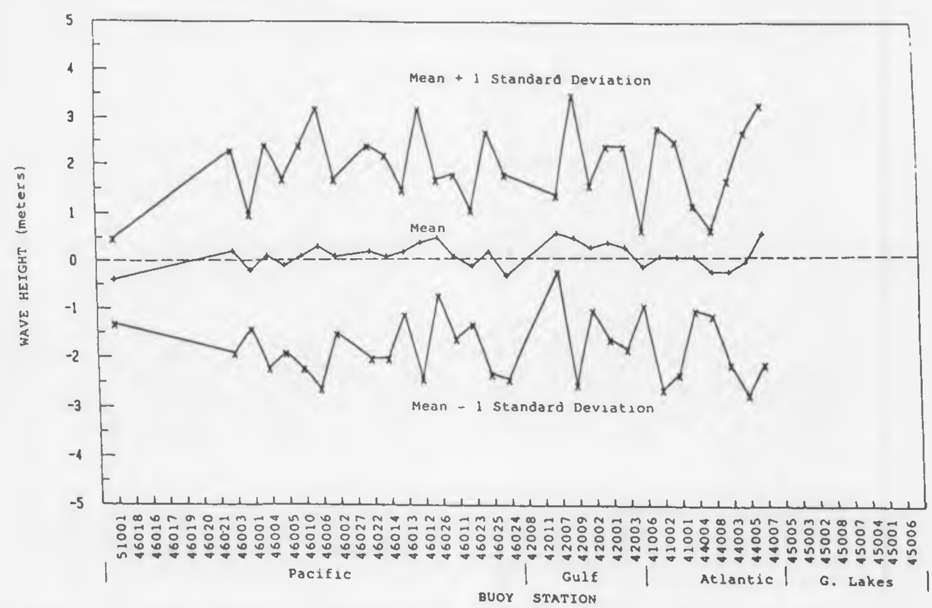

Figure 5. Wave height differences (using highest of ship sea or swell observations) as a function of buoy station (all ships). Results are not shown for the Great Lakes where small numbers of swell observations are seriously in error

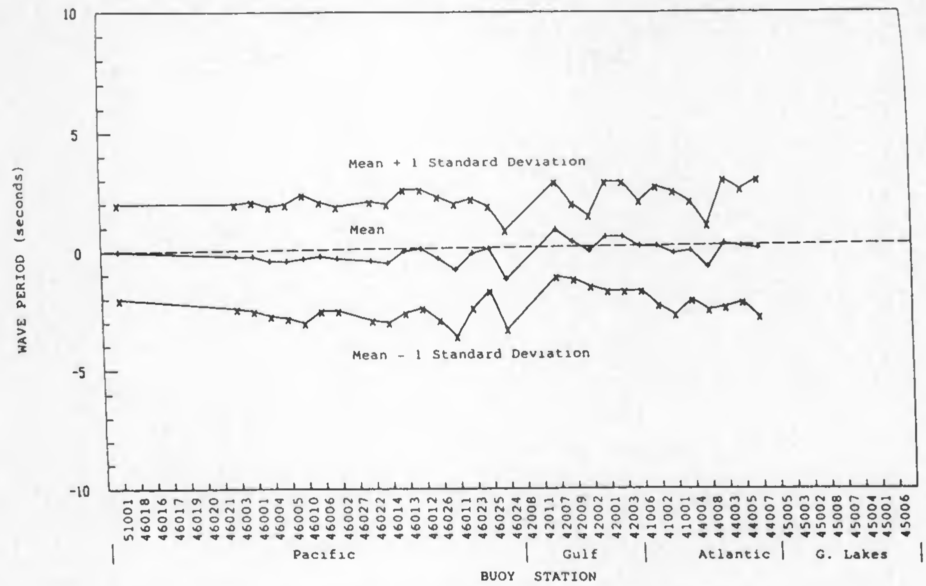

Figure 6. Wave period differences (using period corresponding to highest of ship sea or swell observations) as a function of buoy station (all ships). Results are not shown for the Great Lakes where small numbers of swell observations are seriously in error

```
the occurrences wind speed (in knots)
unknown on the vertical, unknown on the horizontal

  012345678901234567890123456789012345678901234567890     n    avg       var      s

50                                                  0     0
49                                                 0      0
48                                                0       0
47                                               0        0
46        1                                     0         1  -38.0       0.0    0.0
45   1  11           1  11                     0          6  -31.7      80.3    9.0
44                                            0           0
43                                           0            0
42                           2              1             3  -10.0      75.0    8.7
41                                         0              0
40      2                  1 2 1    1     0               7  -18.0     127.3   11.3
39              1                        0                1  -25.0       0.0    0.0
38           1    1            1        0                 3  -19.3      86.3    9.3
37                                     0                  0
36    1 2                    1        0                   4  -25.3     118.3   10.9
35     111     1     1     1  1 111  0                   10  -15.4     121.4   11.0
34  1     1  2      1   1           0                     6  -22.0      50.8    7.1
33            1              1     0                      2  -13.5     112.5   10.6
32  1   1 11      21      1       0                       8  -19.8      51.6    7.2
31            1                  0 1                      2   -8.5     220.5   14.8
30   22211  3312324 211241123 1122 1      1              51  -12.2      78.9    8.9
29      12 2 22   1 21 2  2 1322            1            26   -9.5      83.1    9.1
28             1   22   112 1 4   2                      16   -4.4      32.7    5.7
27   1    21 1 11 1 41 14   13    1 1                    24   -8.0      61.3    7.8
26    1 2  1 12 2   14 12   1  1                         19  -10.1      48.0    6.9
251  444438624958445955347AA6363112     1               154   -7.8      63.5    8.0
24 1112 1251 3 23 2414 4215 214  1                       53   -7.6      63.7    8.0
23  1   2144 2233 5 75 2262 2221  1                      59   -5.8      47.3    6.9
22      3254 A954 727  18 3 2114   1                     79   -6.3      43.5    6.6
21 12 2 1245 4548 754A 83 4 1221                         85   -5.3      40.2    6.3
20$5AC$CC$FCGCFCCED$EACA98AA53343  112  3   1           845   -7.4      47.3    6.9
19  34  4333 5528 678A 6122 321  1312                    97   -2.7      59.0    7.7
18 1664 A8AA $$AA AA$8 A443 31 1 11 1                   237   -4.3      36.6    6.1
17 1274 AAAA AAAA 9AA5 4627 12 2      1                 176   -3.8      40.3    6.3
16 1946 AAAA A$A$ $5A9 3522 13                          212   -3.8      30.9    5.6
1547AA$$CEHFDFHFFEDCE$AAAAA3652 11                      943   -2.9      29.7    5.5
14 49AA $A$$ $D$C $$$A 2324  31                         342   -2.4      28.8    5.4
13 25AA $$C$ CDDC 8AA6 225       2  1                   348   -2.1      24.7    5.0
12 6AA$ DDEC DGCD A$A6 9628  221   1     1    1         532   -1.1      30.7    5.5
11 49AA $DCD DCC$ AAA9 241  322                         383   -0.4      25.3    5.0
10$$FIKJPQSQQMMJHEF$DCAAAA7744    211          11      2083   -0.5      26.5    5.2
 9 6ACC DEGE CD$$'A7A5 2323   1   1    1                504    0.3      23.7    4.9
 8 A$DE HHLE CFCD AAA2 3322 1     2                     728    0.9      21.1    4.6
 7 ACDE FIFE CD$A 79A9 231   2    1                     570    1.2      21.5    4.6
 6 $DED HGFD CC$A AAA9 2 22  2 1  1 3 1                 613    2.3      28.6    5.3
 5FDIOR0STSMJIHEEC$$$A9371632 11 1    1        1       1986    2.6      22.2    4.7
 4 A$DH EFDC $$AA A2A3 2 22 213   1                     475    3.7      25.6    5.1
 3 6CEG DCC$ $AAA 4381 31   1 1                         387    4.0      20.7    4.5
 2 9CDC CD$$ AA18 232   1                               303    4.4      14.2    3.8
 1 7799 AA95 7643 2 2  2111 1                           102    7.0      30.4    5.5
 0F$DDHEGFFC$$CAAAA83161111   11               2        737    6.7      25.9    5.1
  012345678901234567890123456789012345678901234567890
```

Figure 7. Differences in reported wind speeds between two ships within 100 km of each other. Paired reports consist of both ships with and ships without anemometers. (After Ref. 2)

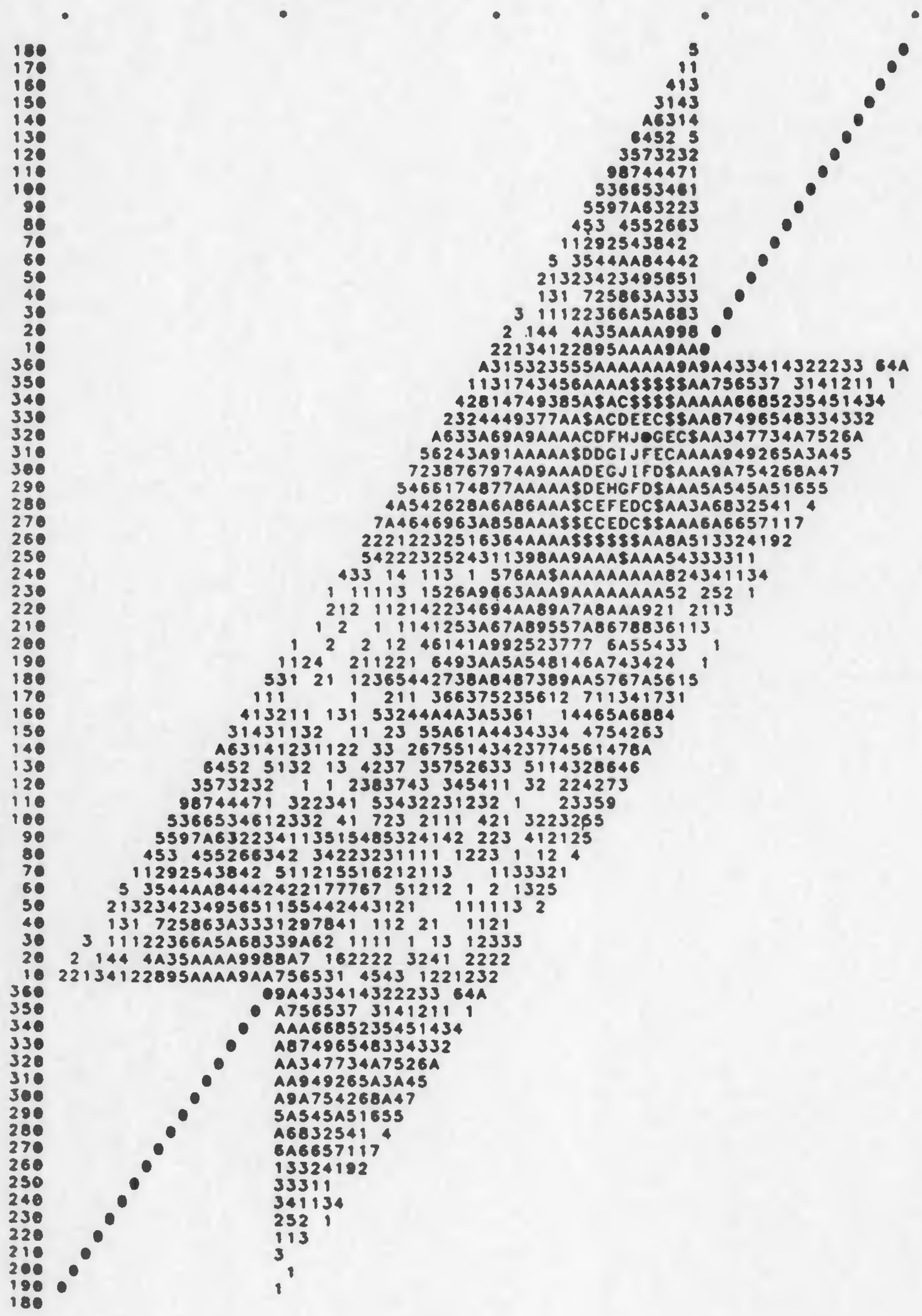

Figure 8. Differences in reported direction between two ships within 100 km of each other. Paired reports consisted of both ships with and without anemometers. (After Ref. 2)

THE ACCURACY AND AVAILABILITY OF OPERATIONAL MARINE SURFACE WIND DATA FOR ERS-1 SENSOR CALIBRATION AND VALIDATION FROM FIXED PLATFORMS AND FREE DRIFTING BUOYS

W A Oost

Royal Netherlands Meteorological Institute (KNMI)
P.O. Box 201, 3730 AE De Bilt, the Netherlands.

ABSTRACT

This paper deals with two items: the problems to be encountered when using data from oil or gas production platforms and a proposal for a calibration experiment, using drifting buoys.
The problems with platforms are discussed on the basis of some recent studies on the K13-A platform in the southern North Sea.
Drifting buoys being at the moment the most cost-effective platforms to obtain data from the high seas a suggestion is made to deploy a group of drifters measuring wind and, possibly, waves. This could be done by co-operation with the COST-43 organization, which maintains drifting buoy programmes in two areas.

1. INTRODUCTION

Comparing winddata, obtained by spacecraft scatterometer and in situ measurements will reveal differences between values measured in the same region. These differences have three main causes:

- A scatterometer measures a spatial, an anemometer a time average. These averages coincide only if Taylor's hypothesis strictly applies and the windfield is homogeneous in the direction transverse to the wind over the footprint of the scatterometer.
- Readings of anemometers are often not representative for the wind at the 10 m (or 19.5 m) level in the area, due to obstructions in the neighbourhood of the instrument or the level where the instrument has been mounted.
- Inadequate calibrations.

In this contribution we will concentrate on two items: the quality of wind measurements from fixed platforms and the contribution free drifting data buoys can make to obtain trustworthy spatially averaged values.

2. PLATFORMS

Oil or gas production platforms provide wind data from rather special areas viz. the continental shelves. Their anemometers are often well exposed, but mounted at heights of 60 m or more. Recently a wind tunnel study on such a platform was performed in the Netherlands (Ref. 1). The platform was the Pennzoil K13-A platform and the study was performed as a co-operative effort of the Organization for Applied Scientific Research (TNO) and the Royal Netherlands Meteorological Institute (KNMI). Two models were placed in one of the wind tunnels of TNO, a 1:200 scale model of the entire platform and a 1:30 scale model of the microwave tower of the platform, on which the anemometers were mounted. The topmost level of the tower, on which the anemometers are mounted on 3.5 m uprights, is 47.5 above the main deck, which again is 25 m above mean sea level, so the anemometers are 76 m above mean sea level. The helideck is north west of the tower, 38 m above mean sea level.

The results of the study indicate that the deviations in the wind speed at anemometer level, due to the main body of the platform, are less than 2%. The obstacles at the tower itself have a far bigger influence and are the main cause for the resulting total deviations which range from -4 to +9%, depending on the wind direction.

The corrections, needed to compensate for the wind field disturbance by the platform, can be obtained from wind tunnel studies. This is not possible for the reduction of the (corrected) anemometer readings to a standard level, e.g. 10 m above mean sea level. Bouws (Ref. 2) performed a statistical study in which he compared the wind as measured at platforms to the 10 m wind, as deduced from analyzed wind fields. His study indicated that for K13-A the reduction factor ranged from 0.65 for wind speeds of 8 m/s or lower to 0.85 for wind speeds of 15 m/s or higher.

The standard reduction factors used in the North Sea area only depend on the height of the anemometer. For K13-A this factor is 0.76. Although this value is not contradictory to the 0.65 and 0.85 for the end points of the velocity range studied, its use would result in an error of +17% (or 0.8 m/s) in the 10m wind, when the anemometer registers 8 m/s, respectively -11% (or 1.4 m/s) at 15 m/s, if the factors 0.65 and

0.85 are correct.

If we did not have the results of these studies at our disposal we would take the anemometer readings without distortion corrections and use a reduction factor of 0.76. This would lead to errors ranging from +12 to +28% (0.6 to 1.5 m/s) in the 10 m wind when the anemometer reads 8 m/s, respectively from -15 to -3% (-1.9 to -0.4 m/s) at 15 m/s, the precise value depending on the wind direction.

As noted in the beginning of this paragraph, platforms will be found in shelf seas, the prime example for Europe being the North Sea. There they are so ubiquitous that their measurements provide a very sizable fraction of the total weather information from this area. In this way systematic errors in the analyzed windfields are apt to occur. Therefore it is strongly recommended to perform studies of the type described in this paragraph on all platforms in an area to be used for calibration/validation of scatterometer before using their data.

3. DRIFTING BUOYS

The most ideal instrument carrier at sea, in terms of correctness of the data, is a buoy. They have low profiles and smooth bodies compared to ships and platforms and do not necessitate substantial height corrections.

Large, anchored data buoys, however, are expensive and therefore rare, especially far from coasts. The most cost-effective instrument carriers there are the small drifting buoys. Several programmes exist, both in the US and in Europe, in which these buoys are being used. The European Organisation COST, Action 43 has two programmes in this field; Norway has an extensive national programme, besides co-operating in COST 43. Other European countries are executing more incidental programmes.

A drifting buoy programme in support of the ERS-1 calibration/validation seems to be well worth pursuing. By selecting an area of the ocean of some 1000 x 1000 km and putting in e.g. 6 to 8 drifters, a calibration programme can be run over an extended period of time. The drifters must be equipped with wind measuring devices (measuring waves with drifters is also possible, but requires simultaneous current measurements, see Ref. 3). A problem arises from the fact that drifters are generally equipped with data transmission facilities for the ARGOS system. This implies that the data must be gathered during the overpass of ERS-1 and transmitted when a NOAA satellite is within sight . Two solutions present themselves: the use of a timing device or registration and transmission of all ten minute means. The latter one requires fairly much transmission time, but has the

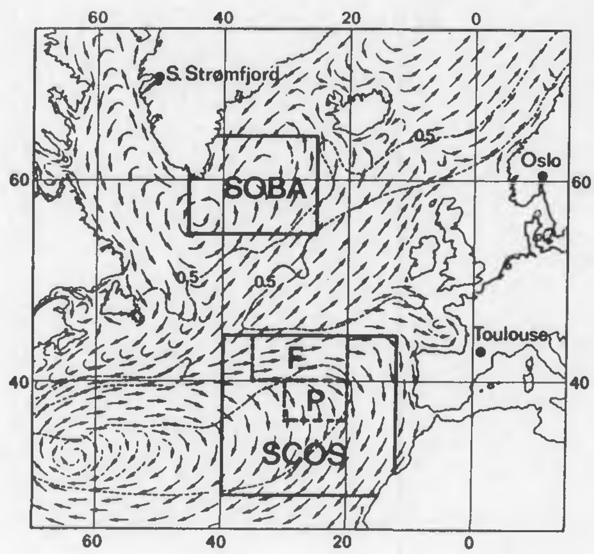

Fig. 1 The COST-43 drifting buoy programmes.

advantage that a record of all significant changes in the weather becomes available. Implementation of such a programme would be relatively simple, as COST 43 is operating two drifting buoy programmes and would probably be willing to incorporate these extra buoys into one of them. This would mean that pre-deployment checks, transport, deployment, day-to-day supervision and primary data handling, could be done by this organization. The programmes cover the area (see fig. 1) 55-63° N, 45-25° W ("SOBA") and 25-45° N, 40-12° W ("SCOS"). The most attractive area is the northerly one, because of its size, the variable wind conditions, the frequent overpasses of polar-orbiting satellites and the possibility of a long residence time of the buoys.

REFERENCES.

1. Vermeulen, P.E.J., Oemraw B. and Wieringa J., 1985: Wind tunnel measurements of the flow distortion near the anemometer positions on Pennzoil K13-A platform.
TNO report 85-01246.

2. Bouws, E., 1985: Wind speed measurements on platform K13-A: a historic overview of the interpretation of the data.
KNMI Report 00-85-22.

3. Lai, R.J. and Bachman, R.J., 1986: Current effects on wave measurements.Proceedings Marine Data Systems '86, Marine Technology Society, p. 541.

SESSION 2 – SUMMARY

W Rosenthal *(Chairman)*

Forschungszentrum Geesthacht
FR Germany

This session contained stimulating contributions how to compare satellite data with other data sources. The intention of the organizing committee was

1. to stimulate critical assessment of quality for conventional data sets and

2. to get proposals for the strategies to calibrate the satellite during the first three months after launch

In the following I will try to comment the content of the session in the context of this issues.

The presentation of A. Cavanie, J. Demurger, P. Lecomte showed a very promising method to check the self consistency of the coefficients in Long's wind algorithm. This method relies on the yaw-steering of the satellite and, therefore, there has been no way to test it so far. The limits to which the coefficients could be determined could probably determined by a numerical simulation experiment. Most likely the method will show its merits in the validation phase.

The contribution of P. Francis proposes to increase the amount of surface data tremendously by using numerical models. These models are available at several meteorological offices on a routine basis and the statistical distribution of the differences between high quality measurements at selected stations and model values is very well known. It depends only on the number of independent comparisons between model data and satellite to get a sufficiently exact relation betwen sea surface- and satellite-parameters. The author goes one step further and describes the improvement of model output by assimilation of satellite data. This step, however, will show its performance after the commissioning phase and all numerical modellers have great hopes in this technique. It may be useful to mention that beside the activities in the national weather centers, that there is an ongoing activity at the ECMWF to develop a third generation wave model especially for the use of ERS-1 data.

In M. H. Freilich's presentation a comprehensive review was given on comparison of SEASAT-SASS with various sources of surface data. The author did not give quality assessments of the conventional instruments but from the regression fits with the SASS there was an evidence of differences between measurements used for comparison with the SASS. In total, from the error limits given by Freilich, we can expect a satisfying data set to be delivered from the ERS-1 sensors.

The contribution of Koch and Ramseier duplicated in the first part the paper of P. Francis. It showed by a few examples the performance of todays wind and wave models. Different to P. Francis's contribution was the derivation of the wind field, which comes from pressure analysis charts in the Koch-Ramseier-paper and directly from a numerical atmospheric model in the Francis-paper. Koch and Ramseier showed in the second part of their paper with SMMR-data of NIMBUS 7 how a comparison with model wind may be done. Their technique to translate the satellite-measured wind into surface pressure differences seems a very promising tool. Before it is not tested with scatterometer data, however, this method cannot be used in the commissioning phase and may show its merits in later validation experiments.

As in previous talks the use of models, calibrated to high quality measurements was suggested to increase the surface data base, the presentation of P. Taylor suggests to use well calibrated VOS-data as a mean to increase the number of surface data. The paper shows the value of the different wind estimates used by VOS, beginning with high quality anemometer winds on research vessels and ending with hand anemometer measurements on VOS (the latter are concluded to be useless under strong wind conditions). The author suggests to use a subset of carefully selected VOS with properly installed anemometers to increase the quality level of the total set of VOS-data.

The presentation of J. C. Wilkerson compares ship operations with the data from the net of NOAA data buoys. Whereas Taylor's work considered mainly wind measurements this paper also treats wave observations from ships using the buoy data as a normal. A large amount of regression fits for a variety of conditions has been shown. In connection with the contribution of P. Taylor which also considers the reliability of wind measurements from buoys this paper gives an estimate on the errors to be expected for ERS-1 calibration, if it is done with the VOS-fleet.

Session 3

DEDICATED MEASUREMENTS

Chairman: A Cavanié (IFREMER)

USING BUOYS AND SHIPS TO CALIBRATE ERS-1 ALTIMETER AND SCATTEROMETER

R Ezraty

IFREMER - Centre de Brest - B.P. 337 - 29273 BREST CEDEX - FRANCE

ABSTRACT

Given the stated accuracy of ERS'1 sensors, this paper addresses the constraints to be dealt with using ships and buoys for a dedicated calibration experiment.

Improved wave measuring buoys, giving directional and non directional informations, are now available to be used remotely in the open ocean.

Wind measurements from ships can be considered as a reference, if ship effects are properly taken into account.

At sea tests of a spar buoy, measuring the wind vector at 4 meters, are presently being conducted. The importance of the continuity of wind data is stressed and has to be accounted for to plan the on-board electronics.

The geometry of wave and wind buoy networks are different since the altimeter and scatterometer don't scan the same area. Tentative network configurations are presented.

INTRODUCTION

From the SEASAT experience, we learned that carefully controlled and selected data are needed to tune the algorithms used to relate the backscatter power or signal signature of radars to geophysical information (i.e. wind vector, significant wave height, wind force).

At present, since too little is known about the physics of interaction between electromagnetic waves and the complex structure of the ocean surface, empirical power laws or semi-theoretical models rely on experimentaly determined constants. Moreover, because of technical limitations due to the open-ocean environment, only a few mean geophysical quantities are believed to be measured accurately enough at sea from ships and buoys, on an operational basis and during a 3 to 4 month period, to suit the spot calibration accuracy requirements.

To assess an order of magnitude of the accuracy of in-situ wind measurements needed for the scatterometer calibration, lets assume that the variance of the global error, E^2g, is the sum of a radar error variance, E^2sig, an algorithmic error variance, E^2algo, and an in-situ data error variance, E^2is, such that : $E^2g=E^2sig+E^2algo+E^2is$, furthermore, lets assume that E^2is contributes to one third to E^2g.

Since the accuracy of ERS1 scatt is anticipated to be 2 m/s (or 10 % of the measured value) between 4 and 24 m/s, $E^2is=4/3\ (m/s)^2$. Furthermore, for one measuring location, during 3 months, on a 3 day repeated orbit, we can expect up to 30 calibration data points for a given incidence angle. Assuming an uniform distribution of measured wind speeds into the considered wind range leads to 1.5 data point/(m/s). So, a spot measurement standard deviation has to be about 1.15*SQR(1.5)=1.4 m/s. It is anticipated that this crude estimation could be further refined when scatterometer performances and in-situ location will be known. Consequently, the measuring systems have to be carefully tested and the data correctly evaluated, using previous experiences and specific at sea experiments, prior to satellite launch.

A major constraint with real-time open-ocean buoys measurements is the data transmission and collection since the power supply on board buoys is limited. Thus, we intend to use the ARGOS positionning and transmitting system. In turns, this implies on-board processing to reduce the amount of data to be transmitted and match the ARGOS capability.

This paper presents some of the equipments and techniques already developed or being planned by IFREMER and other French agencies. This collaboration, within the TOSCANE project, is aimed to the measure of the ocean gravity wave field and the wind vector using ships and buoys, in the context of an open ocean dedicated experiment, to provide inputs to the calibration and validation of the ERS1 satellite active remote sensors.

1. MEASUREMENTS OF WAVE-FIELD CHARACTERISTICS

Since 1974, IFREMER has continuously developed and improved wave measurements from buoys and the corresponding processing and data analysis to

Proceedings of a Workshop on ERS-1 Wind and Wave Calibration, Schliersee, FRG, 2–6 June, 1986 (ESA SP-262, Sept. 1986)

provide reliable experimental results. From the experience acquired during major campaigns (MARSEN 1979, OUESSANT 1981-1982) we have tested and validated the SPEAR"F" and WADIBUOYS buoys which can be used in the open ocean (no range limitations).

The gaussian random process model for ocean waves has been proved to describe the real nature of sea waves in most situations (linear model) ; we employ it for data processing and analysis.

The SPEAR"F" buoy is an improved DATAWELL Waverider (.8 m diameter sphere, 100 kg) which on-board computes the sea-surface elevation spectrum, reduces the data and transmits, via ARGOS, the energy levels in 30 selected period bands from 21 seconds down to 2.5 seconds. A 34 minutes data time series is used to compute a non directional spectrum every hour. From this information the significant wave height, Hs, and a mean wave period, Tm, can be computed. Figure 1 presents a typical data set and the corresponding spectrum ; Hs reaches 7 meters and Tm is 10.5 seconds.

EXP 433

[illegible]

[illegible]	227	123	182	121
	125	112	084	083
	078	076	068	038
	049	042	024	029
	032	032	025	027
	025	027	020	020
	017	018	015	013
	014	018	076	094

ARGOS READY

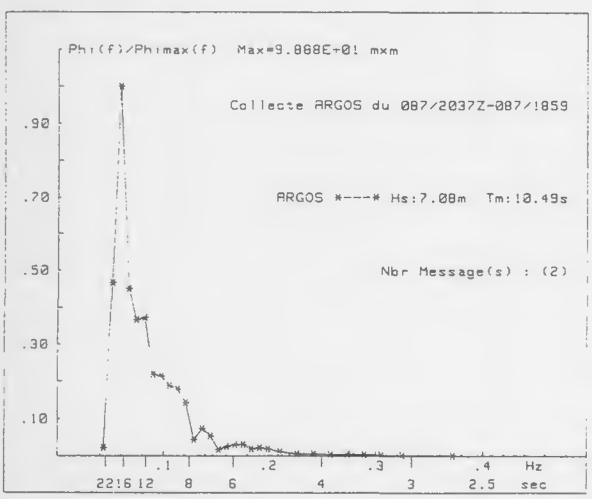

Figure 1. Typical SPEAR "F" data set and corresponding spectra.

Figure 2 shows a sequence of SPEAR"F" results, obtained recently at IFREMER test site, to illustrate the continuity of the information as sampled by ARGOS. It is possible on this graph to follow the wind sea merging with the swell as a fonction of time.

Directional wave measurements are performed using WADIBUOYS (Cone shaped buoy, discus hull, 2.5 m diameter, 800 kg). The heave, pitch, roll and compass information of the surface following buoy is used to compute the first five terms of the angular Fourier expansion of the directional spread (Ref. 1).

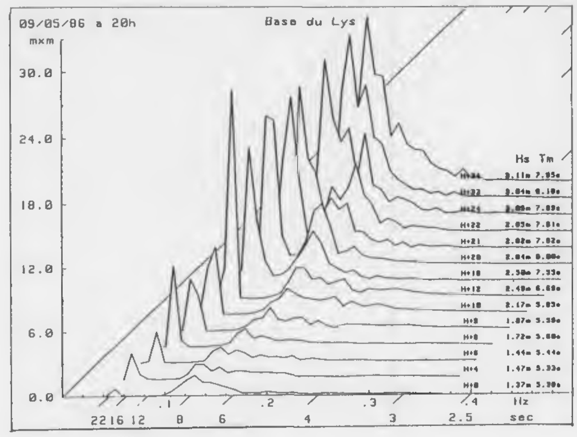

Figure 2. Time series of SPEAR "F" spectra (ARGOS sampling).

Two transmission systems can be used depending on the amount of detailed information wanted. For example, in the vicinity of a receiving station (10 nautical miles off a ship or land), a VHF radio link transmits the raw data and a detailed analysis can be performed using a desktop computer. This method was used during the MARSEN campaign (1979) (Ref. 2) and the USHANT campaigns (1981-1982) (Ref. 3) to validate the buoy and the data quality in the 18s-2.5s band. A recent improvement in data telemetry (1985) permitted a navigational buoy (80 tons, 11 m diameter, 42 nautical miles from main land) to be so instrumented. The data was proven to be valid, in terms of directional sea state analysis, in the 16s-6s band (Ref. 4). Figure 3 is an example of time serie of mean direction of propagation of energy for different periods bands.

To be used with the ARGOS system, the raw data (13000 data values) has to be processed on-board to be reduced to 60 values (energy level and mean direction of propagation in 30 selected period bands). Such a procedure was shown to be feasible using a digital recursive filter during an USHANT campaign (Ref. 5). Recent developments in CMOS microprocessor could be used to implement an on-board FFT procedure.

2. WIND FIELD MEASUREMENTS AND ANALYSIS

2.1. First step : Time average

The design of the experiment has to account for the physics of the wind. The wind vector is a function of time and space, it depends on location, altitude of measurement, atmospheric stability and synoptic conditions. A major difficulty is the interaction of the different time-scales (from days to fraction of seconds).

As an illustration figure 4 presents a time record of wind, collected at sea on R/V "LE SUROIT", during the C-Band PROMESS/TOSCANE 1 campaign. The recorded signal shows a front with a complete different signature before and after. A consequence is that the estimation of a "mean" value depends both on the time, to, at which it is computed and on the duration, T, over which it is computed (Ref. 6).

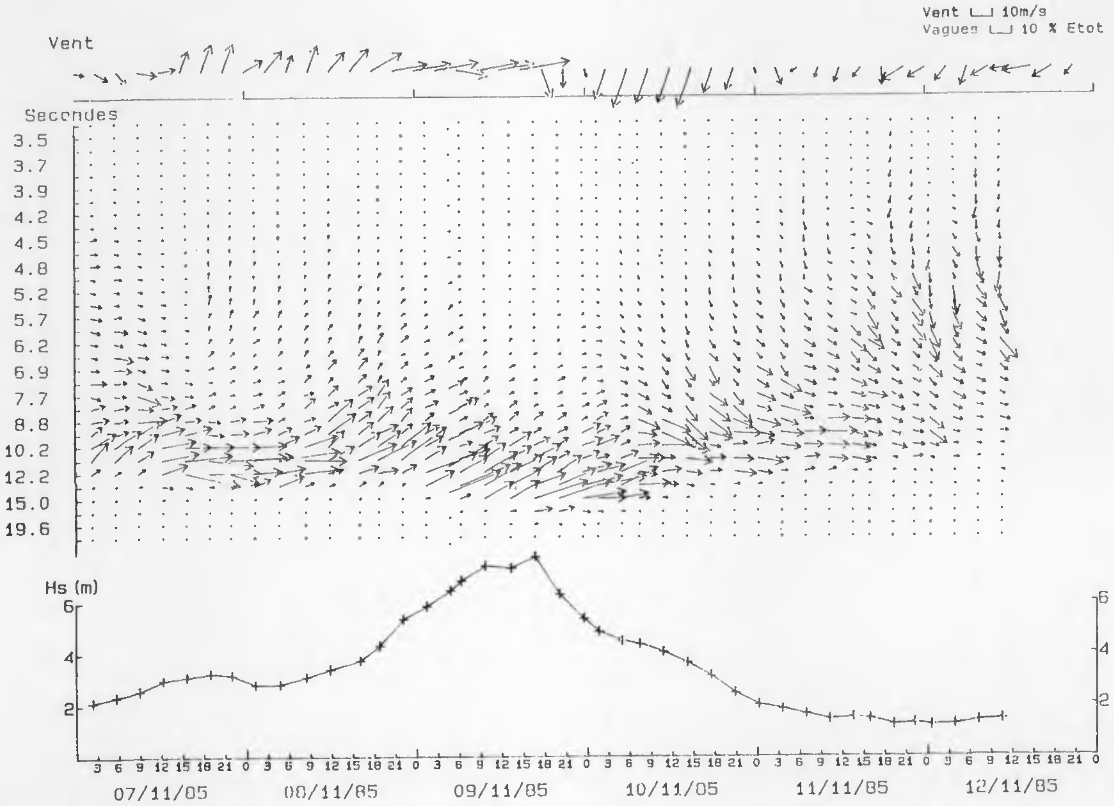

Figure 3. Time series of mean direction of wave energy obtained from a buoy.

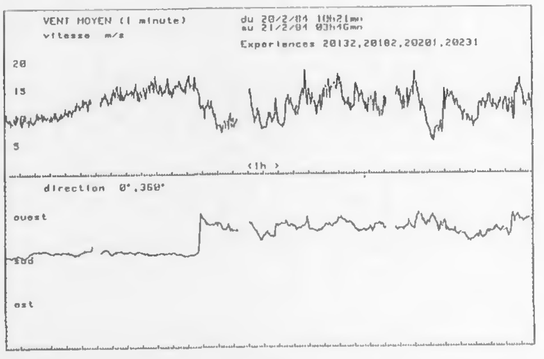

Figure 4. Example of time series of wind force and direction during a front passage.

In this case a mesoscale structure transports, at the measuring location, an air mass whose composition and dynamics differ from the previous one (atmospheric stability effects).

Figure 5 is a spatial wind field obtained from aircraft measurements on March 20, 1985, during the TOSCANE "T" experiment. It shows a wind direction discontinuity probably related to a cloud structure (Ref. 7). Such large discontinuities (in time or space) can be tracked and taken into account during the data analysis and selection process, but for smaller scales the question remains : how to relate a time average to a space average ?

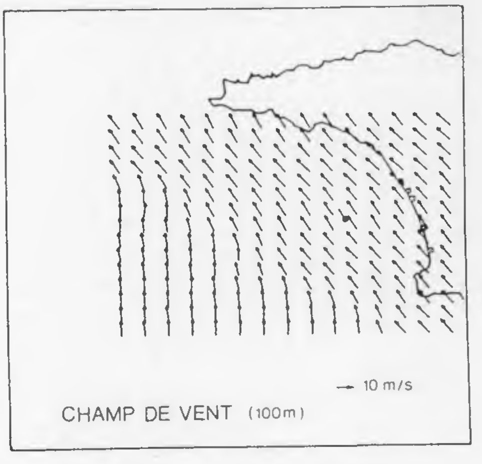

Figure 5. Example of spatial wind field discontinuity.

Figure 6 presents samples of coherence and phase spectra, computed from wind data obtained at neighbouring masts, 12 m height, during the TOSCANE "T" experiment. The distances between mast number 1 and masts 2, 3, 5 are respectively 1.5, 6.9 and 10.1 km. On this data set (wind speed is 10.5 m/s, no mesoscale signature) it can be seen that fluctuations whose periods are lower than 10 minute become incoherent when the distance extends beyond 6.9 km (significant confidence level is about .45). Inferring a fluctuation level or an accuracy statement over a 50 x 50 km^2 area from a single 10 minute wind average becomes a fortune-teller job ! From mast 1 - mast 5 coherence a 20 minute long record seems to be a much better duration for, at least, a 10.1 km distance.

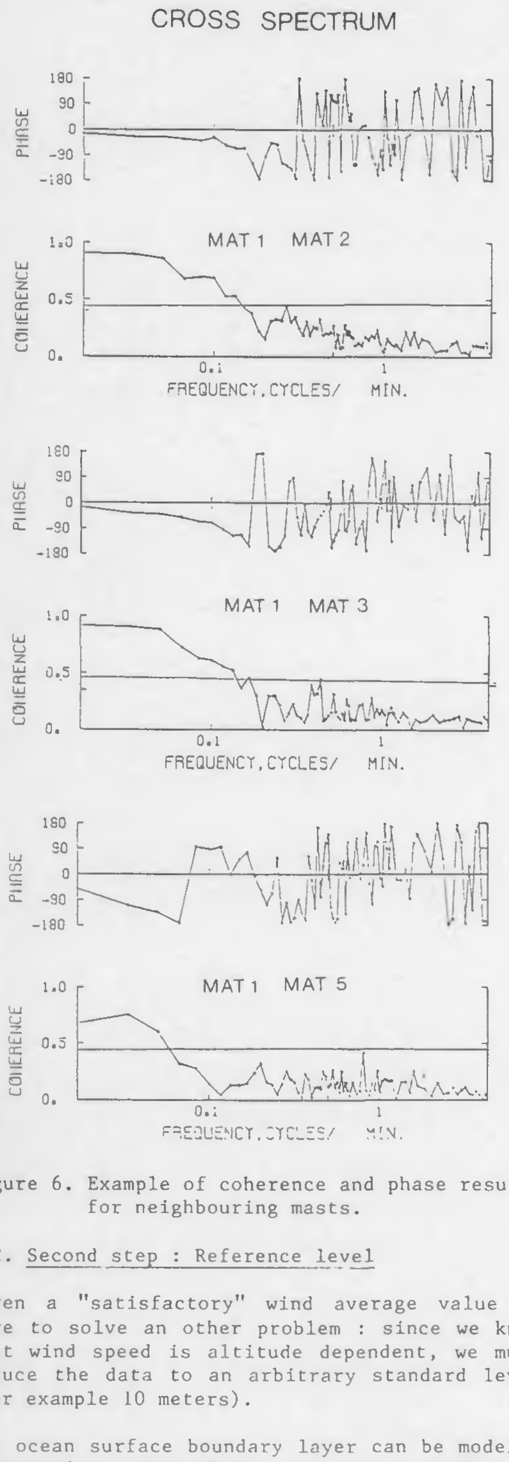

Figure 6. Example of coherence and phase results for neighbouring masts.

2.2. Second step : Reference level

Given a "satisfactory" wind average value we have to solve an other problem : since we know that wind speed is altitude dependent, we must reduce the data to an arbitrary standard level (for example 10 meters).

The ocean surface boundary layer can be modeled using the Log-profile relation, eventually corrected by an atmospheric stability term :

$$U(z)/U^*=(\mathrm{Log}(z/zo)-\mathrm{Psi}(z/L))/K$$

The hydrodynamic roughness height, zo, is related to the friction velocity U*. Since the MONIN-OBUKOV length, L, can be estimated from mean measurements, the above equation can be solved by iterations to compute an equivalent 10 meter neutral atmospheric condition wind, U10n, if a wind value measured at altitude z is known (Ref. 8). It is shown, from model simulations, that the estimation of U10n is practically independent of the zo(U*) (or drag coefficient) parametrisation, even when stability effects become important.

An interesting point concerning the stability correction term, Psi(z/L), is its dependence on z/L : by definition Psi(z/L) tends to 0 as z/L (L->∞ for neutral case). For typical North Atlantic situations (U20=10 m/s, Tair=15°C, 80 % humidity, Twater=12°C), L=120 m. At a 4 meters measuring level, z/L=0.033, the corresponding U10n, using the stability correction would be 8.58 m/s and 8.71 m/s without this correction (1.5 % difference) ; but at 20 meters measuring level, the stability corrected U10n is 8.75 m/s and 9.40 m/s non corrected (7.4 % difference). Conclusion : higher the measuring level is, greater the stability correction has to be. Consequence : low level instrumented wind buoys don't need temperature measurements for wind speed estimation purposes.

2.3. Third step : in-situ difficulties

Among the in-situ difficulties to be dealt with, the moving ocean surface is one of the worse. We will focus on the probe-holder problem (ships and buoys) and present some results on the wavy surface influence on wind measurements.

2.3.1. On-board ships and buoys measurements :

During the PROMESS/TOSCANE 1 experiment on-board the R/V "LE SUROIT" a method was developed to determine and account for the ship disturbance effects and ship movements (Ref. 9, 10). It was shown that the disturbance effect introduced a 12 % wind overestimation when the ship moves slowly up-wind. The influence of pitch and roll induced wind speed could be smoothed out using at least a 30 second running average of the wind. Since the ship log can be carefully calibrated at low speed (1 to 2 knots), it is believed, from our experience, that an absolute accuracy of .4 to .6 m/s can be achieved for on-board ship measurements, using carefully calibrated and operated instruments. Moreover the scientific crew can pay special attention to the sensors (replacing or continuously monitoring and controlling the data quality).

Regular cleaning of temperature probes (dry and wet bulbs, sea-water temperature thermometers) is necessary to provide good quality data for the atmospheric stability correction.

Such dedicated measurements could be considered as a reference for comparison against other techniques.

It might seem trivial to recall that specific experiments can be conducted from the same ships, at the same time, by different specialized groups, but these groups should be already aware of the difficulty of at sea experiments and of the quality of the data they plan to collect. This precaution prevents from strategic conflitcs since all on-board teams use the same probe platform, at worse at the same moment, with different operational constraints.

Since buoys are unmanned platforms, special attention has to be given to the ruggedness of sensors and electronics. To avoid uncertainties and ease comparisons and controls, identical sensor and electronic packages should be used, when feasible, on all platforms (Ref. 11), and two independent systems should be mounted on each buoy. It is now agreed that a vector averaging procedure should be used instead of independent force and direction averages.

2.3.2. Data comparison and qualification :

Recent litterature (Ref. 11, 12, 13) pays special attention to this uneasy problem ; averaging-time, scalar or vector averages, sensors height, sensor behaviours and other installation differencies obscure the task and make difficult to assess the contribution of each effect to the total error budget.

Our experience relies on the TOSCANE "T" experiment data, comparing the wind measurements on a buoy (10 minute scalar averages, every hour, sensor height 3 m, 5 km offshore) to shore based data from 7 masts at 12 m height (Data were reduced to 3 meters height). The sensors where identical at both locations (Ref. 7, 13).

Although the coast was reasonably flat, coastal effects where detected on the individual mast measurements as a function of wind incidence with respect to the coastline. The averaged value of 5 out of the 7 masts was used as a reference. Selecting only onshore winds (To discard data influenced by land-sea transition) leads to a .968 correlation between the reference mast and the buoy data. The regression adjustement shows a 1.13 slope and no significant shift at the origin (0.04 m/s), (fig. 7).

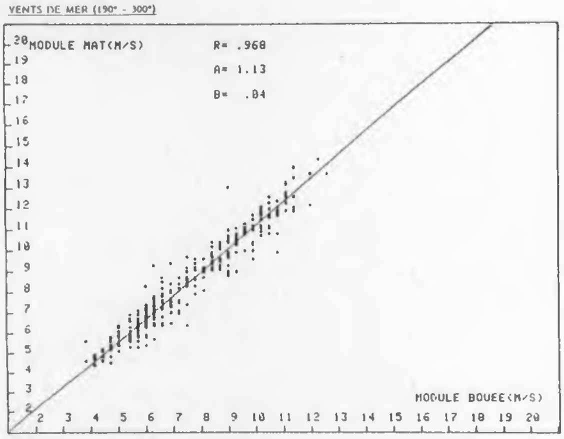

Figure 7. Comparison of buoy and reference mast wind speed data.

This slope value could not be attributed to wave height influence or sea state sheltering effect (if any) : a plot of the relative difference between onshore wind buoy data and the average mast data versus significant wave height, Hs, up to 6.5 m shows no trend at all (fig. 8). The standard deviation of the absolute difference is about 0.3 m/s. Reevaluation of the post experiment results of buoy anemometer comparison against a reference one, revealed that some data formerly taken into account for re-calibration had to be rejected because of the instruments layout. Using the updated calibration coefficients, the average mast and the buoy data match within the anemometer accuracy (0.3 m/s).

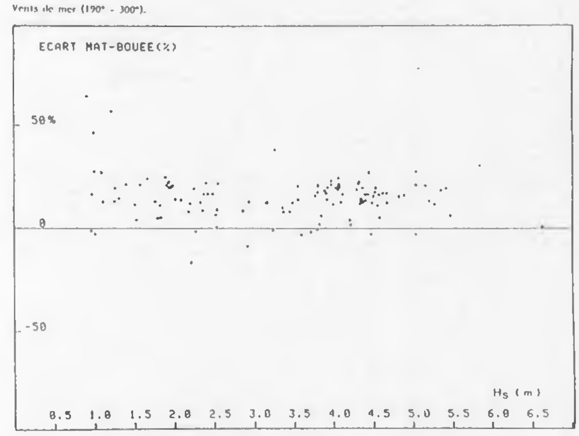

Figure 8. Relative wind speed difference between the buoy and the mast as a fonction of significant wave height.

Figure 9 presents the comparison of offshore wind direction between the buoy and the average mast. Given the 10° buoy data resolution and the compass alignment, results do agree.

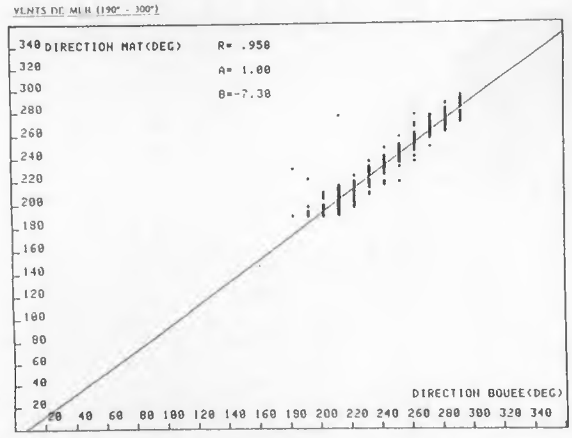

Figure 9. Comparison of buoy and mast direction measurements.

2.4. Fourth step : planned developments

Presently we are conducting at sea tests of a 8 m tall spar buoy (wind measuring level 4 m) to estimate its behaviour. Some mechanical adjustments seem to be necessary to ease buoy handling during the mooring phase, but the concept, size and shape should not vary much. A wintertime experiment is planned for early 1987 to provide comparison data between ship, buoy and shore based wind measurements. The electronic package (ARGOS transmission) is being specified. To do so a simulation has been performed using TOSCANE "T" data. Figure 10 is a 2 day time series of continuous 30 minute vector averaged wind. From top to bottom are plotted the wind direction, wind speed, the standard deviation of the cross wind, Sigv', and along wind, Sigu', computed from one minute long averaged elementary vectors during each 30' period. Such a simulation does indicate that, to correctly select calibration values, the transmitted wind data has to be continuous in time, but also that speed and direction are not enough information to ascertain the variability of

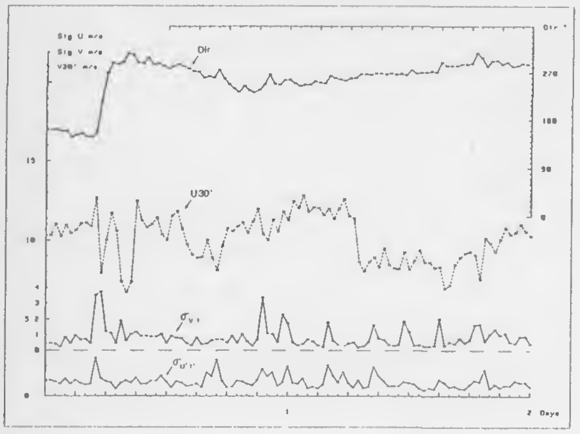

Figure 10. Simulation of planned wind measurements as reported by ARGOS.

the wind field being sampled. This extra information will be important to decide upon any space-time relation. Anyhow such a plot shows that usual meteorological reports (10 mn averages, every 3 hours) can be highly misleading using a single measurement point without any other information.

The planned electronics will include for each wind report the above defined four parameters and, since continuity is a need, the ARGOS message will consist of at least 7 hours of data (ARGOS, ERS1 and NROSS orbits are independent).

3. TENTATIVE NETWORK CONFIGURATION

The preliminary study by Queffeulou (Ref. 14, 15) was used as a guide to the design of a possible network configuration. Since the areas scanned, at a given time, by the altimeter and the scatterometer are not coincident, an optimum geometry for a given sensor will not suit the other.

In the following we will consider using 7 buoys on a three day repeated orbit.

As an illustration, figure 11 focuses on altimeter significant wave height calibration. Such a geometry provides 12 Hs values, since we place 5 buoys at ground track crossing points.

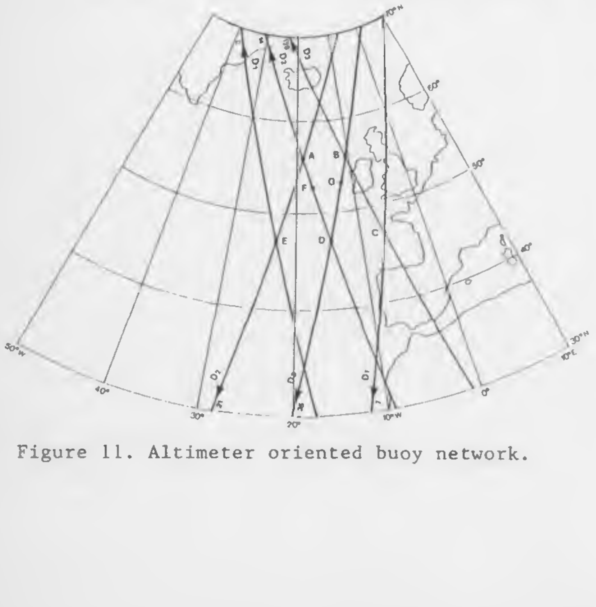

Figure 11. Altimeter oriented buoy network.

The buoys labelled F and G in conjunction with buoys A and B are used to assess an homogeneity wave field criterium on a more restricted area to be used for scatterometer wind calibration. A nice solution, given the earth geometry, is to select the region (between latitude 50° and 60°) where, on a 3 day orbit, the ground tracks of the satellite (altimeter winds) is overlapped by the scatterometer swath. The geometry presented in figure 12 returns 14 scatt and 4 altimeter winds. All scatt incidence angles are scanned. Lets call A to G the buoys and 1 to 10 the incidence angles (1 is the nearest to the ground track). Scatterometer winds will be collected on day 1 (A-1,B-3,E-5,F-6,G-6,C-7,D-9) and on day 3 (A-10, B-8,E-6,F-6,G-5,C-4,D-2), and altimeter winds on day 1 (F,E descending track) and day 2 (F,G ascending one). Such an array extends over 240 nautical miles, it can be easily maintained over a 3 month period, and a suitable mooring area can be selected (for example the HATTON-ROCKALL bank 56°N, 15°W, 800 m water depth). Moreover such a spatial extend coincides with mesoscale structures of physical interest.

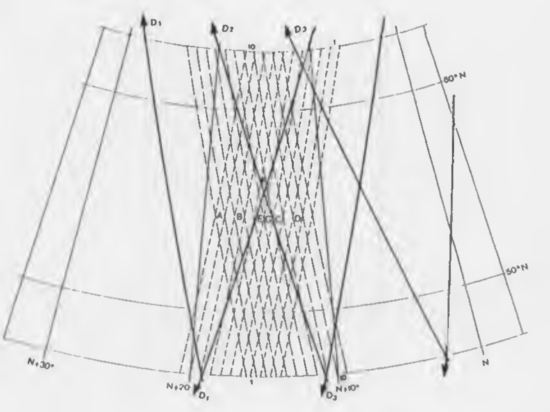

Figure 12. Tentative network geometry.

CONCLUSION

Based on SEASAT in-situ calibration experience, on previous scientific results and technological know-how, we have at our disposal the means to plan and conduct a good quality dedicated experiment to calibrate ERS'1 sensors. Further developments both on the scientific and the technical point of view are still necessary to improve our confidence in the in-situ data quality and on the data interpretation.

Such an in-situ dedicated experiment will require sharing the expertise and resources of many research teams ; we look forward to a cooperative effort.

ACKNOWLEDGMENTS

The results used in this presentation were obtained by the members of the TOSCANE group (R. EZRATY, P. QUEFFEULOU, M. CHAMPAGNE, J.P. GOUILLOU, S. DIDAILLER), the Météorologie Nationale-EERM/CMM Brest-team (N. DANIAULT, M. CAMBLAN, J.N. THEPAUT), and the Service des Phares et Balises (J.F. RACAPE).

I thank P. LECOMTE for his assistance when plotting ERS1 orbits. The comments from Professor W.J. PIERSON are gratefully acknowledged.

BIBLIOGRAPHY

1. Longuet-Higgins H S, Cartwright D E, & Smith N D 1963, Observations of the directional spectrum of sea waves using the motions of a floating buoy, "Ocean wave spectra", proc. Prentice Hall.

2. Ezraty R & Cavanié A 1981, Evaluation de la mesure de la direction des vagues à partir des données d'une bouée instrumentée, Oceanologica Acta, 4(2), 139-149.

3. Ezraty R, Cavanié A & Gouillou J P 1983, Système de mesure de houle directionnelle, campagnes hivernales aux abords d'Ouessant, Rapports Scientifiques et Techniques, n° 53, CNEXO ed.

4. Ezraty R & Racape J F 1986, Directional and omnidirectional sea state information obtained from instrumented buoys, Proc. Marine Data Systems, New Orleans, Louisiana, April 30-May 2, 1986.

5. Ezraty R, Ollitrault M & Ayela G 1983, A wave directional spectrum buoy using ARGOS, Proc. Oceans'83, San Francisco, August 29-September 1, 1983.

6. Pierson W J 1983, The measurement of the synoptic scale wind over the ocean, J Geophys Res. 88(C3) 1683-1708.

7. Camblan M & Thépaut J N 1986, Analyse de la structure spatio-temporelle du vent en mer pendant l'expérience TOSCANE "T", Rapport de stage Ecole Nationale de la Météorologie, mai 1986.

8. Ezraty R 1985, Etude de l'algorithme d'estimation de la vitesse de frottement à la surface de la mer, Contrat ESTEC n° 6155/85/NL/BI.

9. Ezraty R, Queffeulou P & Champagne M 1985, The Promess 84 & Toscane 85 campaigns in-situ measurements, Proc. of the 3rd International Colloquium on Spectral Signatures of Objects in Remote Sensing, Les Arcs, France, December 16-20, 1985, ESA/SP 247-1985.

10. Queffeulou P, Lavanant L & Ezraty R 1984, Remarques sur la mesure du vent en mer. Conférence Marins et Météorologie, Saint-Pierre Quiberon, 5-7 September 1984, Met-Mar n° 124 bis.

11. Weller R A, Payne R E, Large W G & Zenk W 1983, Winds measurements from an array of oceanographic mooring and from F/S Meteor during Jasin 1978, J Geophys Res, 88(14) 9689-9705.

12. Gilhousen D B 1986, An accuracy statement for meteorological measurements obtained from NDBC moored buoys, Proc. Marine Data Systems International Symposium, April 30-May 2, New Orleans, 1986.

13. Queffeulou P, Ezraty R, Champagne M & Gouillou J P, The Toscane "T" experiment, in-situ data report, Rapport interne IFREMER, en préparation.

14. Queffeulou P 1984, Wind speed determination from radar altimeters. ERS1 Radar Altimeter Data Product Workshop, Frascati, Italy, May 1984.

15. Guymer T, Challenor P G, Srokosz M A, Rapley C G, Queffeulou P, Carter D J T, Griffith H D, Lavanant L, Scott R F & Tabor A R 1984, A study of ERS1 radar altimeter data processing requirements, ESTEC contract n° 5681/83/NL/BI-1984.

DFVLR FLIGHT OPERATION ACTING AS A USEFUL SERVICE UNIT FOR ERS-1

H Finkenzeller

DFVLR
Oberpfaffenhofen
Germany

ABSTRACT

The DFVLR (German Aerospace Research Establishment) is a major engineering research establishment and operates also large-scale test facilities and aircrafts. The flight Department is executing flights for internal and external customers. The main advantages of this service unit for ERS-1 activities will be competence and flexibility.

Keywords: Airborne Remote Sensing, Research Aircrafts, Flight Operation.

1. OBJECTIVES AND AIMS OF DFVLR

The objectives of DFVLR (the German Aerospace Research Establishment) in its function as a major engineering research establishment, is to contribute to the strengthening of the technological competence and competitiveness of the Federal Republic of Germany by conducting research and development work, mainly in the aerospace field.
DFVLR constructs and operates large-scale test facilities.
DFVLR cooperates with numerous research institutions, organisations and companies in friendly industrial and threshold countries.
In the field of research
- Remote Sensing of the Earth
- Satellite Communication and Localisation

the use of aircrafts for tests and trials, and also as a test bed for experiments is here a necessity.

2. TASKS FOR FLIGHT DEPARTMENT

- Advise and look after customer's wishes
- Aircraft maintenance
- Design, manufacture and technical support for flight measurements of the aircraft's basic equipment.
- Installation and system integration of scientific devices including the execution of necessary modifications of the aircraft.
- Planning and preparation of missions at home and abroad.
- Investigations for the further development of flight research and flight measurement technology.

3. CHECKPOINTS FOR AN INDIVIDUAL MISSION

Research fligths are never carried out on a routine basis.
For each mission we have to consider special requirements:
- aircraft size and performance in respect of the the mission profile.
- construction, building, strap down devices of sensors and apparatus, weight and volume.
- power supply and type of energy
- number of seats for operators
- qualification in respect of skill and individual character of the team member.
- recording of aircraft- and sensor data
- navigational ground aids in test area (VOR/DME/NDB).
- structure of airspace
- cooperation with local authorities
- procurement of approval for overflights, execution of mission and transfer of the data (film or tape) without break.

4. ADVANTAGES OF OUR FLIGHT DEPARTMENT

- Modern and selected aircrafts
- Continuous advanced planning of aircraft selection including special provisions to be suited for scientific purpose.
- Real engineering background
- Construction, doing production of approved 19" racks mounted on shockmounts.
- Knowledge and experience in data acquisition
- Direct communication between different working groups
- Engineering back-up by company
- With the gain of experience last 20 years received a qualification
- Successful participation in different campaigns and flight activities like

JASIN	Joint Air Sea Interaction Machrihanish NE-Atlantic.
OZON	Northern hemisphere upper atmosphere 1977 - 79.
SIMOC	Simultaneous measurements of minor gasses by microwave, optical and chemical process.
ALPEX	Alpine Experiment 14 aircrafts Geneva, 1982
MIZEX	Marginal Ice Zone Experiment Spitsbergen 1984
AZOREN	Campaign 1984 Air-Chemistry Measurements
ADRIA	82/83 Oceanographic Measurements - Scanner + Radiometer Venice.
ERS-1	North Sea/Sylt 1983
ERS-1	PROMESS/Lorient 1984
ERS-1	TOSCANE-T/Quimper 1985
ERS-1	Campaign Malaga/Trapani 1986
ERS-1	Brazil/Rain Forest 1986

5. SPECIAL WORK AND PREPRATION FOR ERS-1 SCATTEROMETER CAMPAIGNS ON DORNIER 228-101

- Our extensive additional modifications pay off
- Use of apertures in the lower fuselage
- Calculations about the influence of the antennas and scientific payload in weight and balance, performance and behaviour in flight.
- Developping of a flight test program
- Verification and approval of test program by Aeronautical Authority.
- Installation and ground test of scientific payload and antennas in aircraft.
- Realisation of flight tests including behaviour in flight, performance, ascertainment of efficiency limits.
- Careful evaluation of flight test results
- Minor improvements of fixation construction, production of radoms.
- Release of installations for planned activities.

6. CONCLUSION

For all airborne remote sensing activities the DFVLR Flight Department could be your reliable partner.
Take the advantage of research aircrafts to be on the spot in very short time.
Especially our DORNIER 228-101 is able to operate from small airfields for flights with a range of at least 1000 NM. Change of scientific payload can be realised at once.
By request we are able to handle supplementary works, like disposal, transportation, set up and arranging of corner reflectors. We have the competence for all kind of aircraft based research missions.
Due to our organisational structure we are very flexible.
We like to be one of the members in your mobile calibration task force.

CCRS CONVAIR 580 RESULTS RELEVANT TO ERS-1 WIND AND WAVE CALIBRATION

N G Freeman, A L Gray, R K Hawkins & C E Livingstone

Canada Centre for Remote Sensing, (CCRS)
Ottawa, Ontario

ABSTRACT/RESUME

Results from past CCRS Convair 580 wind and wave measurement campaigns are presented to demonstrate the usefulness of such an airborne microwave research facility for ERS-1 dedicated calibration and validation experiments. Scatterometer measurements from the PROMESS campaigns show that C-band sensitivity for wind speeds (2-12 m/s) is 70 to 80% of the Ku-band sensitivity. It is also shown that the ERS-1 AMI Image mode should be able to detect surface oil as a 5-7 dB drop in scattering cross section when observed at 23^{o} incidence angle. Ship targets, however, may be lost in the sea clutter for wind speeds greater than 8 m/s. Preliminary results from the Cape Sable SAR wave imaging experiments, indicate that airborne SAR can be used to investigate the effect of R/V scaling and look direction on azimuthal falloff in SAR derived directional wave spectra.

Keywords: Convair 580, C and Ku-band Scatterometer, C-Band SAR.

1. INTRODUCTION

Canada, as a participating country in the space and ground segments of ESA's ERS-1 satellite, is planning to make extensive use of both Fast Delivery and Off Line ERS-1 wind and wave height products. Fast delivery products such as wind speed from the altimeter, and wind speed and direction measurements from the scatterometer will be incorporated in regional ocean surface wind analyses for the east and west coasts of Canada, as well as in hemispherical numerical weather forecast models run out of the Canadian Meteorological Centre. Significant wave height from the altimeter and wave direction and length from the AMI-wave mode will be used in real-time to initialize and validate operational sea state forecast models on the both coasts.

Offline ERS-1 wind, wave and SST products will be analysed by the Marine Environmental Data Service for integration with their conventional Integrated Global Ocean Services System products.

Some specific SAR satellite products would include:

1) Two-dimensional wave height or slope spectra from the AMI-SAR image mode.
2) Automatic ship detection and enhancement from SAR imagery.
3) Ocean feature mapping of fronts, bathymetry, oil spills, and eddies from SAR imagery.
4) Assimilation of satellite ocean wave data in third generation wave models.

In order to have the necessary algorithms in place prior to the launch of ERS-1, a number of airborne microwave/ocean interaction experiments will be carried out in the next few years. The Convair 580, equipped with a new digital C-band SAR as well as the present Ku- and C-band scatterometers and cameras, will be used to investigate the microwave backscattering mechanisms necessary to improve our understanding of how the SAR images ocean waves and how the scatterometer performs at high wind speeds and under different atmospheric boundary layer stabilities. As a first step in this direction, the Convair 580 will participate in an international experiment next March to examine SAR wave imaging properties under various R/V scalings and extreme wave events. During the same experiment it is hoped to add more data points to the high wind region of the C- and Ku-band scatterometer backscatter versus wind speed observational data base. Additional experiments will be carried out in the following years leading up to the wind and wave calibration campaign proposed for the ERS-1 cross-over point off the coast of Newfoundland in February-March 1990.

The Convair 580 is a twin engine turbo-prop aircraft with cabin pressurization adequate to support an operating altitude up to 23,000 feet. At a crusing speed of 270 knots, it is capable of undertaking 4-5 hour remote sensing missions, including transit and time over site. It presently carries C- and Ku-band scatterometers, with along-track fanbeam antennae and doppler processing used to obtain σ_0 at incidence angles of $15\text{-}60^{o}$. Until December 1984, it also contained X-L-C-band Synthetic Aperture Radars which looked to either side of the aircraft track and recorded data both optically and digitally.

A nadir-looking large format mapping camera (RC-10) is used during the scatterometer runs, which are generally below the cloud ceiling, in order to obtain a large area view of sea surface conditions. A Honeywell YG 7500 radar altimeter provides precise altitude information for the scatterometer flights, while a Litton LTN-90 inertial navigation system and recently installed Loran-C allow precise positioning. The two scatterometers or two of the three SAR's can be operated simultaneously, but SAR's and scatterometers are not normally run together. The operating altitude for the SAR is 8,000 to 23,000 feet while the scatterometer operates between 1000 and 3000 feet. A new C-band SAR (C-IRIS), which has high resolution digital recording with no presummer, is being installed in the aircraft in June, 1986.

In the following sections, the principles of operation of the C- and Ku-band scatterometers are briefly discussed along with results from the wind speed measurement campaigns, as well as special experiments to examine the effect of surface oil backscatter depression, and scattering from a surface vessel relative to background sea clutter. SAR ocean wave imaging mechanisms are briefly discussed with a view to showing how airborne Synthetic Aperture Radars can be used to simulate R/V scaling of satellites. The processing of airborne SAR image intensity spectra is described along with some preliminary spectra from the Cape Sable wave imaging campaign. The theory of operation of the new C-band Integrated Radar Imaging System (C-IRIS) is given along with ground measurements of expected performance, as well as operating geometries and data products. In the last section a dedicated ERS-1 wind and wave calibration and validation experiment is proposed.

2. AIRBORNE SCATTEROMETER MEASUREMENTS OF OCEAN WINDS

Currently, two fanbeam scatterometers, C-band and Ku-band, are operated on the CV-580 in a low altitude ($<$ 5000 feet), continuous wave mode. Data from both straight line and circle flights can be processed although it is preferable to use a relatively small roll angle in circle flights (10^o) so that backscatter estimates can be calculated over a wide range of incidence angles (15^o - 60^o).

Each scatterometer (5.7 GHz and 13.3 GHz) uses four fanbeam antennas, one of two H- and V-polarized antennas for transmission and two H- and V- polarized antennas for reception. The beamwidths for all the antennas are nominally $\pm 60^o$ along track and $\pm 1.5^o$ across track. Coherent, homodyne detection is used with part of the transmitted signal, modulated and injected into the receiver for calibration. Backscatter information as a function of incidence angle is derived from Fourier analysis of the audio frequency Doppler spectrum.

Base-band (audio frequency) in-phase (I) and quadrature (Q) signals are sampled at 26 kHz, for both the like and cross-polarized channels of each scatterometer. Groundspeed, altitude (radar altimeter), heading, track, pitch and roll information from a Litton LTN-90 inertial reference system are also multiplexed into and recorded with the scatterometer data stream onto two tracks of an instrumentation tape recorder.

2.1 Scatterometer Data Processing of Ocean Data

Processing proceeds in several stages: stripping the data to computer compatible tape, running quality control software, creating navigation and aircraft attitude files, preprocessing and processing to scattering coefficient data.

With the fanbeam geometry, simultaneous backscatter measurements are possible over a wide range of incidence angle ($\pm 60^o$) without significant signal-to-noise problems. Fore and aft data can be extracted from the positive and negative parts of the doppler frequency spectra obtained from FFT's of the complex (I and Q) data. A preprocessor calculates an array of centre and bandwidth frequencies for a set of bandpass filters corresponding to the desired central incidence angle and also a corresponding array of correction factors based on the ground speed, altitude, aircraft attitude and the assumed 2-way antenna illumination pattern. An array processor (CSPI MAP-300) interfaced to a PDP-10 computer is used in the processing stage to unpack the 8-bit data and to calculate the fast Fourier transform. For the circle data, a constant bandwidth mode can be used for the bandpass filters (150 Hz C-band and 350 Hz Ku-band) in the 8 k complex transforms so that the speckle statistics for the σ_o estimates do not vary with incidence angle although the instantaneous footprint does. The doppler frequencies and incidence angles are calculated based on the assumption of aircraft horizontal motion only.

Additional, incremental doppler arising from wave orbital motion introduces errors into the scatterometer output data in two ways. Firstly, an incorrect assignment of incidence angle can be made and therefore an incorrect two-way antenna gain correction may be used. Secondly, the along-track distance over which the returns are integrated may be different from what would have occurred for stationary, flat terrain and which is assumed in the processor. This second effect is similar to the familiar "wave bunching" amplitude modulation effect which can arise in SAR imagery with azimuth travelling waves. Estimates of the magnitude of the errors arising from these two mechanisms show that normally the effect on average backscatter is small especially after averaging over many gravity wave periods. In order to minimize these effects higher altitude, larger footprint operation is desirable. A study has been carried out to examine the feasibility of changing the C-band scatterometer to a long-pulse type of operation in order to operate at higher altitude. It is hoped to achieve high altitude, larger footprint operation by the ERS-1 time frame.

2.2 PROMESS Ocean Wind Scatterometer Campaign

Multi-polarized C- and Ku-band fanbeam scatterometer data were collected by the Convair 580 off the coast of Brittany, France in February 1984. A number of straight line and circle flight patterns were flown at altitudes of 1000, 2000, and 3000 feet. Over the 20 day campaign, wind speeds ranged from 1.7 m/s to 12 m/s. The French oceanographic research vessel "Suroit" collected digital wind speed and direction data as well as significant wave height. X-band and

C-band SAR imagery, taken by the Convair were used to infer the spatial variability in the wind and wave field.

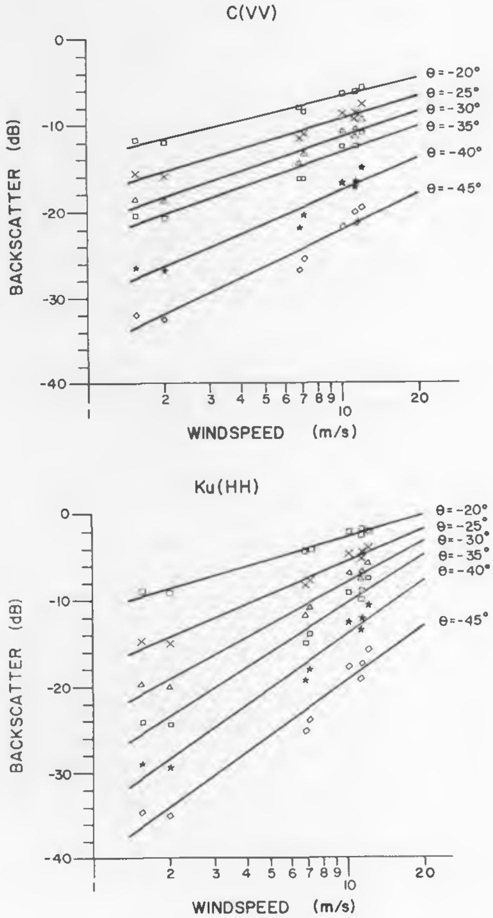

Fig. 1 C- and Ku-band backscatter comparisons or all circle flight winds in the PROMESS Campaign (Feb. 1984).

Figure 1 presents the directionally-averaged backscatter for C(VV) and Ku(HH) circle flight data measured during the PROMESS campaign [1]. The ordinate is σ_0 in dB while the abscissa is windspeed to the log base 10. Unfortunately, no circle flight data were collected for wind speeds between 3-6 m/s and greater than 12 m/s.

Straight lines are fit through the appropriate values for each incidence angle ranging from -45^0 to -20^0. The slopes of these lines represent the exponent on the expression relating wind speed to backscattering coefficient σ_0. The C(VV) slopes are slightly less steep than the Ku(HH) slopes, indicating that the wind speed sensitivity for C(VV) is slightly less than for the Ku(HH). If the low wind speeds are removed from the fit C(VV) values are approximately 70-80% of the Ku(HH) values. It should also be noted that the slopes are smaller for C(VV) than for Ku(HH) at the near swath lower incidence angles.

2.3 C & Ku-band Backscatter Depression from Surface Oil

Backscatter measurements with the Convair C- and Ku-band scatterometers were taken over a controlled oil spill approximately 20 nautical miles off Halifax in October, 1983 [2]. Average backscatter depression values between the oil spill and ocean clutter were computed for a number of straight line flights over the spreading oil plume. In Figure 2, backscatter depression ($\Delta\sigma_0$) is plotted against incidence angle for two wind speeds: 3-6 m/s in the upper diagram and 10-14 m/s in the lower diagram. The shape of the curves in each diagram is approximately the same; however, the maximum backscatter depression is about 4-5 dB lower for the higher wind speed. The maximum Ku-band depression occurs in the 30 to 35^0 incidence angle range, while for C-band this depression maximum is shifted to 45^0 incidence angle and is generally larger in magnitude. It is worth

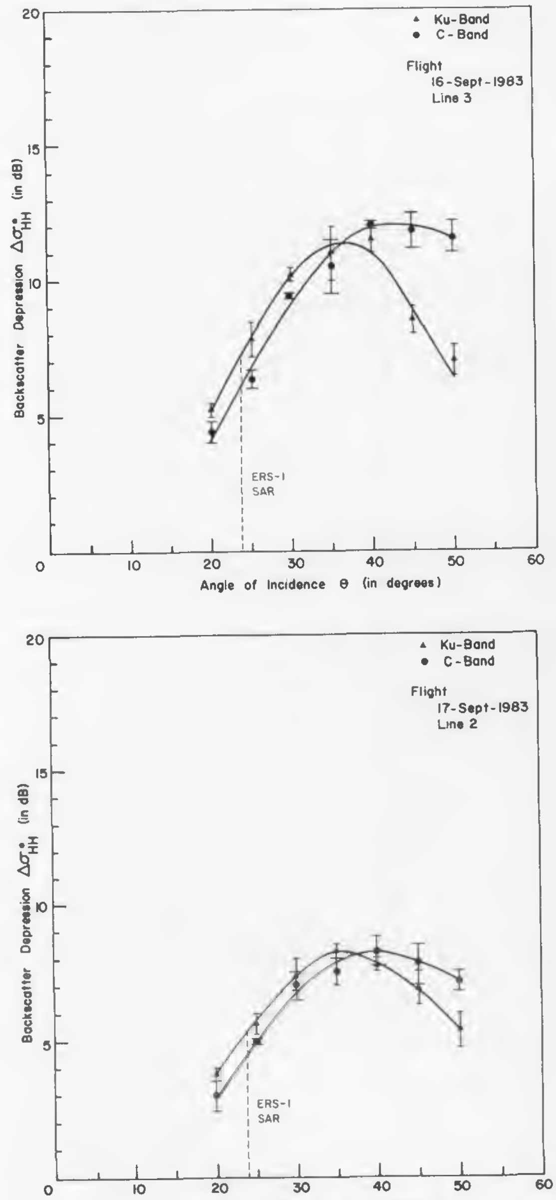

Fig. 2 C- and Ku-band backscatter supression from a controlled oil spill measured at incidence angles of 20^0-50^0.

noting that the ERS-1 AMI SAR Image mode will have a mid-swath incidence angle of 23° which will enable it to detect oil from the background sea clutter as the average backscatter depression at this angle is 5-6 dB.

2.4 Ku-band Backscatter from a Surface Vessel

Figure 3 shows a contrast study of a ship in an ocean background using the Ku-band scatterometer. A cargo vessel crossed the path of the aircraft so that the ship was seen by the forebeam of the scatterometer in the ocean clutter. Fairly high winds prevailed (8 m/s) and large swell waves were also present [3]. The scatterometer measurements are shown as a three-dimensional graph using time, incidence angle and scattering coefficients as axes. In the 3-D graph, the time history first shows the strong fall off of the ocean clutter with incidence angle followed by the pattern generated by the ship itself and then returning to the clutter pattern. It's clear from this piece of data that the ship shows greatest contrast at the higher incidence angles and may be lost in the ocean clutter nearer nadir. The strong modulation in the clutter signal is due to the large gravity waves which manifest themselves in the wave-like pattern in the 3-D graph. Note that the crest at 60° incidence angle leads the same crest at 0° incidence as the wave propagates through ground footprint of the scatterometer. This is a good example of the along track scanning distortion experienced by any moving sensor relative to a scattering facet that is also in motion (the wavelength of these ocean waves is approximately 100 m).

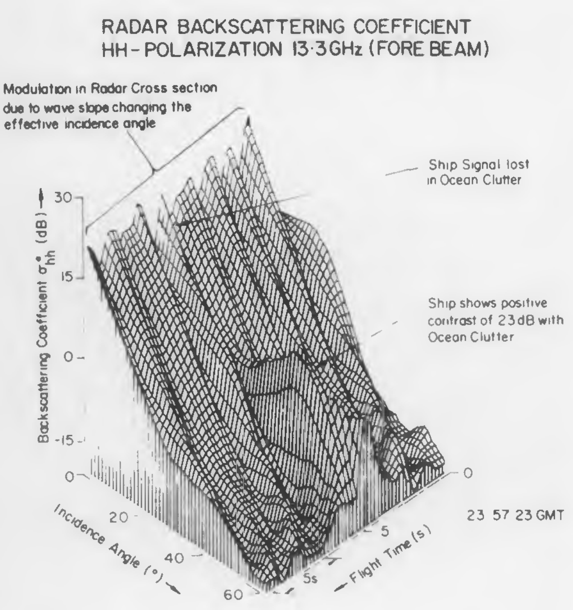

Fig. 3 C-band backscatter from a surface vessel and ocean clutter measured at incidence angles of 0°-60°. (Wind Speed approximately 8 m/s)

3. AIRBORNE SAR MEASUREMENTS OF OCEAN WAVES

During the experiments described in this paper, the Convair 580 carried a multi-frequency (X-L-C) and multiple polarization SAR. The SAR was operated simultaneously at two of the three frequencies; however, due to a malfunction in the C-band antenna only the X- and L-band frequencies were available. Incidence angle ranges of 0 to 88°, over slant range swath widths of 5 to 12 km were recorded. Single-look azimuthal resolution and slant range resolution are both on the order of 3 m for the narrow swath mode, and 6 m in range for the wide swath mode.

The SAR imaging process requires that both the radar and the aircraft be dynamically stabilized. Extreme turbulance, as was encountered at altitudes lower than 8000 feet, created image roll banding and some defocusing. Considerable care was taken in the later selection of the subscenes for digital Fourier analysis so as to avoid these regions.

The X- and L-band SAR data were recorded in three different modes for the experiments discussed here. The X-band Real Time Processor dry silver paper output (6 km slant range; 3m x 3m resolution) was used during the experiment to verify the navigational accuracy and stability of the INS. RTP ship returns from the C.S.S. Dawson as well as land references were later used to verify the aircraft azimuthal angle relative to the wave propagation direction measured by the Wavec buoy. X- and L-band digital raw signal data were recorded on High Density Digital Tapes in the high resolution mode (6 km slant range and ground resolution of 1.44 m). The presummer on this digitally recorded data may be responsible for the generation of parasitic peaks in in the spectrum of the digital data [4]; however, this has yet to be confirmed by digitizing the optically-recorded data. The third method of recording the X- and L-band SAR data was on 70 mm optical signal film. This was later processed at ERIM into 70 mm SAR, wide-swath image film (slant range width of 10.4 km).

3.1 Digital SAR Fourier Analysis

Subscenes of 1054 x 1054 pixels (approximately 1.5 km x 1.5 km) were selected from various regions of the full digital scene (approximately 10 km x 8 km). The sixteen bit intensity data were squared to obtain the radar backscatter values. A 31 x 31 Cartwright filter was applied to the subscene to reduce the speckle and thermal noise in the image. The smoothed scene was resampled by a factor of two and a least square plane fit and trend removal applied to this 512 x 512 pixel image. The variance of the backscatter values was computed and used to normalize the values at each pixel. Then a two-dimensional Fast Fourier Transform was applied to the normalized image and Power Spectral values computed from the resulting I and Q. A five by five Gaussian filter was used to smooth the resulting spectrum. As yet corrections for scanning distortion are made after manual selection of the peaks in the spectrum but work is proceeding on incorporating azimuthal wave number resampling in the Gaussian filtered spectrum.

Figure 4 provides an example of the Wavec spectrum as well as X- and L-band SAR spectra. The directional spread in the WAVEC power spectral density estimates was reduced by using the method of maximum likelihood. The principal axis of the Wavec spectrum is aligned with the corresponding axis of the SAR derived spectra.

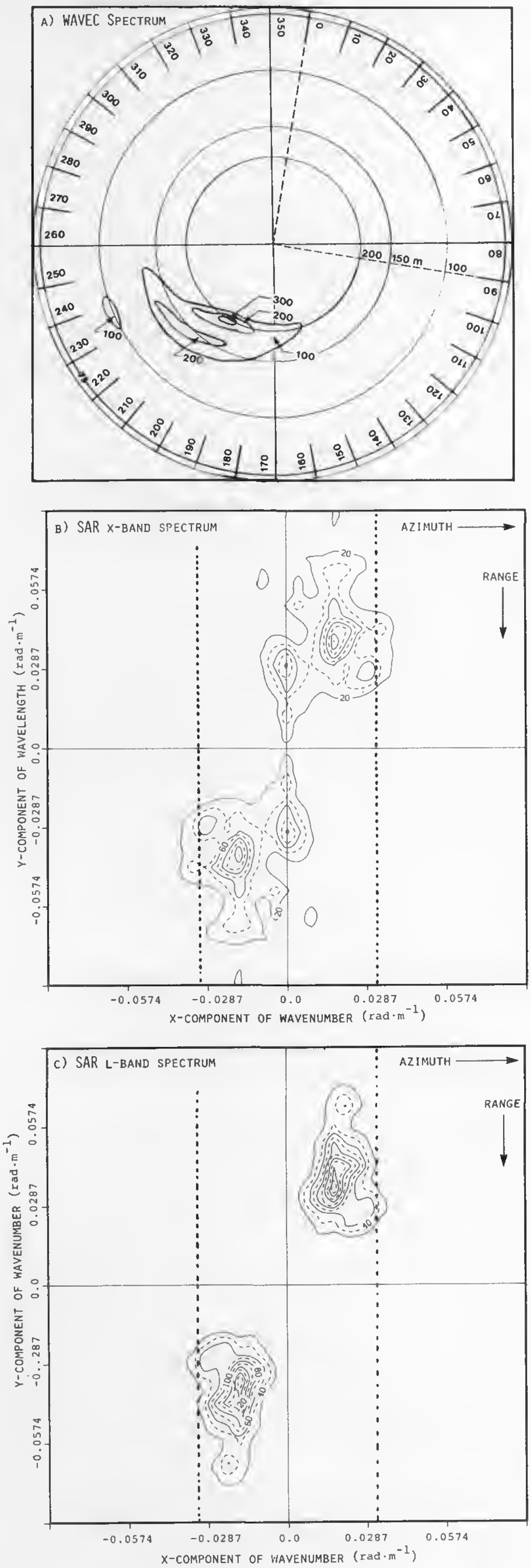

Fig. 4 Two-dimensional power spectral density plots (dashed lines are 2 min. values for this R/V and H_s condition).

The concentric circles represent wavelengths in meters. The primary peak is well-reproduced in both the X- and L-band spectra; however, the peak is rotated in azimuth as one would expect for this case of high R/V scaling (R/V = 110 s). The minimum detectable azimuth wavelength [5] for the R/V ratio (H_s = 3.5 m) is shown by the dashed lines on the two SAR spectra. Note that very little energy is visible outside these limits. The secondary peak on the range axis in the X-band spectrum may be due to parasitic peaks arising from the presummer.

3.2 Cape Sable R/V Scaling Experiment

The Cape Sable campaign took place in November 1984 off the coast of Nova Scotia (Figure 5) in conjunction with the Bedford Institute of Oceanography surface current and wave measurement program. Directional wave spectra were measured every hour during the overflight period and recorded on board the BIO research vessel CSS Dawson. In order to investigate the effects of scanning distortion, look direction and slant-range-to velocity ratio a five star pattern was flown, with each leg transitted in both directions.

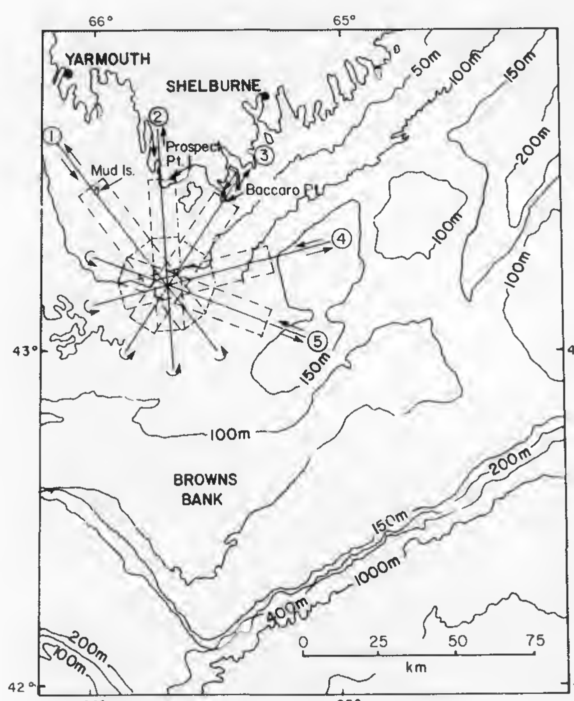

Fig. 5 Five star geometry used for the look direction and R/V scaling for imaging ocean wave properties.

As can be seen from Table 1 a wide variety of radar and ocean wave parameters were encompassed in the Cape Sable experiment. By flying into the wind at four different altitudes along a single east-west line on Nov. 17, R/V ratios of 28 to 111 s were achieved. By flying the five star pattern on Nov. 18, 21 and 22 a range of azimuthal angles from 1^o to 89^o was possible. Also by flying on five different days, significant wave height conditions ranging from 3.5 m to .7 m were encountered. From this data set of 40 X- and 40 L-band SAR scenes it will be possible to address the questions as to whether R/V is the dominant parameter contributing to azimuth fall-off or rather integration time. These questions will be investigated with the present data set as the SAR spectrum analysis become available, and alternatively with the new C-band data set to be collected in March 1987 in the Labrador Sea.

Section 2 gives data on the two receiver channels (A and B). Differences in the two receivers are due to small variations in the component characteristics, most notably the SAW range compression networks.

Three data recording paths are indicated in section 3. The simplest of these is the hardcopy

TABLE 1 CAPE SABLE DATA ACQUISITION PARAMETERS

Overflight Date	Number of Passes	Range of R/V (s)	Range of ϕ_w	Range of H_s (m)	Range of λ_w (m)	Range of Wind Speed (m/s)
Nov. 17	5	28 to 111	-20^o to -59^o	3.4-3.5	108-153	8-12
Nov. 18	11	37 to 81	$\mp 13^o$ to $\mp 85^o$	2.0-2.5	92-100	10-12
Nov. 19	2	32 to 57				
Nov. 21	11	39 to 70	$\pm 1^o$ to $\pm 72^o$	2.0-2.6	100-117	12-16
Nov. 22	11	44 to 67	$\pm 5^o$ to $\mp 89^o$	.7-.8	46-117	3-4

4. NEW C-BAND INTEGRATED RADAR IMAGING SYSTEM ON THE CONVAIR 580

A major design objective for the new CCRS integrated SAR was stability in terms of calibration, performance, and reliability. MacDonald Detwiller and Associates of Vancouver were prime contractors on the system. The new radar is C-band, dual polarized (H and V), and has two receiver channels for the parallel- and cross-polarized returns. The design employs high power TWT and modular digital control with a sophisticated motion compensation system to control antenna pointing, range delay, and signal phase correction. Range compression is done using a SAW (Surface Acoustic Wave) device. In addition, it has a set of 5 selectable Sensitivity Timing Controls (STC) which compensate for the range dependent system gains (antenna pattern, range) as well as the expected scene backscatter behaviour. Up to seven independent looks can be selected on the Real Time Processor (RTP) and the imagery is displayed both on CRT and hardcopy units during acquisition. The new radar is being installed in the CCRS CV-580 aircraft so that no actual performance characteristics other than ground tests are currently available. The subsections below therefore give details of the radar which is to be flight tested in June, 1986.

4.1 Description of the Radar Implementation and Expected Performance

Table 2 lists the major radar characteristics and combines design targets with actual measurements of the system on the ground.

In section 1 of the table the transmitter side of the radar is characterized. The H and V antennas are split out separately as is the chirp for both the high resolution (narrow and nadir swath geometries) and the low resolution (wide swath geometry).

dry silver product produced from the RTP. This is available during data acquisition from one of two receiver channels. The image HDDT (High Density Digital Tape) path is again the RTP product from the selected channel and represents the fully compressed signal. The third path employs a HDDT to record the motion compensated, range compressed signal data. Subsequent azimuth compression must be done on a ground based SAR processor.

Highlights of the system are: its flexibility in operating geometry, high S/N ratio, high resolution, high quality on-board RTP, and the ability to record both image and raw data.

4.2 SAR Operating Geometries

The system has three operational geometries: nadir, narrow, and wide swath. The first two encompass the higher resolution mode of the radar and the wide swath extends the swath but reduces the resolution. In addition, for the wide swath and narrow swath geometries, the near edge of the swath is viewed at 45 degrees incidence angle. (The minimum range delay of the system is 23 microseconds which places restrictions on these limits depending on the altitude). Data on the three geometries are given in Fig. 6 which illustrates the nadir mode. In the figure, the resolutions in azimuth and slant range, the range of incidence angles studied, and the ground swath available are indicated. Note that the STC function is applied to the first 9 km of the image swath for the nadir mode only, but is applied to the full swath in the other modes. The nadir geometry is the mode most applicable to satellite verification work.

4.3 Data Products

Figure 7 illustrates the three data flowstreams and image products that will be available from the system.

TABLE 2 C-IRIS EXPECTED PERFORMANCE

1) **Properties of Radiated Signal**

Frequency (wavelength)	5.3 GHz (5.7 cm)	
Radiated Peak Power	26.4 kW	
Transmitted Polarization	H	V
Azimuth Beamwidth (3 dB one way)	3.6^o	4.2^o
Elevation Beamwidth (3 dB one way)	23^o	27^o
Antenna Gain	23.6 dB	21.8 dB
Polarization Cross Coupling	-40 dB	-40 dB
Modes	High Resolution	Low Resolution
Chirp Length	7 μs	8 μs
Chirp Bandwidth	42 MHz	11.4 Mz
Chirp Coding	Non-linear FM	linear FM
Pulse Repetition Freq./AC Speed	2.32 Hz/m/s	

2) **Properties of the Received Signal**

		Receiver A	Receiver B
Range Pulse Width	High Res.	38 ns	40 ns
	Low Res.	110 ns	130 ns
Range Integrated Side Lobes	High Res.	-18.78 dB	-14.7 dB
	Low Res.	-21.0 dB	-16.8 dB
Range Paired Echos (Worst Case)	High Res.	-45 dB (±1.8 μs)	-40 dB (±1.8 μs)
	Low Res.	-37.5 dB (±4.8 μs)	-37 dB (± 5 μs)
Noise Equivalent σ_o at Far Range	High Res.	-45.8 dB	-41.2 dB
	Low Res.	-40.6 dB	-36.3 dB

3) **Data Recording**

Signal HDDT	- 4096 (8 bit I and 8 bit Q) range cells - full annotation
Image HDDT	- 4096 (8 bit Real) range cells - RTP annotation
Hard Copy	- 2048 range cells (averaged for full, ½ or ¼ swath) - embedded annotation

4) **Special Features**

No Presummer	
Radiometric Resolution	±2.4 dB
Good Relative Stability	
Four Stored Laws for Sensitivity Time Control.	

Data are recorded directly in image form or HDDT using a formatter. A ground computer (currently known as AIR I) is used to transcribe to computer compatible tape (CCT) in standard format. This CCT is available to users and may be imaged on high quality film or used on image analysis systems. It is anticipated that this path would be the most popular since it combines high quality digital data and no necessary post flight processing.

Range compressed data are also recorded on HDDT and CCRS has in place a dedicated ground processing system known as C-SHARP to transcribe, process, and transfer to CCT the data in this stream. The ground processor has potentially more flexibility and resolution than the RTP. It is anticipated that this data path would be more of interest for research on system peformance, quantitative studies of surface properties, or for processing the other recorded receiver channel.

5. CALIBRATION/VALIDATION EXPERIMENTS

In March 1986, the Bedford Institute of Oceanography in conjunction with the Canadian Atmospheric Environment Service as well as numerous government and university participants conducted a major two-month mesoscale air/sea interaction study on the Scotian shelf. The basic oceanographic objective of the program was

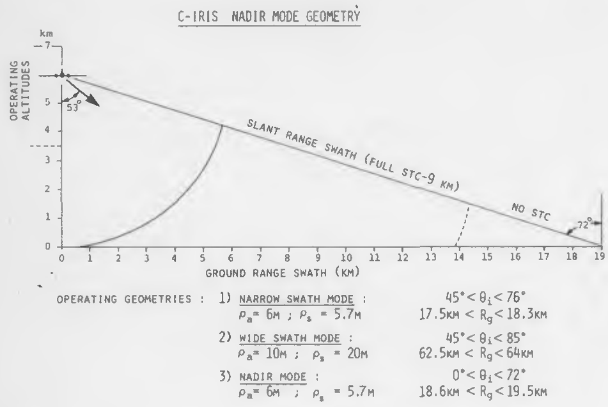

Fig. 6 C-band Integrated Radar Imaging System (C-IRIS) operating geometrics.

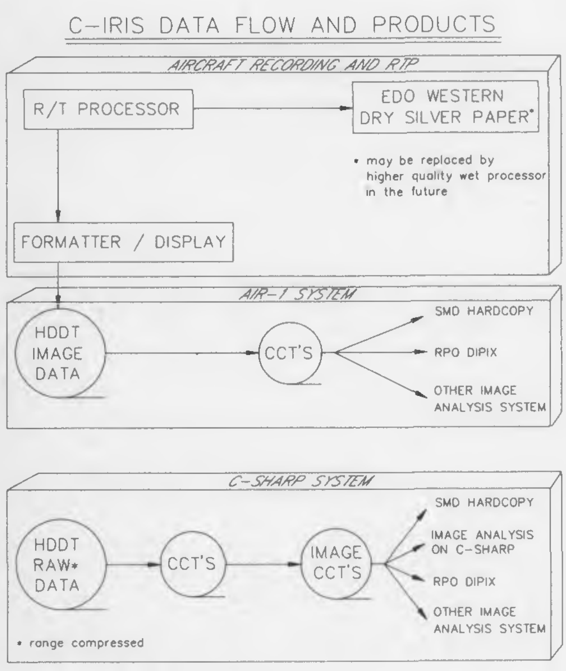

Fig. 7 C-IRIS data flow and products.

to measure the response of the ocean to mesoscale features (10-100 km) embedded in extreme storm events (approximately 1000 km) propagating up the east coast. One of the many experiments carried out during the study was to examine the degree to which mesoscale variability in the wind, modulated the surface wave field. A similar Canadian Atlantic Storms (CASP) field program in cooperation with a US effort is planned for the east coast of Canada in March 1989 but may be shifted by a year to take advantage of ERS-1 and N-ROSS wind and wave observations. These ongoing oceanographic air/sea interaction programs not only provide the necessary understanding of the temporal and spatial variability of wind and wave conditions in the area but also provide an opportunity to link the calibration/validation of ERS-1 wind and wave mode to a strong on-going ocean science program.

5.1 AMI Wind Mode Validation

It is proposed that a minimum of three anemometer equipped minimet buoys be deployed by the Bedford Institute of Oceanography along a line of latitude (approximately 55°N) at the three-day crossover point for ascending and descending passes of the ERS-1 scatterometer (Figure 8).

These buoys would remain in place for the one month observational phase (February or March 1990) during the three month commissioning period. The highest frequency of occurrence of extreme wind and wave events occur at about this latitude in the Labrador Sea off the pack ice. There is a 50% probability of obtaining 6-8 m significant wave height events in this region during March.

The Convair 580 with its C- and Ku-band scatterometers continuously recording, would be flown orthogonal to the ERS-1 wind mode swath along the same latitude as the moored buoys. The straight line σ_0 measurements would be interrupted periodically by evenly spaced circle flights. The ten circle flights correspond approximately to the ten 50 km wind cells of the ERS-1 scatterometer. By beginning the airborne data acquisition 1½ hours before the overpass and by having the anemometer time histories, a good mix of spatial and temporal data can be used for ERS-1 algorithm validation. From the experience gained in the PROMESS campaign, good estimates of the azimuthal variation can be obtained with the fanbeam scatterometers even from one circle (radius approximately 7 km; time approximately 8 mins.) especially if higher altitudes and larger footprints can be used. On the return trip the SAR would be run continuously in the wide swath mode (approximately 60 km swath width) to give a qualitative indication of the spatial variability of the wind field.

The value of airborne scatterometer measurements is to fill in the trends and variations between fixed point surface measurements. As well they permit comparison of backscatter from all incidence angles of the ERS-1 AMI wave mode. Consequently, it is felt that the two scatterometer systems on the Convair 580, along with the in situ meteorological buoys as well as the large range of wind and wave conditions of the Labrador Sea site, will provide an important wind calibration/validation point for ERS-1.

5.2 SAR Wave Mode Calibration

As can be seen in Figure 8, the 80 km ERS-1 SAR swath cross-over point is about 8° of latitude further south than the cross-over for the AMI wind mode swath. This essentially means that a separate experimental site is required for the wave mode validation. Also because of the reduced quantization of the AMI wave mode as well as the inability to carry out spatial averaging of the AMI wave mode spectra, only the AMI image mode will be used for SAR wave calibration. This precludes simultaneous AMI wind mode data over the wave validation site. At this site, it is proposed that four directional wave buoys be deployed along with a single minimet buoy. In addition to the redundancy achieved by four WAVEC buoys, it should also be possible to achieve better directional resolution and some reduction in the observational errors through averaging.

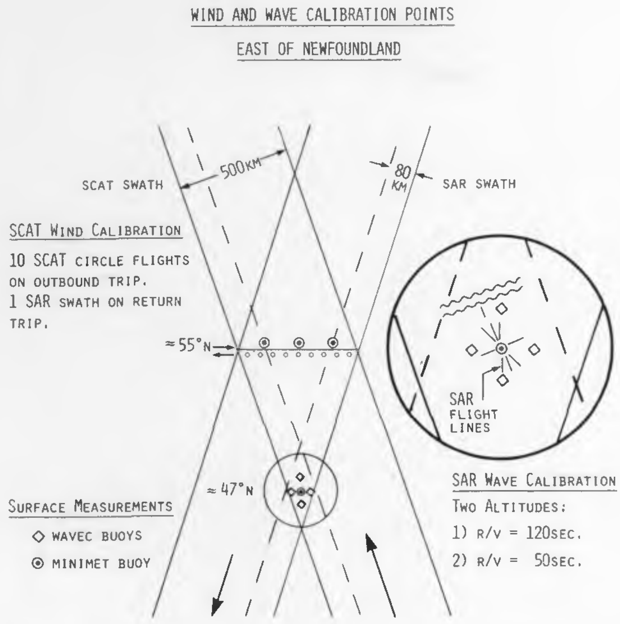

Fig. 8 Proposed wind and wave calibration site off Newfoundland, Canada.

The wind measurement is necessary to interpreting wind direction effects on the SAR imagery of ocean waves.

For calibration purposes, the Convair 580 would be flown at an altitude and azimuthal angle, relative to the propagation direction of the principal wave field component, so as to minimize the R/V scaling and look direction effects. This implies a low altitude/high ground speed and near range travelling waves. These parameters may however change as results from on-going and planned experiments suggest otherwise. For the purpose of assessing the degree of azimuthal falloff in the SAR image intensity spectra, it is also considered important to fly the line pattern at a higher altitude (ie. R/V value). The four star pattern should be flown at both altitudes as recent work by Piau et al. [4] indicates that the airborne SAR may be more sensitive to range-travelling waves than azimuthal-travelling ones.

The new C-band SAR currently being installed on the CV-580 will be further characterized prior to the mission using passive and active reflectors and by carrying out SAR-scatterometer comparisons. In this way, the linear operation of the SAR System necessary for any kind of calibration/validation activity can be checked. Directional wave buoys provide valuable surface measurements for the wave mode, however, by using airborne SAR (possibly also with a lidar altimeter) the quality of the surface information is significantly enhanced. The airborne SAR can be flown in any direction, has a more suitable R/V ratio for wave imaging, and the 2-D image spectra often show a narrower wave directionality than directional spectral derived from pitch and roll buoys.

6. CONCLUSIONS

Past results from the Convair 580 microwave sensor measurements of ocean wind and wave backscattering properties demonstrate that airborne measurements can play a significant role in ERS-1 wind and wave calibration and validation. The new C-IRIS offers the potential for increased instrument stability, very low noise equivalent σ_0 and good dynamic range for airborne imaging of wave properties. BIO/CCRS offer the opportunity for a strong mesoscale air/sea interaction measurements and the Labrador Sea extreme waves experiment provides a pilot test for wind and wave mode calibration prior to the launch of ERS-1.

ACKNOWLEDGEMENTS

The authors would like to gratefully acknowledge the contributions of H. Kimpton in typing the manuscript and B. Moxon in drafting the figures.

REFERENCES

[1] Gray, A.L., R.K. Hawkins (1985) "C- and Ku-band Scatterometer Results from Canadian Participation in the ESA PROMESS Ocean Measurement Campaign", Proceedings of Third International Colloquium on Spectral Signatures in Remote Sensing, LesArcs, France, 1985 (ESA SP 247). pp. 77-82.

[2] Singh, K.P., A.L. Gray, R.K. Hawkins (1986) "The Influence of Surface Oil on C- and Ku-band Ocean Backscatter", to be published in IEEE Geoscience and Remote Sensing, 1986.

[3] Gray, A.L., R.K. Hawkins, C.E. Livingstone, R. Lowry, R. Larson, R. Rawson (1970) "The influence of Incidence Angle on Microwave Returns of 'targets' in an Ocean Background", in Proceedings of the Thirteenth International Symposium on Remote Sensing of Environment, Ann Arbor, Mich., pp. 1815-1837.

[4] Piau, P., C. Blanchet, A.L. Gray (1985) "SAR Imaging of the Sea Surface During the ESA C-band Wind Scatterometer Campaign", Proceedings of the Third International Colloquium on Spectral Signatures on Remote Sensing, Les Arcs, France, 1985 (ESA SP 247).

[5] Beal, R.C., D.G. Tilley, F.M. Monaldo (1983) "Large and Small-scale Spatial Evolution of Digitally Processed Ocean Wave Spectra from SEASAT Synthetic Aperture Radar", J.G.R. Vol. 88, No. C3, pp. 1761-1778.

OCEANOGRAPHIC MEASUREMENT CAPABILITIES OF THE NASA P-3 AIRCRAFT

E Mollo-Christensen, F C Jackson, E J Walsh & F Hoge

Laboratory for Oceans
NASA Goddard Space Flight Center
Greenbelt, Maryland 20771, USA

ABSTRACT/RESUME

NASA's P-3A Orion aircraft is equipped with a suite of unique sensors which are capable of providing high resolution directional wave spectrum measurements as well as other oceanographic measurements in support of the ERS-1 validation. The wave sensors include the 36 GHz Surface Contour Radar (SCR), the Ku-band Radar Ocean Wave Spectrometer (ROWS), and the Airborne Oceanographic Lidar (AOL). The other sensors include a C-band scatterometer, video camera, radiation thermometer, and AXBTs. The SCR and ROWS directional spectrum measurements are discussed in some detail. When planning for an underflight mission, the limited endurance of the aircraft (6 hrs) and flight cost (2.7 K$/hr) must be considered. The advantage of the redundancy afforded by the several waves instruments is another important consideration.

Keywords: NASA P-3 aircraft, ERS-1 underflights, radar wave sensors, directional wave spectra, C-band scatterometer, lidar.

1. INTRODUCTION

NASA's P3-A Orion aircraft (Figure 1) is operated by the Goddard Space Flight Center's Wallops Flight Facility (WFF) located in Wallops Island, Virginia. The aircraft is the prototype version of the production P-3. Unlike the production P-3, it has a rather limited fuel capacity and hence a limited endurance (approx. 6 hrs). Since its acquisition by WFF in 1978, the aircraft has been used for rocket range work and for remote sensing instrument development and scientific data gathering. Unlike most other of NASA's scientific research aircraft, the WFF aircraft are not block-funded by NASA Headquarters, and so flight expenses must be paid for directly by individual research or project funds. The present cost of the aircraft is $2,700 per hour.

The aircraft navigation is by Inertial Navigation System (INS) and Omega. A GPS (Global Positioning System) receiver will be installed in the near future. A large bomb bay and several other ports can accommodate a number of remote sensing instruments. Permanent facility instruments on the aircraft include a PRT-5 infrared radiometer, video camera, and AXBT launch tube.

Much of the research use of the aircraft is now in the ocean sciences. The principal oceanographic instruments which either have flown on the aircraft, or which are planned for the aircraft are given in Figure 1. This paper will describe several unique experimental sensors which could contribute significantly to the ERS-1 validation effort. These instruments are: The Surface Contour Radar (SCR), Radar Ocean Wave Spectrometer (ROWS), Airborne Oceanographic Lidar (AOL), and C-Band Scatterometer (C-SCAT). They form an exceptionally good suite of sensors for an ERS-1 underflight mission directed to evaluating the performance of the SAR and scatterometer wind and waves measurements. Particularly relevant to an ERS-1 underflight mission is the Shuttle Imaging Radar-B (SIR-B) underflight mission which took place off the coast of southern Chile in October 1984 (Beal et al., 1986). This mission well illustrates the use of the P-3 wave sensors for a spaceborne SAR validation.

2. SURFACE CONTOUR RADAR

The Surface Contour Radar (SCR) is a 36-GHz computer-controlled airborne radar (Kenney et al., 1979) which generates a false-color coded elevation map of the sea surface below the aircraft in real time, and can routinely produce ocean directional wave spectra with post-flight data processing which have much higher angular resolution than pitch-and-roll buoys. The high spatial resolution and rapid mapping capability over extensive areas make the SCR ideal for the study of fetch-limited wave spectra, diffraction and refraction wave patterns in coastal areas, and wave spectra associated with hurricanes and other highly mobile events. The SCR is also being applied in areas other than producing directional wave spectra such as determining the scattering characteristics of waves and the topography and backscatter characteristics of ice. The SCR is one of the most straightforward remote sensing instruments in measurement concept. It provides great ease of data interpretation since it involves a direct range measurement.

AIRCRAFT TYPE — P-3A ORION
AIRSPEED — 180 TO 315 nts
ALTITUDES (OVER OCEAN) — 500 ft TO 25,000 ft
CRUISING RANGE — 2,000 n mi (APPROX 6½ HRS)

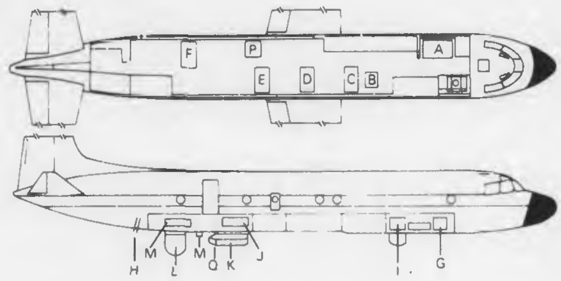

INSTRUMENTATION

LEGEND	SENSOR	FREQ.	MEASUREMENTS
A,G	SURFACE CONTOUR RADAR (SCR)	35 GHz	DIRECTIONAL WAVE SPECTRA BACKSCATTER VS. ANGLE & RANGE
B,C,I	WAVE DIRECTIONAL SPECTROMETER (ROWS) & K-BAND SCATTEROMETER (K-SCAT)	13.9 GHz	DIRECTIONAL WAVE SPECTRA DIRECTIONAL WINDS
D,E	AIRBORNE OCEANOGRAPHIC LIDAR (AOL)	OPTICAL	BATHYMETRY CHLOROPHYLL (INDUCED FLUORESCENCE) DIRECTIONAL WAVE SPECTRA
F,L	STEPPED FREQUENCY RADIOMETER	4.3-6.8 GHz 160 STEPS	WINDS
H	AXBT DEPLOYMENT TUBE		VERTICAL TEMPERATURE SOUNDINGS
J, K	C-BAND SCATTEROMETER (C-SCAT)	4.5 GHz	DIRECTIONAL WINDS
M	TV RECORDER SYSTEM	OPTICAL	FOAM
P	AAFE ALTIMETER	13.9 GHz	SWH WINDS
Q	PRT-5	IR	SURFACE TEMPERATURE

Figure 1.

Figure 2 shows the nominal measurement geometry and the horizontal resolutions in terms of the aircraft altitude, h. An oscillating mirror scans a 1.42° half-power width pencil-beam laterally to measure the elevations at 51 evenly spaced points on the surface below the aircraft. The nonscanning receiving antenna is a 1.3° x 40° fan beam with the 40° dimension oriented cross-track. The combination of the transmit and receive antennas narrows the along-track interrogated region to a half-power width of 0.96°. At each of the 51 points across the swath the SCR measures the slant range to the surface and corrects in real time for the off-nadir angle of the beam to produce the elevation of the point in question with respect to the horizontal reference.

The elevation measurements are false-color coded and displayed on the SCR color TV monitor so that real-time estimates of significant wave height, dominant wavelength, and direction of propagation can be made. The real-time display allows optimal selection of aircraft altitude and flight line direction even during a flight over a cloud-covered sea without prior knowledge of the wave conditions. The radar has range resolution cells of 0.15, 0.3, 0.6, and 1.5 m, although the last two have never been used for oceanographic studies. The 15 cm resolution has generally been used, with the 30 cm resolution employed when the significant wave height reaches 5 m, or when the SCR is operating at 800 m altitude. Walsh et al. (1985) describe in detail the data processing used to produce directional wave spectra.

The SCR measured the directional wave spectrum in the vicinity of the Delaware Bay on January 5, 1982. The wind was blowing offshore, nearly parallel to the bay axis, at approximately 17 m s^{-1}. The left side of Figure 3 indicates a flight line flown parallel to the shoreline, starting off the New Jersey coast and ending on the axis of the Delaware Bay. The heavy dots indicate the center positions of contiguous sets of 1024 scan lines used to produce the spectra indicated on the right of Figure 3. The radial direction from the center of the mouth of the Delaware Bay to the center of each data set was determined and indicated by the dotted radials. The spectra on the right side of Figure 3 are numbered consecutively from north to south. They show only the right-half plane (0°-180°) and the wave number region from 0.1 to 0.3 radian/m. Arrows have been included to indicate the direction from the Delaware Bay, corresponding to the dotted radials on the left side of Figure 3. A number of interesting things are apparent in the sequence. In general, the spectra shift from northeast to southeast, following the radials from the Delaware Bay, indicating that the waves were originating in the Bay. However, the two northernmost spectra are actually propagating more northerly than the radials. Since the left side of Figure 3 indicates that these radials graze the shoreline, part of the wave energy may have arrived in that region due to refraction. That might also account for the energy being highest in the first spectrum and then waning over the next three.

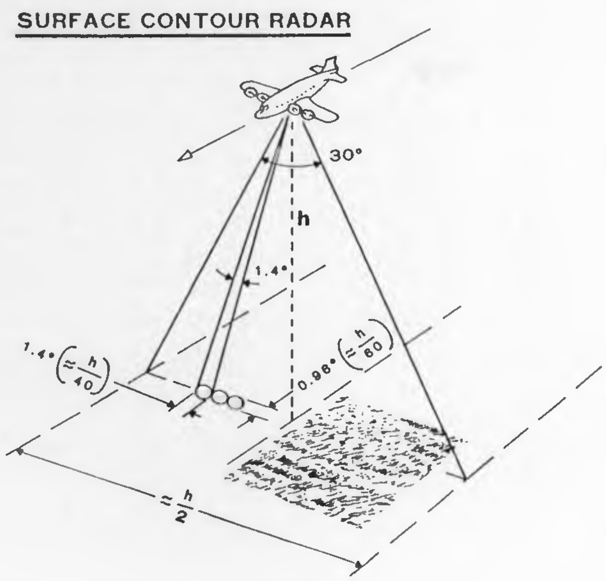

Figure 2.

Spectra 5 through 10 of Figure 3 have peaks which are south of the radial from the Delaware Bay, which is reasonable since the radials were drawn from the center of the mouth of the Bay which has a significant width. The radial associated with the last spectrum, which is also the most intense, is centered on the spectral peak and the associated radial is nearly aligned with the axis of the Delaware Bay.

The technique of producing directional wave spectra with the SCR has some similarities to stereophotography (e.g., Holthuijsen, 1983), except that the stereophotographic technique provides the instantaneous topography of the sea surface so there are no Doppler effects present. An instantaneous topographic map could represent waves traveling in either of two directions, separated by 180°. As was pointed out by Holthuijsen (1983), it is not possible to discriminate between the two spectral lobes direction of propagation as frequency increases, using stereophotography and a priori knowledge must be introduced to reject the ambiguous lobe. While that process might not be too difficult near a shoreline, it could be quite troublesome far out to sea. Since it takes approximately 52 seconds to acquire each SCR data set used to produce a directional wave spectrum, the data do But far from being a disadvantage, the SCR Doppler effects are easily corrected (Walsh et al., 1985) and provide a means of uniquely determining the direction of propagation of the waves being measured. Figure 4 shows overlays for two different ground tracks of the Doppler corrected directional wave spectra for the bimodal system of swell measured on October 28, 1980, off Duck, North Carolina. The spectral data on a 100 x 0.01 m^{-1} wave number grid were slightly smoothed by averaging over 3 x 3 points with the surrounding eight points each weighted one eighth that of the center point. The solid curves are the average of four spectra and the dashed curves are the average of two, all from data obtained at 400 m altitude. All of the spectral components were Doppler corrected assuming that they were real. The corrections cause the actual spectral components (propagating towards the north and west) to coalesce for the two flight directions. But the corrections are in the wrong direction for the ambiguous lobes (south and east) and cause the mismatch apparent in Figure 4 that allows them to be rejected.

The SCR can determine even a complex spectrum in great detail. The top of Figure 5 shows a directional wave spectrum generated from data taken at 860 m altitude approximately 240 km west of the eye of Hurricane Debby on September 17, 1982. The significant wave height was 4.3 m and the spectrum shown is the average of five spectra gathered with the interval 1810 to 1815 GMT. The aircraft was traveling at 98 m/s along a 319° ground track with a drift angle of approximately 7°. The SCR beam was scanning at 9.6 Hz, producing one crosstrack raster scan line of elevations every time the aircraft advanced 5.1 m. The spectrum shows the presence of both sea and swell generated by the hurricane. By flying along different ground tracks the ambiguous spectral lobes were rejected and are shown crossed out in the figure. The swell peak spectral density is at 0.09 Hz and has a 25° half-power width which Walsh et al. (1985) indicate is the resolution limit of the SCR at that frequency. The peak spectral density of the sea is at 0.12 Hz with a 35° half-power width which is about three times as wide as the SCR resolution for those conditions. The bottom of Figure 5 shows the aircraft position relative to the ground track of the hurricane obtained from the forecasts. Also indicated is the expected wind at the aircraft position from the hurricane forecast, confirmed by the wind measured at the aircraft altitude.

The hurricane spectrum gives an indication of the detail that the SCR can provide to people studying wave growth and dissipation under these highly nonlinear circumstances. The sea and swell spectral lobes both turn through 30° in direction of propagation as frequency increases, the sea in a clockwise direction and the swell in a counterclockwise direction. The extrapolated positions indicated for the swell indicate it was generated at approximately 1000 GMT in a region 140 km from the eye of the hurricane. It would have been impossible for a pitch-and-roll buoy to produce this spectral detail.

3. RADAR OCEAN WAVE SPECTROMETER

The Radar Ocean Wave Spectrometer (ROWS) is a 13.9 GHz, 12.5 ns resolution pulse compression radar with characteristics similar to the Geos-3 altimeter. It is presently equipped with two antennas, a broad-beam (70°) nadir-pointing antenna, and an off-nadir, conically scanning antenna. A mode change command from the radar control panel switches the radar between these two antennas. The nadir-pointing antenna is used in the instrument's 'altimeter' mode to measure significant wave height, and the surface mean square slope and wind speed from the trailing edge of the waveform. The off-nadir 'spectrometer' mode uses a 6-rpm, 10° elevation by 4° azimuth beamwidth antenna boresighted to 16° incidence to measure the directional slope

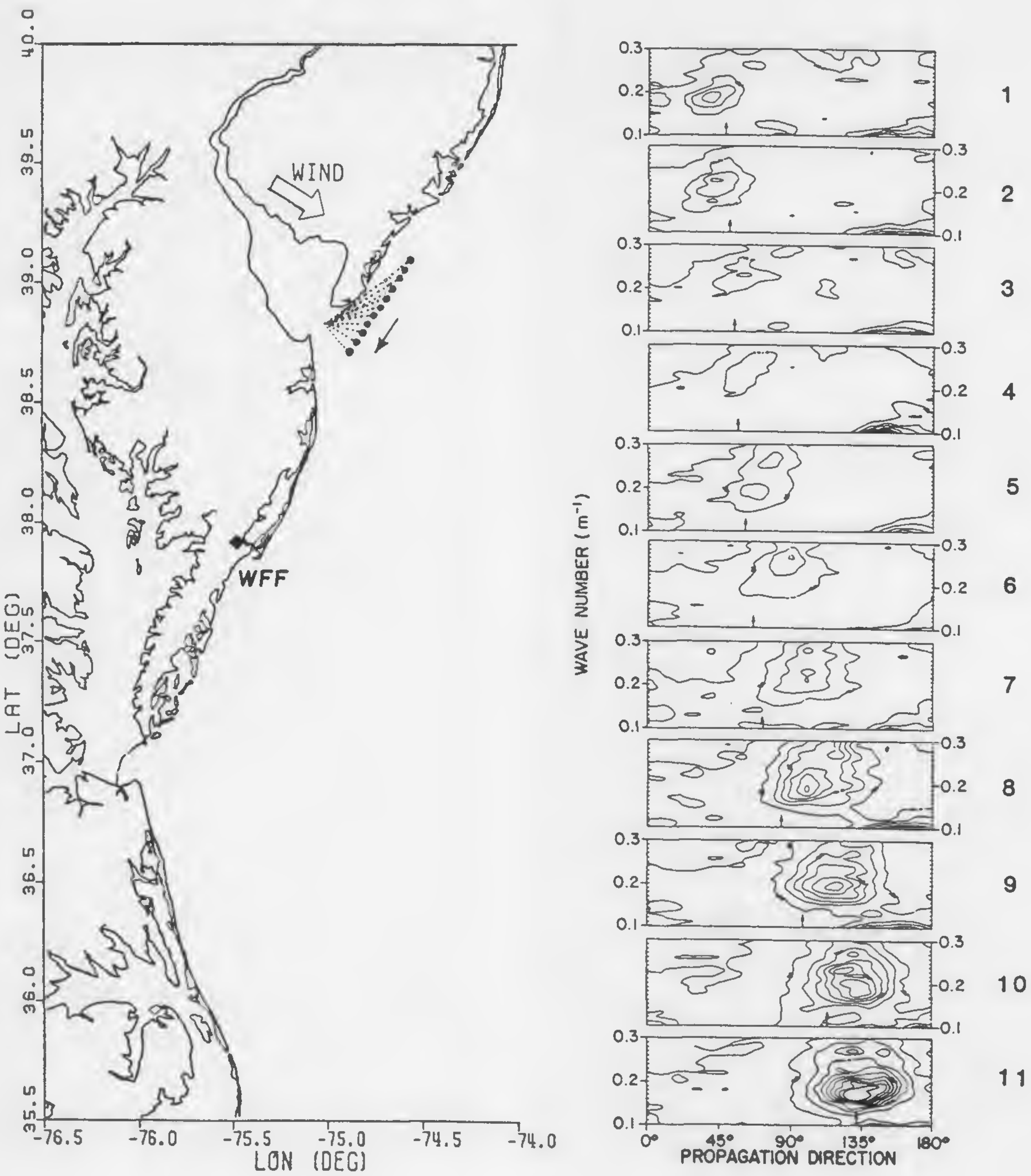

Figure 3.

spectrum. At the nominal P-3 operating altitude of 7 km, this antenna produces a footprint of ca. 1000 m in range and 500 m in azimuth. The surface range resolution is about 8 m at 13° incidence, the nominal angle for peak power return. The spectrometer mode geometry is depicted in Figure 6.

The spectrometer technique is described in detail by Jackson et al. (1985a, b). The technique is similar to the two-frequency technique developed by ESA for Spacelab I. In both techniques, wave directionality is determined by a matching of the ocean wave and electromagnetic phase fronts across the lateral extent of the beam (cf. Fig. 6). The ROWS technique differs from the two-freqency technique in that the range reflectivity modulation is detected in the time domain using short pulse waveforms. The square-law detected backscattered pulses are sampled with a high-speed A/D converter, integrated for a time corresponding to 15° of azimuth movement, and spectrum analyzed for the spectrum of the range reflectivity modulation. The actual processing, which is presently done off-line on a general purpose computer, is rather involved and the reader is referred to Jackson et al. (1985a, b) for details.

In the near-nadir, quasi-specular scatter regime in which the ROWS operates, the reflectivity modulation mechanism is predominantly geometrical tilting. Thus, the spectrum of the range reflectivity modulation is to a first approximation proportional to the directional

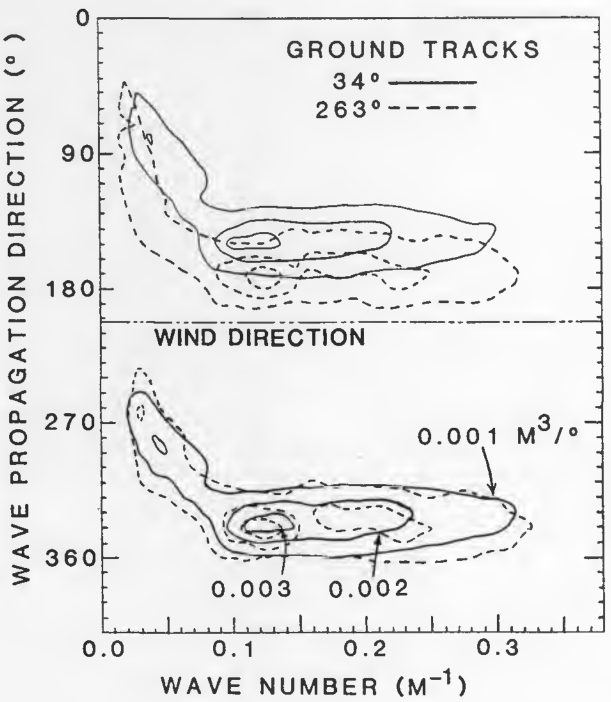

Figure 4.

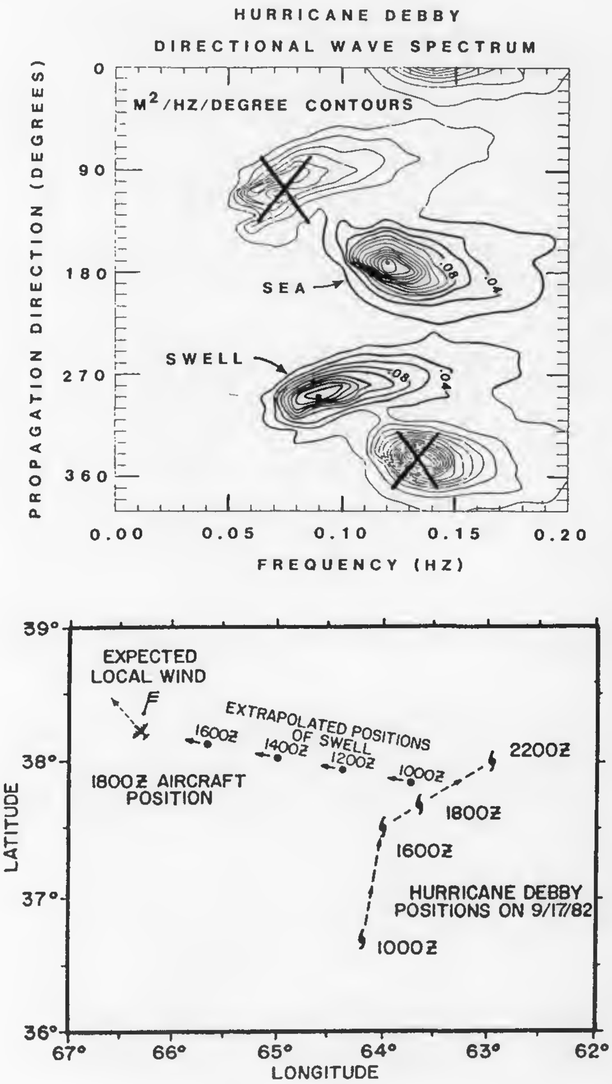

Figure 5.

slope spectrum evaluated for the particular azimuth of look. The sensitivity coefficient relating the slope spectrum to the measured modulation spectrum depends on the cross section roll-off, which in turn depends on the surface mean square slope. Since the cross section near nadir is weakly azimuth dependent, the sensitivity is also azimuth dependent, varying by about 20% over all azimuths. The sensitivity is presently calculated using mean square slope data from the altimeter mode (Jackson et al., 1985c). The measured slope spectrum can also be scaled simply by using the altimeter mode wave height estimates directly. Generally, the technique can be expected to produce spectra with good fidelity out to wave numbers several times the peak wave number provided there is sufficient small-scale roughness. Thus, the wind speed must be greater than several meters per second.

The directional resolution is a function of the azimuth footprint dimension and the wavefront curvature and also of the finite movement of the antenna beam during the pulse integration time (15°). This resolution varies with water wave number and is about 20° for the shortest waves and about 45° for the very long waves (400 m). Regardless of the resolution, ROWS spectra are output in 15° bins. The wave number resolution is determined soley by the 1000 m range footprint dimension. The wavefront curvature effect in the elevation plane is corrected for in the time-domain processing when the data are re-arrayed in equally spaced 12 m range bins prior to spectrum analysis by FFT. The measured 360° modulation (or slope) spectra are symmetrized by averaging looks 180° apart and final spectra are produced by averaging spectra from at least 10 antenna rotations.

This gives directional spectra with a minimum of 40 degrees of freedom. The corresponding spatial coverage is a swath of some 2 km by 15 km. Final conversion to height spectra is done simply by dividing the spectra by k-squared.

The ROWS technique was first demonstrated with data obtained during the CV-990 Nimbus-G underflight mission in 1978 (Jackson et al. 1985a, b). Comparison with a large buoy data set showed good spectral fidelity, and the ability to measure absolute spectral amplitudes rather accurately was demonstrated.

A remarkable set of ROWS spectra was obtained on the 1978 mission during an intense storm in the Norwegian Sea. Figure 7 is a synoptic chart showing the storm at 1800 Z the day before the flight on November 3, 1978. The map shows the prior positions of the low every six hours and the flight pattern on the third. Between 0800 Z and 1000 Z on the third, the 990 flew a box pattern at 10 km altitude measuring 150 km in the NS direction and 700 km in the SW-NE direction. In this flight box, the ROWS obtained ten files of

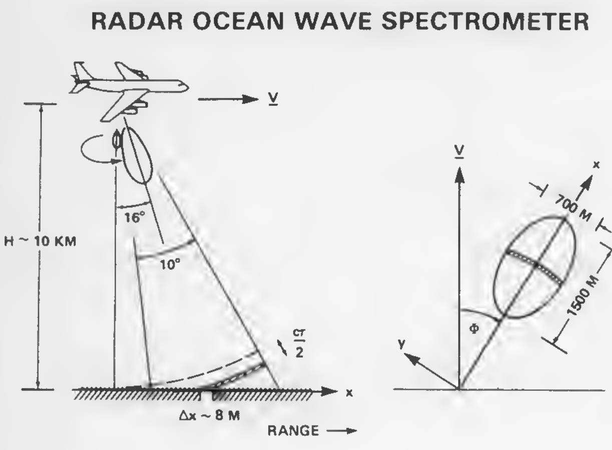

Figure 6.

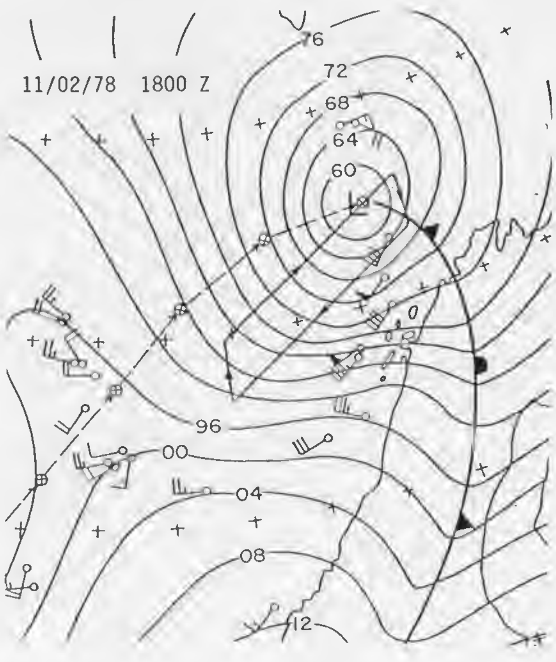

Figure 7.

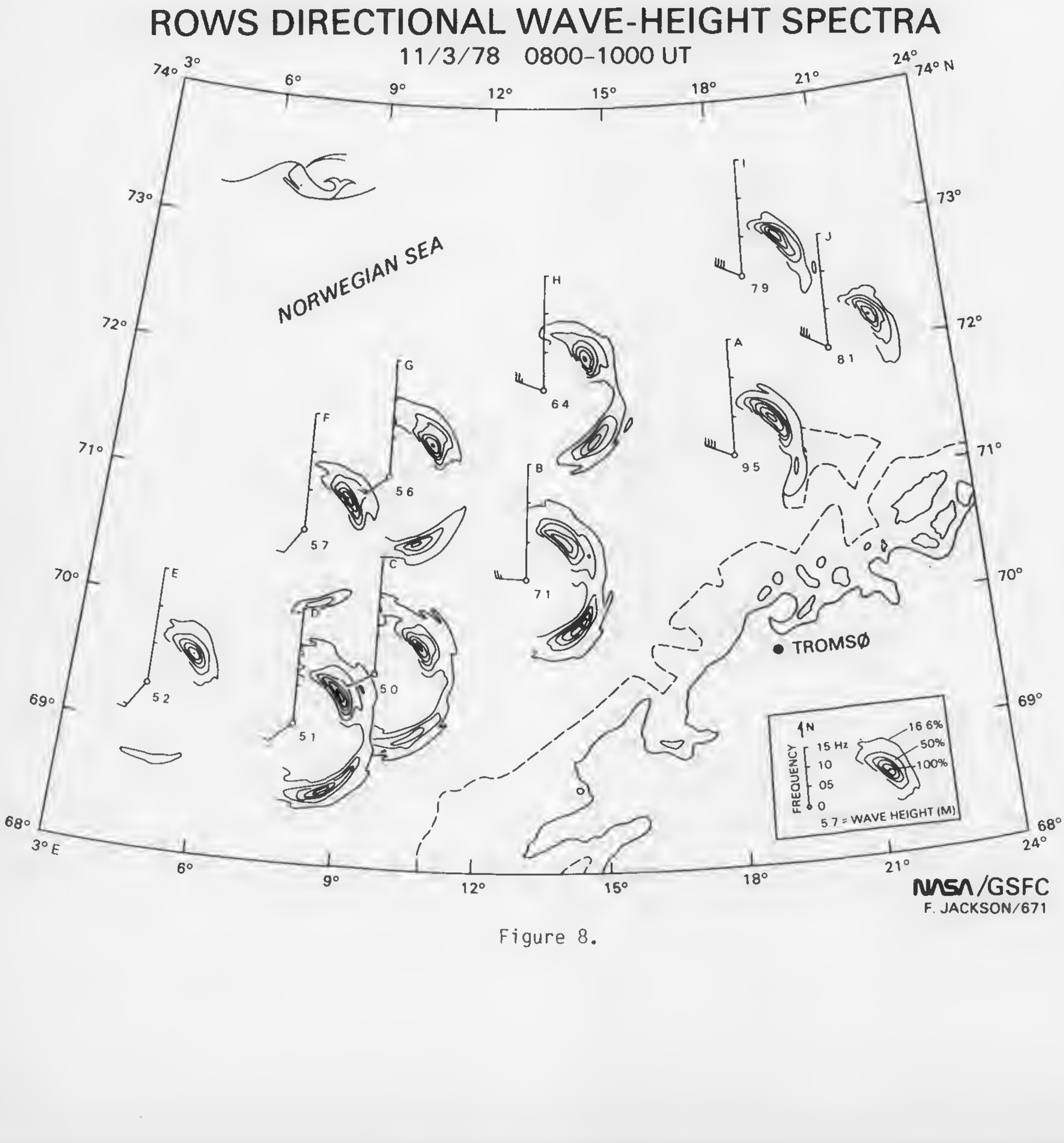

Figure 8.

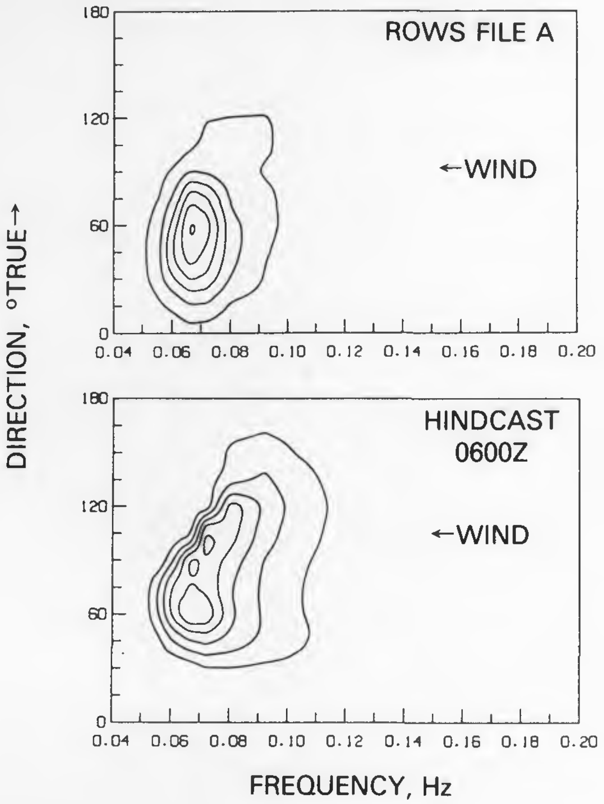

Figure 9.

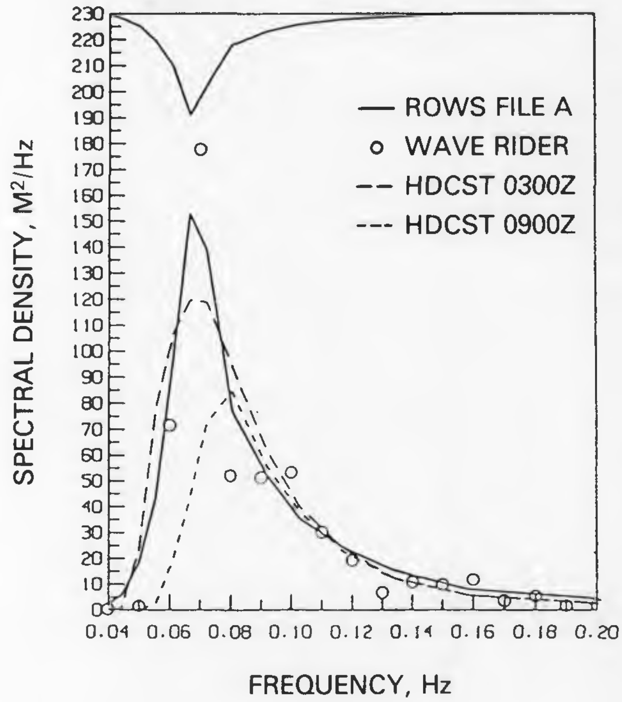

Figure 10.

spectrometer data, some as long as six minutes. The spectra from these files are shown in Figure 8 as height-frequency spectra displayed on a map of the Norwegian Sea. For this presentation, the 180° ambiguity in the ROWS spectra was removed based on the synoptic weather picture. The ROWS spectra reveal a complex wave system consisting of a 330 m component travelling NE parallel to the Norwegian coast and a 200 m component travelling at right angles to the SE. Estimated wave heights range from 5 m in the south to nearly 10 m in the north. The NE travelling component is basically the trailing edge of the wave train produced by an intense episode of southwesterly winds two days before north of Scotland. The local high winds in the northern portion of the box seen in Figure 7 are not the generating winds since the waves acted on by these winds have mostly moved out of the flight box at the time of flight 15 hours later. The SE travelling system is in the nature of transient pulse of energy produced by the fast-moving fetch region in the western sector of the cyclone seen in Figure 7.

The ROWS spectra of Figure 8, along with 3-hourly spectra from a Waverider buoy located at the northern end of the box near the ROWS file 'A', have been used to test the performance of two numerical wave models, the SAIL and ODGP models developed by V. Cardone of Oceanweather, Inc. (Greenwood et al., 1986; Cardone et al., 1976). These models were run in a hindcast mode on a fine-mesh grid (100 km) with carefully prescribed wind fields. Comparison with the ROWS and Waverider data showed that the two models performed remarkably well considering the complexity of the wind field, the speed of the cyclone (25 ms^{-1}), and the lack of real wind data to the northwest. The models produced both wave systems with basically the same spatial distribution observed by the ROWS. Differences between the models and the ROWS and Waverider observations can be attributed to phasing errors in the models caused by the crude wind-field update interval (6 hours) and to a tendency for the models to put too much energy into the local wind direction. (This tendency was more pronounced for the SAIL).

Figures 9 and 10 compare the ODGP hindcast spectra for the grid point closest to ROWS file A and the Waverider buoy. The ROWS observation was at 0800 Z, the Waverider observation at 0830 Z; these are compared with the hindcasts for 0300 Z, 0600 Z, and 0900 Z. The comparison shows excellent agreement between the ROWS and Waverider and the 0300 Z hindcast. In the ROWS and hindcast directional comparison for 0600 Z, it appears that the hindcast is putting too much energy into the local wind direction. However, examination of the nondirectional spectra shows that the wind-sea energies are actually quite close. Apparently, the model is advecting away the 0.067 Hz swell faster than is occuring in actuality. By 0900 Z, the 0.67 Hz swell has been nearly entirely advected away, leaving the ca. 0.08 Hz wind sea as dominant constituent. It is possible that in this case the swell is being maintained, or regenerated, in the local wind field, compensating for the advection, but this needs further study.

Since 1982, the ROWS has flown on the NASA P-3 in concert with the SCR. Both the ROWS and SCR

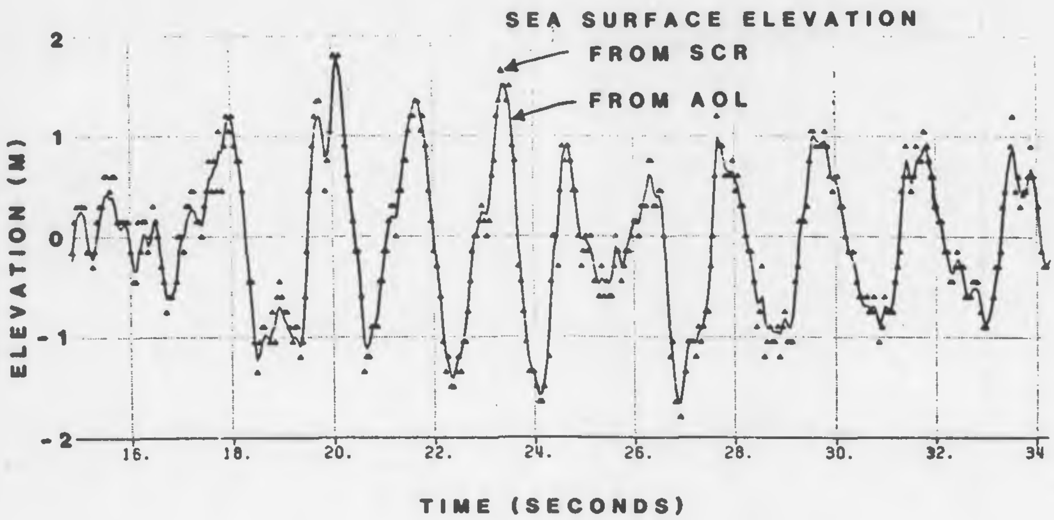

Figure 11.

were exercised in Hurricane Debby (section 2), and some excellent fetch-limited wave data have been obtained with both instruments; unfortunately, space does not permit showing the ROWS results for these experiments. Example comparisons with the SCR can be found in the discussion of the SIR-B experiment in section 6.

4. AIRBORNE OCEANOGRAPHIC LIDAR

The Airborne Oceanographic Lidar (AOL), described by Hoge et al. (1980), was developed in the late 1970's by NASA in cooperation with several other federal agencies for the purpose of investigating and developing potential remote sensing appliications that can benefit from lidar technology performed from a high speed, fixed-winged airrcraft. Basically, the system utilizes a pulsed laser transmitter(s) optically co-aligned with a receiving telescope and electrooptical components. The sensor presently possesses the capability to temporally and spectrally resolve backscattered laser or laser stimulated fluorescence emission from ground or ocean targets. In either mode, the AOL measures the range between the aircraft and the ground or ocean surface. After aircraft vertical motion is removed through post-flight processing of the ranging data and simultaneous measurements obtained with a vertical accelerometer, the system provides a high precision measurement of the topographic features of the surface under investigation. This laser system can profile the waves at a 400 Hz rate to provide independent corroboration of the elevation data measured by the SCR at the center of its swath.

Figure 11 shows comparative data taken at 230 m altitude by the SCR and AOL flying perpendicular to the crests of the waves. The AOL data have been averaged to correspond to the SCR spot size in the along-track direction. The agreement is remarkable considering that one system is microwave and the other is optical; they use entirely different ranging techniques; and the AOL is located 10 m aft of the SCR in the aircraft and was looking aft at 15° off-nadir. A relative shift in the time origin of approximately 0.7 s was required for the comparison of profiles between the two instruments. The 15 cm range quantization of the SCR is apparent in Figure 11.

In the temporal, or ranging mode, the instrument has successfully been utilized to demonstrate the practicality and potential accuracy of bathymetric surveying to depths in excess of 30 m.

Considerably more emphasis has been placed on developing the spectral measurement or fluorosensing capabilities of the lidar system. In this mode, the laser induced fluorescence of marine or terrestrial targets are spectrally resolved in 32 contiguous channels, each 11.25 nm in width, to provide 360 nm coverage. The position of the spectrometer can be varied depending on the wavelength of the laser transmitter and expected fluorescence responses. Flight tests with the instrument have established the feasibility for utilizing an airborne laser fluorosensor to measure oil spill thickness and fluorescence, map the distribution of tracer dye released in marine water masses, delineate ocean fronts, and resolve phytoplankton pigment concentrations.

Shown here are results obtained during investigations conducted over a Gulf Stream warm core ring in April 1982. During this experiment, the AOL was equipped with a frequency doubled Nd:YAB laser with an output wavelength of 532 nm. Figure 12 provides the approximate location and size of the ring at the time of the study. The top of Figure 13 is a profile of laser induced chlorophyll fluorescence obtained on a SE to NW flight track through the ring. Similarly, laser induced phycoerythrin (an auxiliary pigment contained in marine phytoplankton) is plotted in the middle of Figure 12. Both photopigments have been normalized with the water Raman backscatter signal acquired along with the fluorescence signals. This technique has been shown to effectively remove variations in fluorescence signal level due to changes in water attenuation properties along the flight path. The ocean surface temperature profile

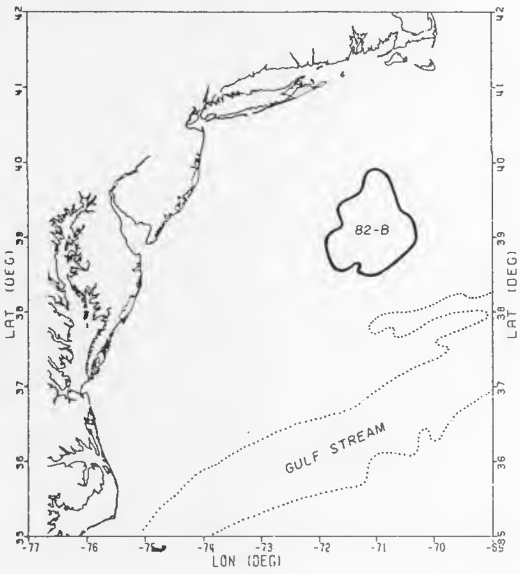

Figure 12.

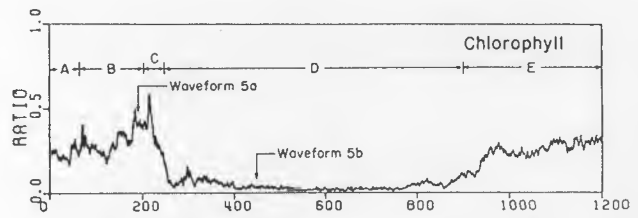

Profile of chlorophyll a fluorescence across Ring 82B.

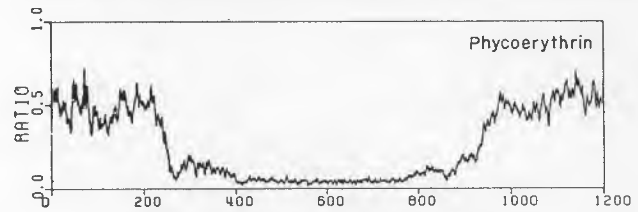

Profile of phycoerythrin fluorescence.

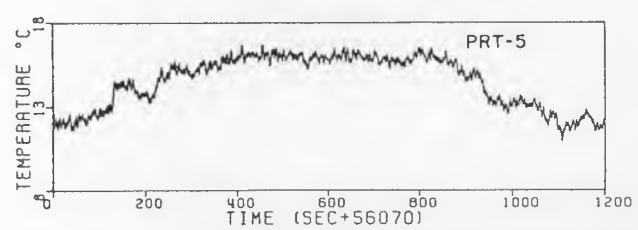

Profile of ocean surface temperature obtained with a PRT–5 infrared radiometer.

Figure 13.

acquired from the PRT-5 infrared radiometer and recorded by the AOL system is shown at the bottom of Figure 13. Note the characteristic rise in water temperature as the ring is encountered during the transect. Higher concentrations of the photopigments are confined to the ring boundary regions where nutrient rich shelf and slope waters are warmed by contact with the ring.

5. C-BAND SCATTEROMETER

The University of Massachusetts Microwave Remote Sensing Laboratory C-Band step-frequency radiometer has flown on the GSFC P-3 aircraft in the past, but it is planned to replace that system by the C-Band Scatterometer being developed by them. The C-Band Scatterometer is designed to operate at any selected frequency between 4 and 5.2 GHz. In its normal configuration, it transmits 100 mw of power, however an available solid state amplifier can be externally attached to put out 2 watts of transmitted power. The front panel has several controls to adjust the pulse width from 100 ns to 100 us which corresponds to ranges varying from 90 m to 3000 m. In addition, the pulse repetition frequency is user selectable as is the receiver bandwidth to match the pulse width. The receiver contains both a linear and logarithmic amplifier, and an array of switches are on the front panel to adjust the attenuation level of the received signal.

A 1.22 m dish has been ordered for the system which will provide a 3° by 3° pencil beam so that the system can operate in a beam fill mode to reduce receiver bandwidth and therefore boost the over-all signal to noise ratio.

The system accepts commands from a commercial HP9826 computer which also records and reduces the data. The absolute accuracy of the scatterometer is better than 0.8 dB at this time using an 8-bit A/D converter. A 12-bit A/D converter is being procured which will further improve the accuracy.

It is planned to install the C-Band Scatterometer on the GSFC P-3 using the 1.22 m dish looking at nadir and combine its output with the other P-3 systems to measure EM bias in support of the TOPEX mission. The P-3 would fly at 200 m altitude so that all instruments would have high spatial resolution. The SCR would measure the ocean surface topography in two dimensions while the backscattered power would be measured simultaneously at optical (AOL), Ka-band (SCR), Ku-band (ROWS) and C-band (UMASS scatterometer) frequencies. This collection of measurements would allow EM bias determination at all four frequencies simultaneously. In the ERS-1 time frame, UMASS expects to have a scanning antenna system incorporated in the scatterometer.

6. SIR-B UNDERFLIGHTS

The NASA P-3, equipped with the SCR, ROWS, AOL, and AAFE Altimeter, underflew the Shuttle Imaging Radar-B (SIR-B) off the coast of Southern Chile in early October, 1984. The purpose was to provide surface truth for establishing the SAR's performance in measuring directional wave spectra (Beal, 1985; Beal et al., 1986). Five nighttime underflights out of Punta Arenas, Chile were made in a five day period. The basic flight plan consisted of a low-altitude (800 m) outbound leg for the SCR and AOL and a high-altitude (7 km) return leg for the ROWS. This plan, besides providing for a maximum of over-

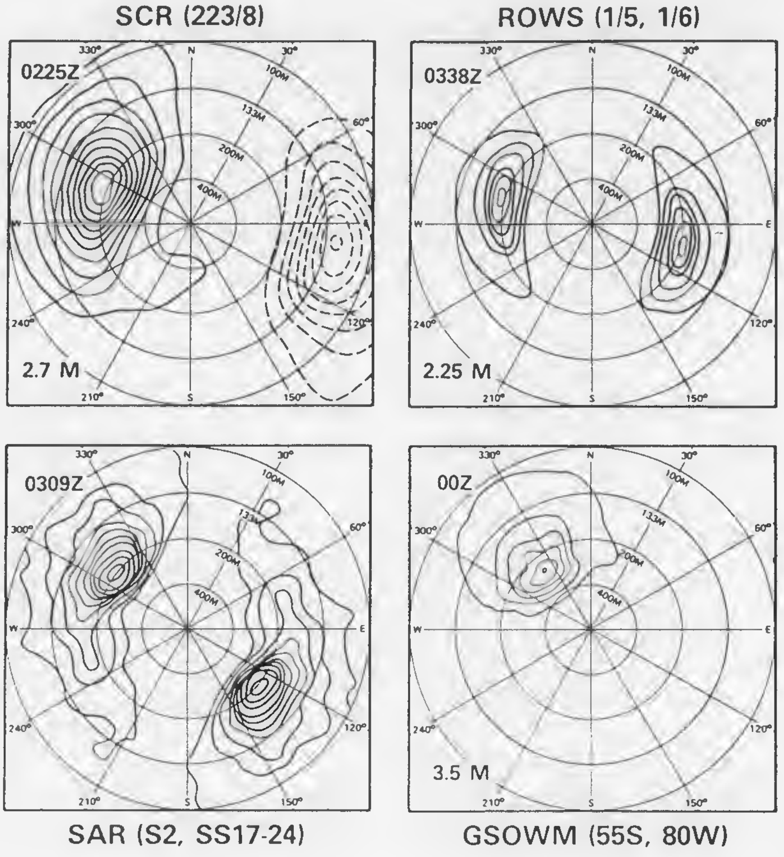

Figure 14.

lapping for the SCR, ROWS, and SAR, also provided for the contingency that if the SCR failed to operate by the end of its leg, then the ROWS would assume the SCR's role as the prime verification instrument on the return leg. Indeed, this situation did occur on one of the flights. On another flight, both the ROWS and the SCR failed to operate, and for this flight the AOL assumed the role of the primary surface truth instrument.

Figure 14 is an example of a four-way comparison of directional spectra from the second underflight. The comparison is between the SIR-B, SCR, ROWS, and a Global Spectral Ocean Wave Model (GSOWM) forecast made by the U. S. Navy's Fleet Numerical Oceanography Center. The spectra are shown as wave number height spectra referenced to true north. In the case of the GSOWM spectra and the SCR spectrum (solid lines), the direction of travel is indicated as direction from. The SIR-B heading in both cases was about 80° true. Both the SCR and ROWS show a simple ca. 200 m wavelength system travelling toward 110°. The significant wave heights estimated by the SCR, AOL, AAFE altimeter and ROWS agreed within 0.4 m, with a mean value of 2.7 m. The SCR and ROWS spectra are in excellent agreement (note that different levels are used for the two spectra); the SIR-B spectrum exhibits a rotation of about 15° clockwise toward the SAR's range direction (350°). The GSOWM prediction is a slightly longer wave system rotated slightly further north than the SAR modal direction. The rotation of the SAR spectrum is consistent with an azimuth fall-off effect, but further investigation is required to see whether a simple azimuth filter is adequate to describe the response (Beal, personal communication). The rotation of the GSOWM with respect to the SCR and ROWS observations also was exhibited on three other flight days and may be due to a mislocation of the FNOC generating wind fields to the north and west of the observation area.

Preliminary SIR-B results are given by Beal et al. (1986) and by Beal (1985) and by the subsequent papers in the IGARSS'85 Digest.

7. CONCLUSIONS

We have described some of the instrumentation available to provide ground truth for the ERS-1 mission. The same high/low flight scenario utilized during the SIR-B underflights should prove effective for ERS-1. The P-3 would fly outbound along the ground track at a 400 to 800 m altitude while acquiring data with the SCR, the AOL and the C-Band scatterometer. At the turn around point the aircraft would climb to a 7 km altitude and the ROWS and C-Band scatterometer would acquire data on the return leg. This procedure could effectively document the temporal and spatial variation of the wind and wave field.

8. REFERENCES

Beal, R. C., 1985: The SIR-B extreme waves experiment in the southern ocean. 1985 International Geoscience and and Remote Sensing Symposium (IGARSS'85) Digest, IEEE Cat. No. 85CH2162-6, 787-791.

Beal, R. C., F. M. Monaldo, D. G. Tilley, D. E. Irvine, E. J. Walsh, F. C. Jackson, D. W. Hancock III, D. E. Hines, R. N. Swift, F. I. Gonzalez, D. R. Lyzenga, and L. F. Zambresky, 1986: A comparison of SIR-B ocean wave directional spectra with aircraft scanning radar scanning-beam radars, Science, in press.

Cardone, V. J., W. J. Pierson, and W. G. Ward, 1976: Hindcasting the directional spectra of hurricane-generated waves. J. Petrol. Tech., 28, 385-394.

Greenwood, J. A., V. J. Cardone, and L. M. Lawson, 1986: Intercomparison test version of the SAIL wave model. In Ocean Wave Modeling, Plenum Press, New York, pp. 221-233.

Hoge, F. E., R. N. Swift, and E. B. Frederick, 1980: Water depth measurement using an airborne pulsed neon laser system. Appl. Opt., 19, 871-883.

Holthuijsen, L. H., 1983: Observations of the directional distribution of ocean-wave energy in fetch-limited conditions. J. Phys. Oceanogr., 13, 191-207.

Jackson, F. C., W. T. Walton, and P. L. Baker, 1985a: Aircraft and satellite measurement of ocean wave directional spectra using scanning beam mirowave radars. J. Geophys. Res., 90, C1, 987-1004.

Jackson, F. C., W. T. Walton, and C. Y. Peng, 1985b: A comparison of in situ and airborne radar observations of ocean wave directionality. J. Geophys. Res., 90, C1, 1005-1018.

Jackson, F. C., W. Glazar, D. E. Hines, and C. Y. Peng, 1985c: ROWS estimates of wave height, wind speed and directional wave spectra for SIR-B underflights off Chile. International Geoscience and Remote Sensing Symposium (IGARSS'85) Digest, IEEE Cat. No. CH2162-6, 804-812.

Kenney, J. E., E. A. Uliana, and E. J. Walsh, 1979: The Surface Contour Radar, a unique remote sensing instrument. IEEE Trans. Microwave Theory and Techniques, MTT-27, 1080-1092.

Walsh, E. J., D. W. Hancock III, D. E. Hines, R. N. Swift, and J. F. Scott, 1985: Directional wave spectra measured with the Surface Contour Radar. J. Phys. Oceanog., 14, 5, 566-592.

A PROCEDURE FOR ESTIMATION OF TWO-DIMENSIONAL OCEAN HEIGHT-VARIANCE SPECTRA FROM SAR IMAGERY

F Monaldo

The Johns Hopkins University/Applied Physics Laboratory
Johns Hopkins Road, Laurel, Maryland 20707

ABSTRACT

A step-by-step procedure is outlined to convert synthetic aperture radar (SAR) imagery into estimates of the ocean surface wave spectra. The procedure is based on a linearized version of a model to convert SAR image intensity spectra into either wave slope- or height-variance spectra. The outlined procedure is applied to SAR imagery from the SIR-B mission and shown to produce spectra which are highly correlated to two-dimensional spectra measured independently.

1. INTRODUCTION

A number of investigators have demonstrated the general correspondence of SAR image spectra with ocean wave spectra [1,2,3]. The wavenumber and propagation direction derived from SAR image spectra have agreed well with independent measures of these parameters.

The more complete verification of the potential of spaceborne SAR's to produce reliable wave spectra estimates has awaited two developments: (1) alternate airborne techniques to estimate two-dimensional wave spectra with wavenumber and angular resolution comparable to that of SAR image spectra, and (2) an integration of various SAR wave imaging theories into a procedure for converting SAR image spectra into ocean wave slope- or height-variance spectra.

During the shuttle imaging radar (SIR-B) mission in October 1984, SAR imagery was acquired off the southern coast of Chile. Simultaneously, two-dimensional wave spectra were also acquired by a NASA P-3 aircraft equipped with a radar ocean wave spectrometer (ROWS) [4] and a surface contour radar (SCR) [5]. Both of these instruments have been tested and verified in previous experiments.

In 1981, Alpers et al. [6] proposed a comprehensive approach to interpretation of SAR image modulation in terms of ocean surface wave slope. A linearized and simplified version of the wave imaging models detailed by Alpers et al. was included in a proposed method by Monaldo and Lyzenga [7] to convert SAR wave imagery into estimates of ocean wave slope- and height-variance spectra.

In this paper, we will review the procedure for converting SAR imagery to wave spectra, as well as emphasize some still uncertain aspects of the procedure. In addition, we will compare SAR wave spectra computed using this procedure with independent spectral estimates from the ROWS and SCR. The comparison will reveal the ability and limitations of a SAR to estimate wave spectra. A preliminary comparison of the spectra from this experiment is provided in Beal et al. [8].

2. WAVE SPECTRUM ESTIMATION PROCEDURE

A five step procedure, used to estimate wave slope- and height-variance spectra, is schematically shown in Figure 1 [7]. The initial input is the two-dimensional SAR intensity image. The digitally processed, geometrically and radiometrically corrected, imagery used in this paper has been provided by the Jet Propulsion Laboratory. The imagery is then divided into image frames 512 pixels x 512 pixels on a side. Each pixel corresponds to an area 12.5 m x 12.5 m on the surface, so that the entire image frame covers an 6.4 x 6.4 km area.

Image normalization is performed by subtracting off the mean image intensity and then dividing by this mean. The resulting image is then in units of fractional modulation. SAR wave imaging theories are generally characterized in terms of fractional image modulation.

Fourier transformation of the image and squaring results in a level 1 spectrum, $S_1(k_a,k_r)$, where k_a is azimuth (along track) wavenumber and k_r is range (cross track) wavenumber.

All imaging systems have finite resolution and SAR's are not exception. The effect of finite resolution on SAR image spectra is to reduce spectral response at high wavenumbers. The spectral values at large wavenumbers are smaller than they would be in an infinite resolution system. Tilley

[9] has been able to estimate and partially correct for this reduced response. Applying Tilley's "stationary response" correction to increase high frequency spectral response, a level 2 spectrum, $S_2(k_a,k_r)$ is produced.

The spectral estimate at each wavenumber bin located at any given k_a and k_r has only 2 degrees of freedom with an associated uncertainty of 100%. It is, therefore, not very statistically reliable. To improve statistical reliability, a level 2 spectrum is smoothed with a Gaussian-weighted running average. The full-width of the Gaussian kernel at the point where it falls to 60% of its maximum value is approximately 7 wavenumber bins or 6.885 x 10^{-3} rads/m. The resulting smoothed spectrum is designated as a level 3 spectrum, $S_3(k_a,k_r)$.

Although the spectral estimate in any particular wavenumber bin in a level 3 spectrum is no longer independent of values in neighboring wavenumber bins, it is far more statistically reliable. Each spectral estimate now has 300 degrees of freedom with an associated uncertainty of 6%. Others, who process SAR imagery, might like to use more or less averaging in the tradeoff between statistical reliability and spectral resolution.

Because a SAR is a coherent imaging system, SAR imagery has the unfortunate quality that it is corrupted by multiplicative, speckle noise. The amount of this noise is dependent on the number of looks used to form the image and the mean and variance of the SAR image. This speckle noise manifests itself in the spectral domain as a white noise pedestal upon which wave spectrum rests. The level of this pedestal is predicted by Goldfinger, [10]. The noise pedestal, calculated from [10], is subtracted from the level 3 spectrum to generate a level 4 spectrum, $S_4(k_a,k_r)$. Any spectral value less than zero is set equal to zero.

A level 4 spectrum can be considered to be an enhanced SAR image spectrum. Up to this point no model of how SAR image intensity modulation is related to ocean surface wave slope or height has been invoked. Using the imaging models developed by Alpers et al. [6] and linearized by Monaldo and Lyzenga [7], a SAR modulation transfer function $R_{SAR}(k_a,k_r)$ is used to convert a level 4 spectrum into a level 5 height-variance spectrum, $S_5^H(k_a,k_r)$ using

$$S_5^H(k_a,k_r) = \frac{S_4(k_a,k_r)}{R_{SAR}^2(k_a,k_r)} \tag{1}$$

Since the wave slope-variance spectrum is related to the height spectrum by k^2 $(=k_a^2+k_r^2)$, a level 5 slope-variance spectrum is generated by

$$S_5^S(k_a,k_r) = \frac{S_4(k_a,k_r)\ k^2}{R_{SAR}^2(k_a,k_r)} \tag{2}$$

It is interesting to note that the $R_{SAR}^2(k_a,k_r)/k^2$ is nearly constant so that a level 4 spectrum is nearly proportional to a slope-variance spectrum.

3. OCEAN SURFACE MOTION

Because a SAR is Doppler device, movement of the ocean surface affects the resulting SAR image. A scatterer with a component of velocity in the radar look direction results in an azimuth displacement of the scatterer in the image by an amount proportional to the scatterer velocity and R/V, the range-to-velocity ratio of the SAR platform. The periodic shifting of scatterers by orbital velocities of the long (>50 m) azimuth traveling waves is one mechanism by which azimuth traveling waves are imaged by a SAR [6]. When velocities cause displacements comparable to the ocean wavelength or the velocities are not highly correlated to the long wave, however, azimuth position shifts caused by surface velocities tend to degrade, rather than enhance, the SAR image.

The formally nonlinear remapping of the position of scatterers causes a smearing of the image in the azimuth direction and can be thought of as a loss of resolution in the azimuth direction [7,11]. The reduced azimuth resolution, like the effect of finite image resolution discussed earlier, results in a spectrum with reduced response at large azimuth wavenumbers. Attempts have been made to correct for this "dynamic response", similar to the "stationary response" correction, with some success [11]. The correction schemes, however, do not yet seem robust enough to be included in Section 2 and Figure 1. For example, it is still not clear to us how the azimuth falloff might affect the amount of speckle noise present and presumably subtracted off in obtaining a level 4 spectrum.

Nonetheless, inspite of difficulties, a "dynamic response" correction ought to be applied, if possible.

Even with a "dynamic response" correction, examination of SAR image spectra from SEASAT and SIR-B have resoluted in an empirical estimate of the minimum detectable wavelength, λ_m, given by

$$\lambda_m = \left(2\ \frac{m^{1/2}}{S}\right)\ \frac{R}{V}\ H_s^{1/2} \tag{3}$$

where H_s is ocean significant wave height (SWH) [7,8,11]. Interestingly, this limitation seems to be most severe in relatively mild sea states. Low sea states usually have dominant wavelengths short enough to be lost in the falloff of azimuth response. In high sea states, although the minimum detectable wavelength increases, typical dominant ocean wavelengths are sufficiently long, at least a shuttle altitudes, to avoid the azimuth falloff problem. Since the effect is proportional to R/V, there is a strong argument in favor of reducing satellite altitudes for spaceborne SAR's dedicated to measuring ocean surface waves.

The low, 235 km altitude of the SIR-B SAR turns out to have roughly a factor of four smaller minimum detectable wavelength than the SEASAT SAR. For example, equation 3 would predict a minimum detectable wavelength of 50 m at a typical 3 m SWH sea state for the SIR-B SAR as compared to 200 m for the SEASAT SAR which orbited at 800 km.

4. COMPARISONS WITH INDEPENDENT SPECTRA

Comparisons between ocean wave spectra derived using the process described in Section 2 with estimates of the wave spectra from the SCR and ROWS serve both to illuminate the potential for SAR measurement of waves and reveal some inherent limitations. SAR spectral data was acquired over five days, from October 8-12, 1984. We choose here to concentrate on the last three days, when the SAR signal to noise ratio was a minimum of 5 dB.

Figure 2 shows contour plots of three height-variance spectra from October 12, from the SAR, ROWS and SCR. The center of the spectrum corresponds to zero wavenumber and the outer circle corresponds to a wavenumber of $2\pi/100$ m. This day is particularly interesting in that the dominant 400 m wave system was almost exactly azimuth traveling. The imaging of azimuth traveling waves is perhaps less well understood. Note that all three instruments clearly show the wave system at the same wavenumber and direction. It seems that shapes of the SAR and SCR spectral peaks are in most agreement, although all agree well.

On October 11, 1984, there is only a limited amount of SCR data available so we compare only the ROWS and SAR slope-variance spectra in Figure 3. In this case, there are two, nearly range traveling wave systems at 375 m and 135 m wavelength, respectively. The spectra are within 50 km in space and 3 hours in time apart. The two spectra show very good agreement. The wavelengths, propagation directions, shapes and relative magnitudes of the two peaks are very similar.

Spectra from October 11 and 12 clearly demonstrate the SAR's ability to image both range and azimuth traveling wave systems. The spectral comparisons from October 10 demonstrate the limitation caused by azimuth falloff. Figure 4 shows height-variance spectra from the ROWS, the SCR, and the SAR. In Figure 4, the maximum wavenumber is $2\pi/50$ m. This mild, nearly 2 m, sea state shows some low frequency peaks as well as an angularly broad wave system stretching to almost 50 m in wavelength. This system is clearly present in the SCR and ROWS spectra. However, because much of the angular breath of the spectrum extends in the SAR azimuth direction, the high frequency end of the broad wave system is abruptly cutoff.

The spectra we have shown are all relative spectra, without absolute units attached to the contours. Although SAR imaging theories are probably not sufficiently well developed that they can estimate slope- and height-variance spectra in absolute units, it is interesting to compare the SWH estimate from the SAR and other instruments aboard the P-3. In addition to SCR and the ROWS on the P-3, a profiling lidar (AOL-airborne optical lidar) provided one-dimensional spectra and a nadir looking altimeter (AAFE-advanced airborne flight experiment) provided SWH estimates.

Table 1 is a listing of SWH estimates from the P-3 instruments and the SAR. For October 10, the SAR estimated the SWH as being 1.3 - 1.4 m while the SCR and ROWS estimated slightly higher SWH's. Similarly on October 11, the SAR measured a SWH between 3.2 and 4 m while all four other instruments had slightly higher estimates. On the last day, October 12, the SAR's SWH of 5.6 to 6 m is a factor of two larger than the estimates by the other instruments. It is interesting to note that the days October 10 and 11 had much of the wave energy traveling the rangedirection. On October 12, the wave system was azimuth traveling. Clearly, the magnitude of the component of the $R_{SAR}(k_r, k_a)$ in the azimuth direction is a factor of two too small. The range component of the function is slightly too large.

It is important to remember that the fact the SWH can be estimated this closely with SAR spectra is somewhat of a surprise and indicative of the fact that the linearized SAR imaging model is a fairly good. In an operational environment, it would probably be better to normalize relative SAR spectra with SWH estimates from an altimeter, for example.

5. CONCLUSIONS

A specific procedure for estimating slope- and height-variance spectra from SAR imagery has been developed which seems to produce relative spectra in close agreement with independently measured spectra. More work is required in specifying the exact magnitude of the SAR wave imaging function $R^2_{SAR}(k_a,k_r)$.

The most important limitation in SAR wave imagery is the azimuth falloff caused by ocean surface motion. Although correction for the "dynamic response" function can alleviate the problem, low satellite orbits are required to maximize the usefulness of spectra derived from spaceborne SAR imagery.

6. REFERENCES

[1] Beal, R.C., D.G. Tilley, and F.M. Monaldo, "Large- and small-scale spatial evolution of digitally processed ocean wave spectra from the SEASAT synthetic aperture radar", J. Geophys. Res., Vol. 88, pp. 1761-1778, 1983.

[2] Beal, R.C., T.W. Gerling, D.E. Irvine, F.M. Monaldo, and D.G. Tilley, "Spatial variations of ocean wave directional spectra from the SEASAT synthetic aperture radar", J. Geophys. Res., Vol. 91, pp. 2433-2449, 1986.

[3] Shuchman, R.A., J.D. Lyden, and D.R. Lyzenga, "Estimates of ocean wavelength and direction from X- and L-band synthetic aperture radar during the marinelane experiment", IEEE J. Oceanic Eng., Vol. OE-8, 99, 90-96, 1983.

[4] Jackson, J.C. and W.T. Walton, "Aircraft and satellite measurement of ocean wave directional spectra using scanning-beam microwave radars", J. Geophys. Res., Vol. 90, pp. 987-1004, 1985.

[5] Walsh, E.J., D.W. Hines, III, R.N. Swift, and J.F. Scott, "Directional wave spectra measured with the surface contour radar", J. Phys. Oceanogr., Vol. 15, pp. 566, 1985.

[6] Alpers, W., D.B. Ross, and C.L. Rufenach, "On the detectability of ocean surface waves by real and synthetic aperture radar", J. Geophys. Res., Vol. 86, pp. 6481-6498, 1981.

[7] Monaldo, F.M. and D.R. Lyzenga, "On the estimation of wave slope- and height-variance spectra from SAR imagery", IEEE Trans. Geosci. and Remote Sensing, in press, 1986.

[8] Beal, R.C., F.M. Monaldo, D.G. Tilley, D.E. Irvine, E.J. Walsh, F.C. Jackson, D.W. Hancock III, D.E. Hines, R.N. Swift, F.I. Gonzalez, D.R. Lyzenga, and L.F. Zambresky, "A comparison of SIR-B directional wave spectra with aircraft scanning radar spectra and spectral ocean wave model predictions", Science, in press, 1986.

[9] Tilley, D.G., "Use of speckle for estimating response characteristics of Doppler imaging radars", Optical Eng., in press, 1986.

[10] Goldfinger, A.D., "Estimation of spectra from speckled images", IEEE Trans. Aerospace Electronic Systems, Vol. 18, pp. 675-681, 1982.

[11] Monaldo, F.M., "Improvement in the estimate of dominant wavenumber and direction from spaceborne SAR image spectra when corrected for ocean surface movement", IEEE Trans. Geoscience and Remote Sensing, Vol. GE-22, pp. 603-608, 1984.

Significant Wave Height
Comparisons (meters)

Day	SAR	P-3 Instruments			
		ROWS	SCR	AOL	AAFE
3	1.3 - 4	1.9	1.7	--	--
4	3.2 - 4	4.6	4.1	4.4	4.6
5	5.6 - 6	3.3	3.3	3.7	3.5

Table 1

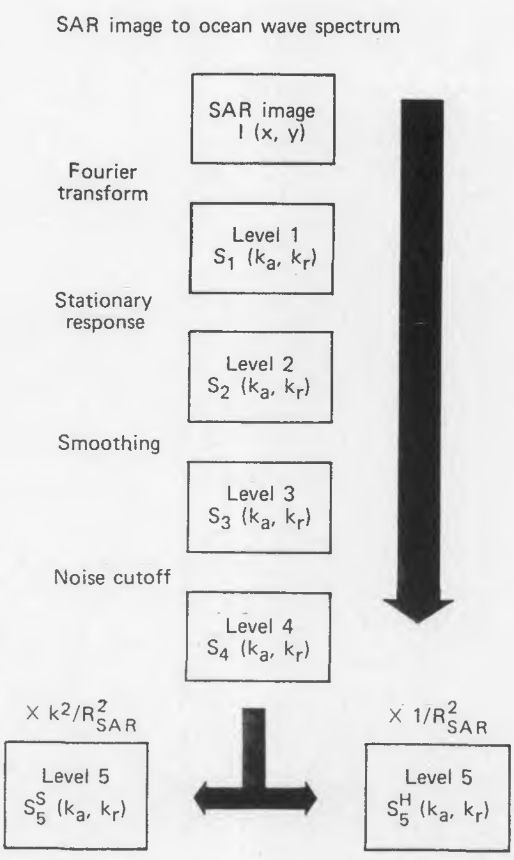

Figure 1

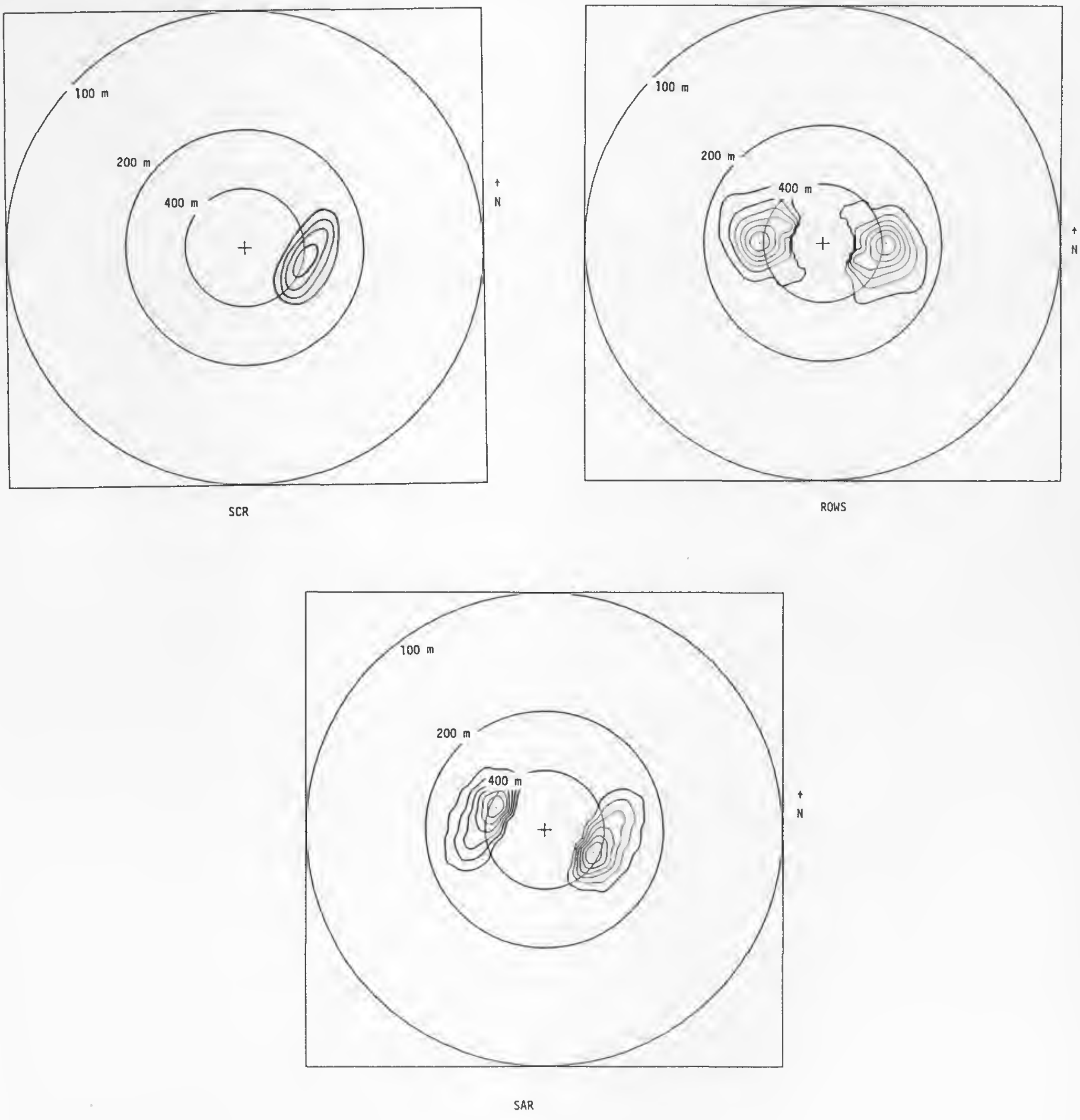

Figure 2
Height-variance spectra
October 12, 1984

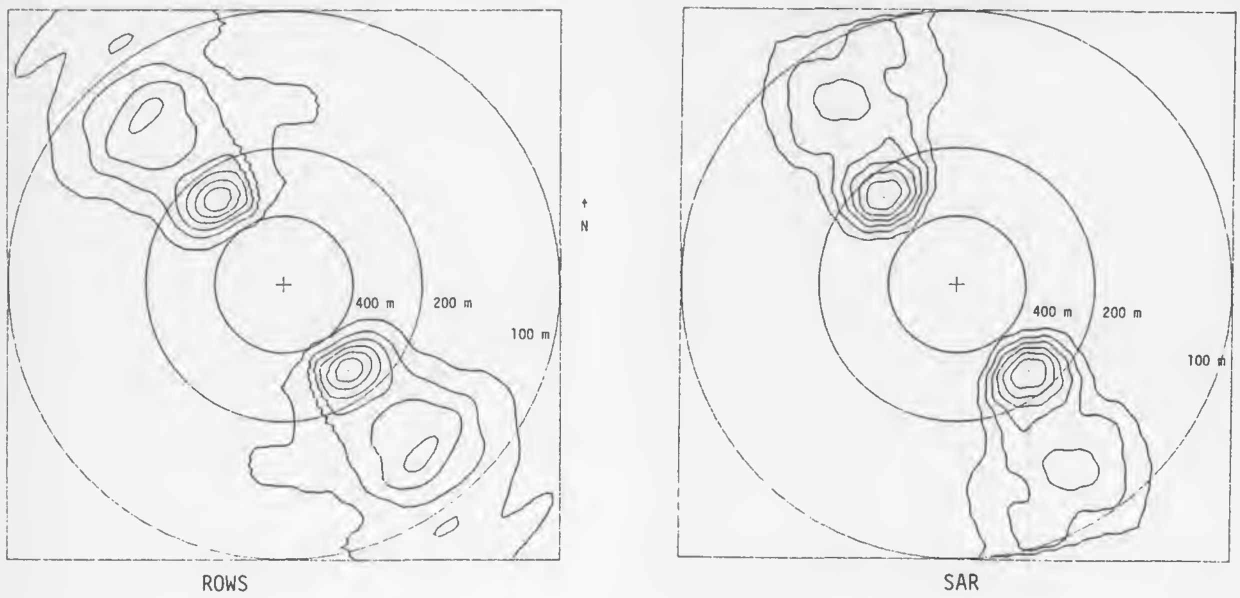

Figure 3

Slope-variance spectra
October 11, 1984

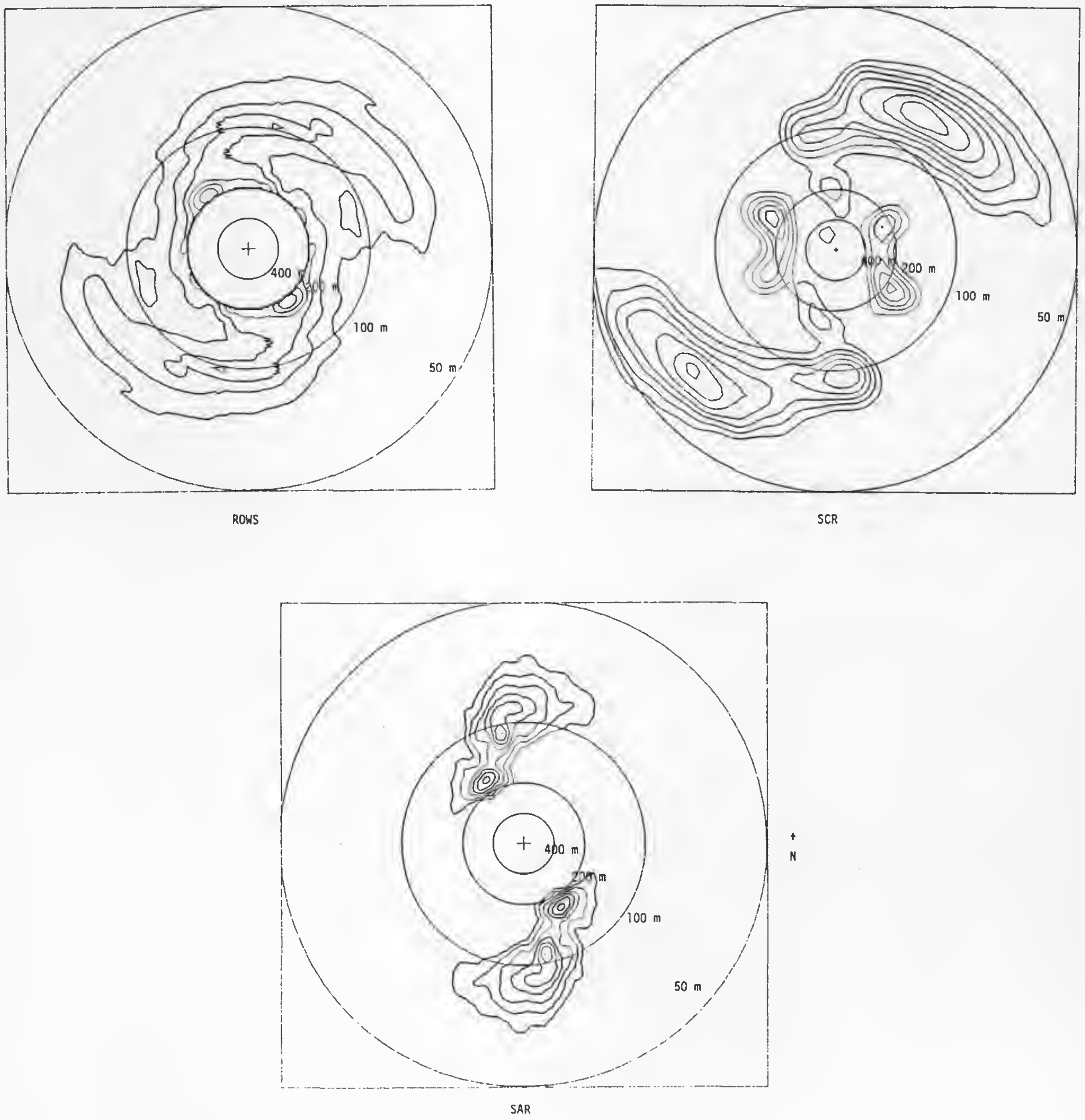

Figure 4

Height-variance spectra
October 10, 1984

THE USE OF AIRCRAFT FOR WIND SCATTEROMETER CALIBRATION

D Offiler

Meteorological Office, Bracknell, UK

ABSTRACT

The UK Meteorological Office plans to use the ERS-1 Fast Delivery products in its operational atmospheric and wave forecast models. However, unless these data are properly calibrated and validated, there cannot be full confidence in the ERS products, and their use will be limited. In order to support the commissioning phase of the spacecraft in the first three months after launch, the Meteorological Office could deploy its Hercules aircraft to assist in the calibration and verification of the wind scatterometer products. The capabilities of this aircraft, its advantages and its possible use are described, and compared to other sources of calibration data.

Keywords: Winds, Calibration, Validation, Scatterometer, ERS-1, Aircraft.

1. INTRODUCTION

The UK Meteorological Office is keen to use ERS-1 data operationally in its weather forecasting activities. ERS-1 Fast Delivery (FD) wind data can make a contribution to global and regional atmospheric and wave numerical forecast models, and is potentially directly useful for ship routeing, storm tide warning services and forecasting for the offshore industry. The global nature of the products also have application to ocean climatology.

However, unless the FD products are properly calibrated, and there is full confidence in the ERS-1 data, or at least its error characteristics are well known, the operational use of the data will be limited. To help in this learning process (including feedback to ESA for improvement to the retrieval algorithms), the Meteorological Office is willing to deploy its Hercules (Lockheed C-130) instrumented aircraft in support of ERS-1 wind calibration during the first three months commissioning phase.

The measurement capabilities of the aircraft will be described, and how these may be used in a campaign. The complementary nature of such measurements compared to ship and buoy data will also be discussed. At this relatively early stage of calibration planning, cooperative international campaigns and the types and regions of deployment are to be addressed during workshop discussions, in preparation for coordination under the umbrella of the ESA Announcement of Opportunity (AO).

2. AMI WIND SCATTEROMETER GEOPHYSICAL VALIDATION

In order to validate the wind vector output from the AMI wind scatterometer processing algorithms, various forms of comparison data are needed. These may be special observations in support of ERS-1, other coincident campaigns (such as JASIN was for SEASAT), or conventional, long-term meteorological measurements from ships, buoys and other platforms. Grid point data, as derived from meteorological analyses could also be used.

2.1 Conventional meteorological observations

An estimate of the quality and likely quantity of collocations between the scatterometer and ship/buoy measurements is required. The number will impact the size of the various datasets in the validation processing, and there will be a trade-off between the frequency of geophysical validation and wind extraction algorithm tuning, and the significance of the results. For instance, if the number of collocations was small - a few per day - then the tuning would have to wait for several months until there were sufficient collocations to ensure good results. As a round figure, perhaps 1000 good quality collocations would be required.

The UK Meteorological Office receives most global meteorological data rapidly over the Global Telecommunications System (GTS), and these observations are immediately placed in a comprehensive data-base for general use. Currently, data is available on-line for 5 days before being archived to tape. Typically, there are around 4000 observations from dedicated weather ships, buoys, merchant ships and fixed platforms and oil rigs daily. However, it should be noted that:

- over 90% are in the Northern Hemisphere
- the majority of these are in the North

- Atlantic and North Sea
- many are close to coasts
- the frequency of observation is dependent on the particular platform, but most report several times a day (every hour for weather ships, every 3 or 6 hours for most of the others)
- very few merchant ships are instrumented, the wind force being estimated from the sea condition
- nearly all averaging periods are short (2-10 mins), therefore making satellite comparisons difficult to interpret
- as a general rule, conventional data from the majority of platforms is probably accurate to 2-5 m/s and 20-30 deg. Dedicated platforms such as ocean weather ships, oceanographic vessels and well maintained buoys will have the better accuracy. Comparisons of good quality wind measurements made between ships and buoys during JASIN suggest accuracies of 1-2 m/s and 10-20 deg. (Ref 1)

The number of occasions that surface-based observations will collocate with the scatterometer swath within 2-3 hours in very small, perhaps 130-150 per day (Ref 2). There will be very few collocations in the Southern Hemisphere. The number of collocations with weather ships and other good-quality oceanographic vessels and (relatively) short-lived buoys may well be under 10 per day. The rest will be from merchant ships and oil rigs, etc., whose data is of unknown quality. There is also no guarantee that the Atlantic weather ships will still be operating in 1990. To offset this small number, several scatterometer measurements (especially on a 25 km grid) may be compared with a single ship observation, and although these are not totally independent, they will provide more stable statistics. Data from special campaigns will give additional good quality surface data.

2.2 Grid point data

Another source of comparison data is gridded winds from the above surface observations. These analyses (either from operational models run by ECMWF or the UK Meteorological Office for example, or from custom-made models) have the advantage of averaging out individual measurement noise and are more consistent spatially and temporally with the scatterometer measurement. They also are constrained to be meteorologically consistent with other parameters (eg surface pressure) and other atmospheric levels.

This technique (though only analysing the wind vectors) was successfully used for SEASAT to increase the number of comparisons for GOASEX and JASIN. Numerical analyses will certainly be used in the verification of ERS data (Ref. 3), but only after they have been fully calibrated and then validated (using all available sources of comparison data) will they be assimilated into numerical models.

2.3 Aircraft data

Data from low-flying aircraft with suitable instrumentation may be used to supplement surface observations during the commissioning phase. Consideration is being given to the use of meteorological data gathered from aircraft in support of special validation campaigns because of the unique capabilities of such platforms. Their usefulness was amply demonstrated in the TOSCANE-T campaign off Brittany in 1985 (Ref. 4).

3. THE MRF HERCULES AIRCRAFT CAPABILITIES

The Meteorological Research Flight (MRF) of the UK Meteorological Office operate a modified Hercules (Lockheed C-130) aircraft, shown in Figure 1. This has extensive instrumentation for atmospheric observation of winds, temperature, humidity, clouds, aerosols and chemistry. In brief, the relevant features of such a platform for wind measurement include:

- accurate wind vector determination
- low level flight possible
- stable platform
- long range and endurance
- Fully instrumented support data
- optimum sub-swath deployment

Detailed capabilities of the MRF Hercules relevant to wind measurement are given in Table 1, and Ref. 5 contains a discussion on the use of aircraft for meteorological observations, and gives details on all of the Hercules sensors.

Range:	7500 km)	Depending on payload and
Duration:	14 hours)	altitude etc.
Min. height:	down to 100 ft (exceptionally 50 ft in calm conditions and for short periods), by radar altimeter.	
Wind vector:	U, V components from INS, verified by Doppler radar and Navaids (Refs. 6, 7, 8). Also fast response U, V, W turbulence vanes (Ref. 9)	
Sea surface	temperature from Barnes IR radiometer (8-14 microns)	
Ambient air	temperature/humidity from fast response, compensated Platinum resistance and hygristor probes.	

Measurement	Accuracy	Sampling
U, V comp	+/-0.4 m/s	40 Hz (2.5 m))
Speed	+/-0.6 m/s	) 10 m/s
Direction	+/-3 deg	)
SST	+/-0.3 K	4 Hz (25 m)
Air temp	+/-0.3 K	20 or 4 Hz (5 or 25 m)
Altitude	+/-1 %	

Table 1. Measurement capabilities of the MRF Hercules

4. WHY USE AIRCRAFT?

It is arguable that conventional sources of calibration data (principally from surface observations) are often of unknown or insufficient quality, and

Figure 1. The Meteorological Research Flight Hercules

will be few and far between when paired with satellite data. Such surface data may be more suitable for the longer-term monitoring, tuning and validation of the wind extraction algorithms both for the FD processing and off-line precision processing. For the commissioning phase, it is likely that special campaigns, such as could be cordinated under the ESA AO, will be necessary. A variety of platforms will form a complementary dataset of near-surface observations for the initial calibration task.

One problem in interpreting the comparison of spacecraft and conventional measurements is their fundamental differences in observing technique. Ship or buoy wind measurements are made at a single point, and typically may not be averaged over more than 10 minutes. The satellite measurement, on the other hand, is spatially averaged over 50 x 50km without time averaging. It has been estimated that a point measurement should be averaged for not less than an hour to be comparable with the scatterometer footprint (Ref. 10). Another problem is the low repetitivity of the spacecraft overpassing a ship (every three days), even assuming the ship is in the correct location.

The use of large aircraft like the Hercules can partially overcome some of these difficulties. Although they cannot be deployed for weeks on end, their long range and flight endurance enable them to fly to a predicted overpass location, make fairly extended measurements across the whole swath, and could still be able to intercept another pass, if the region were at high latitudes. The region of coverage (within limits) can also be chosen flexibly during the campaign. Cross-calibration with surface observations could be made in transit to and from the test area.

Although the flight level is not ideal (perhaps 30-50 metres, depending on wind strength), the bulk stability may be derived from the other instruments carried, and the equivalent 10-metre neutral stability wind (as "measured" by the scatterometer) estimated to an acceptable accuracy for calibration purposes.

5. CONCLUSIONS

In order to properly calibrate the ERS products, all tools that can be used for this purpose should be used. The ultimate use of the FD products will be in large numerical models for the atmosphere and oceans, and these require good quality, global data. Individual poor observations from ships can be detected during quality control stages, but satellite data has both the strength and weakness of being globally self-consistent and of vast quantity, so any biases must be calibrated out before use.

The geophysical calibration of wind vector data from ERS-1 and similar satellites will in turn require surface-based observations of a high quality. The source for such data will be limited, but may be supplemented by airborne low-level wind measurements. Cross-calibration of aircraft winds with ship and buoy data will enable the comparison dataset to be extended, and their different characteristics to be understood. The Meteorological Office Hercules aircraft can help in this task.

5. REFERENCES

1. Offiler D 1984, A comparison of SEASAT scatterometer-derived winds with JASIN surface winds. Int J Rem Sensing 5 365-378

2. Long A E, Offiler D and Wolff T 1984, Report of the Scatterometer Algorithm Development (SAD) Group. ESA ERS-1 AMI Team report, Ref. SAD01.

3. Francis P E 1986, The use ofnumerical wind and wave models to provide areal and temporal extensions to instrumental calibration and validation of remotely sensed data. Paper in these conference proceedings.

4. Attema E 1986, An experimental campaign for the determination of the radar signature of the ocean at C-band. Proceedings of First ISPRS Colloquium on Spectral Signatures, held at Les Arcs, December 1985.

5. Readings C J 1985, The use of aircraft to study the atmosphere: the Hercules of the Meteorological Research Flight. Met Mag, 114 66-77.

6. Broxmeyer C 1964, Inertiall navigation systems. McGraw-Hill Book Co, New York.

7. Axford D N 1968, On the accuracy of wind measurements using an inertial platform in an aircraft and an example of the measurement of vertical meso-structure of the atmosphere. J Appl Met 7, 645-666.

8. Meredith J S 1983, Global navigation systems. Proc IEEE 71, 1123-1227.

9. Nicholls S 1978, Measurements of turbulence by an instrumented aircraft in a convective boundary layer over the sea. QJRMS 104 653-676.

10. Brown R A 1983, On a satellite scatterometer as an anomemeter J Geophys Res 88 (C3) 1663-1673.

MEASUREMENT OF THE DIRECTIONAL SPECTRUM OF OCEAN WAVES USING A CONICALLY-SCANNING RADAR

A R Birks

Rutherford Appleton Laboratory, Chilton, Didcot, UK

ABSTRACT

A short-pulse radar altimeter, modified by the addition of a steerable antenna which can scan a cone about nadir, may be used to measure the directional spectrum of ocean waves. The method can be used from either a satellite or aircraft; in this presentation the application of the method from an aircraft will be described, having in mind its use in the validation of satellite instruments. Near simultaneous measurements of significant wave height and of the directional wave spectrum are possible with the same instrument, and this capability will enhance the value of both measurements.

Trial airborne measurements have been made by Rutherford Appleton Laboratory (RAL), using a 13 GHz radar developed at RAL, during a campaign with the NASA CV-990 aircraft in 1984. The analysis of this data is currently in progress at RAL.

1. INTRODUCTION

The radar altimeter has amply demonstrated its value for the remote measurement of significant wave height and wind speed from satellite platforms such as Seasat. With only minor modification, the same instrument may be used to measure the directional spectrum of ocean waves. The simple modification is the provision of a steerable antenna which can scan in a cone about nadir.

The essential principle of the measurement is as follows. The radar altimeter is a short (3 ns) pulse radar which illuminates the surface vertically. If the antenna is tilted to illuminate the ocean surface obliquely, at an angle of incidence of about 10°, the delay of the echo maps onto horizontal range from nadir. The backscattering cross-section at a given illuminated point depends on the local slope of the ocean surface; the analysis of the echo as a function of delay is thus equivalent to a measurement of the spatial variation of surface slope. Thus the measured echo as a function of delay can be related to the two-dimensional spectrum of surface slope. For the case of a periodic swell propagating in the direction of increasing range, the measured echo power as a function of delay will show a periodic variation the period of which is equal to the delay between successive wave crests. Jackson (Ref. 1) has shown that the spectrum of this modulation is proportional to the cross-section, in the direction of the antenna pointing, of the function $|\underline{K}|^2\ F(\underline{K})$, where $F(\underline{K})$ is the two-dimensional spectrum of the ocean surface. If the antenna is rotated about a vertical axis, this function can then be built up, as a sequence of radial cross-sections.

The method can be applied using a radar deployed either on an aircraft or on a satellite. Jackson et al, (Ref. 2) have demonstrated the technique using an airborne radar. Brooks and Dooley (Ref. 3) suggested that an instrument such as the Seasat altimeter could be easily adapted to make this measurement using a conically scanning antenna and also an analog filter bank spectrometer to analyse the power spectrum of the radar return. The "full-deramp" method of signal processing used by the Seasat instrument depends on the analysis of a comparatively narrow range of delays, such as is appropriate to the altimeter measurement, whereas the ocean wave spectrum measurement requires a wider range (~ several μs).

A microwave radar combining the functions of a radar altimeter and a short-pulse conically scanning scatterometer has been developed at the Rutherford Appleton Laboratory (RAL) to be used in airborne experiments. This instrument was used, primarily in its altimeter mode, during campaigns in 1983 and 1984 during which trials of the instrument in the ocean wave spectrum mode were made.

2. OUTLINE OF THE METHOD

A full analysis of the short pulse method for measuring the ocean wave spectrum has been presented by Jackson (Ref. 1), and the following simplified description is mainly based on that paper.

The radar illuminates the ocean surface obliquely at an angle of incidence θ_0 (typically 10 degrees). The antenna beam will thus select an area of the ocean which, if we assume the beam pattern to be circularly symmetric, will be elongated in the direction of look of the antenna. The contours of constant delay will be approximately straight lines crossing the footprint at right angles to the direction of look, such that the relationship between delay τ and horizontal range x is

$$x^2 + H^2 = \left(\frac{c\tau}{2} + H\right)^2 \quad (1)$$

In this expression, H is the height of the radar above mean sea level, c is the velocity of light, and the origin of τ is taken to correspond to the return from the nadir point. The x axis is the projection of the antenna axis onto the horizontal plane. From (1) we can derive the approximate linear relationship

$$dx = \frac{1}{2} c d\tau / \sin\theta_o. \quad (2)$$

Strictly, it is necessary to take into account the non-linear relationship (1) between x and τ when aircraft measurements are being analysed (Ref. 2), but in the following the approximate linear relationship implied by (2) will be used.

The radar transmits a short pulse of radiation, $d\tau$, so that at any delay the return in the receiver will consist of power from a strip of the ocean surface of width dx (equation 2), where dx is small enough to resolve the dominant ocean waves present. Resolution in delay corresponds to resolution in the x coordinate. At small angles of incidence the scattering mechanism will be dominated by specular returns from correctly orientated slopes, and in these circumstances, as noted in the introduction, the received power will show modulation in delay related to the wave slopes.

The received echo is detected, with a square law detector, and the power spectrum of the resultant signal is measured. Jackson (Ref. 1) shows that the power spectrum of the detected echo is proportional to

$$P(\omega) = \left|\int E_o(\nu) E_o^*(\nu-\omega) d\nu\right|^2 \{\delta(\omega) + P_{mod}(\omega)\} + \int E_o^2(\nu) E_o^2(\nu-\omega) d\nu \quad (3)$$

Here $E_o(\omega)$ is the amplitude spectrum of the transmitted pulse, ω is angular frequency, and $P_{mod}(\omega)$ is the modulation spectrum which is related to the two-dimensional spectrum of the ocean surface by

$$P_{mod}(\omega) d\omega = \mu K^2 F(\underline{K})\, dK \quad (4)$$

where the spatial frequency variable $\underline{K}$ is evaluated on the section parallel to the look direction (the x axis) and where

$$K = 2\sin\theta_o\, \omega/c \quad (5)$$

The proportionality factor μ depends on the antenna geometry and on the sea state; in the first order model here,

$$\mu = \frac{\sqrt{2\pi}}{L_y}\left[\cot\theta_o + \frac{2\tan\theta_o}{s^2}\right]^2 \quad (6)$$

where L_y is the width of the antenna pattern and s^2 is the mean square slope of the waves.

As is usual in radar experiments, the signal after detection is an exponentially distributed noise process which is modulated by terms representing the distribution of scatters in delay and the antenna pattern. The final term in equation (3) represents the power spectrum of this exponential noise process. Superimposed on it are the terms representing the quantity of interest $P_{mod}(\omega)$ and the term which we have represented as a δ-function which represents the d.c. component of the detected signal.

The weighting function

$$\left|\int E_o(\nu) E_o^*(\nu-\omega) d\nu\right|^2$$

in equation (3) is the square of the Fourier Transform of the envelope of the transmitted pulse (the point target response of the radar), so that its width will be of the order of 1/(delay resolution of radar). It represents the fact that the modulation is measured with delay resolution determined by the width of the transmitted pulse, so that Fourier components corresponding to wavelengths shorter than this will not be measured.

If the function $E_o(\nu)$ is assumed to have a gaussian form;

$$E_o(\nu) = \exp\left[-\frac{1}{2}(\nu/\beta)^2\right] / \sqrt{2\pi}\,\beta \quad (7)$$

then it is easy to show that the signal to noise ratio, defined as the ratio of the term in equation (3) involving $P_{mod}(\omega)$ to that representing the underlying noise process, is

$$\mathrm{SNR} = \sqrt{2\pi}\,\beta\, P_{mod}(\omega) \quad (8)$$

This is a measure of how strongly the desired function P_{mod} stands out against the noise background. Note that if the signal bandwidth increases, over and above the minimum necessary for range resolution, so does the SNR. This is because, for a given transmitted energy, the power in the exponential noise process is independent of β but it is spread out over a wider bandwidth, $\sim\beta$, as β increases.

The above discussion applies to the case of the analysis of a single echo. In this case the measurement of the spectrum will be affected by random errors the magnitude of which will be comparable to the mean level of the noise background. Thus SNR (equation 8) represents the detectability of the signal in this sense. The level of these random errors will be reduced by a factor of $N^{1/2}$ if N spectra, corresponding to the same look direction, are averaged. Alternatively, pulses may be averaged before the power spectrum is calculated. If the integration time is short, and if successive pulses in the average are displaced to compensate for the motion of the radar, the modulation will be unaffected but the variance of the exponential noise will be reduced by a factor N; the effective signal-to-noise ratio will increase by N.

The spread of look directions of the pulses included in a given average must be less than the intrinsic angular resolution of the measurement if the angular resolution with which the spectrum is measured is not to be degraded. The angular resolution of the basic measurement depends principally on the lateral width of the antenna beam; angular resolution is inversely proportional to L_y so long as L_y is not so large that wavefront curvature is important (Ref. 2).

3. THE RAL RADAR ALTIMETER/SCATTEROMETER

The RAL Radar Altimeter/Scatterometer is a high resolution pulsed radar which operates at a frequency of 13.81 GHz (λ = 2.2 cm) and is intended for aircraft installation. It uses a pulse compression scheme based on a pair of matched surface-acoustic wave (SAW) filters to provide an effective pulse width of 4 ns. The returned echo is digitized with a sampling interval of 3.3 ns and its delay recorded. The instrument is controlled by an HP 1000 computer which stores the data on magnetic tape for subsequent analysis.

The pulse compression scheme is similar to that used on the GEOS-C altimeter, not the 'full-deramp' method used by the altimeter on SEASAT, and so all digitization and processing takes place in the time domain. The merits of this scheme are that we do not need any on-line tracking, in the altimeter modes, and the range of delays sampled (the width of the delay window) may easily be varied over a wide range. This ability to expand the delay window to exceed 1 μs in width is, as noted previously, one of two features which permit the instrument to be used for the ocean wave spectrum measurement. The other is of course the provision of the steerable antenna.

Three antennas are provided; two horns, with their planes of polarization at right angles to one another, are directed at the nadir and are intended for altimetric operation; the third, a paraboloidal dish, is steerable and in particular can be scanned in a cone about the vertical. The horn antennas are identical, and each has a beamwidth of 10°. The parabolic antenna has a diameter of 48 cm and a beamwidth of 3° (between half-power points). It can be tilted away from the vertical up to about 25°, and rotated continuously about the vertical axes.

The main characteristics of the radar are given in Table 1, and a block diagram of the radio frequency section is shown in Fig. 1. Fuller descriptions of the instrument appear in Refs. 4 and 5.

Table 1.

THE RAL RADAR

Frequency	13.81 GHz
TWT power	20.0 W
PRF	100.0 Hz or 66.6 Hz

Antennas:

	Beamwidths (degrees) E-plane	H-plane	Gain (+/-0.35 dB)
Horn (X)	8.9	13.1	23.3 dB
Horn (Y)	9.1	13.2	23.4 dB
Parabolic dish	3.1	2.9	33.05 dB

Pulse Compression System:

Transmitted pulse length	320 ns
Bandwidth	320 MHz
Compressed pulse width	4 ns
Compression ratio	80 (19 dB)

Pulse Digitization:

Digitizer	Biomation Model 6500
Sampling frequency	300 MHz
Resolution	5 bits + sign
Input bandwidth	100 MHz
Number of delay channels	1024

If the system is operated at an altitude of H = 10 km with θ_0 = 10°, the longitudinal extent of the beam is 540 m corresponding to a delay range of 626 ns. This sets the upper limit on wavelengths which can be detected, and defines the spatial frequency resolution with which spectra are measured. The lateral width of the beam is defined by L_y = 222 m. This sets the angular resolution for the system; from equation (2) of Ref. 2, which incorporates wave front curvature effects, we find a potential angular resolution of 21° at a wavelength of 200 m. The antenna is rotated at 3 rpm.

Because the only essential difference between the conically scanning and the altimeter modes of the instrument lies in the antenna used, it is possible for the operating mode to be switched very rapidly between the two; for example a one-second cycle might be chosen. If this is done, a near-simultaneous altimetric measurement of the significant wave height is obtained to accompany the ocean wave spectrum measurement.

The RAL Radar was one of several instruments flown on the NASA Convair CV-990 aircraft during the Marginal Ice Zone Experiment (MIZEX) in 1984, and also during an earlier campaign (MIZEX-WEST) in 1983. The principal emphasis of the radar operations during these campaigns was to gather altimetry data over ice-covered surfaces (Ref. 5). However, the opportunity was taken to collect data in the conical scanning mode both in transits over the open ocean to validate the technique, and in the vicinity of the Marginal Ice Zone to acquire data relevant to wave propagation in the Marginal Ice Zone. In all, somewhat over six hours of data was measured in the conically scanning scatterometer mode, and the analysis of these data is currently in progress.

4. CONCLUDING REMARKS

The RAL Radar is designed to operate both as an altimeter for the measurement of significant wave height and as a conically-scanning short pulse scatterometer for the measurement of the directional spectrum of ocean waves, and these two modes can be time-shared.

Airborne radar measurements of the ocean waves are expected to play an important part in the campaigns for calibration and validation of the ERS-1 ocean data products. The instrument described here represents the development in Europe of a radar suitable for these measurements.

REFERENCES

1. Jackson, F.C., 1981. An analysis of short pulse and dual frequency radar techniques for measuring ocean wave spectra from satellites. Radio Science 16(6), 1385-1400.

2. Jackson, F.C., Walton, W.T. and Baker, P.L., 1985. Aircraft and Satellite Measurement of Ocean Wave Directional Spectra using Scanning-Beam Microwave Radars. J. Geophys. Res. 90(C1), 987-1004.

3. Brooks, L.W. and Dooley, R.P., 1975. Technical Guidance and Analytic Services in support of Seasat-A. NASA Contractor Report CR-141399.

4. McIntyre, N.F., Powell, R.J. and Squire, V.A., 1985. A radar altimeter and the validation of its data products over ice surfaces. Proc. EARSeL/ESA Symposium "European Remote Sensing Opportunities", Strasbourg 31 March - 3 April 1985. ESA SP-233, 3-11.

5. McIntyre, N.F., Griffiths, H.D., Birks, A.R., Cowan, A.M. and 6 co-authors, 1986. Analysis of altimetry data from the Marginal Ice Zone Experiment. ESA CR-5948/84/NL/BI.

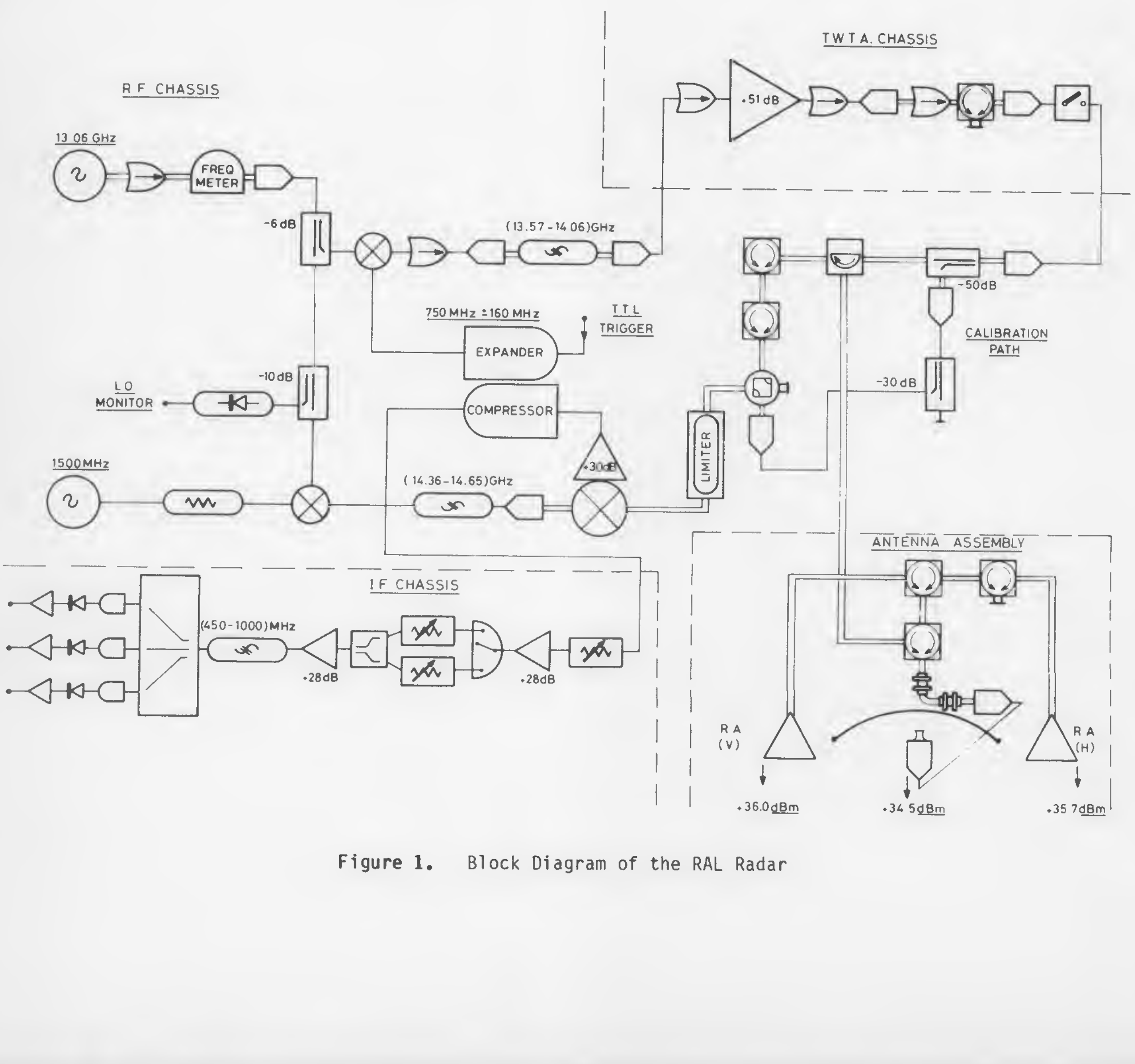

Figure 1. Block Diagram of the RAL Radar

LABORATORY STUDY OF MICROWAVE SCATTERING BY WATER SURFACE WAVES

A Lifermann
CNES/GRGS
TOULOUSE FRANCE

A Ramamonjiarisoa
INSTITUT MECANIQUE STATISTIQUE
DE LA TURBULENCE
MARSEILLE FRANCE

B Jahne
UNIVERSITAT HEIDELBERG
HEIDELBERG

Studies of microwave scattering of the sea generally refer to either of two kinds of experimental supports, namely open field experiments or wave tank simulations. Although validation and calibration of the algorithms during the commissioning phase clearly appeal to the first kind, laboratory measurements can still provide valuable contribution in the parameters definition and sensors selection for a test field campaign.

The experiments conducted in the IMST large wind wave facility with the CNES Ramses 2 scatterometer led to first results about the identification of the phases of swell and wind waves motions which contribute to the microwave (C and K bands) reflection.

At vertical incidence, for geometrical reasons or non linearity of the waves profiles the wave troughs tend to be better reflectors than the wave crests.

When the swell steepness is high enough to induce local breaking, a local large enhancement of the reflected microwave power occurs.

The reflection was seen to be highly sensitive to the presence of wavelets propagating along the swell or the dominant wind wave profile. This is questionning for the reliability of models that completely ignore this fact.

The scattering by swells is comparatively well understood with help of the one point-temporal measurements provided by classical wave height and slope gauges. Nevertheless for a wind driven field the 2-dimensional spatial structure of the waves need to be taken into account in the data analysis. This requires new kind of devices performing spatial measurements of the sea surface. This opportunity exists now at IMST with the recently developped visualisation technique which combines an optical system, a video camera and a digital image processor and images the surface slopes within its field of view. The location and statistics of the specular facets (seen by the radar) in relation to the sea state may then be studied from these pictures.

It happens that the wave field characteristics basically related to the radar response (the wave number spectrum or the joint distribution of surface elevation and slopes, depending upon the incidence angle) have been scarcely studied up to now, partly due to the lack of relevant spatial measurements.

It seems thus that the advent of satellite and airborne radar technics emphasizes studies and measurements adressing the spatial properties of the wave fields - as functions of the parameters (H1/3, wind speed, u*) to be determined.

This will be the main concern of the next investigations planned at IMST.

Proceedings of a Workshop on ERS-1 Wind and Wave Calibration, Schliersee, FRG, 2–6 June, 1986 (ESA SP-262, Sept. 1986)

Session 4

PLANNED/ONGOING PROGRAMMES

Chairman: R Frassetto (CNR)

AN OVERVIEW OF THE NSCAT/N-ROSS PROGRAM

B D Martin, M H Freilich, F K Li & P S Callahan

NASA Scatterometer Project
Jet Propulsion Laboratory
California Institute of Technology
Pasadena, CA 91109 USA

ABSTRACT

The NASA Scatterometer (NSCAT) will be one of four instruments to fly on the U.S. Navy Remote Ocean Sensing System (N-ROSS) mission. This paper briefly describes the overall N-ROSS mission, the NSCAT flight instrument and ground-based data processing/distribution system, and NASA-supported science and verification activities.

Keywords: Scatterometer, Remote-sensing, Ocean Winds

1. INTRODUCTION

Microwave instruments mounted on polar-orbiting satellites can provide data with the coverage and spatial resolution required for the study of many oceanographic and atmospheric phenomena. The U.S. Seasat mission in 1978 demonstrated the capabilities of several microwave instruments for gathering all-weather information about the air-sea interface. Several dedicated ocean remote sensing missions are being carried out as follow-ons to Seasat, including the ERS-1 and U.S. N-ROSS missions. The data from these missions will play an increasingly large role in studies ranging from weather and wave forecasting to investigations of the long-term variability of climate and ocean current systems. The global nature of the data will make them especially valuable to planned large-scale experiments such as the World Ocean Circulation Experiment and the Tropical Ocean/Global Atmosphere experiment.

In the next section, we briefly summarize the U.S. N-ROSS mission. Section 3 outlines the high-level science requirements established for the NSCAT system. Sections 4 and 5 discuss the designs of the NSCAT flight instrument and the ground data systems, respectively. NASA-supported science and planned validation activities associated with the NSCAT system are summarized in Section 6.

2. N-ROSS DESCRIPTION

N-ROSS is a satellite system designed to provide measurements of near-surface wind, ocean topography, wave height, sea-surface temperature, and atmospheric water content over the global oceans. The N-ROSS mission will involve inter-agency collaboration between the U.S. Navy, NASA, the U.S. National Oceanic and Atmospheric Administration (NOAA), and the U.S. Air Force. Planned as an "operational demonstration," data from the N-ROSS mission will be assimilated in near-real time to enhance operational Navy environmental predictions. In addition, NASA will process NSCAT data within two-weeks for use by the research science community.

In all, N-ROSS will have four microwave instruments mounted on a single satellite in a near-polar orbit:

(1) A scatterometer (described more fully in the following sections).

(2) A microwave altimeter, similar to that flown on Seasat, to measure ocean topography and surface wave conditions.

(3) A Special Sensor Microwave/Imager (SSM/I), a four-frequency (19, 22, 37, and 85 GHz) scanning microwave radiometer, that will be used to acquire data on sea-surface temperature, scalar wind speed, atmospheric water content, and ice characteristics.

(4) A low-frequency (5.2 and 10.4 GHz) scanning microwave radiometer that, in conjunction with SSM/I data, will be used to measure sea-surface temperature with a resolution of 25 km.

A schematic diagram of the possible configuration of the spacecraft is shown in Figure 1. Figure 2 illustrates the planned measurement swaths of the instruments.

Although mission parameters have not yet been fully established, present plans call for N-ROSS to be launched aboard a Titan-II in late 1990. N-ROSS will be placed in a sun-synchronous orbit at an altitude of $\sim$820 km and at an inclination angle of about 98.7°. The orbit will be maintained to assure a 19-day repeat to within 1 km. The designed mission duration is three years, although spacecraft consumables sufficient for a 5-year mission are planned.

Proceedings of a Workshop on ERS-1 Wind and Wave Calibration, Schliersee, FRG, 2–6 June, 1986 (ESA SP-262, Sept. 1986)

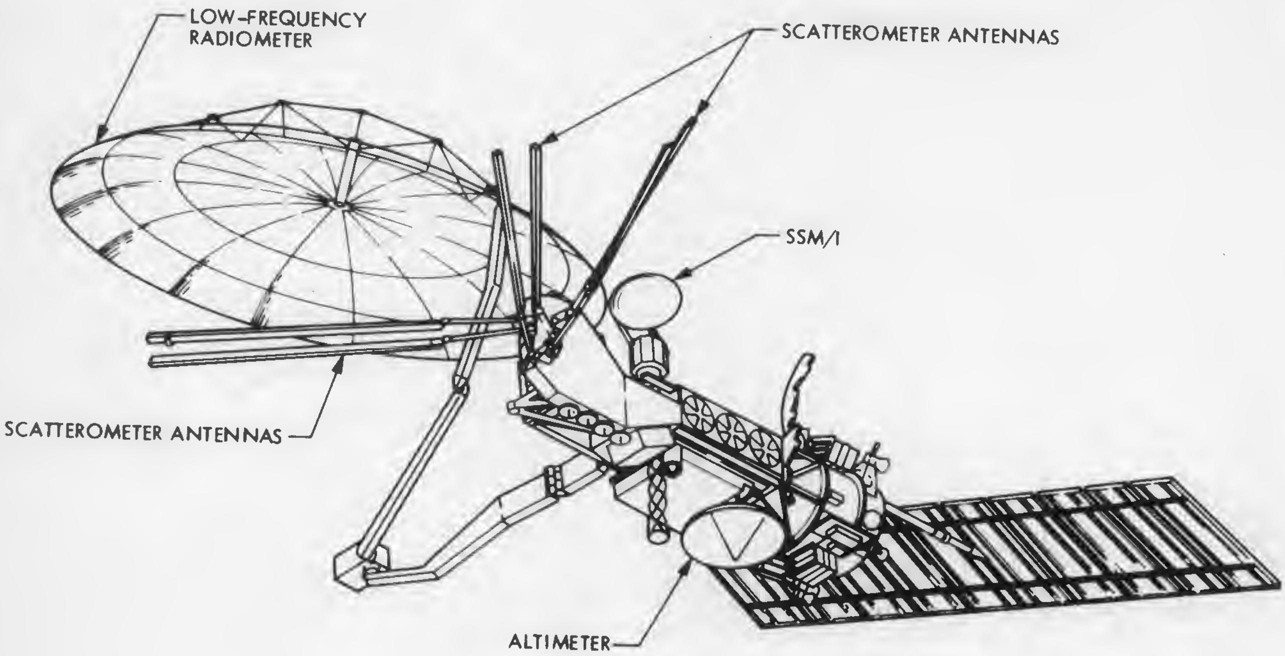

Figure 1. Schematic configuration of the N-ROSS spacecraft, showing the locations of the scatterometer, SSM/I, low-frequency radiometer, and altimeter antennas.

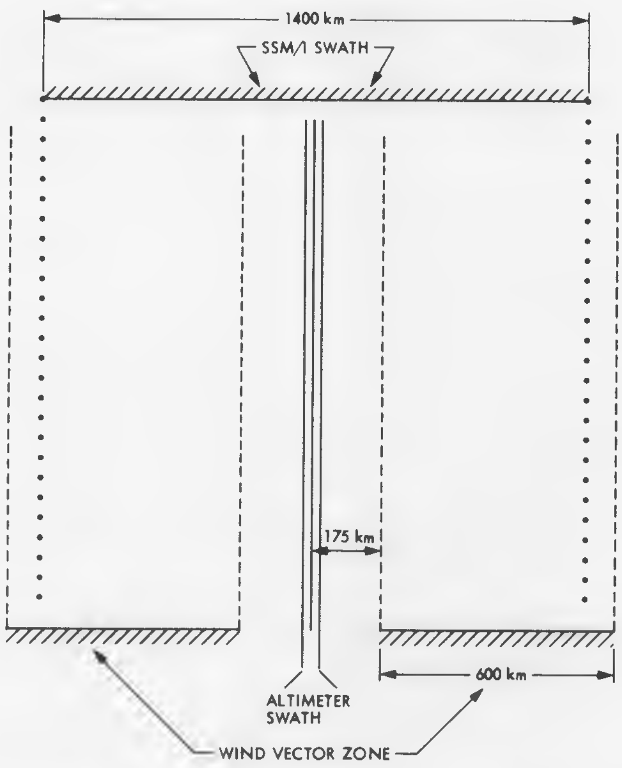

Figure 2. Plan view of N-ROSS measurement swaths on the earth's surface. Swath widths are drawn to scale. Details of the measurement swath for the high-resolution radiometer are not yet known.

Table 1
A Comparison of the Nominal System Parameters for the NSCAT and SASS Scatterometers

	NSCAT	SASS
Orbit Altitude	830 km	800 km
Orbit Inclination	98.7°	108°
Operation Frequency	13.995 GHz	14.599 GHz
Receiver Noise Figure	4.0 dB	5.7 dB
Transmitter Pulse Length	5.0 ms	4.8 ms
Transmitter Duty Cycle	31 %	17 %
Peak RF Power Output	110 W	110 W
Antennas	6	4
Number of σ_o Measurement Cells	25	12
σ_o Measurement Cell Resolution	25 km	50 km
Doppler Filtering	Digital	Fixed-Frequency

3. NSCAT MISSION REQUIREMENTS

The NASA Scatterometer, NSCAT, represents NASA's contribution to the N-ROSS mission.

NSCAT will obtain frequent, accurate, high resolution measurements of near-surface vector winds over the global oceans. NSCAT measurements will be applied to a variety of oceanographic and meteorological research studies, as well as to near-real-time operational weather and wave predictions for the Navy and other users (see Ref. 1 for a more detailed review of the NSCAT systems and potential scientific uses of scatterometer data). Although similar in design to the Seasat scatterometer (SASS), NSCAT will have enhanced capabilities leading to more accurate and higher resolution measurements and greater coverage than was possible with SASS.

Performance requirements for NSCAT were established by the NASA Satellite Surface Stress working group, S^3, and by the Navy (Refs. 2-3). NSCAT is required to measure vector winds over at least 90% of the global, ice-free oceans at least once within every two-day period. Wind speed measurements for NASA research users must have an rms accuracy of the greater of 2 m/s or 10% for wind speeds ranging from 3-30 m/s. The dynamic range of the instrument must not preclude measurements of wind speeds up to 50 m/s, assuming that the geophysical model function of remains valid at such wind speeds. At least 90% of the vector winds retrieved must have no more than two ambiguities approximately 180° apart. Wind direction rms accuracy must be 20° or better for the ambiguity closest to the true wind direction. Winds must be retrieved with a resolution of 50 km. The absolute location of the center of each vector wind cell must be known to better than 50 km (rms), and the relative locations of the centers of adjacent vector wind cells must be known to better than 10 km (rms). Since the absorption due to liquid atmospheric water can alter the observed σ_o and, therefore, can degrade the vector wind measurements beyond specifications, a rain flag is necessary to identify those and vector wind cells retrieved from regions of excessive atmospheric absorption. Data derived from the SSM/I will be used to set the rain flag. For near-real time operational use, the Navy requirement for speed rms accuracy is 4 m/s at a spatial resolution of 25 km or less.

In order to assure that useful data are available in a timely fashion for NASA research studies, S^3 has also put forth requirements on data processing throughput and data distribution. Vector wind data from NSCAT must be processed to wind field maps and be made available to research users with two weeks of data acquisition from the Navy. Raw as well as selected volumes of the processed data will be archived for later use.

4. NSCAT INSTRUMENT DESCRIPTION

The design of the NSCAT flight instrument is based heavily on the SASS design and the results from several previous studies of spaceborne scatterometers (Ref. 4). Table 1 provides a comparison of the nominal system parameters of NSCAT and SASS. A block diagram of the NSCAT instrument is shown in Figure 3.

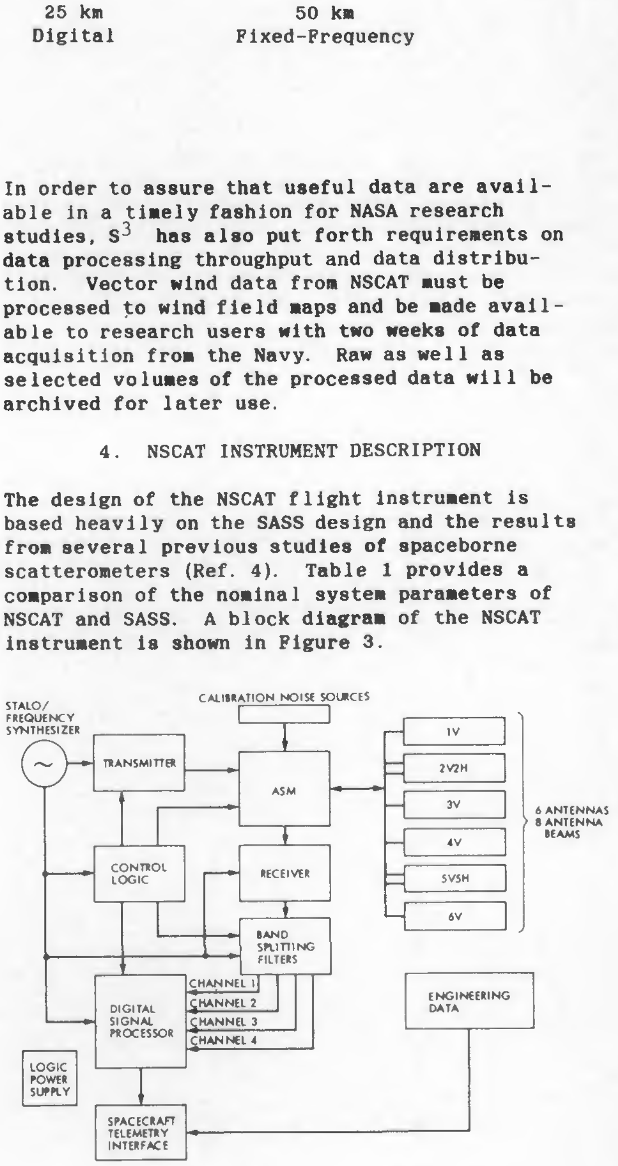

Figure 3. Block diagram for the NSCAT instrument.

The nominal NSCAT operation frequency will be 13.995 GHz, compared to the SASS frequency of 14.599 GHz. This change in frequency is in response to a reallocation of the frequency spectrum available for remote sensing.

NSCAT will use six fan-beam antennas with surface illumination patterns shown in Figure 4. The SASS illumination pattern was similar, but without the center antenna beams. The measurements of σ_0 by NSCAT at a third azimuthal angle, made possible by the center antenna beams, greatly increase the instrument's skill in removing directional ambiguities, with the result that more than 90% of the retrieved winds will consist of two ambiguities which are nearly 180° apart.

In the baseline design, two of the six antennas will be dual-polarized while the other four will be singly polarized. Thus, there will be eight antenna beams (see Figure 3). The baseline antenna configuration and polarization was selected based on the results of an extensive series of system performance simulation studies.

Spatial resolution of σ_0 measurements is achieved by subdividing each illumination pattern in the along-beam dimension by Doppler filtering. NSCAT will have 25 σ_0 cells, each with a characteristic area of $(25\ km)^2$. It is envisioned that 16 σ_0 cells will be combined in retrieving winds at 50 km resolution for the NASA users, while four cells will be used to retrieve winds at 25 km resolution for Navy applications.

One of the measurement cells from each of the antenna beams will be at an incidence angle of approximately 11°. The data obtained from these cells will be used for monitoring the instrument performance, since at these incidence angles, σ_0 is relatively insensitive to wind velocity (Ref. 5).

A stable local oscillator (STALO in Figure 3) will provide reference frequencies for the transmitter, receiver, and digital processor. The transmitter subassembly is designed with redundant traveling wave tube amplifier units in order to enhance the system reliability. The transmitter will provide pulses with 110 W peak power at a 31% duty cycle. The antenna switching matrix (ASM) will sequentially cycle through the eight antenna beams in approximately 3.75 s

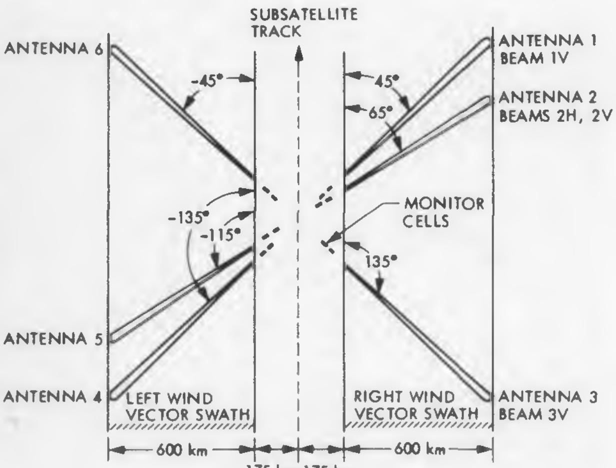

Figure 4. Antenna illumination patterns.

to achieve the desired along-track resolution of 25 km. In the baseline design, for each antenna beam, 25 pulses will be transmitted and the return signal powers will be averaged. An additional set of four "listen only" measurement intervals for each antenna beam, during which pulse transmission is inhibited, will be used to estimate system noise and the natural emissivity of the ocean.

A GaAsFET receiver will be used to amplify the return signal. This improvement in receiver technology provides a lower overall system noise temperature relative to SASS (refer to Table 1). The receiver output will be split into four channels of different, partially overlapping bandwidths by the band-split filters. The channel splitting will be used to reduce the amount of computation required in the digital signal processor (DSP).

In SASS the Doppler filtering for along-beam resolution was achieved through the use of fixed-frequency band-pass filters (Ref. 6). As the frequencies and bandwidths of the analog filters were fixed, the latitude-dependent Doppler shift caused by the Earth's rotation distorted pattern and size of the σ_0 measurement cells from the fore and aft beams. Except at the extreme latitude of the orbit, one pattern was compressed while the other was expanded, leading to misregistrations between the fore and aft beams and a reduction in the effective width of the vector wind measurement swath.

For NSCAT, Doppler filtering and associated data windowing and power detection will be performed using an on-board Fast Fourier Transform digital signal processor. A closed-form analytic expression describing the normalized standard deviation of σ_0 estimates from a digital filter system (such as that in the baseline design) has been derived and used in the detailed design of the DSP (Ref. 7). The DSP compensates for latitude-dependent Doppler shifts due to the Earth's rotation by adjusting the frequency ranges of the band-pass Doppler filters. Both the orbital period and a set of parameters for the filters will be stored onboard the spacecraft in random access memory and may be modified as the orbital parameters are varied. The orbital position computation in the DSP will be synchronized with equator crossing times. This compensation for the Earth's rotation will ensure that the measurement cells from the different beams will be nearly coregistered and thus will maximize the swath width over which vector wind measurements can be made. Details of the system are described in Refs. 7-8.

5. NASA RESEARCH-MODE GROUND DATA PROCESSING SYSTEM FOR NSCAT

A research-mode NSCAT Ground Data Processing System (NGDPS) will be established at JPL to reduce the raw NSCAT data and to distribute NSCAT data products to NASA investigators in a timely manner. Figure 5 shows a schematic diagram of the data flow through this system. The input to the NGDPS will consist of NSCAT telemetry (radar return data, calibration data, and engineering data) orbit and attitude data, and partially processed SSM/I brightness temperatures. The NGDPS will first convert all

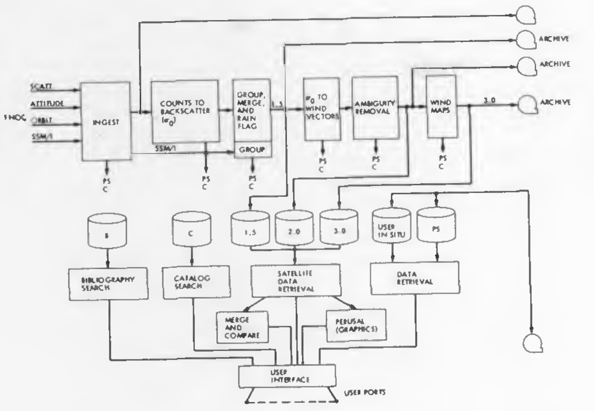

Figure 5. Schematic diagram of the NSCAT ground data processing system.

NSCAT telemetry to engineering units. Earth locations for the σ_0 measurement cells will be calculated using the orbit and attitude information. Scatterometer radar return data will then be converted to σ_0 estimates using the radar equation. At this stage any σ_0 cells containing land or ice will be removed from further processing. SSM/I brightness temperatures, where available, will be used to detect excessive atmospheric absorption due to the presence of rain and corresponding σ_0 cells will be flagged.

The σ_0 estimates from various antenna beams will then be binned into 50 km "wind cells" preparatory to wind retrieval. Although the "SASS-I" model function relating σ_0 to wind velocity was used in the design of the NSCAT flight instrument, several studies in recent years (Refs. 9-11) have demonstrated various errors and inconsistencies in the Seasat data due to inadequacies of the SASS-I model and the SOS wind retrieval algorithm (used to invert the model function, given a small number of σ_0 measurements). Careful re-analyses of the SASS data as well as new theoretical work and experimental data will be used to develop and test an improved model function and retrieval algorithm for pre-launch implementation in the NGDPS.

An additional processing step will be used to select a unique vector wind from among the (nominally two) ambiguities. The ambiguity removal process will utilize the intrinsic skill provided by the instrument as well as correlations between neighboring vector wind cells. While the exact form of the ambiguity removal algorithm remains under active study, simulations indicate that a technique based on "median filtering" has very favorable properties (Ref. 12). Using a variety of simulated wind fields based on SASS data, the ambiguity removal technique chooses the "correct" solution more than 90% of the time when the instrument first alias skill exceeds 55%. Furthermore, the technique has been shown to restrict errors to local regions, such that the skill in each 600 km x 600 km region of NSCAT data is greater than 85% more than 99% of the time.

Wind field maps will be constructed by spatially and temporally averaging the unique wind vectors. It is expected that the maps will be used by research investigators to assess data availability and to identify regions of space and time containing large-scale phenomena of interest. The maps and associated statistical information may also be used directly for the construction of even larger-scale spatially and/or temporally averaged data sets for the study of large-scale air-sea interactions.

The NGDPS must be in place and tested at launch. In addition, in order to meet the timeliness requirement (data available within two weeks of receipt from the Navy, see Section 2 above), the system must process and make data available at least at a real-time rate.

Data will be available to users through a data management system (DMS). The DMS will support on-line access to selected scatterometer data and will allow the specification of longitude, latitude, and time boundaries of desired data. The requested data will be transmitted to the user either electronically or on magnetic tape. The data available on-line will include:

(1) All wind-field maps.

(2) All unambiguous vector winds.

(3) A selected 5% of σ_0 data for the most recent 12 months.

The science investigators and Project personnel will determine which regions are included in the 5% of σ_0 data that are stored on-line.

In addition to the scatterometer data the DMS will host in situ data for comparison purposes. It will be possible to host certain user data sets that meet format and validation criteria established by the DMS. These in situ data will also be available through the on-line selection procedures used for the scatterometer data.

The DMS will have catalogs of available data organized in convenient ways. It will also maintain an on-line bibliography of relevant Project and external literature on scatterometry and related subjects.

The DMS will archive data (off-line) at several levels. The plan is to archive all of the following:

(1) Data received from the Navy.

(2) σ_0 data.

(3) Ambiguous vector winds.

(4) Unambiguous vector winds.

(5) Wind-field maps.

(6) In situ data.

An operations staff will be available to extract and distribute selected portions of the archived data in response to users' requests. All archived data will be sent to NOAA/NESDIS and appropriate NASA data systems for long-term archiving and access by the general community. These data may also be made available directly to other national and international agencies.

6. NSCAT SCIENCE AND VERIFICATION

A team composed of 14 science investigation groups has been chosen by NASA based on technical proposals submitted in mid-1985. The main goal of the team is to demonstrate the utility of satellite scatterometer data for the solution of geophysical research problems. To this end, the team's expertise and interests encompass a wide range of oceanographic and meteorological subjects.

The team will advise and closely monitor the NSCAT Project during the pre-launch years. It is expected that the team will make significant contributions to the data processing system (described in Section 5 above) and the validation activities in order to maximize the scientific utility of the NSCAT data.

The wind data from the NSCAT system will be verified in the first year following launch. The goal of the verification will be to quantitatively assess the overall accuracy of the data in terms of location, σ_o, wind speed and direction, and the presence or absence of the rain flag. The sensor (location and σ_o) and geophysical (wind vector and rain flag) verification efforts currently planned for NSCAT are briefly described below. Although the studies described are limited in temporal and geographical extent, similar comparisons are expected to be made between the scatterometer data and high-quality in situ data collected by oceanographic and meteorological field programs such as WOCE and TOGA, and by similar validation efforts conducted by other U.S. and international agencies.

The σ_o measurements and location accuracies will be verified using up to three mobile ground monitoring stations, onboard calibration sources, data obtained from σ_o monitoring cells, isotropic scatterers, and airborne scatterometer measurements. The ground monitoring stations will measure the transmitted power as received on the surface (over land) as the satellite passes overhead. Some additional information on the antenna gain pattern will be obtained from these data. Onboard calibration sources will be used to monitor gain characteristics of the instrument. Data obtained from cells at ~11° incidence angle (where σ_o is fairly insensitive to wind velocity) will be used to monitor and calibrate σ_o measurements over the ocean. The backscatter from isotropic scatterers, such as large regions of rain forest, can be used to identify and correct biases in the gain pattern for any individual antenna (Ref. 12). Finally, comparisons between measured σ_o from the NSCAT over the ocean and suitably averaged aircraft under flight measurements of σ_o will provide direct, if limited, verification of σ_o accuracy over the ocean under realistic conditions.

A quantitative assessment of σ_o accuracy will be made within the first six months after launch. However, data for monitoring purposes (ground stations, calibration sources, and isotropic scatterers) will be collected and routinely examined throughout the mission. The σ_o data processed in the first six months of the mission will be called "interim" data because the σ_o validation will not have been completed.

To evaluate the accuracy of the geophysical measurements (wind vector and rain flag) the system will be verified by comparing NSCAT winds with winds measured or inferred by conventional, non-NSCAT means. Present plans call for acquiring in situ conventional wind data from two experiments conducted at different geographical regions, each lasting approximately two months. The regions will be chosen to encompass a wide range of oceanic and atmospheric conditions, and to complement, insofar as possible, field work being simultaneously performed by others. Direct measurements of surface winds will be obtained from buoys (both National Data Buoy Center [NDBC] type moored buoys and drifting buoys), aircraft (such as the National Center for Atmospheric Research [NCAR] Electra or the NOAA P3, and possibly oceanographic ships and instrumented platforms. In addition to direct comparisons between in situ and scatterometer winds, plans call for preparing high-quality wind-field maps for the validation regions based on the conventional measurements as well as all other available meteorological information. These maps, which represent an interpolation and smoothing of the wind field, will provide vector wind estimates that can be compared with scatterometer measurements.

Although the direct comparisons discussed above provide an estimate of the intrinsic accuracy of the scatterometer system, many oceanographic and meteorological uses of the data will involve both spatial and temporal averaging of measured winds. As the scatterometer data are irregularly distributed in both space and time, it is not clear how errors in individual measurements will affect averages constructed from many scatterometer measurements. The errors in averaged winds are much smaller than the random errors in the individually measured winds. However, systematic biases, if any, remain in the averaged products. The two-month duration of the system verification experiments, as well as their regional extent (as opposed to isolated point-comparison data sets), will allow estimates of the accuracy of averaged NSCAT data.

The quantitative accuracy of the NSCAT geophysical measurements will be summarized by the end of the first year of the mission. At that time, the NSCAT Project, in conjunction with the science team, will determine the necessity for and the nature of any changes to the geophysical model function used to reduce σ_o measurements to wind vectors. All ambiguous vector wind and higher level data processed during the first 12 months of the mission will be labeled "interim" data to denote that the geophysical wind products will not have been validated during this period.

ACKNOWLEDGMENTS

This work was carried out at the Jet Propulsion Laboratory, California Institute of Technology, under contract with the National Aeronautics and Space Administration.

7. REFERENCES

1. Freilich M H 1985, Science Opportunities Using the NASA Scatterometer on N-ROSS, JPL Pub. 84-57.

2. O'Brien J J 1982, Scientific Opportunities Using Satellite Surface Wind Stress Measurements Over the Oceans, NOVA University N.Y.I.T. Press.

3. JPL D-2483 (NASA) 1983, NASA Scatterometer JPL Proposal.

4. Grantham W L et al 1982, Performance evaluation of an operational spaceborne scatterometer, IEEE Trans Geoscience and Remote Sensing Vol GE-20(3).

5. Schroeder L C et al 1982, The relationship between wind vector and normalized radar cross-section used to derive Seasat-A satellite scatterometer winds, J Geophys Res Vol 87, 3313-3336.

6. Johnson J W et al 1980, Seasat-A satellite scatterometer instrument evaluation, IEEE J Oceanic Eng Vol OE-5(2), 138-144.

7. Chi C-Y et al 1986, Radar backscatter measurement accuracies using digital Doppler processing in spaceborne scatterometers, IEEE Trans Geoscience and Remote Sensing Vol GE-24(3), 426-437.

8. Long D C et al 1984, Digital filter processing design for spaceborne scatterometers, Proc 1984 IGARSS, Strasbourg, France, 569-572.

9. Wentz F J et al 1984, A model function for ocean radar cross sections at 14.6 GHz, J Geophys Res Vol 89(C3), 3689-3704.

10. Woiceshyn P M et al 1986, The necessity for a new parameterization of an empirical model for wind/ocean scatterometry, J Geophys Res (accepted).

11. Plant W J 1986, The physical basis of scatterometry, J Geophys Res (accepted).

12. Schultz H 1985, A median filter approach for correcting errors in a vector field, Proc 1985 IGARSS, Amherst, Massachusetts, USA, 724-728.

N-ROSS VALIDATION

D R Johnson

NORDA, Code 321
NSTL, MS 39529

ABSTRACT

The N-ROSS (Navy Remote Ocean Sensing System) satellite is currently scheduled for a three year mission starting in late 1990. This satellite will acquire information over the global oceans on sea surface temperature, topography and waves, ice fields, atmospere and soil moisture content, and near surface winds. Since its mission time frame, orbital characteristics and sensor packages are similar to those of ERS-1, collaboration of efforts to validate the satellites makes sense, both from the point of view of sharing resources and experience, as well as from the potential dividends from enhanced coverage and performance comparisons of intercalibrated systems.

Keywords: Validation, GEOSAT, N-ROSS, ERS-1, Operational Products.

1. INTRODUCTION.

The U.S. Navy Remote Ocean Sensing System (N-ROSS) has been designed principally as an operational instrument, to provide environmental products on a near real time basis. Measurements of sea surface temperature and topography, ice fields, atmosphere and soil moisture content, and near surface winds over the global oceans are expected to improve short and medium range forecasting capabilities. A second, but equally important component of the N-ROSS mission is to contribute to a data base which can be used for climatology studies as well as for specific research applications.

In order to achieve its mission requirements, it is recognized that a high quality scientific effort is needed, not only to calibrate and validate the spacecraft sensor output, but to test models of geophysical processes which use this output and to determine the validity of the models for producing global and mesoscale fields. At present, we are learning by experience and testing our abilities to do near real time analysis using current GEOSAT data.

The N-ROSS calibration and validation effort will encompass a broad scope. Broken roughly into three parts, this effort will include

* validation of the geophysical parameters,
* validation of the data base synthesis and geophysical model products,
* determination of the usefulness of NROSS as an operational system.

The third part is understandly subjective, but a necessary precursor to future N-ROSS missions. As part of our planning for such future missions, we also have an interest in evaluating the advanced sensor designs onboard ERS-1. It is hoped that by collaboration and by sharing of expertise, methods and data products, the ERS and NROSS systems will produce significant scientific and engineering advances which can benefit everyone.

Since the ESA/ERS-1 community will be facing a similar task, I will begin the paper with a discussion of our efforts at developing operational products using the current GEOSAT data base. The second part will deal with the direction that our ground validation effort is taking and, finally, some areas of collaboration will be discussed.

2. GEOSAT OPERATIONAL PRODUCTS.

Table 1 shows some of the areas in which we are trying to develop operational products using near real time data from GEOSAT. Each area has its own schedule requirements based upon its parameter duration of usefulness. The most restrictive limitation on operational utility is that the primary mission of the GEOSAT program has been to measure the geoid by filling in gaps left by the premature failure of SEASAT. This requirement has meant that it is placed in a non-repeat orbit and, hence, has limited usefulness as an oceanographic satellite. In the Autumn of this year GEOSAT is due to be placed in a collinear orbit with 17 day repeat track. This should improve our efforts in some areas, but will have little effect in others.

Table 1: GEOSAT APPLICATION PRODUCTS

Parameter	Coverage	Schedule
surface wind speed	global (50K pts)	2/day
signif. wave height	global (50K pts)	2/day
Ice Edge	Northern Hemisphere	daily
Meso-scale features	NW Atlantic	2/week

At present, and continuing through the GEOSAT Extended Repeat Mission, surface wind speed and significant wave height will be of limited operational value due to its 12 hr. lag time (limited reception times at a single ground receiving station). Some efforts are being made to use the significant wave height as a quality control check on an operational Global Spectral Ocean Wave Model and as a check on Visual Sea Height Analysis. In addition, first efforts are being made in melding the surface wind speeds with a Marine Winds Analysis, taken primarily from ship and buoy winds. Perhaps the most useful result from the GEOSAT wind/wave fields, however, will be a data set encompassing seasonal changes which can serve as a test bed for N-ROSS and ERS-1 software.

Ice edge from GEOSAT altimetry has only recently been distributed as a useable product. Figure 1 shows a portion of the bi-weekly output of ice index profiles along the ground track of GEOSAT. Comparisons of the ice index locations with multichannel imagery has generally been encouraging. However, incorporation of the index into an automated ice edge distribution field is a significant problem which must be met before the launch of N-ROSS.

Two programs of interest here concern the description and the analysis of mesoscale oceanographic features. Since GEOSAT is not in an exact repeat orbit and, hence , cannot separate the geoid from topographic variations, these programs have been limited to the NW Atlantic where the best gravimetric geoids have been measured. But it is also in this area that a rich field of warm core and cold core spin-off eddies occur and where the rapid development of Gulf Stream meanders provide the strong signals needed for testing our programs.

Figure 2 shows a product from this area which combines IR imagery with GEOSAT altimetry to produce a map of the major features. The IR imagery is not entirely reliable as an indicator of upper ocean structure, particularly in defining cold core eddies and in resolving strong current boundaries. In this case it is most useful as an interpolator between the sparse altimeter ground tracks. At present, the system relies on skilled interpretation. However, efforts are being made to incorporate the product into models which can both help with interpretation and provide information on subsurface structure.

A second program in the NW Atlantic, termed the Regional Energetics Experiment (REX), is a multidisciplinary approach using (1) GEOSAT altimetry, (2) long time series of sea surface and thermocline fluctuations from bottom mounted instrument arrays and (3) extensive temperature sections from aircraft. Figure 3 shows a temperature section across the Gulf Stream with a superimposed altimeter residual taken during a REX study. The inverse relationship between sea surface and isotherm slope is obvious. But noise due to geoid uncertainty and long wave orbit error tend to limit its quantitative usefulness at present. The program has two objectives: (a) a scientific study of the variability of the region and, (b) a validation effort for altimetry and for models which project surface information into the ocean interior

3. N-ROSS GROUND VALIDATION.

At present, the N-ROSS ground validation effort is only in the rough conceptual stage. Although this may be frustrating to the ESA/ERS-1 community who are trying to define their effort in more detail, it actually represents a major opportunity to develop significant interaction at the start. With sufficient interest and sufficient determination from both communities, the exciting prospect of an intercalibrated dual satellite system can be achieved.

3.1 Validation Objectives.

The objectives of the N-ROSS ground validation effort are

* to determine quantitatively the precision and accuracy of the N-ROSS system product at the geophysical parameter level and,
* to define and to recommend changes (if necessary) in order to bring the system accuracy to within specified mission requirements.

The N-ROSS community recognizes that there are heavy problems to be met before a quality validation effort can be accomplished. Among these problems are (1) the inherent space and time scale differences between satellite and ground truth measurements and (2) the lack of measurement "standards" at appropriate scales. In addition, N-ROSS validation planning is driven by the relatively short response time required for an operational capability.

The solutions to the problems are universally recognized: a "global" scale validation effort is required, involving numerous institutions and countries, and involving a variety of methodologies. In addition, opportunities must be provided for intercalibration of in-situ instruments and methods. Finally, in order to meet the short post launch response time, preparations must involve prelaunch collaborative exercises to work out problems and to rehearse the participants.

3.2 Validation Activities.

The major activities surrounding the validation effort will be, in order,

* the formation of a validation working group for detailed planning of the field validation effort,
* prelaunch in-situ validation of airborne sensors and cross calibration of instrumentation during Prelaunch Validation Field Experiments (PVFE),
* post launch Validation Field Experiments (VFE),
* "quick-look" comparison workshop with problem flagging and recommendations,
* validation workshop,
* algorithm refinement workshop.

3.3 Validation Working Group (VWG).

In order to create as much opportunity as possible for cross calibration and sharing of expertise, methodology and equipment, the Validation Working Group will include participants from,

* U.S. Navy oceanographic laboratories,
* NASA/JPL
* NOAA
* ESA/ERS-1
* Universities

The VWG will be organized into teams according to geophysical parameters. Although the final organization will depend on the individual expertise in the group, it is expected that the teams will be organized into parameter groups something like the following:

* wind and boundary layer stability,
* wind waves,
* sea surface temperature,
* sea surface topography,
* ice,
* atmospheric and soil moisture.

Each team leader will be responsible for designing the special field experiments, obtaining comparison data from all possible sources, analysis of the data, reporting the results and recommending changes.

3.4 Prelaunch Validation Field Experiments (PVFE)

Prelaunch efforts at organization and intercalibration are considered to be a necessary part of the overall plan if an effective postlaunch validation is to be accomplished. The objectives of the prelaunch phase, in order of priority, are

* prepare for the postlaunch VFE,
* evaluate instruments and methods,
* intercalibrate,
* obtain data in areas of scientific and operational interest.

Prelaunch field experiments will be undertaken at several different locations and times as chosen by the VWG. An effort will be made to collaborate the field programs with other field programs, such as the NASA/JPL validation of NSCAT, the ESA/ERS-1 validation program and other large and regional intensive projects such as TOGA and WOCE.

Following each field experiment, reports will be issued. In addition, a special effort will be made to encourage scientific publications since this is an effective means of bringing a quality effort to bear on the problem.

3.5 Postlaunch Validation Field Experiments (VFE)

The postlaunch field program will be designed by the Validation Working Group. At present, it is expected that there will be something like four field experiments. Although the locations will be chosen by the VWG, to meet Navy requirements, the final choice will emphasize locations where,

* greatest ranges are expected,
* knowledge of sea conditions are most limited,
* fleet components are most likely to operate,
* sea conditions have impact on ship and air operations.

The validation field experiments must be completed within 6 months of the N-ROSS initial operational checkout phase after launch. However, for the "quick-look" and flagging of potential problems, one of the experiments will be done within two weeks after the initial checkout.

4. AREAS OF POTENTIAL COLLABORATION.

There are several areas in which collaboration between the N-ROSS community and the ERS-1 community could bring substantial benefit to everyone involved. Sharing of experience, methods, hardware, software and data can be done only when a strong effort is made to do so. Specifically, sharing can be done in the following areas,

* GEOSAT - share experience in developing operational products.
  - contribute data for testing.

* ERS-1 - evaluation of advanced sensors for future N-ROSS satellites.
  - share experience in validation.
  - contribute satellite/satellite validation (ERS-1/N-ROSS).

* N-ROSS/ERS-1
  - share data and experience.

It seems apparent, however, that these collaborative efforts must involve more than memorandums of understanding. It will depend strongly on the desire of principal investigators to work together.

5. SUMMARY

Validation plans for N-ROSS are only in the conceptual stage. Although this can be frustrating, it does provide the opportunity for making collaborative efforts with the ESA/ERS-1 community a part of the planning process. It can be expected that by addressing these linkages now, later problems with data exchange may not be so difficult.

Since the ERS-1 has an operational mission, some of the efforts on developing operation products with GEOSAT has been discussed. Some of the major problems with using GEOSAT data for operational products can be traced to the fact that its primary mission has been to measure the geoid. Oceanography has been added as an opportunistic mission. Nevertheless, experience gained with GEOSAT can be transferred directly into N-ROSS and ERS-1 operational efforts.

Finally, in Figure 4 an enhanced version of an IR image in the region of the Gulf Stream in the NW Atlantic is shown, with ground tracks from two satellites crossing the area. The satellites (one black and the other white) have 19 day repeat orbits, but with 3.5 hr differences in equatorial crossing times. This image, which covers 7 days of tracks, is presented as a graphical way of demonstrating the problems faced in defining the energetic features in this area with only one satellite. Even in a retrospective time sense, only about 7 days, or less, can be used since the features move and smear on a longer time scale. Hence, it is distinctly to our advantage to work out methods of sharing our oceanographic capabilities.

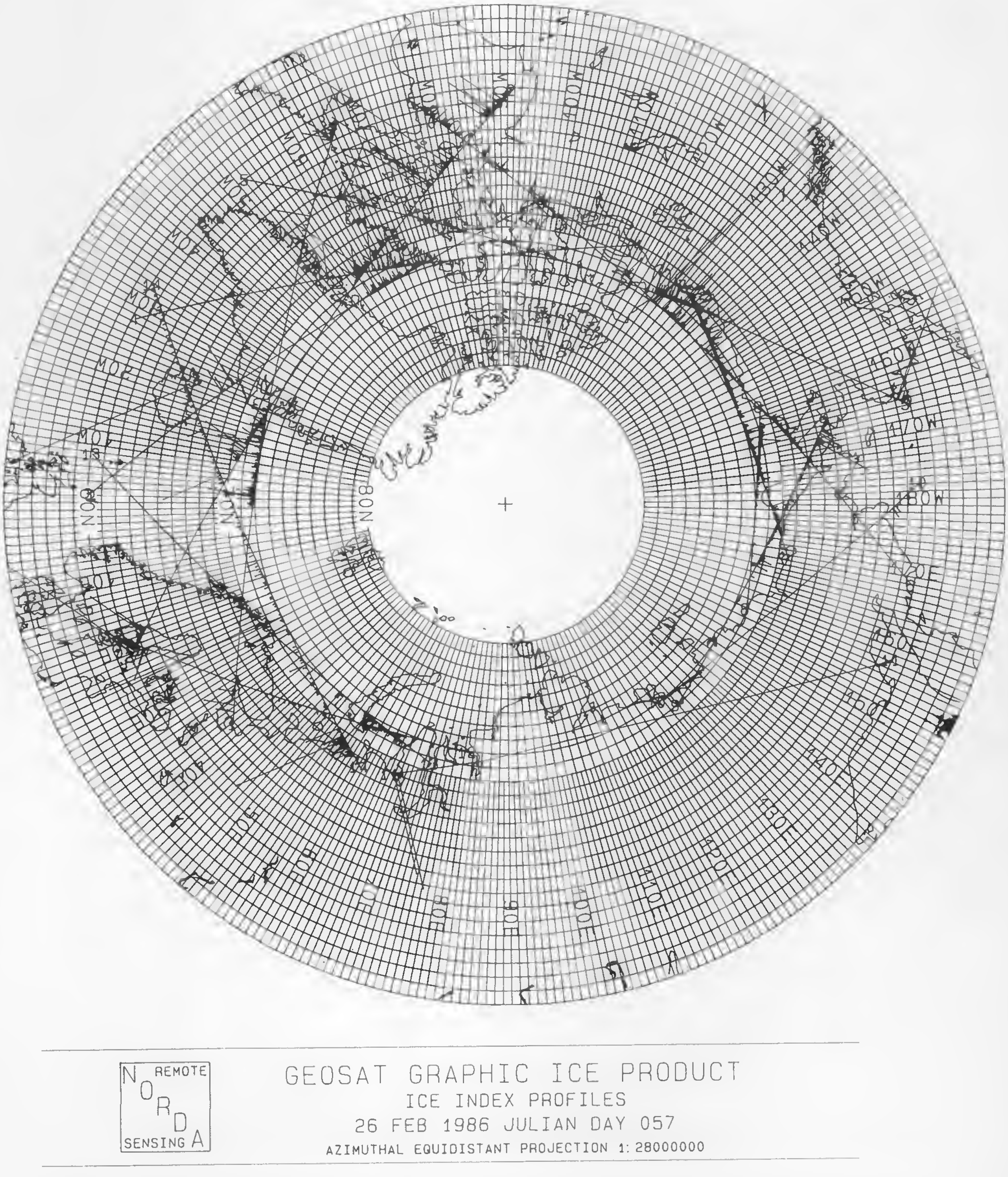

FIGURE 1: Ice Index profiles along GEOSAT ground track. Comparisons with multi-channel imagery has shown good agreement although some problems persist. Note the false indices along the descending pass through Iceland, thought to be due to loss of tracking window.

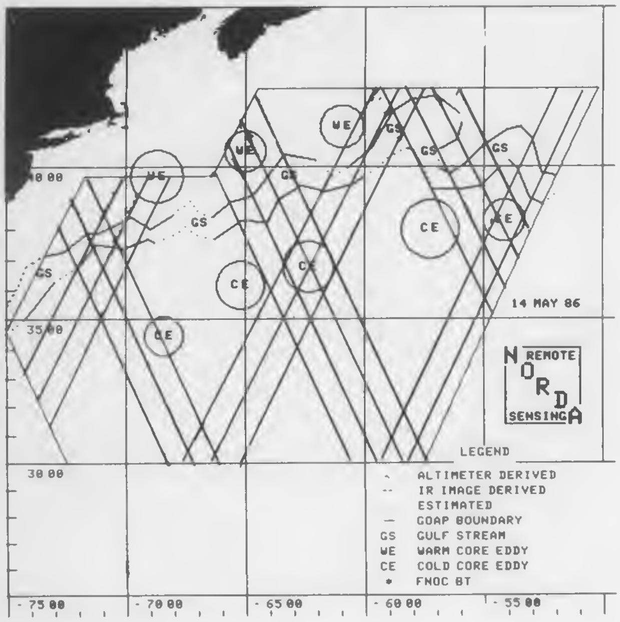

FIGURE 2: Ocean feature analysis in test area of NW Atlantic showing Gulf Stream and several mesoscale eddies. The product has been derived from 7 days of GEOSAT altimetry plus the most recent IR image (courtesy of R. Crout).

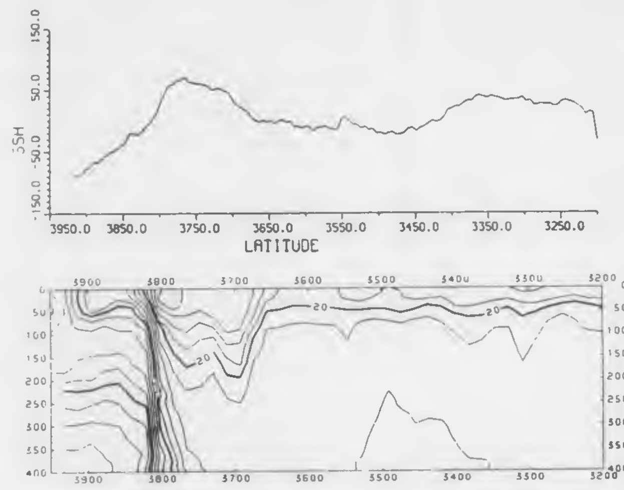

FIGURE 3: (lower) Temperature section across Gulf Stream along ascending pass of GEOSAT in NW Atlantic. (upper) GEOSAT altimeter residual collocated with the temperature section (courtesy J. Mitchell)

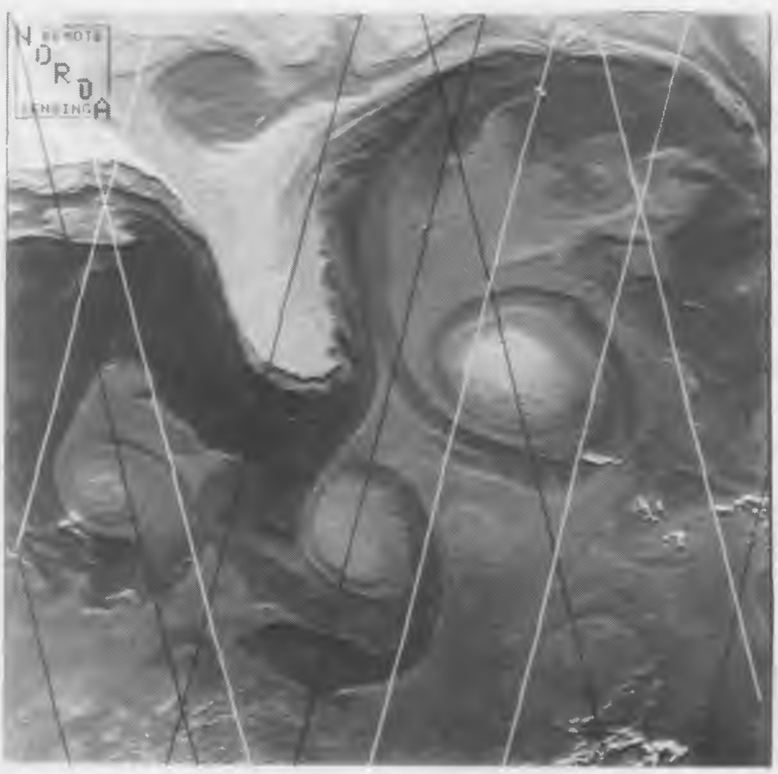

FIGURE 4: Edge inhanced IR image of Gulf Stream meander (dark ribbon) with several cold) core eddies (light) and a warm core eddy (dark). Ground tracks from 2 satellites (19 day repeat orbits) for 7 days are superimposed. The dark track satellite covers most features, while the white track satellite misses. Data exchange from two satellites would help to avoid the uncertainties caused by aliased samples. (courtesy of M. Lybanon)

INTERSENSOR COMPARISONS FOR VALIDATION OF WIND SPEED MEASUREMENTS FROM ERS-1 ALTIMETER AND SCATTEROMETER

C T Swift
University of Massachusetts
U.S.A.

N M Mognard
CNES
U.S.A./France

ABSTRACT

Global and regional wind speed measurements comparisons using the SEASAT altimeter (ALT), scatterometer (SASS), and scanning microwave multichannel radiometer (SMMR) show discrepancies in the magnitude of the observed features. The SMMR consistently measures wind speed on the average 20% higher than the SASS which measures wind speed consistently 20% higher than the ALT.

Such comparisons will be continued using available GEOSAT data and the forthcoming Special Sensor Microwave/Imager (SSM/I) wind speed data. Statistical analysis of the ERS-1 altimeter and scatterometer should be used as a means to validate, on a periodical basis, the ERS-1 wind speed fields. Extensive buoys comparisons with SSM/I data will be done by the University of Massachusetts during the validation phase after launch which is expected in 1987. Either the same validation techniques can be applied to ERS-1 or SSM/I can be used on its own to be compared to ERS-1 winds.

1. INTRODUCTION

Analysis of the data obtained from the three wind sensors on board SEASAT, namely the radar altimeter (ALT), the scatterometer (SASS), the scanning microwave multifrequency radiometer (SMMR) show systematic discrepancies in the measurements of the wind magnitude. These discrepancies are shown and analyzed both on a global and regional scale for time periods varying from the entire three-month SEASAT period, to a monthly, and a 3-day time scale. The data are analyzed in the Southern Oceans where, during the SEASAT lifetime, the highest sea state conditions were found (Mognard et al., 1981). The algorithms used to process each data set are the official JPL SEASAT algorithms. The results point to a more detailed verification activity for future satellite systems such as the SSM/I, NSCATT and the ERS-1 scatterometer.

2. SOUTHERN OCEANS SEASAT WIND SPEED FIELDS

2.1 Global Southern Oceans Three-Month Mean Wind Speed Fields From July to October 1978

The three-month mean wind speed fields over the Southern Oceans for the whole SEASAT mission - from July 7 to October 10, 1978- are presented in Figure 1. The zonal banding characteristic of climatoligical wind speed fields is clearly defined on the three mean SEASAT fields. The geographical locations of the different mean wind speed bands agree remarkably well in the SASS and the ALT fields. In the SMMR field, the light winds of the Horse Latitude regions do not appear. A comparison of the magnitude of the seasonal wind speed features by the three SEASAT microwave wind sensors is presented in Table 1.

	SASS	ALT	SMMR
Doldrums	<6	<6	<6
Trade Winds	8-11	7-8.5	9-13
Horse Latitudes	7-9	5.5-7	
Southern Westerlies	10-15	9-13	12-19

Table 1. Ranges of mean wind speed in m/s estimated by the SEASAT wind sensors over the Southern Oceans during the satellite lifetime from July to October 1978.

The three-month fields deduced from each sensor have significant variations in magnitude. The mean SASS field has features approximately 20% higher than the ALT and 20% lower than the SMMR. The best quantitative agreement is found in the Equatorial regions where the Doldrums are well defined with wind speeds less than 8 m/s. The high winds of the Southern Westerlies are well defined in the three fields but not with the same magnitude. The ALT reports lower winds and the SMMR higher winds than the SASS. However, radiometric contamination by the Antarctic sea ice edge within the large SMMR wind speed algorithm spatial resolution (85x85 km) is in part responsible for the very high SMMR mean wind speeds at extreme southern latitudes. The light winds of the Horse Latitudes are not delineated in the SMMR field, probably also due to the poor spatial resolution of the SMMR.

The ALT and the SASS wind speed fields have good agreement in detail in the location of the long-term hemisperhical seasonal wind features, whereas much detail is missing in the location of the SMMR derived features. This lack of precision in the location of the wind features of the three-month SMMR field is partly due to the large footprint of the SMMR compared to the ALT and SASS footprints. It is also due to rain, land, or ice radiometric contamination which have not been completely removed from the official JPL data set (Mognard and Campbell, 1984).

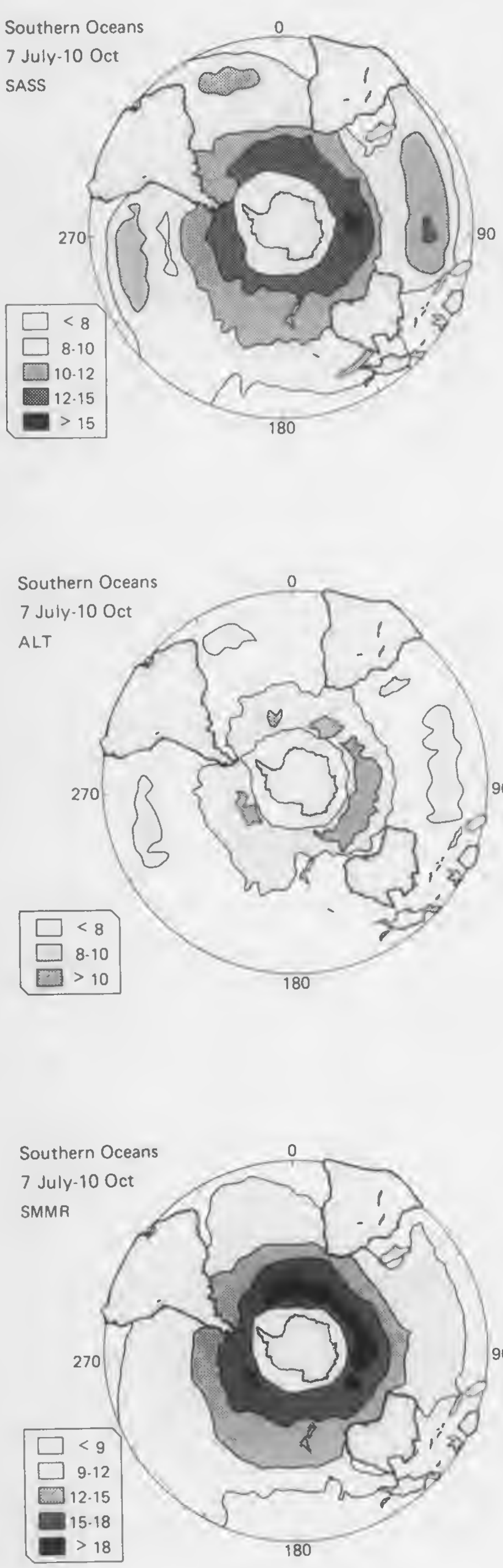

Figure 1. Three-month mean wind speeds as derived from SASS, ALT, and SMMR.

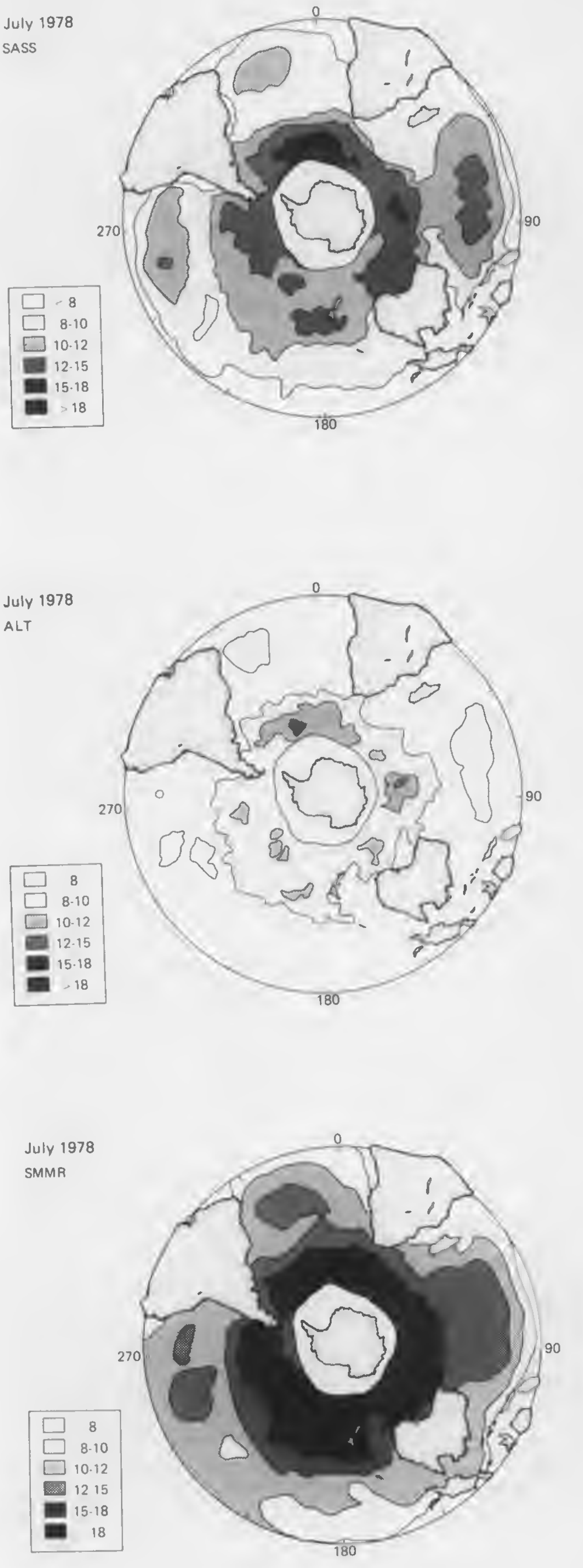

Figure 2. Average wind speed fields as derived from SASS, ALT, and SMMR for July 1978.

2.2 Global Southern Oceans Mean Monthly Wind Speed Fields

The monthly wind speed fields (Figures 2-4) show a pronounced mesoscale variability (with horizontal scales as small as 1,000 km) superimposed on the climatological zonal banding dominant in the three-month fields (Figure 1). As in the three-month fields, differences in the wind speed magnitudes appear in the monthly fields obtained with each sensor. The monthly SASS fields have mean wind speeds about 20% higher than the monthly ALT fields and 20% lower than the monthly SMMR fields.

A pronounced monthly mesoscale variability appears in each monthly wind speed field derived from each sensor data set. An eastward migration of the highest winds in the Southern Westerlies from July to September/October, first noticed in the monthly ALT wind speed fields (Mognard et al., 1983), is also present in the SASS and SMMR mean monthly fields. Significant differences appear in the geographical location of the monthly mesoscale features for each sensor. These differences can be attributed to the differences in footprint size and coverage patterns of the three sensors. This is especially so for the ALT which samples only a narrow band along the satellite track, and therefore undersampling can occur.

The conclusions drawn for the three-month wind speed fields about differences in the magnitude of the wind fields obtained with each sensor and the constraints associated with the SMMR wind fields remain true for the monthly fields. Some significant differences in the geographical locations of mesoscale features show that for monthly wind fields, differences in the sensor footprints and in the coverage patterns of each sensor have to be taken into account in the interpretation. These differences, which were averaged out in the three-month fields, become even more significant in the analysis of the three-day fields.

2.3 Regional Southern Oceans Three-Day Wind Speed Fields

The sensor with the poorest spatial coverage is the ALT (about 3 km footprint). In order to establish a meaningful comparison of the fields deduced from each of the three sensors, the minimum time period required to obtain sufficient spatial coverage to obtain coherent quasi-synoptic wind speed fields is three days which corresponds for the ALT to a 800 km east-west separation between tracks at 35 degrees latitude.

Two three-day periods in the West Pacific, July 10 to 12, and September 22 to 24 are presented Figures 5 and 6. In both cases, the ALT measures the lowest wind speeds and the SMMR the highest one. The first three-day period (Figure 5), shows relatively low winds with a total 10 m/s wind variation range on the ALT and 15 m/s on both the SASS and the SMMR. Individual features in each field are poorly correlated in the detail, but a large scale correlation between the geographic location of high and low wind features can be found.

The second three-day period (Figure 6) shows a more dynamic wind fields with a total variation in range over about 20 m/s in each field. There is a good large scale agreement in the location of the main wind features with the highest winds located in the south-west region and the lowest along a band oriented north-west to south-east and also in the north-east sector.

The histograms for each case show close agreement between the SASS and the SMMR, whereas the ALT histograms are asymetric, with more low wind speeds measured.

A common feature for the three time periods analyzed is that the SMMR always measures the highest mean wind speeds and the ALT the lowest. There is approximately a 20% discrepancy between the speeds measured by each sensor. On the three-month fields there is a very good agreement in the geographical location of the climatological features for each of the three sensors. In the monthly fields, some of the mesoscale features vary in location in the fields of each sensor. Part of these differences are due to footprint/spatial coverage interplay of the three sensors. The differences in the geographical location of the wind features become predominant in the three-day maps.

The official algorithms that have been used to obtain the wind fields are based upon the sea-truth data that were collected during the satellites lifetime, mainly during the GOASEX and JASIN experiments. However, the sea state sampled during these experiments were mostly low and the wind speed recorded were mostly under 15 m/s. The lack of data to validate the SEASAT instruments specially for high sea state sets a limit in the improvement of the geophysical algorithms for each of the three sensors.

3. A LOOK TO THE FUTURE

3.1 Re-examination of Historical Data

Clearly, there is only one true measurement of wind speed, yet each of the SEASAT sensors show some measure of disagreement. It therefore seems appropriate to re-examine historical SEASAT data to resolve the issue. To some extent this activity is underway with regard to the SMMR. In hand at the University of Massachusetts are the entire SMMR data tapes for brightness temperature and buoy data that were compiled by the NASA Langley Research Center to verify the SASS performance. The University of Massachusetts has developed an alternative SMMR wind speed algorithm which will be used to re-establish the SMMR wind speed retrievals. It is assumed that a similar activity will be undertaken at the Jet Propulsion Laboratory to further refine the SASS algorithm. Hopefully, the result will converge to a common measurement of wind speed.

3.2 Future Satellite Data

At the present time, GEOSAT is collecting altimeter data and it is expected that a limited data set will be available to the general research community. Within the coming year, the Special Sensor Microwave/Imager (SSM/I) will be launched by the United States Department of Defense. The SSM/I data will be available to the general research community. The University of Massachusetts (UMass) is committed to the wind speed verification program for the SSM/I, and GEOSAT can be easily woven into this program. The UMass activity will consist of using buoy data with near coincident SSM/I measurements to establish confidence intervals for the SSM/I wind speed retrieval. To this end, the effort relative to the post-verification of the SEASAT SMMR data will be modified to accommodate the SSM/I.

With regard to the SSM/I, progress to date has included generation of the SSM/I orbit to estimate the frequency of expected spatial and temporal "hits" of the NOAA buoy network shown in Figure 7. This figure indicates the deployment of the NOAA buoys near North America. Data products include 8 minute averages of wind speed, gust, and wind direction transmitted at hourly time intervals. Other useful data products such as air and sea temperature are also available to assess atmospheric stability. Figure 8 shows the number of SSM/I hits that will occur over a three week time period for a buoy located at 43.5° latitude/-70.1° Longitude as a function of distance from the buoy. Less that 500 "hits" are required to establish a 95% confidence interval that the buoy and the satellite measure the same quantity. Thus, an adequate number of measurements are available within this time frame to establish verification within the 50 km footprint of the SSM/I. A similar histogram for the temporal frequency of "hits" is shown in Figure 9. Here we see that 500 "hits" are achieved within 10 minutes between the time the buoy and satellite data are received. Statistical analysis is presently underway to optimize the trade-off of spatial vs. temperal averaging. In addition, the optimum temperal averaging of buoy data are being evaluated in cooperation with other international colleagues.

We view the SSM/I and GEOSAT verification effort as a first step in developing a resource for future related satellite missions. Clearly the same skills developed by UMass for SSM/I can be woven into next generation satellite wind speed measurement programs such as NSCATT and ERS-1.

4. REFERENCES

1. Mognard, N. M., W. J. Campbell, R. E. Cheney, J. G. Marsh, and D. B. Ross, Southern Ocean Waves and Winds Derived from SEASAT Altimeter Measurements, Proceedings of the Wave Dynamics and Radio Probing of the Ocean Surface, in press, Miami, Florida, 1981.

2. Mognard, N. M., W. J. Campbell, R. E. Cheney, J. G. Marsh, Southern Ocean Mean Monthly Waves and Surface Winds for Winter 1978 by SEASAT Radar Altimeter, J. Geophys. Res., Vol. 83, No. C3, p. 1736-1744, 1983.

3. Mognard, N. M., and J. J. Campbell, Comparison of Sea Surface Wind Speed Fields by SEASAT Radar Altimeter, Scatterometer, and Scanning Multichannel Microwave Radiometer, with an Emphasis on the Southern Ocean, Proceedings of IGARSS'84 SYMPOSIUM, EAS SP-215, p. 403-409, Strasbourg, France, 27-30 August 1984.

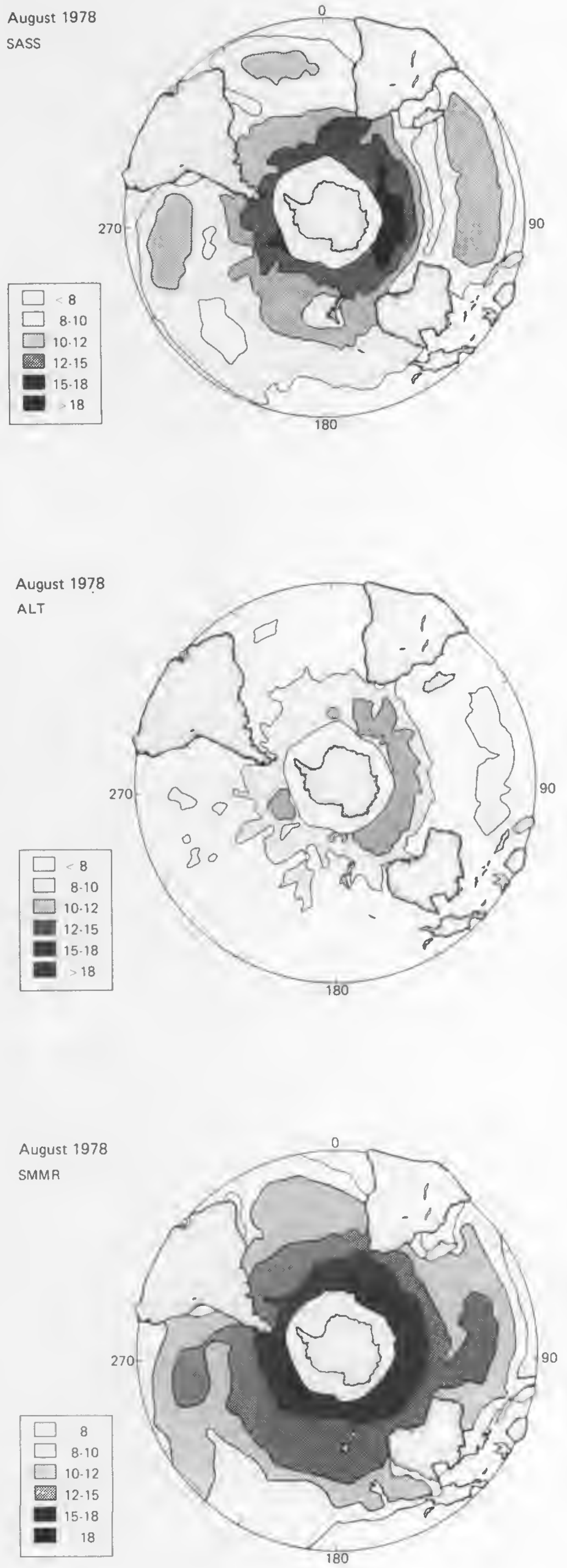

Figure 3. Average wind speed fields as derived from SASS, ALT, and SMMR for August 1978.

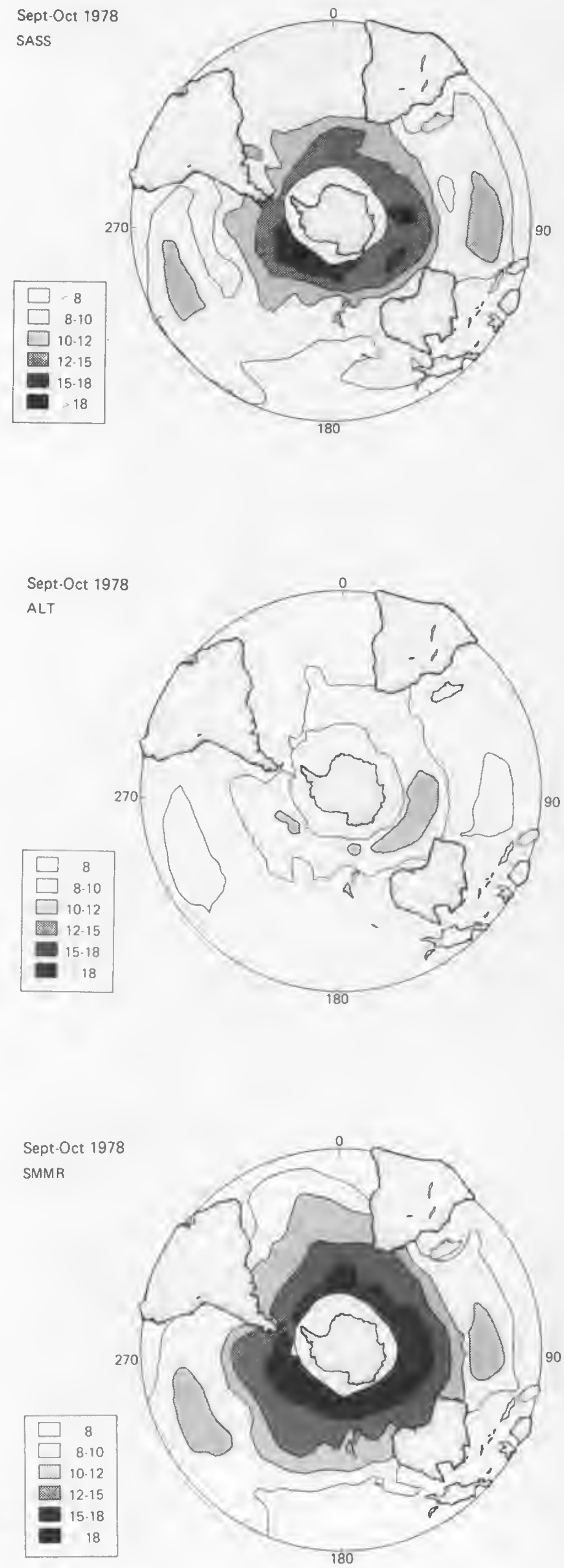

Figure 4. Average wind speed fields as derived from SASS, ALT, and SMMR for Sept.-Oct. 1978.

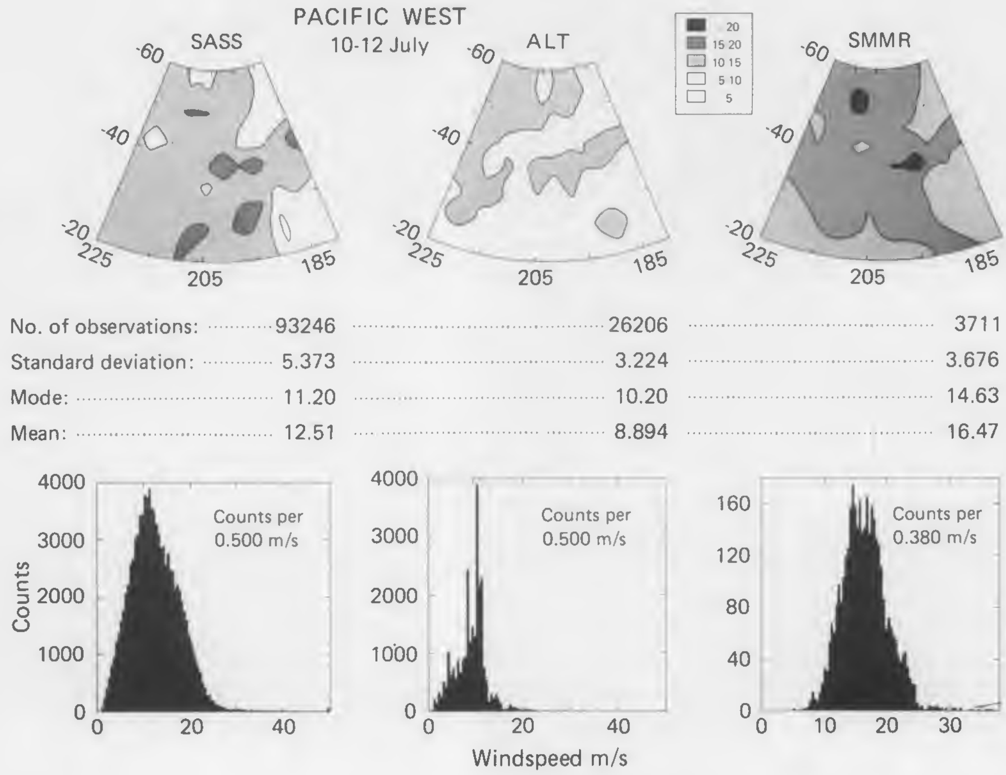

Figure 5. Histograms of wind speed from the SASS, ALT, and SMMR for 10-12 July 1978.

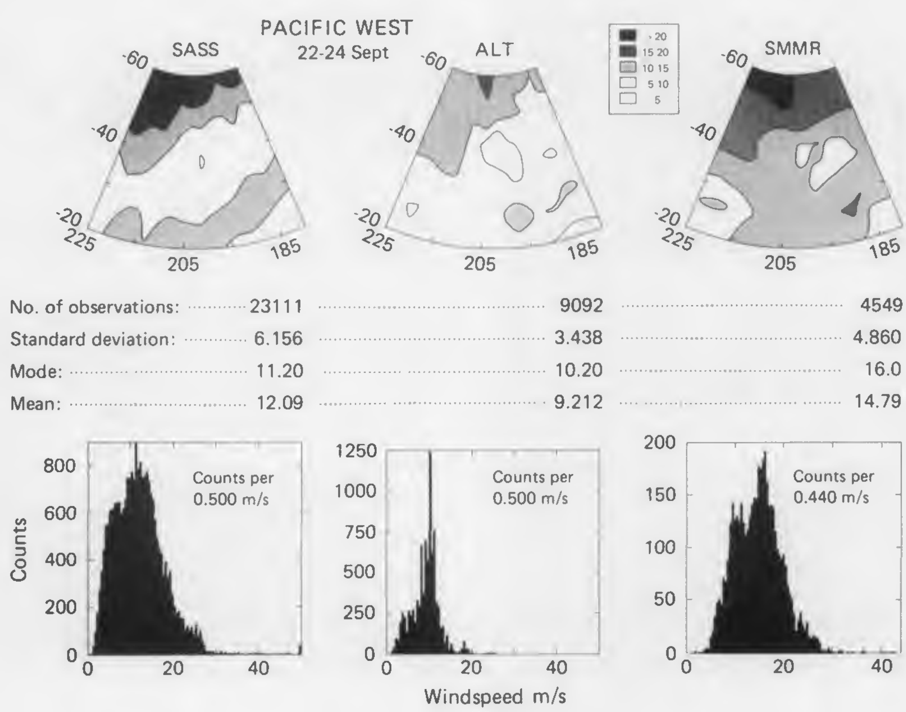

Figure 6. Histograms of wind speed from the SASS, ALT, and SMMR for 22-24 Sept. 1978.

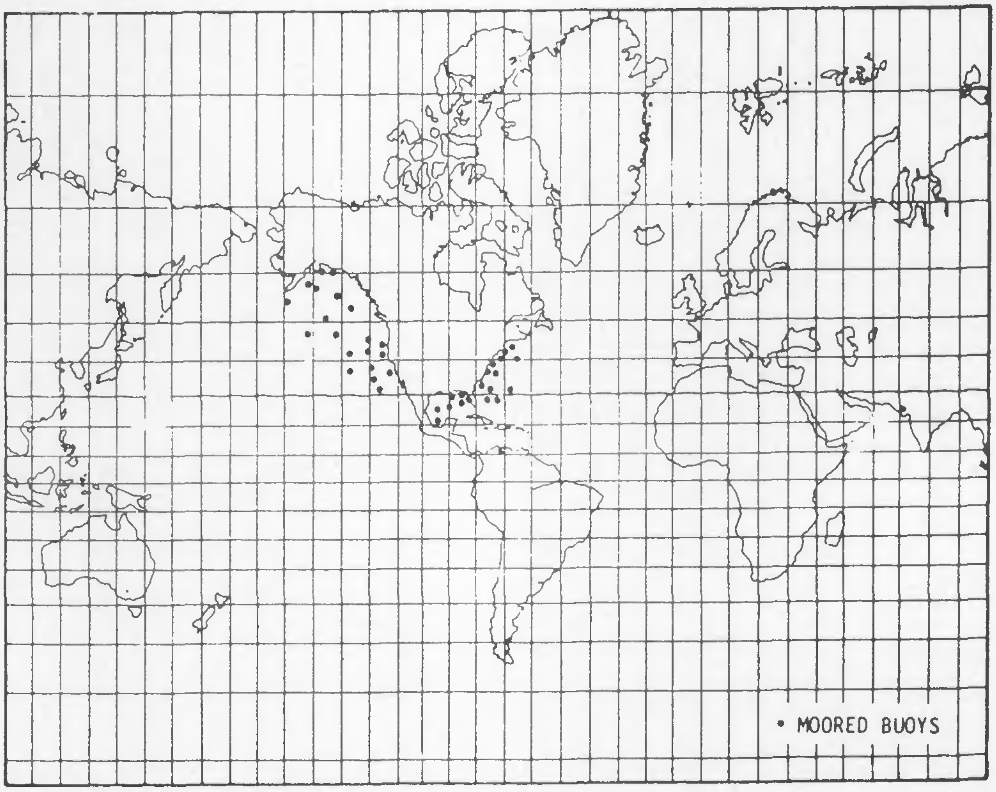

Figure 7. Location of NOAA buoys.

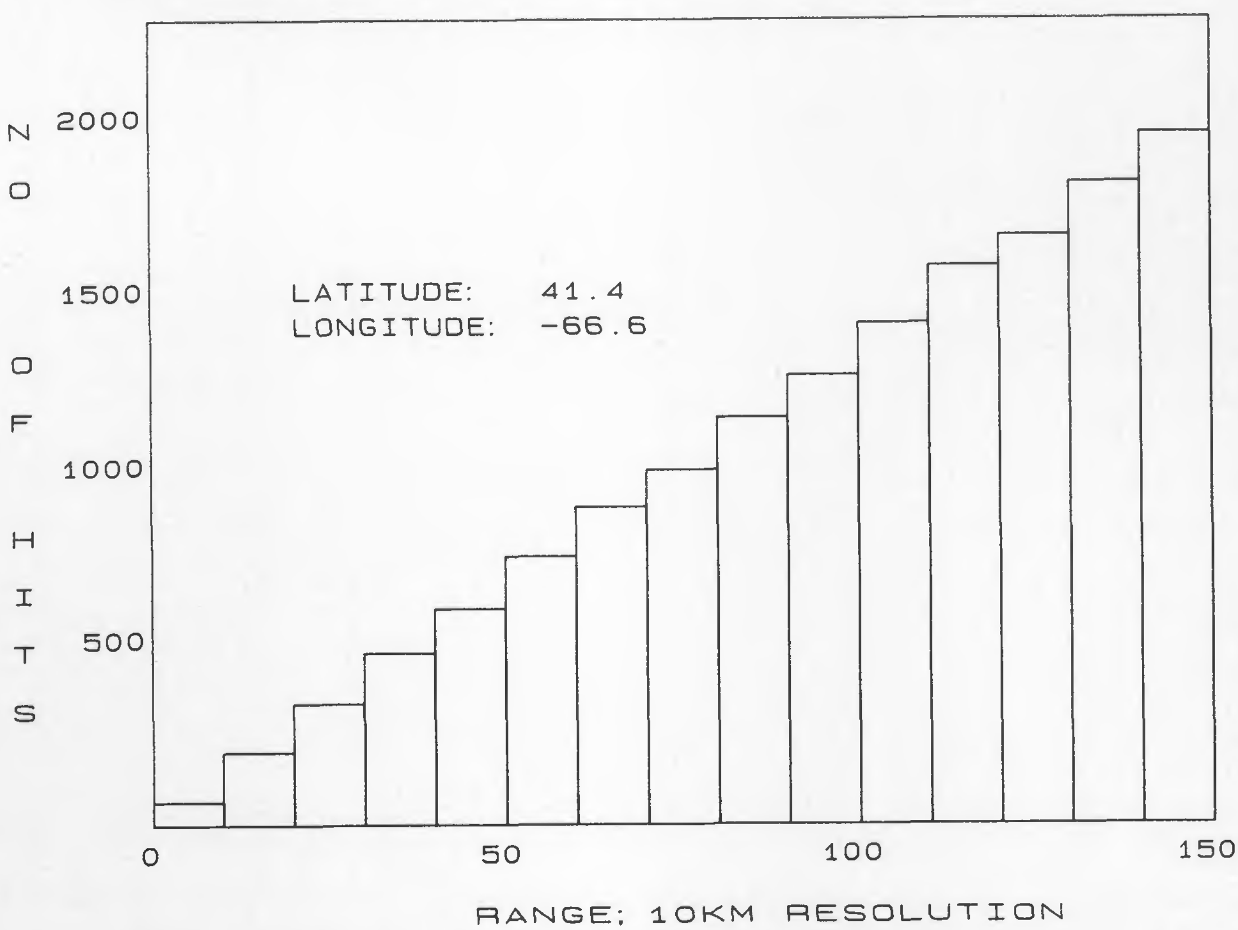

Figure 8. Number of SSM/I buoy hits as a function of distance from the buoy.

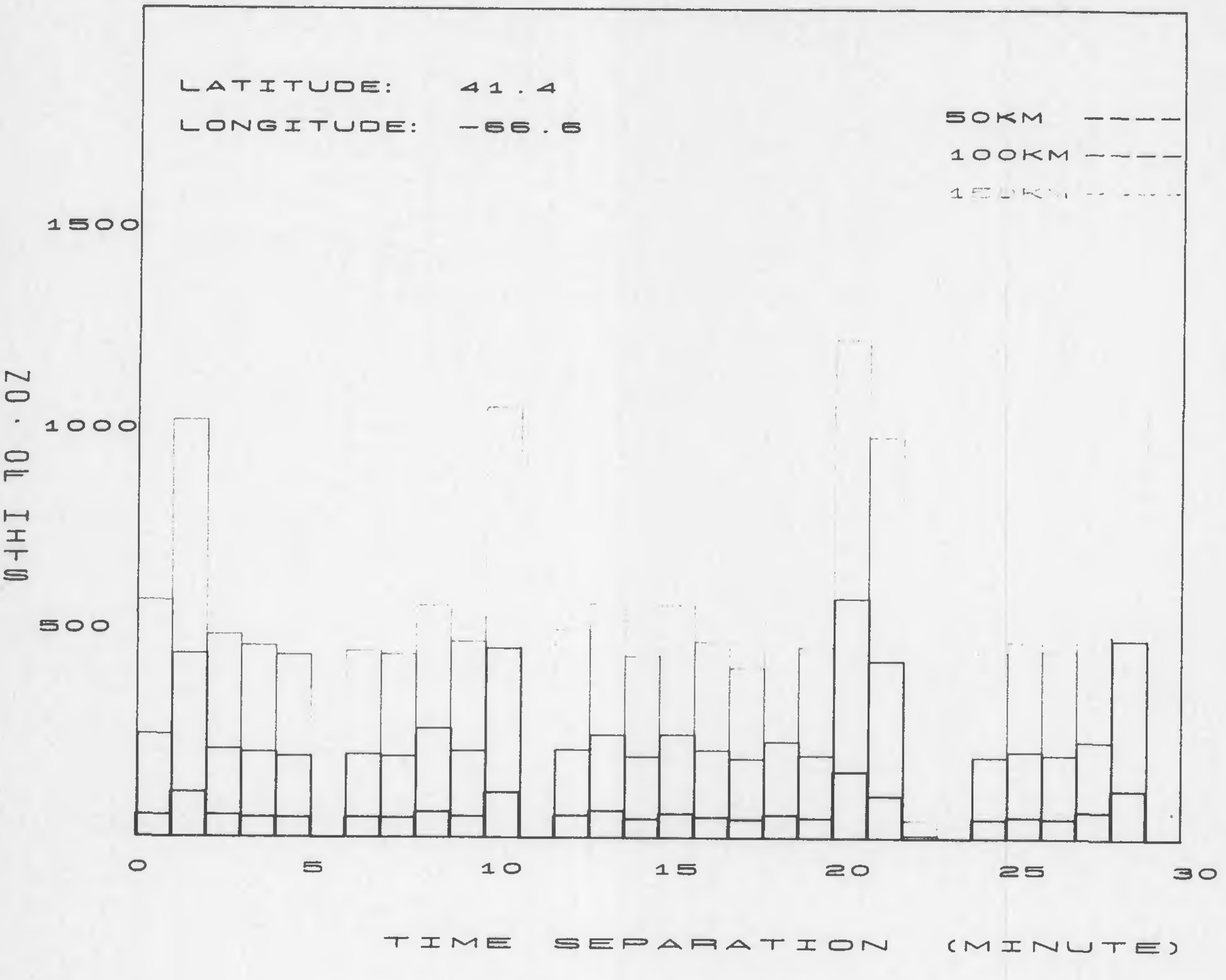

Figure 9. Number of SSM/I buoy lists as a function of time relative to buoy data transmission time.

AUSTRALIAN VALIDATION PLANS FOR ERS-1

I J Barton

CSIRO Division of Atmospheric Research, Aspendale, Victoria 3195, Australia

ABSTRACT

Details of Australian calibration/validation plans for the instruments carried on the ERS-1 satellite are described. A large experiment (SAVE) is planned for 1990 in the tropical waters to the north-east of the continent. Although the prime concern of this experiment is the validation of the ATSR instrument in tropical areas there will be side programs involving the validation of the products from the microwave instrumentation. Extended comparison between measurements from two HF radars (one ground-wave and one sky-wave) and the ERS-1 data will also be attempted as part of the Australian involvement in the ERS-1 program. Other studies planned relate to the calibration and general use of data both over land and ocean surfaces and in Antarctica.

Keywords: ERS-1 Validation, ATSR Validation, Australia, Tropical Measurements, Ground Truth Data, Wind/Wave Validation, HF Radar

1. INTRODUCTION

Australia, as a vast and sparsely populated continent, has in the past been a prolific user of remote sensing data to explore and manage her natural resources. Much use has been made of both airborne and space platforms for gathering these data. The LANDSAT station in the centre of the continent at Alice Springs is sited so that complete coverage of Australia and her surrounding oceans are possible from orbiting environmental satellites. In recent years Australia has also been following the global trend towards an increased awareness of the importance of the oceans in climate, meteorological and biological research as well as in our management of natural resources. This awareness is evident in the several oceanographic satellites planned for the next decade. Hitherto, the only satellite dedicated to oceanography has been the ill-fated SEASAT that supplied data for three months in 1978. Australia's interest in these oceanographic "radar" satellites does not stop at the ocean boundaries. There are many institutions that are planning to use the microwave data to supplement the LANDSAT data for land use applications. Preliminary involvement in the SIR-A and SIR-B flights have given a useful guide to the use of such data over both land and sea. Airborne investigations using SLAR and other instruments are continuing. Participation in experiments such as TOGA and WOCE are also evidence of a strong involvement in international science programs.

Australia also recognizes the technical advantages of a country being involved in the planning and implementation of international space programs. To be a user only of satellite data means that the technological skills of the nation's industries will fall behind. Therefore there is a strong movement within Australia for both science and industry to become involved in all aspects of remote sensing from space. The country is now a major contributor to the ATSR project and part of this instrument is being manufactured in Australia. Also, the government has recently confirmed plans for the development of an X-band tracking receiving station at Alice Springs that will be capable of receiving SAR data from ERS-1.

The important link between space hardware and the use of satellite data is the calibration/validation of the satellite instruments. In this field there are several plans for such activities relating to ERS-1 in the Australian region. Given the strong involvement in the ATSR program it is logical that a major component of the calibration/validation activities should be related to this instrument. There are also a number of institutions that are keen to be involved in validation exercises related to the AMI on ERS-1. Details of these activities will be formulated as a response to the A.O. for ERS-1 but a general guide to our calibration/validation plans is presented in this paper. Australia recognizes the importance of her geographical isolation in the southern hemisphere and her scientists anticipate participation in global experiments relating to ERS-1. Australia also has active continually-manned bases in Antarctica and appreciates the potential value of ERS-1 data in polar regions.

2. SAVE

A Satellite Validation Experiment (SAVE) is planned for 1990 in the tropical waters off the north-east coast of Australia (See Figure 1). The experiment will last for two months and will commence soon after the launch of ERS-1. A major component of this experiment will be the validation of the sea surface temperature (SST) products from the ATSR instrument. Such an experiment needs to be performed in tropical waters because it is in these areas where SST measurement from satellites is most difficult. Also, it is in these areas where changes in SST are climatically most important.

For the following reasons the SAVE area will extend from 30°S to north of the equator and from 140°E to 170°E:

(a) The Australian north-east coast is an ideal area for the experiment. There is good coverage by satellite ground stations, logistical support is available from the many ports along the Queensland coast and there are advantages of operating in the waters of a single, developed country. Australia can also offer the support of a modern well equipped weather service.

(b) Surface temperatures near 30°C will be included in the area.

(c) The following recommendation from the COSPAR International Workshop on Satellite-Derived Sea Surface Temperatures for Global Climate Applications will be satisfied; viz "It is recommended that a program for regional validation of satellite derived SST be initiated. The large area of high SST over the Indian Ocean to the western equatorial Pacific should be given the highest priority for regional validation."

(d) The SST in this area is emerging as one of the most important parameters in the development of the El Nino phenomenon. SAVE will thus supply an important data set in this hitherto data sparse region.

(e) CSIRO Division of Oceanography and other Australian institutions are developing important oceanographic programs in this area.

Several ships and aircraft are planned for SAVE and work on the design of a multichannel precision infrared radiometer for the supply of accurate ground truth data has commenced. There is already considerable scientific interest and activity in the Great Barrier Reef and several towers and platforms are available for SAVE.

The SAVE experiment will also include the validation of other ERS-1 sensors. Some of these plans are detailed later in this paper. The aims of SAVE are:

(a) To provide intensive accurate ground truth measurements for validation of the ATSR instrument on the ERS-1 satellite.

(b) To evaluate the accuracy and need for surface based SST measurements.

(c) To provide oceanographic ground truth data for validation of the other products from the ERS-1 satellite.

(d) To compare the products from, and performance of different satellites e.g. ERS-1, NOAA, GMS, N-ROSS.

(e) To improve satellite SST determination in the presence of clouds.

(f) To study air-sea interaction processes (including the skin effect) with particular reference to satellite measurements.

(g) Evaluation of satellite data for net radiation studies in the tropics.

(h) To study the effect of maritime aerosols on satellite measurements.

(i) Others - that may be specified by co-investigators.

Given the large investment planned for SAVE a strong scientific program is becoming incorporated into the experiment. This relates to studies of the heat budget of the surface layers of the tropical oceans. Further scientific programs will no doubt emerge as planning continues.

The UK ATSR team are also planning a validation experiment in the North Atlantic but will be supporting SAVE as the <u>tropical</u> validation experiment. The involvement of other countries in this Australian experiment will be most welcome.

3. HF RADARS FOR WIND/WAVE MEASUREMENTS

There are two Australian groups that operate HF radars for observing sea state: one uses a ground-wave system for near coastal measurements (COSRAD) while the other uses a sky-wave via the ionosphere (JINDALEE). The measurements from both these radars are ideal for comparison with the ERS-1 derived product as they all give an average measurement over a large surface area and not a spot measurement.

3.1 COSRAD

The Coastal Ocean Surface Radar (COSRAD) is operated by James Cook University at Townsville, Queensland and is described by Heron et al (Ref. 1).

COSRAD is a portable HF ground-wave terrestrially-based radar designed to observe ocean surface parameters in the coastal zone. The observations are made within 30 km of the shoreline on a spatial resolution of about 1.5 km and a time resolution of the order of 30 minutes. The radar uses a wide-aperture beam-forming array and the beam can be steered over a coastal area. The HF radar uses backscatter processes and consequent Doppler shifts to observe ocean surface parameters. The primary response is a resonant back-scatter from sea-waves of $2k_0$ where k_0 is the radar wavenumber. Secondary responses, from double-scatter processes allow rms wave height to be estimated. During ERS-1 truthing it is proposed that two coastal radars be deployed in North Queensland, within the waters of the Great Barrier Reef. The deployment will be made to optimise the determination of the directional pattern of the λ = 5m sea-waves and the rms waveheights. If we assume that the wave directional polar pattern is constant over an area of water then pointing the beam successively in different directions gives the required polar pattern. By using two stations with overlapping sweeps the area of water under study is effectively halved. The average rms waveheight is derived from each station independently of the other. Supporting observations of sea-surface wind, and temperatures of the air and sea will be made from a buoy moored in the study area.

COSRAD will be operated throughout the SAVE experiment but will also be involved in a longer term comparison between satellite and ground based data. The radar can measure wind velocity with accuracies of $\pm$ 3m sec^{-1} and $\pm$ 10°, wave height to $\pm$0.15m and $\pm$current to 0.02m sec^{-1}.

3.2 JINDALEE

The JINDALEE skywave radar has been developed by The Defence Research Centre, Salisbury, South Australia and is located near Alice Springs some 1300 km from Australia's north coast. The radar is linked to the Australian Bureau of Meteorology regional forecasting centres by a facsimile transmission network. Wind maps surveying over one million square kilometers of ocean can be produced automatically in real time at the radar facility and transmitted directly to forecasters, (see Figure 2). This capability, which became operational in January 1985, is supported by active research programs directed at improving the scope and accuracy of the measurements as well as investigating a variety of meteorological and oceanographic phenomena. Currently only wind direction is supplied with an accuracy of $\pm$12° but future measurements of wind speed and wave height are planned.

The area sampled by JINDALEE is outside that planned for SAVE, but a long term program for comparing ERS-1 data with that from this radar and other in situ measurements are planned. Calibration targets are planned for deployment in this area and these will be viewed by both ERS-1 and JINDALEE.

A comparison between data collected by SIR-B in October 1984 and JINDALEE is currently in progress. Further information on the JINDALEE system is given in Reference 2.

4. ALTIMETER CALIBRATION

Altimeter calibration in the southern hemisphere is recognized as being an essential component of studies relating to geodesy, oceanography and precise orbit determination. Australia is thus considering an altimeter calibration program to be incorporated into SAVE and other validation experiments. Most of the essential oceanographic components for altimeter calibration are already incorporated into SAVE. A mobile laser tracking station and a network of GPS receivers are being planned for 1990. Several institutions are already planning for use of altimeter data in oceanographic and Antarctic studies. The University of New South Wales is involved with a German company in planning for use of ERS-1 data in geodetic research.

5. PHYSICAL OCEANOGRAPHY

Many Australian institutions are interested in physical oceanography processes in our surrounding oceans. There are many tide gauges, current meters, wave-rider buoys and other oceanographic instrumentation around the continental shelf. In the past study areas have included the Great Barrier Reef, the Leeuwin and East Australian currents, the Tasman Sea and Bass Strait.

A large experiment is planned over the next decade aimed at modelling changes in the SST of the tropical waters north of Australia. This experiment will be part of the international TOGA effort. Some ships of opportunity have already been carefully instrumented to provide surface data on the Australia-Japan shipping lanes and more such vessels are planned. This experiment hopes to have access to ERS-1 data for surface currents, winds and SST.

Many other experiments are planned that relate to measurement and modelling of wind-wave spectra at various locations including Bass Strait, West Tasmanian waters and the *Tasman Sea*. ERS-1 data including SAR imagery will assist in these studies.

6. GENERAL ERS-1 PLANS

6.1 ERS-1 data

A survey of Australian institutions in early 1985 revealed a large diverse interest in the use of ERS-1 data.

More recently these interests have been channelled into four major areas that will form the basis of Australian responses to the ERS-1 A.O. These areas are:

(a) Calibration and validation as described in Section 2 (SAVE).

(b) Physical oceanography which will include some validation as well as the general use of data from all ERS-1 instruments.

(c) Land surface applications which will incorporate some calibration of the AMI over land surfaces using calibrated corner reflectors.

(d) Antarctic studies which include the possibility of installing a ground station in polar regions as described below.

Outside the responses to the A.O. there is a general interest in using ERS-1 data for a multitude of purposes ranging from meteorology and oceanography to agriculture and mining.

6.2 Ground segment plans

An X-band tracking antenna is planned to be sited at Alice Springs in the centre of the continent. This facility will be capable of receiving both the high bit rate (SAR) data and the low bit rate data from the ERS-1 satellite and will give coverage well beyond the coastline in all directions (see Figure 1).

The upgrade of AVHRR receiving stations to receive the LBR data from ERS-1 is being considered. Plans will probably be included in the responses to the ERS-1 A.O.

A recent study (Ref. 3) has investigated the feasibility of installing an X-band HBR data reception facility in Australian Antarctic Territory.

7. CONCLUDING REMARKS

The calibration and validation of the ERS-1 data products in the southern hemisphere is an important component of the ERS-1 scientific program. By virtue of her geographic location Australia is well sited to make a valuable contribution to this sophisticated remote sensing system. Plans for various calibration/validation exercises have been presented here and already there is some co-operation with European countries. Hopefully, by ERS-1 launch, the Australian plans for ERS-1 validation may be well integrated into those from Europe.

8. REFERENCES

1. Heron M L et al 1985, Parameters of the air-sea interface by high frequency ground-wave Doppler radar, **Aust. J. Mar. Freshw. Res.**, 36, 655-670.

2. Anderson S J 1986, Remote sensing with JINDALEE skywave radar, **IEEE J. Oceanic Eng.**, OE-11, No. 2.

3. CSIRO Office of Space Science and Applications (COSSA) 1986, Reception of remote sensing satellites in Australian Antarctic Territory - A technical feasibility study, **COSSA Publication 004A, ISBN 0643 038450**, 48pp.

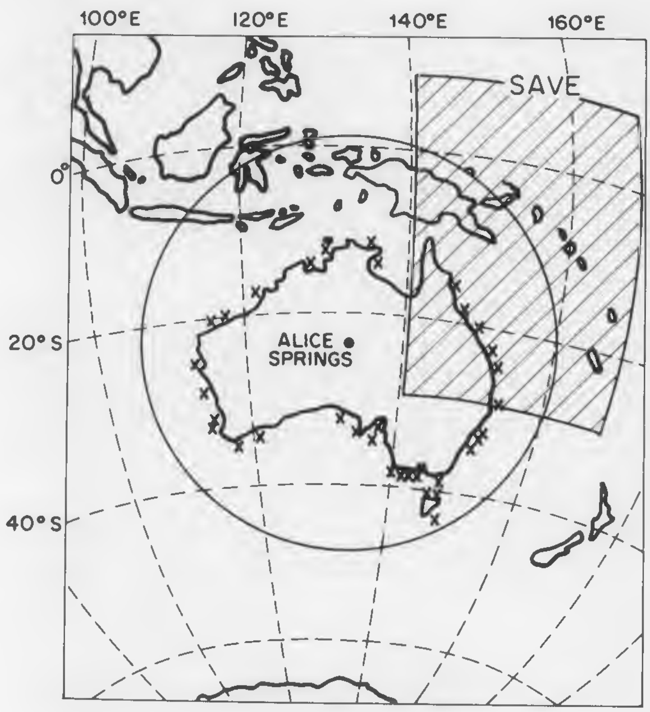

Figure 1 The Australian region showing the SAVE area, the coverage of the LANDSAT station of Alice Springs, and the location of tide gauges around the Australian coastline.

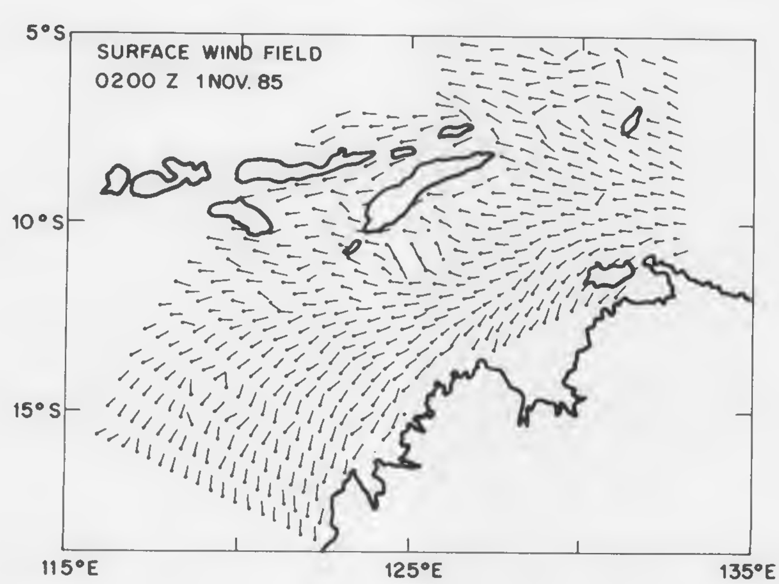

Figure 2 A typical wind field as measured by the JINDALEE radar.

AN OVERVIEW OF THE IMPLEMENTATION OF THE WORLD CLIMATE RESEARCH PROGRAMME

T Kaneshige

Joint Planning Staff for the WCRP, Geneva, Switzerland

ABSTRACT

The World Climate Research Programme was established in 1980 with the overall goal of understanding climate variability and its causes, whether from natural or human origin. The research strategy has been formulated in terms of three specific objectives or streams. Each objective is a stepping stone for the next, which encompasses a wider range of interactions between the atmosphere, ocean, ice and land surface, and calls for a more refined treatment of energy sources and sinks. This paper briefly reviews the activities which need to be implemented to attain the objectives of the WCRP.

1. BACKGROUND

The World Climate Research Programme (WCRP) is a joint undertaking of the International Council of Scientific Unions (ICSU) and the World Meteorological Organization (WMO) (Ref. 1). The programme was formally established by an agreement between the two organizations, which came into force in January 1980. The overall goal of the WCRP is the understanding of climate variability and its causes, whether from natural or human origin.

WMO and ICSU also agreed to call upon other national and international organizations to collaborate in the implementation of the Programme. Recognizing the importance of oceanographic research, WMO and ICSU called upon the Unesco Intergovernmental Oceanographic Commission (IOC) to co-ordinate oceanographic activities in support of WCRP. The Committee on Climatic Changes and the Ocean (CCCO) was established jointly by ICSU's Scientific Committee on Oceanic Research and the IOC. CCCO has been charged with planning the oceanographic component of the WCRP, as well as establishing the requirements for an ocean observing system.

2. OBJECTIVES OF THE WCRP

The major objectives of WCRP are to determine:

- to what extent climate can be predicted, and
- the extent of man's influence on climate.

The research strategy of WCRP has been formulated in terms of three specific objectives or streams:

- Stream 1: Establishing the physical basis of long-range weather prediction.
- Stream 2: Understanding the predictable aspects of global climate variations over periods of several months to several years.
- Stream 3: Assessing the response of climate to natural or man-made influences over periods of several decades.

These objectives constitute a natural progression for the implementation of the WCRP. Each objective is a stepping stone for the next, which encompasses a wider range of interactions between the atmosphere, ocean, ice and land surfaces, and calls for a more refined treatment of energy sources and sinks. The progression of scientific objectives is, to some extent, reflected in the implementation schedule. Most activities in support of the first stream are in their final planning stages or are already underway, while activities in the second stream, and especially the third stream, may only be in their early definition phase.

2.1 First Stream

The growing capability of global weather forecasting, which is a result of the successful Global Atmospheric Research Programme, has brought the knowledge of atmospheric dynamics to the point where the response of the global atmosphere to various forcing influences can be simulated. It has been shown that the evolution of atmospheric flow is unstable and therefore unpredictable, in a deterministic sense, beyond a certain time range on the order of one to two weeks for meteorological disturbances which affect weather on the regional scale. However, meteorologists have recognized the existence of relatively persistent weather patterns which may be the result of various combinations of specific surface boundary conditions. These findings offer promises for statistical weather prediction extending well beyond the range of meteorological forecasting. Significant advances in the representation of energy sources and sinks in the atmosphere are still needed, however, if atmospheric general circulation models are to provide unambiguous information on long-range weather as well as long-term climate changes.

2.2 Second Stream

The link between the oceanic circulation and the year-to-year changes of the mean weather, including in some instances catastrophic events such as observed during the 1982-83 El Niño episode, has become increasingly clear. It is believed that the dynamic behaviour of the interactive system constituted by the tropical ocean and the global atmosphere holds the key to understanding and predicting a significant fraction of the year-to-year climate variability, especially in the tropical zone. The objectives of the Tropical Ocean and Global Atmosphere (TOGA) Programme are to determine the time-dependent behaviour of the tropical ocean and the overlying atmosphere, as well as to develop coupled ocean-atmosphere models which can be applied to scientific investigations and climate predictions. Together with the activities planned for Stream 1, those planned for TOGA and coupled ocean-atmosphere boundary layer research constitute the basis for achieving the second objective of the WCRP.

2.3 Third Stream

The increasingly precise information about the rate and range of past climate variations gives rise to the concern that similar changes could be caused in the future by man's influence on the environment. Evidence points to the fact that a slow and relatively minor variation of the solar energy input to the earth's atmosphere could cause relatively fast and large climatic changes. The same conclusions could apply to man-made modifications of the environment, such as the potential climate impact of the well-documented rise of the concentration of carbon dioxide and other radiatively active gases which is expected to significantly increase the blanketing effect of the earth's atmosphere during the next century. No assessment of the long-term sensitivity of climate to external influences can be made reliably without taking into account the response of the global ocean circulation as an interactive component of the climate system. The World Ocean Circulation Experiment (WOCE) will be the first attempt to consider the global pattern of ocean currents and describe the world ocean as a continuous fluid system interacting with the atmosphere.

Research on cryospheric processes is, at present, focussed on modelling the large-scale, air-sea-ice interactions which determine the changes in the extent and thickness of sea ice in response to changes in atmospheric and oceanic forcings. Climate sensitivity assessment studies are focussed on the detection of climate trends and the understanding of their relationship to changes of external forcing factors or environmental parameters. These research programmes, together with WOCE and activities planned in the first and second streams, constitute a comprehensive scientific strategy for achieving the objectives of the third stream of the WCRP.

3. IMPLEMENTATION OF THE WCRP

After several years of in-depth scientific discussions about the Programme, conceptual planning reached the stage where consultations could be taken, at the inter-governmental level, on the implementation of the WCRP. The First Implementation Plan for the WCRP was published in late 1985 (Ref. 2) to provide an overall view of the ensemble of observational projects, data processing and analysis tasks, and numerical modelling activities, which are considered to be essential components of the Programme and which could be specified in sufficient detail at this time. The following sub-sections briefly describe the activities which need to be implemented.

3.1 Meteorological Observing Systems

The highest priority requirement for WCRP is for consistent, long time series of global data describing the components of the climate system and extending over many years. For atmospheric data, WCRP must rely on the operational World Weather Watch (WWW) System. In particular, the continuity in operation of the basic system of two polar orbiting and five geostationary meteorological satellites is fundamental to providing the spatially complete observations of the global atmosphere needed by the WCRP.

In general, WCRP would benefit directly from any advances made in the performance of the WWW and in some cases, depends critically upon specific improvements such as additional upper-air wind soundings and surface observations, and improved satellite instruments and information retrieval algorithms. The following specific augmentations are required:

3.1.1 Upgrade the density of wind observations in the tropics (to allow the determination of both the rotational and divergent components of the horizontal flow).

3.1.2 Upgrade the network of upper air wind observing stations in the tropics and improve their operational performances (to resolve the three-dimensional structure of planetary-scale, wave-like disturbances, which account for most of the perturbation energy of the large-scale tropical atmospheric circulation).

3.1.3 Improve significantly the coverage and timely availability of Voluntary Observation Ships (VOS) measurements, and upgrade the quality of information from a subset of the VOS fleet (to provide better coverage in the tropics and southern hemisphere, and more accurate measurements for use in the calibration and validation of satellite estimates).

3.1.4 Improve the coverage of sea level pressure information over the southern hemisphere with satellite-tracked meteorological drifting buoys (to provide input for reconstructing the three-dimensional structure of the atmospheric circulation).

3.2 Oceanic Observing Systems

Ocean processes play an essential role on the time scales considered by the WCRP. For this reason, WCRP incorporates two major projects (TOGA and WOCE) aimed at understanding and modelling ocean dynamics and thermodynamics. Although these projects rely on the extensive use of remote observations of the ocean surface by existing meteorological satellites and a new generation of experimental oceanographic satellites, in situ oceanographic observations are also needed. Requirements for these observations are described below.

3.2.1 Monitor and expand the existing island and coastal tide gauge network in the framework of the IOC Global Sea Level Observing System (to determine relatively fast changes in the tropical ocean surface topography which reflect much larger changes of the depth of the tropical thermocline and corresponding variations of ocean heat content, and to study the dynamics of ocean gyres and smaller-scale eddies).

3.2.2 Upgrade the network of systematic and repeated expendable bathythermograph (XBT) launchings from merchant vessels and other ships of opportunity (to map the time-dependent thermal structure of the upper tropical oceans and understand the evolution of heat content anomalies, and to better determine the rates of formation and ventilation of water masses that influence the climate system with time constants of several years to several centuries).

3.2.3 Acquire high quality profiles of temperature, salinity and chemical concentrations extending from top to bottom of the ocean, and spaced at intervals close enough to resolve eddies along sections crossing ocean basins from continent to continent (to assess the large-scale variability on annual and interannual time scales).

3.2.4 Design and develop a system of surface drifters in support of TOGA and deep ocean drifters for WOCE (surface drifters are a unique source of direct near-surface current velocity information for validation of model diagnostics, and deep ocean drifters permit the exploration of large-scale circulation around gyres and the statistics of transient eddies).

3.2.5 Continue support of present current meter mooring programmes, with priority given to TOGA and WOCE during 1985-1995 (to provide information on vertical structure of the velocity field).

3.3 Experimental Satellite Systems

The development of oceanographic observation satellites from space has been slower than for meteorological satellites because the electromagnetic signals received by satellite sensors carry only the signature of oceanic phenomena which can be detected at the ocean surface, or within the upper 10-30 meters for imaging radiometers. Nevertheless, the SEASAT mission in 1978 demonstrated the capability of satellite systems to provide systematic global observations of variables needed in determining the large-scale circulation of the ocean. The implementation of an oceanographic satellite system incorporating these technical advances would make it possible to undertake, for the first time in the history of oceanography, the synoptic description of large-scale ocean circulation phenomena and to envisage the world ocean as a single fluid dynamical system on the planetary scale.

The development and successful operation of these satellite systems is a prerequisite for launching WOCE and would greatly enhance the oceanic observation network of TOGA. However, space observations must be complemented by a wide variety of simultaneous or nearly simultaneous in situ measurements. The following missions are required.

3.3.1 Ocean surface topography missions (TOPEX/POSEIDON, ERS-1, MOS-2).

3.3.2 Wind stress scatterometer missions (NROSS, ERS-1, MOS-2).

3.3.3 Imaging microwave radiometer missions (USA, MOS-2).

3.3.4 Along Track Scanning Radiometer (ERS-1).

3.4 WCRP Data Projects

Progress in understanding climate mechanisms and assessing climatic impacts requires consistent and, if possible, complete global fields of significant climate quantities during appropriate periods of time. Such global descriptions of climate variables will generally be inferred from several kinds of primary data obtained from different sources. Since the step from basic observations to the production of a homogeneous global field constitutes a major data processing task, specific WCRP data projects need to be organized.

The WCRP data projects are essential scientific activities which must, normally, be performed by operational services or agencies. It is important to recognize this dual aspect, experimental in purpose and operational with respect to implementation. The following data projects have been specified for the WCRP.

3.4.1 International Satellite Cloud Climatology Project (ISCCP) (to collect and analyse satellite observed radiances to infer the global distribution of the radiative properties of clouds, as needed to improve the modelling of cloud effects on climate).

3.4.2 Radiation Budget Climatology Project (to establish a long-term data set describing the spatial (regional and global) and temporal (monthly) statistics of the components of the earth's radiation budget at the top of the atmosphere and at the surface).

3.4.3 Global Sea Surface Temperature (SST) Data Project (to provide a global description of the time-dependent SST field).

3.4.4 Tropical Wind Data Project (to provide a more comprehensive collection of existing wind observations in a delayed mode).

3.4.5 TOGA Marine Climatology Data Project (to accelerate the availability of marine climatology data to meet TOGA objectives).

3.4.6 Global Precipitation Climatology Project (to acquire a global description of area/time-averaged precipitation).

3.4.7 Continental Water Runoff Data Project (to provide information for closing the ground water budget over continental areas).

3.4.8 TOGA Tropical Sea Level Data Project (to collect and analyse sea level data available in near-real time, producing synoptic maps and indices of sea level anomalies on ocean basin scales, and distribute them in a timely fashion to TOGA users for rapid assessments of impending climate developments and for research planning purposes).

3.4.9 TOGA Tropical Ocean Sub-surface Data Project (to collect and quality control available XBT data from the tropical ocean networks and other temperature and salinity measurements, on a faster time scale than would be available via IODE).

3.4.10 Level III Data Project (to produce and make available averaged global fields of the basic meteorological variables and other relevant physical quantities for the duration of TOGA, 1985-1995).

3.4.11 International Satellite Land Surface Climatology Project (ISLSCP)/Global Land Surface Data Project (to acquire global fields of observable land surface variables inferred from satellite measurements).

3.5 Global Environmental Monitoring

One goal of WCRP is the early detection of possible climate change and assessment of causal links with relevant environmental factors which may influence climate. The observational programmes already implemented in the WWW or being planned as special WCRP projects will provide time series of the most useful indicators of atmospheric climate trends. Closely associated with the detection of such trends is the requirement to monitor the terrestrial and extraterrestrial factors to which climate is potentially sensitive. The following factors have been identified in the first implementation plan.

3.5.1 Atmospheric carbon dioxide (the projected increase over the next century is expected to cause a significant enhancement of the atmospheric greenhouse effect and an associated warming of the earth's surface).

3.5.2 Stratospheric and tropospheric aerosols (aerosols can affect climate through absorption and scattering of solar and long wave radiation and/or through modifying cloud optical properties).

3.5.3 Solar radiation flux (changes in solar luminosity could affect the earth's climate).

3.6 Process Studies

WCRP requires detailed investigations of several thermodynamic (or diabatic) processes, which control the energy sources and sinks in the climate system. Detailed observational field studies or experiments, involving intensive observations over a limited time interval and limited area, will be necessary to elucidate the mechanisms which are effective on climatologically significant scales and to provide an observational basis for their parameterization. These regional process studies can most effectively be mounted by national or multinational groups. Nevertheless, international co-ordination mechanisms are necessary to ensure that planned initiatives provide optimal support to WCRP objectives, make optimal use of other planned WCRP activities, and provide information which can be used by the international climate research community.

3.6.1 Cloud radiation process studies (to provide for a more physical approach to the parameterization of clouds, based on detailed case-by-case comparisons of computed cloud fields with comprehensive in situ observations; e.g. USA/First ISCCP Regional Experiment; Japan/Western North Pacific Cloud-Radiation Experiment).

3.6.2 Land surface process studies (to provide for the validation of parametric formulations of land surface processes against detailed field measurements of the physical quantities needed to estimate area-averaged surface fluxes of heat, moisture and radiation, area-averaged water runoff ground storage as well as significant meteorological parameters on a scale comparable to the resolution of climate models; Hydrological and Atmospheric Pilot Experiments: HAPEX-1 in France, HAPEX-2 in USA).

4. INFORMAL PLANNING MEETING ON THE WCRP

The first Informal Planning Meeting on the WCRP was held in Geneva, Switzerland from 12-16 May 1986 to review the national climate research plans of countries wishing to participate in the implementation of various aspects of the Programme. Delegates from 25 countries and 4 multinational organizations participated in the meeting. In general, there has been a willingness among scientists, individually and collectively, to contribute towards the planning and implementation of various components of the WCRP. The meeting showed that there is also a corresponding willingness among governments of Member countries of WMO and IOC to support the implementation. A summary of the present state of contributions is being prepared for submission to the thirty-eighth session of the WMO Executive Council (2-13 June 1986).

5. REFERENCES

1. WMO 1984, Scientific Plan for the World Climate Research Programme, WCRP Publication Series, No. 2, Geneva.

2. WMO 1985, First Implementation Plan for the World Climate Research Programme, WCRP Publication Series, No. 5, Geneva.

WAVE MODELLING ACTIVITIES OF THE WAM GROUP RELEVANT TO ERS-1

K Hasselmann

Max-Planck-Institut für Meteorologie, Hamburg, FRG

ABSTRACT

An improved third generation wave model has been developed and successfully tested in various hindcast studies by the WAM (WAve Modelling) Group in both global and regional, deep and shallow water versions. The model will be applied to assimilate wind and wave data from ERS-1. For this purpose the model will be embedded in a comprehensive data assimilation system based on a global atmospheric circulation model together with the WAM wave model. The availability of such an operational system already at the time of the ERS-1 commissioning phase would greatly assist the calibration and validation of the ERS-1 wind and wave sensors.

Keywords: Satellite Wave Data, Ocean Waves, Wave Models, Data Assimilation

1. INTRODUCTION

The availability of global wind and wave data through the launch of ERS-1 and other oceanographic satellites in the nineties opens entirely new perspectives to wave modellers. It also poses major new challenges. One of the principal motivations for the formation of the WAM (WAve Modelling) group in 1982 was to respond to these challenges (Ref. 1). The major goals of the WAM programme with respect to ERS-1 may be defined as:

(1) The development of an improved operational 3rd generation wave model that can make effective use of the satellite data for both global and regional applications.

(2) The incorporation of wave data assimilation methods in operational wave forecasting.

(3) The embedding of wave models and wave data assimilation schemes in a more comprehensive wind and wave data assimilation system which will be able to process all available wind and wave data from both conventional observing systems and oceanographic satellites in a joint operation.

(4) The testing and application of these techniques to assist in the validation of ERS-1 wind and wave instruments during the commissioning phase of the satellite.

Although only the fourth point of this list is directly related to the main subject of the present workshop, it will be shown below that the goals (1) - (3) will already need to have been achieved in order to be able to effectively carry out the last task.

The need for sophisticated models and data assimilation techniques for an optimal instrument calibration and verification exercise follows on the one hand from the incomplete nature of both conventional and satellite wave data (quantitative measurements of the complete two-dimensional wave spectrum cannot yet be obtained by any standard measurement technique) and on the other hand from the coupling of wind and wave signatures in the satellite microwave sensor signals.

2. THE DEVELOPMENT OF A THIRD GENERATION WAVE MODEL

A detailed investigation of nine operational first and second generation wave models in the Sea Wave Modelling Project (Ref. 2) revealed that current wave models of both types suffer from basic deficiencies. First generation models, developed during the sixties and early seventies, are based on physics of wind-wave growth which we know today to be incorrect. It is in principle impossible to tune models of this type to yield correct predictions for all forms of generating wind fields. Second generation models, although based on our present, revised physical picture of wave growth (characterized by an order of magnitude reduction of the wind input and a corresponding enhancement of the nonlinear transfer) suffer from basic limitations in the parameterization of the nonlinear transfer and the representation of the spectrum. This prohibits reliable computations, for example, of the evolution of complex windseas in rapidly changing wind fields or of the transition of a windsea into swell as the waves propagate out of a generation region.

Methods of overcoming these shortcomings were indicated already in the SWAMP study and have since been realized in the third generation wave model developed by the WAM group (Ref. 3). The WAM model is available in both global and regional versions and has been extensively tested in hindcast studies of six Eastern Atlantic storms and three Gulf of Mexico hurricane cases. Third generation wave models may be defined as models which compute the full two-dimensional wave spectrum by integrating the basic spectral transport equation for a prescribed form of the source functions without any prior side conditions on the form of the resultant spectrum. Thus the models can be integrated for arbitrary wind fields, yielding arbitrarily complex wave spectra. The transition between windseas and swell is modelled as a continuous process without changes in the formulation of the basic physical processes controlling the transition.

Although the present WAM third generation model overcomes the basic shortcomings of first and second generation models and has been shown to be able to successfully simulate complex windsea and swell spectra for highly variable wind fields, more extensive applications of the model will presumably reveal deficiencies also in this model. However, the principal advance of the third generation model, namely the formulation of the model alone in terms of the transport equation, without any prior restrictions on the spectral shape, will make it possible to introduce future improvements of the model at the proper level. This is at the source functions, which describe the physical processes controlling the spectral energy balance, rather than in the form of the spectrum obtained by integrating the transport equation.

3. ASSIMILATION OF WAVE DATA INTO WAVE MODELS

Very little experience exists yet in the assimilation of wave data into wave models. Current wave models are routinely run using only the driving wind fields as input, without subsequent correction of the model wave prediction or hindcast with the aid of independent wave observations. The problem of wave data assimilation differs in several important aspects from standard atmospheric data assimilation methods for atmospheric models (Ref. 4).

(1) Wave data assimilation may be expected to significantly improve wave model prediction, but is not essential for the operation of wave models. Wave prediction is not primarily an initial value problem. As the wave field is continuously being generated by the prescribed wind field, the wave prediction skill is maintained after the initial wave field information has lost its impact on the evolving wave field.

(2) The region of influence of a wave measurement is strongly dependent on the wave field itself. Swell from a distant storm, for example, will generally have a significantly larger spatial correlation scale than a locally generated windsea.

(3) The correction of a predicted model wave field on the basis of wave measurements will in many cases require a simultaneous modification of the generating wind field which produced the erroneous wave field. Otherwise the uncorrected wind field will regenerate an erroneous wave field.

(4) Wave measurements by both conventional techniques (wave buoys, wave staffs, wave pressure measurements, visual estimates, etc.) and remote sensing techniques (altimeter wave heights, SAR image spectra) are invariably incomplete. One therefore requires additional information from a wave model prediction to reconstruct the best guess two-dimensional wave spectrum required as model input. In the case of SAR image spectra, information on the local wind is also needed in order to determine the modulation transfer function which enters in the relation between the SAR image spectrum and the wave spectrum.

The impact of these features on wave data assimilation is discussed more fully in Ref. 4. Here we note only that the coupling between wind and wave data mentioned in (3) and (4) above imply that wind and wave data assimilation need to be carried out jointly within the framework of a comprehensive data assimilation system including both types of data.

4. COMPREHENSIVE WIND AND WAVE DATA ASSIMILATION SYSTEMS

The requirement for a joint data assimilation system for wind and wave data follows not only from the interdependence of the information from both types of data in the assimilation cycle, but also from the cross coupling of these data in the satellite sensor signals. One of the motivations for designing the principal microwave instrument AMI of ERS-1 with a common C-band for both the scatterometer and the SAR was to obtain simultaneous mean backscatter and backscatter modulation data at the same microwave wavelength. It was anticipated that this would aid in the separation of the wind and wave influences in the signals of these two instruments. To develop improved sensor algorithms which take these effects into account, first guess wind and wave fields from models are required. It follows that the assimilation schemes will need to include the satellite data already at the level (Ib) of calibrated physical sensor data, rather than at the higher level (II) of retrieved geophysical data. The structure of such a general data assimilation system, and its relation to other processing centres planned for ERS-1, is discussed in Ref. 5.

5. APPLICATION TO ERS-1 WIND AND WAVE DATA CALIBRATION AND SENSOR VALIDATION

During the commissioning phase of ERS-1, wind and wave data derived from ERS-1 sensors will be compared with in situ data obtained by conventional measurement techniques during specific experimental campaigns or from continuously operating measurement stations. As discussed above, a simple one-to-one comparison between satellite sensor data and conventional measurements is not possible, as the remote sensing and in situ instruments measure different quantities. A relation between the two types of measurement can be established only with the aid of algorithms which, for optimal application, require first guess fields derived from models. Thus a reliable assessment of the optimal satellite instrument performance can be carried out only in the context of a fully operational wind and wave data assimilation system in which all available data are brought together and tested with respect to their mutual consistency with the aid of dynamical wind and wave models.

6. REFERENCES

1. Komen G J 1985, Activities of the WAM (Wave Modelling) Group, in *Advances in Underwater Technology. Ocean Science and Offshore Engineering,* Vol. 6 Oceanology, 121 - 127, Graham and Trotman Ltd.

2. The SWAMP Group 1985, Sea Wave Modelling Project (SWAMP). An intercomparison study of wind wave prediction models, Part 1: Principal results and conclusions, *Ocean Wave Modeling,* Plenum, 256 pp.

3. Hasselmann S, Hasselmann K, Janssen P A E M, Komen G J, Bertotti L, Guillaume A, Cardone V J, Greenwood A, Reistad M & Ewing J A, The WAM model, a third generation ocean wave prediction model (in preparation).

4. Hasselmann K (editor) 1986, Report of workshop on assimilation of satellite wind and wave data in numerical weather and wave prediction models, *WCP Report,* WMO, Geneva (in press).

5. Hasselmann K 1985, Assimilation of microwave data in atmospheric and wave models, *Proceedings of a Conference on the Use of Satellite Data in Climate Models,* Alpbach, Austria, 10-12 June, 1985 (ESA SP-244, Sept. 1985).

MARINE CLIMATE PROGRAM

J J Conde, J E Luis & A Maron

Dirección General de Puertos y Costas
Ministerio de Obras Públicas y Urbanismo
Madrid. España

ABSTRACT

The present and future activities of the Spanish "Programa de Clima Maritimo" are described. Special emphasis is put on those points which can be more or less directly related to ESTEC projects. These activities are separated into three main areas: prevision area, wave data analysis and wave data base.

Keywords: Marine Climate, Wave Prevision, Wave Analysis, Buoy Data, Data Base, Directional Spectra, Wave Groups.

1. INTRODUCTION

The "Marine Climate Program" began working by mid 1983. In addition to the works on wave forecasting and analysis of wave time series, which are described in paragraphs 2 and 3, the Program is also working in the field of flow propagation and is creating a Wave Data Base.

In the field of flow propagation, a finite element model for wave refraction-diffraction, based on Berkhoff equations and a finite difference model for wave propagation following the non lineal Boussinesq equations have been developed. The second model admits as input a time series and considers all the phenomena which participate in wave propagation up to the breaking zone. We are also implementing a three dimensional model for wind and tide induced currents, developed by Dr. J. Backaus from the Institut fur Meereskunde (Hamburg).

The Program has implemented the SIR Data Base Handling System and has developed a model for quality analysis of wave records. Wave information from on route ships collected by the Meteorological Office (Bracknell) has been incorporated to the Data Base and a model for its exploitation has been developed. Presently, models for the explotation of wave data from buoy records as well as wave and wind data from the hindcasting models are at developing stage.

Program activities up to the end of 1986 were mainly aimed to the creation of a numerical infrastucture and a data organization which will permit, on the next phase, a systematic application of them in order to define the structural conditions of Spanish Maritime Climate.

2. AREA OF PREVISION

We are mostly involved with wave hindcasting projects.

2.1 Configuration.

The models used, are the second generation ones, HYPA and its shallow water version HYPAS, for both scalar and vector processors. These are well known models, so there is no need to describe them.

These models have been developed by the GKSS Wave group, W. Rosenthal & H. Gunther. They implemented the models for us on May-July 1985, and have provided us with scientific formation for the model usage. At present, we are working on some related areas in close co-operation with them.

We have developed a North Atlantic Wave Hindcasting scheme with the following characteristics:

- 100 Km. grid size.
- 2546 grid nodes convering from parallel 20N, up to parallels 75 N, and from the Caribean Area to the European and African Coasts.
- 1 hour time steps.
- HYPA model using 20 frecuency bins and 24 direction bins for swell description, and 3 JONSWAP parameters plus directions for the windsea.

The Western Mediterranean Wave Hindcasting scheme has the following ones.

- Higher resolution, 25 km. grid size.
- 1392 nodes, covering the Western Mediterranean Area, from Italy to Gibraltar.
- 20 minutes time steps.
- HYPAS model using only 16 frequency bins, and the rest as above. All points with depth smaller than 200 meters have been included as shallow water points.

Both schemes can use any grid wind information. Cur rently, we are running them on winds calculated from grid pressure data, interpolated from the digitized synoptic surface pressure charts by the Spanish National Institute of Meteorology, and we will run them shortly on the ECWMF data.

2.2 Projects for short and medium terms.

For the next future, we plan to take the following projects, excluding from this list any possible cooperation that may result from this workshop:

We will keep operative the current hindcasting schemes, and we may try to develop new ones for forecasting purposes.

We plan to do 25 years hindcasting, for both the Atlantic and Mediterranean. The Mediterranean hindcasting, will be run using the same scheme, probably. The Atlantic hindcasting, will use a new scheme: a multigrid one, where the model application on a sparse grid will provide border conditions for a denser grid, with the same resolution, 25 km, as the Mediterranean model. This denser grid, will cover from the British Islands down to the Canary Islands; we have not fixed yet how much this denser grid will extend to the west. The source for these hindcasting input has not yet been fixed, although we may use data from different sources. These hindcasting will be run on a vector computer.

As members of the WAM group, we plan to participate actively on the model development.

2.3 Computational means for hindcasting use.

Our computational means, up to now, consists on a CDC Cyber 830 which is used for software developing purposes as well as for running short hindcastings; For this last purpose we have available up to 12 CPU hours every night. This is enough to do storm hindcasting, for example.

For mass productions runs, we plan to use external means: we will run shortly two 30 months experimental hindcastings on a vector CDC Cyber 205.

3 ANALYSIS OF WAVE RECORDS

One of the tasks of the Program is the analysis of wave records obtained from the net of buoys deployed along the coastal waters of Spain in order to get insight into the wave climate characteristics of Spanish shores. As one important result of such analysis, combined with the results obtained from the hindcasting model for the same areas, we hope to obtain a wave climate atlas of Spain.

The main part of this task is to create the computer tools needed for such analysis. Therefore we are developing a program library containing the routines that traditionally have been used on this field, including: short and long term statistics, FFT spectral analysis and extremal analysis.

The Program is not only aimed at rutinary analysis of wave records using conventional theories that have been widely tested in the past, but it also wants to apply new techniques and theories proposed recently and to investigate the results obtained. In this sense, programs for the analysis of wave groups and maximum entropy spectral estimation are being implemented.

Finally, although all the buoys actually available in Spanish shores are of scalar type, directional buoys of pitch and roll type will be deployed in the near future. Programs for the analysis of such kind of buoys are being developed based on both FFT and maximum entropy techniques. Moreover, it is our intention to take measurements of wave directional spectra from conventional radars on board ships.

In the following, a short description of each of the items previously referred to, is presented.

3.1 Short and long term statistical analysis of wave records.

Wave records are analysed by the zero up crossing method. The statistics of heights, amplitudes and periods are calculated, including marginal and conditional frequency distributions. Selected mathematical distributions can be fitted to the results by several procedures.

The outputs from this calculations corresponding to successive records give time series of sea state which are analysed by the long term statistical program. Long term distributions are calculated and plotted on many different types of probabilistic paper. Theoretical distributions are fitted to the results. An analysis of threshold exceedances can also be made.

3.2 Spectral analysis of wave records.

The spectra of wave records are obtained using FFT techniques. Smoothing of raw spectra can be performed with different spectral windows and arbitrary degrees of freedom. Spectral moments and characteristic parameters are obtained from the results. JONSWAP spectra can be fitted to the computed ones.

Programs have being developed for the estimation of autorregresive (AR) and autorregresive and moving average (ARMA) processes corresponding to given wave height time series. Several published procedures have been programmed on computer (Burg's method, Marple algorithm, Levinson's recurrence, etc.). The obtained AR and ARMA models are used for spectral estimation as well as simulation and prediction of time series. The efficiency and reliability of the different methods is being compared among then and with those of conventional FFT methods.

We hope that these new methods will be of great help in the knowledge of waves and the recovery of partially lost wave data.

3.3 Extremal analysis.

In connection with the long term statistical analysis of wave data, we are implementing programs for the extremal analysis of sea state time series. Programs for fitting extremal distributions to data by different methods and drawing them in probabilistic papers of different scales are being implemented.

The resulting theoretic distributions will be extrapolated to obtain return values for the variables involved.

3.4 Analysis of wave groups.

The group characteristics of waves are great interest both for design and for a better understanding of wave structure and formation.

We have written programs for analysis of groups in waves following the statistical theories of Goda and Kimura, the envelope theory and the SIWEH method by Funke and Mansard. We are going to apply these programs to real data obtained in different parts along spanish shores. This will give us the opportunity of checking different theories and to compare the results for deep and shallow waters. Another objective is to try to find differences, if they exist, between different points (i.e. Atlantic Ocean and Mediterranean Sea).

3.5 Analysis of directional buoys.

Programs for the cross spectral analysis of pitch and roll buoys by FFT method are available at the Program. The results of the cross spectral analysis are used to estimate the main characteristics of the wave directional spectrum following the theory by Longuet Higgings. Different theoretical directional distributions can be fitted to the result.

Presently, this program will be applied to data recorded by buoys deployed on the North Atlantic Ocean by foreign countries. The results will by used for the calibration of the HYPA model.

In the near future, directional buoys will be deployed in the spanish shores.

Similary to the scalar case, we have implemented programs for the cross spectral estimation using maximum entropy methods. The application of these theories to directional buoy data will be the next phase. A method, connected with the maximum entropy estimation, for better filtering out the effects of buoy resonances is being investigated.

3.6 Ship radar measurements of waves.

The program is interested in taking measurements of directional characteristics of waves from conventional radars mounted on board of ships. The method has been developed by F. Ziemer from GKSS, Germany. The present stage is the implementation on our computer facilities of the programs developed by GKSS.

4. BUOY NETWORK FOR THE SPANISH LITTORAL

4.1 Current Stage

Buoys are grouped as follows:

4.1.1. R.E.M.R.O. Sponsored and owned by the Ministry of Public Works and City Planning.
- Information gathered by 18 buoys. Starting from 1981 sampling 1024 points records until 1985; then changed to 2048 data point records.
- Depths range from 7,5 to 70 meters.
- Original tapes were inspected and 80% of the information was saved. Subsequently, records were uniformized.
-80% of this information has been processed and systematically quality controlled. Only 20 to 30% of it passed successfully the implemented tests; and another 20% was rejected.
-The remaining 50 to 60% of suspicious records are being visually inspected. Out of the 10% of records of this kind already checked, 60% of them were accepted.

4.1.2. Harbours. 10 buoys belonging to Local Harbour Authorities.
-Starting form 1975, records hold 1024 data points.
-Depths range from 10 to 52 meters.
-As in REMRO, records were previously uniformized. 90% of this information has been processed and systematically quality controlled. Test precentages are as those already mentioned.
-20% of suspicious records have already been visually inspected.

4.1.3. Special projects. 8 buoys relating 3 different projects.
-Data collected from 1978 to 1984.
-Depths range from 10 to 105 meters. The former corresponds to the 3 buoys deployed in the Gulf of Biscay.
-75% of all the information regarding the projects located in the Gulf of Biscay and Almeria has been accepted as good. Remaining records, 50% of the total, are waiting to be visually inspected.

All buoys are expected to be calibrated in a rotating arm rig, before the spring of 1987.

4.2. Future stage

On the first phase there will be a one year pilot campaign starting on the spring of 1987, that will deploy two ocean meteorological buoys in dephts over 250 meters, and up to 300 meters.

Signal will be radio transmitted; though at least storms will be recorded on board. Tracking of the buoy will be via satellite (possibly Argos System). Parameters observed by the buoy will be: directional ocean waves, wind, pressure and temperature.

On a second phase a national network will be defined, depending on the experience and results obtained on the first phase.

A SCATTEROMETRY RESEARCH PROGRAMME

I A Ward

Remote Sensing Group - MSDS Laboratory
MARCONI RESEARCH CENTRE
GEC RESEARCH LIMITED

ABSTRACT

A long term (6 years) research programme suitable for co-ordination at the national, or international level has been designed. The aim of the programme is to enhance the understanding and interpretation of SAR images of the sea-surface. The programme is primarily an experimental programme with supporting theoretical and SAR data-analysis programmes.

Keywords: Sea-imaging, scatterometry, SAR, research programme.

1. INTRODUCTION

Microwaves are scattered by small-scale (~cms to 10's of cms) roughness generated on the sea-surface by winds. Large scale variations in the sea-surface structure impose large-scale variations on the scattering efficiency of these small-scale waves. The temporal and spatial correlations of the backscattered microwave signal thus contain information about the large-scale temporal and spatial structure of the sea-surface.

In the case of a SAR, phase coherent detection of the return signal is employed. A coherent phase variation is superimposed on the return signal by the motion of the radar platform causing a steadily changing Doppler shift in the return signal from a stationary target as it passes through the beam.

Convolving the return signal with a matched filter that describes the phase variation (or Doppler frequency variation), with suitable weighting to account for the beam pattern, produces a high-resolution image. Simulation of a large antenna in this manner facilitates imaging of long-waves by the modulations they impose on the spatial distribution of the scatterers (small-scale gravity waves), and the modulations they impose on the motions of the scatterers (via the effect on their Doppler frequency shifts).

Improved understanding of SAR sea-surface imaging requires research into the fundamental scattering-mechanism, and its dependence on sea-state and incidence angle, and long-wave imaging theory and its implications for the imaging of a variety of sea-surface phenomena such as long wave spectra and amplitudes, ship wakes, oil-slicks, ice, internal waves and shallow water features.

The questions concerning fundamental scattering mechanisms address:

a) Bragg-scattering - what spatial property of the surface provides the Bragg-regions, what is the coherence time of a Bragg-region, what is its size?

b) Specular-reflection - this dominates at normal incidence but what is the range of incidence-angles over which specular contributions are significant, how does this range change in the presence of swell-waves and breaking waves?

c) Wedge-diffraction - this appears to dominate in ripple-tanks but it is unclear how wind-wave situations relate to the monochromatic situation, it also depends on the curvature of a wave-crest with respect to the radar wavelength, also near-range studies may not be applicable to airborne radars.

The key questions concerning imaging theory are:

d) Are speckle statistics Gaussian or non-Gaussian?

e) Why is there a bias to longer wavelengths in azimuthally travelling-waves?

f) Is it the orbital or phase-velocities of swell waves that is important?

g) Does velocity-bunching occur?

h) Is the degradation of azimuthal resolution reversible?

i) Can we extract information from nonlinear imaging situations?

j) Can imaging theory be developed to incorporate breaking-waves?

In order to resolve these problems a long term (6 years) research programme suitable for co-ordination at the national, or international level has been designed. The programme is primarily an experimental programme with supporting theoretical and SAR data-analysis programmes.

The experimental programme can be divided into two programme-packages, a microwave programme and an optical programme. The microwave programme has the main objective of determining the dominant scattering mechanism under different wind and wave conditions. To achieve this, the development of an airborne multi-frequency dual-polarised scatterometer that can be used in conjunction with an airborne SAR is advocated. Suggested procedures to diagnose the scattering signatures and investigate their inter-relationships are described as well as the possible uses of such an instrument.

The optical programme has the main objective of determining a detailed database on sea-surface characteristics and the development of techniques that can be used in support of the airborne scatterometer.

The theoretical programme has the main objective of improved understanding of the nature of the wind roughened sea-surface, its interaction with microwaves, and the impact of this improved understanding on SAR sea-imaging theory. To achieve this, both a theoretical development and a simulation programme are advocated.

The SAR data-analysis programme has two objectives. The first is to complement the experimental and theoretical programmes by analysis of current and future SAR datasets -

(in particular, at the raw data and complex image stage). The second and the final objective of the whole research programme, is the development of applications-specific data-processing procedures that take into account consideration of scattering-mechanisms as well as the improved understanding of the behaviour of the small-scale sea-surface roughness and its interaction with microwaves.

2. EXPERIMENTAL PROGRAMME

2.1 Experimental Programme I

2.1.1 Characteristics of Wind-Waves

2.1.1.1 Measure the directional distribution with respect to wind-direction of:-

Amplitudes of gravity-waves;
Wavelengths of gravity-waves;
Spectrum of gravity-waves;
Dispersion relation for gravity-waves;
Number density of capillary-waves;
Amplitudes of capillary-waves;

(If possible) spectrum of and dispersion relation for capillary waves.

The role of these waves in backscatter mechanism for microwave radar can be qualitatively assessed by consideration of the surface wavelength wave-amplitude, crest curvature, face-curvature and radar wavelength. We might expect the dominant scattering mechanisms at different wavelengths to be as in Table 2.1.

	mm	X-band	C-band	L-band
Gravity waves	W,S	W,S,B,	(W),S,B	(S), B
Capillary-waves	S,B	B	(B)	-

where W = Wedge-diffraction
S = Specular reflection
B = Bragg-scattering

Table 2.1

2.1.1.2 Measure the dependence of these (spatial) distributions on wind-strength.

2.1.1.3 Measure the probability of occurrence of breaking-waves and its dependence on wind-strength.

2.1.1.4 Study occasions of specular reflection in detail to determine:

a) Typical scale-sizes in three dimensions. - important (particularly vertical scale-size) for applicability of conclusions on specular reflections' significance to the situation of microwave incidence (wavelengths - cms).

b) Directional distribution of specular surfaces with respect to the wind-direction.

c) Occurrence probability in different look directions as a function of wind-strength.

2.1.2 Microwave Studies

To establish a technique for distinguishing occasions of Specular reflection, Wedge diffraction and Bragg-scattering by identification and validation of signatures of the three scattering mechanisms.

2.1.2.1 Multifrequency (mm, X-band, C-band, L-band) scatterometer illuminating same area of water-surface simultaneously at four frequencies, dual-polarisation.

2.1.2.1.1 The measurement of Doppler spectra - hence dispersion relation - in different frequency regimes simultaneously might (armed with prior knowledge from programme element 2.1.1) be used to identify the different scattering mechanisms (c.f. Table 1).

2.1.2.1.2 Dual polarisation studies could identify specular reflections.

2.1.2.1.3 Scattering-region coherence-time (variable pulse-length) studies could identify occasions of Bragg-scattering. Measurements aimed at this should involve.

a) Cross/Auto-correlation measures, possibly using a hardware correlator to distinguish such occasions.

b) Using a fixed spatial location and studying coherence-time changes as wave-systems propagate through.

c) Varying the angle of incidence and/or varying the receiver-antenna angle to observe Bragg-conditions from "sin θ" variations.

d) Varying the size of the illuminated area - increasing it to study typical sizes of Bragg-regions.

e) Moving the radar platform to follow wave-systems - to cover distances ≈ SAR resolution cell-size.

2.1.2.1.4 Possible simultaneous near-field/far-field (treating the water surface as an antenna) measurements comparing signature-differences, investigating the possibility that near-range wedge-diffraction forms (short-lived) Bragg-regions in the far-field.

2.2 Experimental Programme II

This is mainly to extend the laboratory techniques to natural situations and introduce larger illumination areas of sea-surface that are more typical of the SAR situation. The work envisaged involves progressing from a tower through airship/helicopter platforms to an airborne SAR situation progressively increasing the scale of the waves present by moving from reservoir to coastal sea-studies to the open sea situation, but restricting the latter to "closed" type seas where the longer swell-waves are predominantly locally generated.

2.2.1 Stereophotography, flash-photography, high-speed video in conjunction with a multi-frequency, dual-polarised scatterometer - to study the objectives of Section 2.1.1 of programme I simultaneous with the observation of known signatures of backscattering mechanisms (Section 2.1.2) in the presence of turbulent wind conditions and in the presence of relatively large swell-waves with their accompanying modification of the air-sea interaction and its consequences on the generation of small gravity-waves and capillary-waves.

2.2.2 Airship/helicopter platforms for microwave studies to determine near-field/far-field effect on radar return signatures in presence of long gravity waves, and extend the Bragg-region size studies (Section 2.1.2.1.3d). Stereophotography (simultaneous) from similar platforms would assist in assessing the reliability of microwave scattering-mechanism signatures (particularly specular reflection signatures) when averaged over large illumination areas. Can also test out motion compensation techniques (Section 2.1.2.3) in presence of natural turbulence.

2.2.2.1 Assess relative strengths of tilt and hydrodynamic modulation mechanisms on different scattering-mechanisms - possibly distinguishing the two by V-V/H-H comparison for wedge diffraction and Bragg-scattering occasions, need a different technique for specular reflections.

2.2.2.2 Alter aspect angle with respect to swell-wave propagation direction.

2.2.2.3 Investigate Bragg-scattering region size variations with respect to wind-speed and wind-direction relative to look direction.

2.2.3 Simultaneous sea-truth experiments will be required for experimental programme II to establish swell-wave conditions - wave buoys, short range bistatic H.F. radar. floating transponders/transmitters/reflectors (Microwave), for intercomparison of remotely sensed sea-conditions.

2.2.4 Introduce (simultaneous with microwave scatterometer signature recognition studies) airborne SAR studies.

2.2.4.1 Varying incidence angles, range, platform velocity, aspect-angle with respect to swell-wave propagation direction.

2.2.4.2 Comparison of velocity-bunching imaging mechanism with tilt and hydrodynamic modulation by studying ship-wakes and making azimuth shift comparisons, azimuth defocussing measurements; possibly identify different parts of ship-wake from scattering mechanism signatures.

2.3 Experimental Programme III

This would be an extension of experiments listed under Section 2.2.3 and 2.2.4 to the "open" sea situation and the deep ocean to provide larger ranges of wind-conditions, mixtures of sea-state (locally and remotely generated swell-waves) and very long swell-waves.

Sea-truth measurements would be provided by long-range H.F. radar, floating radar reflectors, pitch and roll buoys.

The "open" sea work could be extended to under-flights of spaceborne SAR by airborne SAR and multifrequency scatterometer to establish wave-imaging constraints and investigate wave-height extraction techniques in the presence of layover.

Applications-specific oil-slick imaging, ice monitoring etc.) measurement campaign should be undertaken to examine system-design and data-processing procedure optimisation for different applications.

3. THEORETICAL PROGRAMME

The theoretical programme can be divided sequentially into a Theoretical Development Programme and a simulation programme. The latter will use as input the results of the theoretical development programme for the analytical tools and the results of the experimental programme (particularly the dispersion relations for gravity waves and their directional distribution with respect to wind-direction, and the probability of occurrence of different fundamental scattering-mechanisms) for the simulated sea-surfaces.

3.1 Theoretical Programme I
(Theoretical Developments)

3.1.1 Further developments of all theories to a stage where the prediction of the behaviour of image parameters as a function of systems and sea-state parameters can be made.

Inclusion of non-Bragg scattering and its impact on predictions e.g. implications for speckle-statistics.

3.1.2 Clarification of the role of intermediate scales of wavelength and the effect of their inclusion on the results of 3.1.1 included in here must be a resolution of the 2-scale complementarity question.

3.1.3 The development of imaging theory for non-linear situations in particular.

3.1.3.1 Identification of the conditions for non-linearity.

3.1.3.2 Identify what information can be reliably extracted under nonlinear imaging.

3.1.3.3 Extend inversion-theory on velocity-bunching modulation in the nonlinear situation to include tilt and hydrodynamic modulation mechanisms.

3.1.4 Study of air-sea interactions in the presence of breaking-waves:-

3.1.4.1 Derive implications for the generation of short gravity-waves (or their destruction).

3.1.4.2 The effects of breaking-waves on Bragg-region coherence times.

3.1.4.3 An explanation of the phenomenon of wind-rows and their possible significance at all wind-speeds.

3.4.4.4 The effects of ship wakes on the generation (or destruction) of small waves, and their effect on local Bragg-region coherence-times (shielding from wind).

3.1.5 An investigation of the effects of rain on the generation of small surface ripples and/or the destructive influence of rain on Bragg scattering-regions.

3.1.6 Study of the effects of currents, bathymetry and internal waves on surface waves and the implication for SAR imaging of these phenomena.

3.1.7 Development of general scattering theories suitable for numerical analysis and/or simulation studies.

3.2 Theoretical Programme II
(Simulations)

Parallel simulations of SAR imaging of the sea-surface according to all formulations of theory need to be performed. (These should also be extended to two-dimensional simulations). The simulations should include:-

3.2.1 Wind-directional distributions of gravity and capillary wave spectra.

3.2.2 Wind-strength dependence of these small waves' amplitude.

3.2.3 Stationary arrays (followed by dynamic arrays) including specular reflectors and wedge-diffractors of varying number densities with both random and deterministic spatial distributions.

3.2.4 Simulations of incoherent radars including wedge-diffraction events and specular reflections for comparisons of statistics with K-distributions.

3.2.5 A study of coherence-time effects, Bragg-region size effects, wedge-diffractors and specular reflections on imaging capabilities according to all theories.

3.2.6 The introduction of intermediate scale-size wavelengths, and their directional distribution with respect to wind-direction.

3.2.7 Extension to non-linear imaging situations.

3.2.8 Comparisons should be made on the basis of predictions for:-

a) Modulation Transfer Function in the presence of swell-waves;

b) Azimuth defocussing effects and dependence on wind-strength, wind-direction, swell-wave propagation direction and their various "crossed" parameters.

c) Image statistics - identifying regions of simulated images that are predominantly Gaussian or 'Specular' in their speckle statistics.

d) The dependencies of parameters as in Alpers et al (1981)

4. SAR DATA ANALYSIS PROGRAMME

The SAR data analysis programme has two objectives:

i) To complement the experimental and theoretical investigations of fundamental scattering-mechanisms.

ii) To investigate applications specific data-processing techniques.

The programme can be subdivided into considerations for raw data processing, complex image processing and real image processing. Objective (i) can best be attained from consideration of raw data and complex image processing, whereas objective (ii) can be attained from complex image and real image processing considerations.

4.1 Raw Data

4.1.1 Applications of Doppler domain autofocussing and centre-frequency tracking techniques.

4.1.1.1 Analysis to identify systematic df/dt (focussing parameter) variations across a swell wavelength and its possible use as a measure of large wave orbital acceleration.

4.1.1.2 Search for identifiable reflectivity anomolies and their possible systematic behaviour - possible implications are the identification of specular scattering events (in particular from dual polarised imagery), tilt and strain modulation mechanisms, occasions of overlay.

4.1.1.4 Characterisation of different regions of ship-wakes from their Doppler spectra/ spectral distortions and possible associations of signatures in the spectra with different scattering-mechanisms.

4.2 Complex Image

4.2.1 Speckle statistics studies.

4.2.1.1 Gaussian/Non-Gaussian region identification, use of ship-wakes to provide different scattering surfaces under the same wind-conditions.

4.2.1.2 Correlations in the speckle - wind-rows, large scale-size Bragg-regions.

4.2.1.3 Wave-height extraction - 'phase-unwrapping' algorithms; could also be useful for identifying overlay situations.

4.2.2 Inverse methods - deconvolution, speckle reduction, correcting for sea-imaging mechanisms;

- is inversion possible under nonlinear conditions?

4.3 Real Image and Spectra

4.3.1 Wind-rows - their identification and characterisation at different signal to noise ratios, the possible use of Hough Transforms; their relation to wind-fields from scatterometer measurements.

4.3.2 Large-scale features - alternative image-processing procedures to identify and track large-scale features such as oil-slicks, icebergs (segmentation), internal waves, ship-wakes (line detection) through series of images.

4.3.3 Automatic ship recognition from high resolution backscatter contours - possible application for locating reflector-buoys in sea-truth experiments.

4.3.4 Tracking of ocean waves

- relating to sources of storms and local wind-fields;
- refraction round islands and the evolution of waves in shallow waters, relation to bottom topography.

4.3.5 Investigation of alternative transform to Fourier Transform e.g. Hough Transform where latter has problems e.g. isolated wave-crests, rapid changes in wavelength.

5. SUMMARY OF RESEARCH PROGRAMME

The elements of an experimental research programme have been described in terms of objectives and suggested experiments and techniques for attaining these objectives. At this stage some of these elements, particularly the techniques, can only be tentatively suggested as feasibility studies are required to assess which techniques are most suitable to the different situations of laboratory, coastal and open-sea.

In parallel with this experimental programme there should also be theoretical research programme and a SAR data-analysis research programme. The developments requiring most attention in these areas have been identified as elements of each research programme.

6. ACKNOWLEDGEMENTS

This work was carried out under contract to the Royal Aircraft Establishment, Farnborough, U.K. who are thanked for permission to publish this paper.

BULK RICHARDSON'S NUMBER ISOGRAMS DEDUCED FROM SAR DATA

B Fiscella, P P Lombardini, P Trivero & C Cappa

Istituto di Fisica Generale Università di Torino, Italy
Istituto di Cosmogeofisica CNR Torino, Italy

ABSTRACT

Elaborating SAR data taken by SEASAT-A over the Ligurian Sea, it is shown that when sufficient information on wind and surface sea current are available, both Richardson bulk number and air-sea temperature difference may be mapped on the basis of SAR observation from space of a marine area.

Keywords: SAR, wind-stress, air-sea interaction.

1. INTRODUCTION

SAR images of marine data directly depend upon the spatial distribution of wind surface stress (Ref. 1)

In this paper we have attempted to extract meteorological information from SAR images observed by SEASAT-A in its passage on orbit 762 over the Ligurian Sea (scene 209; site: Monaco, France) on August 19, 1978. Fig. 1 presents a hard copy of the digital data, after correction due to vertical antenna pattern.

The rationale supporting this attempt involves the fact that the pixel intensity of sea echoes is proportional to the local frictional velocity, u*, i.e.:

$$z \propto u^{*\alpha} \qquad (1)$$

where α is an experimental constant.

Now, the wind strength at a reference hight Z may be written (Ref. 2):

$$|\vec{U}(Z)-\vec{U}_s| = (u^*/k)\,(\ln(Z/Z_0)+R_i\gamma/4 \qquad (2)$$

where k is Karman constant, Z_0 the roughness length, $\gamma/4 \simeq 3.8$, $\vec{U}(Z)$ and $\vec{U}_s$ are the vector velocity of wind and sea-surface current, respectively, and R_i the bulk Richardson's number, defined by (Ref. 3):

$$R_i = g(\partial\theta/\partial Z)\ /\ T\cdot(\partial U/\partial Z)^2 \qquad (3)$$

In (3) T is the absolute temperature, θ the potential temperature, and g the acceleration of gravity.

For a shallow height Z an approximate expression of R_i in SI units is:

$$R_i = 10\ g\ Z\ \Delta T\ /\ T\cdot|\vec{U}(Z)-\vec{U}_s|^2 \qquad (4)$$

where $\Delta T = T_{air}-T_{sea}$.

Clearly, if sufficient information on the in-situ distribution of $\vec{U}(Z)$ and $\vec{U}_s$ is available, the knowledge of z allows the acquisition of R_i and ΔT for the area considered.

2. MEASUREMENTS OF SEA ECHOES

The SAR tapes have been processed on a DEC VAX-11/780 computer. After swapping bytes, matrix compression, and along-range correction, images similar to that of Fig. 1 are obtined by 16 grey level method and common dot printer.

We are interested in areas where sea clutter exists. In an effort to better characterize the information content in the signals, we have subdivided the scene

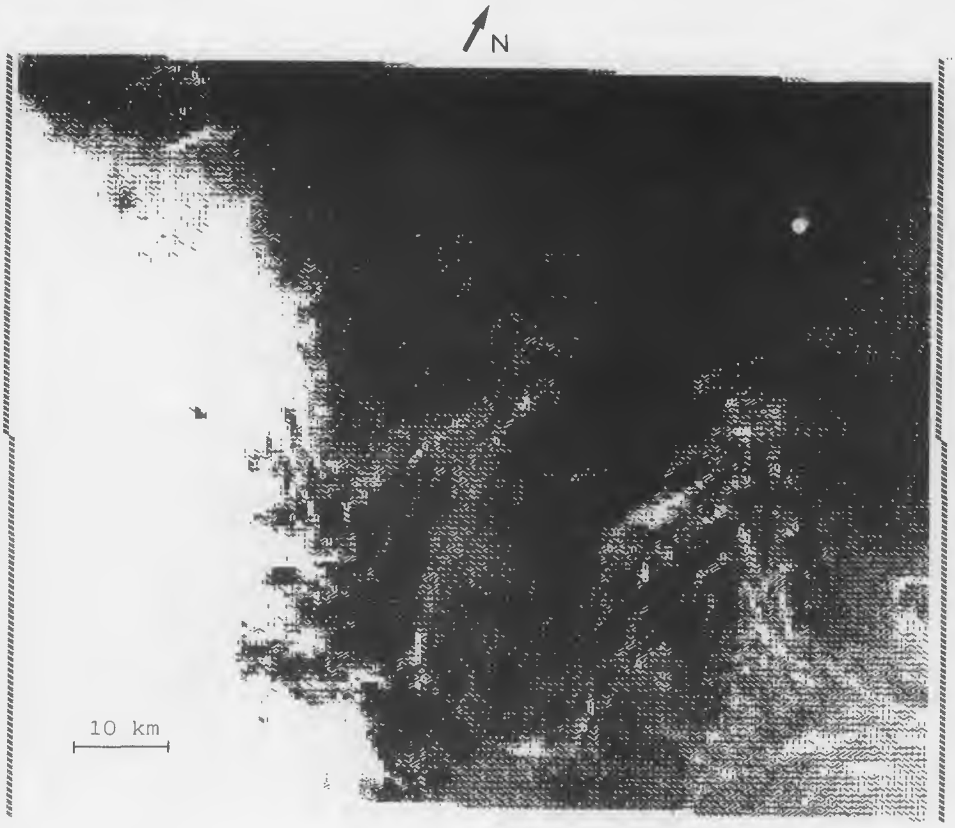

Figure 1. Hard-copy of a 77 x 93 km region of the SEASAT-A. Scene 209 near Monaco - France; orbit 762; August 19, 1978, at 6:40 a.m. U.T.
- Matrix compresssion 256 to 1
- Range correction
- 16 grey level rapresentation.

in many (1200) sub-areas and have calculated the signal mean value $\bar{z}$ and the square-rooth variance σ_z.

Fig. 2 plots σ_z versus $\bar{z}$: before a) and after b) range correction. In the figures, we notice a straight line passing through the origin, on and above which lie all points.

Points on the line belong to sub-areas in which fading is unmodulated. As matter of fact this line may be derivable from the probability distribution function of SAR systems (Ref. 4). Looking at Fig. 2b, we find a threshold z_c below which no signal occurs. We identify this threshold with the threshold described by Pierson and Stacy (Ref. 5) above which the frictional wind arouses the sea. The points far from the straight line pertain to sub-areas crossed by this threshold.

We also notice that the dynamic range of $\bar{z}$ in Fig. 2b is just what is expected with a wind speed less than 4 m/s and surface current of about .5 m/s that likely was present in the scene.

3. SIGNAL AND BULK RICHARDSON'S NUMBER

Formula (2), with the hypotesis (1) may be re-written as follows:

$$U_r/U_c = (z/z_c)^{\beta} \left(1+\frac{\gamma R_i}{4 \ln(Z/Z_0)}\right) \quad (5)$$

where $U_r = |\vec{U}(Z)-\vec{U}_s|$, U_c is the threshold of wind velocity (3.52 m/s), $\ln(Z/Z_0) \simeq 11.5$, $\beta = 1/\alpha = .714$, z and z_c derived from the mean values reported in Fig. 2b.

From (5) one has:

$$R_i = \left(\frac{U_r/U_c}{(z/z_c)^{\beta}} - 1\right) 3.0 \quad (6)$$

and

$$\Delta T = .128\, R_i\, T\, (U_r/U_c)^2/Z \quad (7)$$

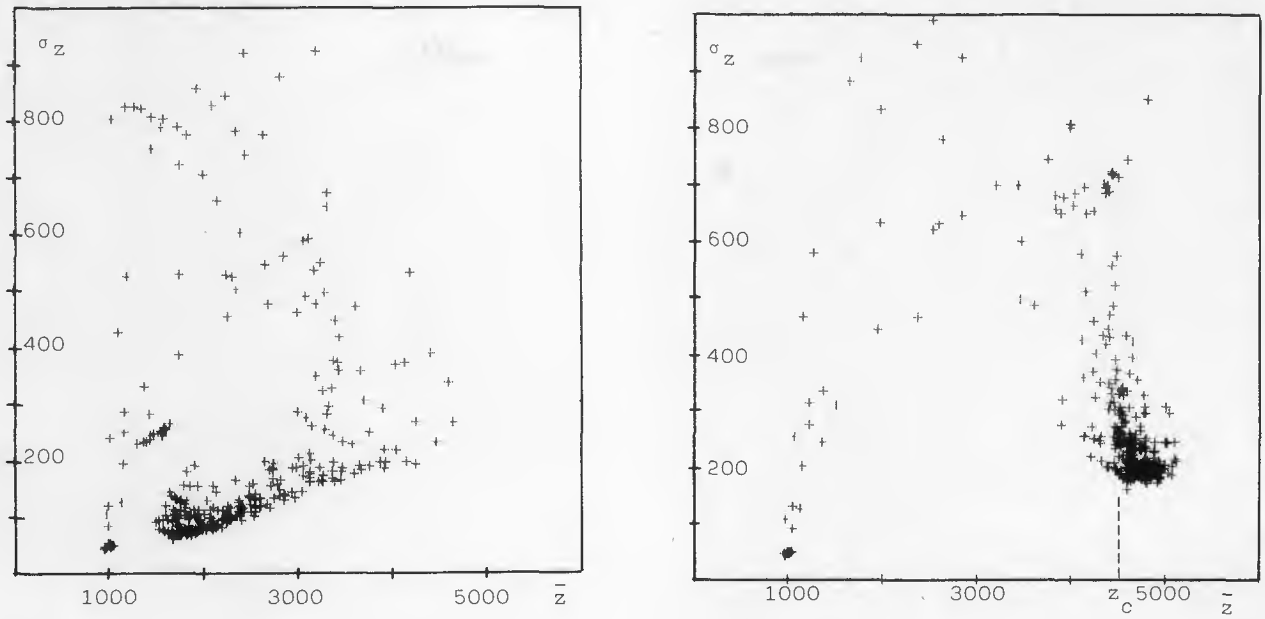

Figure 2. a) Plot of square-root variance versus mean value of pixel intensity on data matrix relative to Fig.1 before range correction.
b) Same as figure a) after correction. Statistic performed on 1200 2 x 2 km^2 sub-areas.

In Fig. 3 data computed from formula (6) are plotted for several values of U_r/U_c. In the scene of Fig. 1 z/z_c ranges from 1 to 1.16, what excludes wind speeds larger than $U_r = 1.15\ U_c = 4.0$ m/s.

On the other hand plots of equal pixel intensity of the scene show that: a) the top left region, having very low pixel levels, is sharply separed from the remaining part, U_r is weakened below threshold as the effect of the surface current; b) elsewhere the contours are so irregular to suggest that mean signal variations are due to temperature variations rather than to wind changes; c) the level $z/z_c = 1.06$, see Fig. 4, divides the visible image in two equal area regions, so presumably wind speeds must be close to $U_r = 1.05\ U_c = 3.7$ m/s and air sea temperature differences have to be confined between + .4 and - .4 °C.

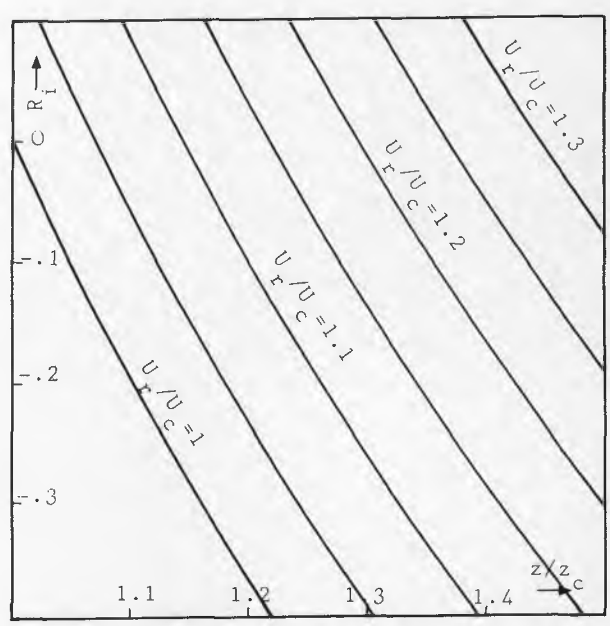

Figure 3. Diagrams of Richardson's number R_i versus mean pixel intensity. Parameter: wind speed.

4. CONCLUDING REMARKS

No doubt that the isograms we have found accuse the crudeness with which "sea-truth" has been assumed.

However, they indicate the feasibility of deriving meteorological data, once sufficient sea-truth is available.

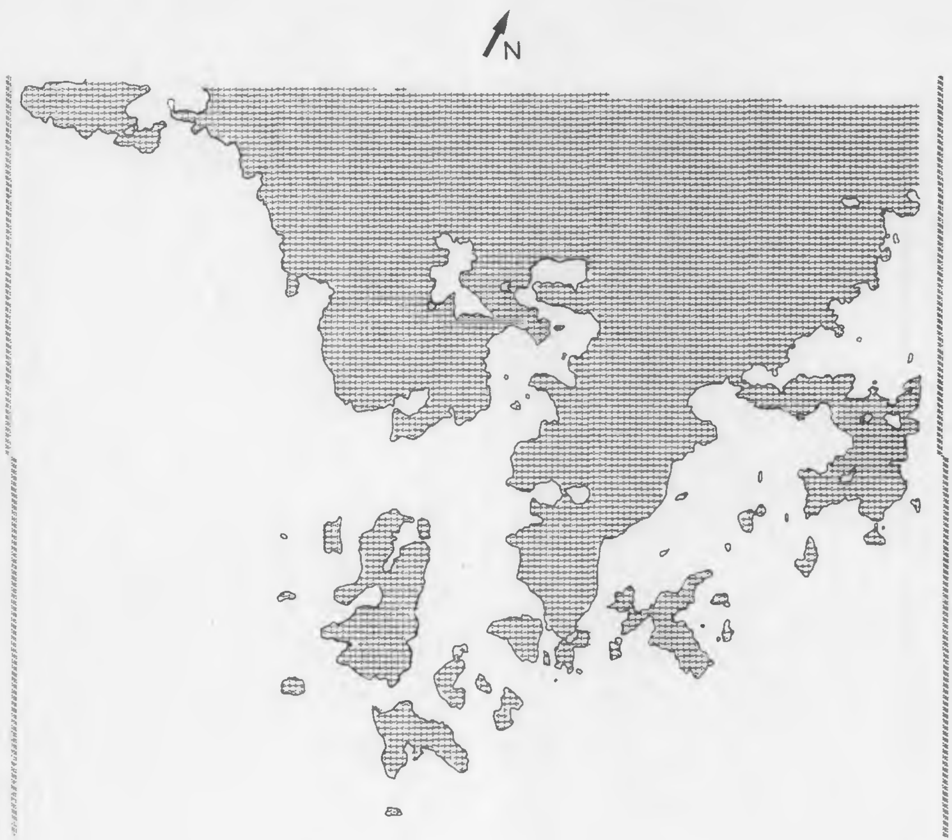

Figure 4. Plot of contours of pixel intensities after compression (256:1), corrections and integration.

The presence of dense waters between Corsica and Ligurian coast has been observed independently, as published elsewhere (Ref. 6).

5. REFERENCES

1. Weissman D E, Thompson T W & Legeckis R 1980, Modulation of sea surface radar cross section by surface stress: wind speed and temperature effects across the Gulf Stream, J.G.R. vol 85, 5032-5072.

2. Paulson C A 1970, The mathematical representation of wind speed and temperature profiles in the unstable atmosphere surface layer, Jour. of Applied Meteor. vol 9, 857-861

3. Lumley J L & Panofsky H A 1964, The structure of atmospheric turbolence, Interscience Pub. N. Y.

4. Ulaby F T, Kayate F, Brisco B & Lee Williams T H 1986, Textural information in SAR images, IEEE Trans. on Geo. Remote Sens. vol GE-24,235-245

5. Pierson W J & Stacj R A 1973, The elevation, slope and curvature spectra of wind roughened sea surface, NASA CR 2247, December

6. Giuseppe M & Manzella R 1986, Influenza sul clima del Mediterraneo Occidentale, Boll. Geof.vol IX, 55-62.

SESSION 4 – SUMMARY

R Frassetto *(Chairman)*

M.H. Freilich illustrated the NSCATT Programme which develops in two selected regional field experiments of 2-months duration with advanced in-situ measurements on a wide parameter range. One site is near the Gulf of Alaska, the other in the Gulf of Mexico.

P. Johnson described the NROSS sensor system, its orbit, 19-day repeat cycle with descending equatorial crossing a0715. He proposed collaboration to calibrate and validate NSCATT and ERS-1, using merged resources and experience, and to enhance coverage and inter-comparisons. A Ground Validation Working Group is to be formed.

C.T. Swift illustrated results of synergetic use of ALT, SCATT, SMMR of Seasat for statistical wind fields studies of the Southern Ocean in particular. Discrepancies between sensors data suggested evaluation of new algorithms. SMM/I, operating in 1987, may be used in wind and wave models improvements - the high speed winds may be comparable to those of SCATT, if not better. He showed an example of SMM/I hits that will occur over a 3-week time period for a buoy located at 43° lat., 70° long. Less than 500 'hits' are required to establish a 95% confidence interval that the buoy and the satellite measure the same quantity.

I.J. Barton described facilities and planned in-situ observation systems and networks to be deployed North East of Australia for tropical oceanography programmes to be used for validation and calibration for ERS-1 in the southern hemisphere. SAVE (Satellite Validation Experiment) should take place, possibly in March-April 1990. Collaboration with European institutes is planned. One programme of energy fluxes using ATSR is agreed with UK.

T. Kaneshige described the general objectives of WCRP (World Climate Research Programme) in its 3 streams: long range weather prediction, global climate variations and response of climate to natural or antropogenic influences. TOGA and WOCE are the main international study programmes of streams 2 and 3. Meteorological observing systems rely on the WWW (World Weather Watch) system to obtain intensified observations of winds at different levels, including the surface wind and pressure, temperature from the VOS (Voluntary Observing Ship) fleet. WMO, CCCO, IOC and other international organisations are now planning the recommendations to enhance this service.

Ocean observing systems rely mostly on IOC, CCCO activity to obtain an increased tide gage network, ships observations in best possible quality and time-spaced distribution, surface drifters and current meters mooring programmes (TOGA, WOCE). Models are available or in development to plan operational programmes for different processes and scales, also of the two boundary layers (air-water).

Although the major programmes are expecting an input from satellites, and for this reason they plan to start in 1990, it is feasible to encourage the use of observing systems in strategical areas and of the available models as a support for validation of ERS-1.

K. Hasselmann described the WAM (wave modelling) programme, the objectives of which are:
1) to develop operational '3rd generation' global and regional wave models for applications;
2) use the 3rd generation model to exploit satellite wind and wave data in the nineties;
3) apply wave models to provide input wave data for Scatterometer wind and SAR wave model algorithms;
4) incoporate wave models in comprehensive operational wind and wave data assimilation system.

He illustrated a cross-coupling between wind and wave microwave sensors and a scheme of wind and wave data assimilation, forecasting and archiving facility.

According to the WOCE workshop on 'assimilation of wind and wave (satellite) data in numerical weather and wave prediction models' (ECMWF, March 1986) it was recommended to establish (at least) one wind and wave global data assimilation system in both Europe and the US at operational global weather prediction centres and to create a WRCP 'Air-Sea Flux Group' to produce continuous gridded global flux data using all available data on operational basis.

PANEL REPORTS

REPORT OF WORKING GROUP 1

THE USE OF OUTPUT PRODUCTS FROM MODELS, ON BOTH REGIONAL AND GLOBAL SCALES

P E Francis *(Chairman)*
J Guddal
W J de Voogt
R Frassetto
P S Callahan
A Ratier
J Reiff
J E de Luis
J Stum
W Koch

TERMS OF REFERENCE

(i) What model products are available and which centres are involved.
(ii) What range of models are available; surface wind, spectral waves, global and regional coverage.
(iii) Which models might be used.
(iv) How are models to be used in relation to both conventional surface data and satellite data.
(v) What is the potential of this technique and what are the limitations, both for the commissioning phase and in the longer term.
(vi) Prepare recommendations for the procedure and the required planning.

1. INTRODUCTION

The aim of this WG is to assess the usefulness of treating numerical wind/wave models as a source of information for ERS-1 data validation. A strategy is proposed, implying the application of
- numerical models
- conventional surface data
- "dedicated" measurement campaign data

By model output data we mean values extracted from model generated parameter fields, by spatial/temporal interpolation to the appropriate position and time for comparison with satellite and conventional data.Model characteristics, such as resolution, performance etc., will have to be clarified, also the mode of assimilation of different kinds of surface data, in any model considered for this purpose.

In principle, the same strategy applies for both wind and wave data,although emphasis may be shifted to different aspects when going from wind to waves.

The logistics of the commissioning phase, i.e. the likely delay in collecting data from any dedicated surface observing network, and the likely initial intermittancy of satellite data on purely regional scales, appear to indicate that work on model - data comparisons should be constructed with the following priorities

a) global assessment
b) regional assessment
c) dedicated network assessment

2. WHAT IS AVAILABLE

One may differentiate between operational (forecasting) models and more dedicated models, i.e. for research purposes, to be found within universities etc. It is more easy to list the operational forecasting institutions and their models, in Europe and the US, but quite a potential also exists in Japan, Australia and New Zealand.

Atmospheric global models are available at ECMWF, UK Met. Office, US NMC, FNOC, and from next year also in France. Probably also in Germany (FRG) and Japan.
Regional atmospheric models with fairly updated physics and adequate (50 km) resolution are operating in most European countries, US, Canada, Australia, Japan.

A comprehensive WMO report (in preparation) will describe characteristics of these models and their pre-processing.

Global wave models are run at FNOC, UK Met. Office, and ECMWF (although not presently operational). Regional wave models also seem to run operationally in most of the coastal countries mentioned above.

Numerical models of atmosphere and ocean surface are steadily improving and their products being used more widely and with growing confidence.

Model outputs are normally at 3 or 6 hourly intervals.
The parameters derived as model output may include:

U, V and/or U*, V*, (10 m and/or "friction" wind)
T(air), T(sea surface)
sea level air pressure
H_s (significant wave height)
separated into sea/swell if required
mean/peak wave period
peak wave direction
1 or 2D wave spectrum

3. COMPARISON OF MODEL DATA WITH MEASUREMENTS FROM THE SURFACE

The following strategy is based on the assumption that FDP data will be ready for real time application in the routine set-up of operational forecasting centres. However, quasi real time dissimination of FD Products is uncertain during the commissioning phase: it is anticipated that PAFs' main activity will then be devoted to non-real time processing of limited, but significant amounts of data for calibration and validation purposes. The use of model outputs for such purposes should therefore be performed in close connection with the Processing and Archiving Facilities during this period.

It can be anticipated that two major sources of surface information will be available during the commissioning phase:

a) 'conventional' data i.e. from regularly reporting meteorological and oceanographic stations, ships, buoys.
b) 'dedicated' data from short-period, planned networks of buoys, ships and airplanes (even though at a low priority due to possible delays in data collection and processing)*

Comparing these two classes of information against values from co-located model points can yield valuable information for use in other areas of the assessment campaign.

Comparing the models against conventional data can be done in two istinct ways. Firstly, by using a short period model forecast (or hindcast in the case of present wave models) it is possible to quality control the conventional data. Secondly (and presently for NWP models only) it is then possible to assimilate the quality controlled data and to assess how well the model can fit them. The model assessment can be further classified by area, e.g. identifying variation in performance between dense and sparse areas of data input. A classification by instrument type, in a dense area, could also give an indication of variation in spatial and temporal representativity between different instruments.

With data from possible dedicated networks it would be more appropriate to omit the assimilation stage and to proceed directly to a comparison at co-located model points. In this way model performance at fixed, well-instrumented locations becomes well-defined, giving a means of assessing differences between model values and satellite values in that area.

The strength of the whole approach, however, is that movement away from the dedicated network is now possible, since (satellite to model) comparisons can be assessed against (ground data to model) comparisons as long as the latter information is well defined by carefully conducted model verification exercises. Such exercises should be performed with the chosen models just prior to launch.

---

* In the case that a dedicated measurement campaign cannot be realised, one should draw attention to the North Sea/Norwegian Sea measurement network, which already consists of modern wind/wave sensors with flexible sampling procedures, buoys and radar units. These systems are not reporting via GTS, but may be accessed through arrangements with national meteorological agencies.

4. COMPARISON OF MODEL DATA WITH SATELLITE DERIVED DATA

Proceeding directly to comparisons with analyses (i.e. no assimilation procedure) we can consider the three levels of conventional data coverage already defined i.e. at dedicated network locations, in densely measured areas, in sparsely measured areas.
Moving into areas of dense conventional observational coverage, we are able to compare many more satellite data than would normally be considered, simply by using the whole extent of the model grids in these areas. The differences between satellite and (co-located) model values can be assessed by using the previously defined behaviour of the model when compared to conventional data in such areas. It would be hoped that the 'error' distribution was similar. Finally one is allowed to proceed into wider areas, and make use of even more satellite data, by comparing model and satellite values in sparsely measured (conventionally) areas. Again, the comparison of 'error' distribution with the pre-determined model performance in these areas should indicate whether or not this large volume of satellite data is physically consistent, hence whether the algorithms, developed from perhaps a sub-set of limited range, are reliable over a much wider range of environmental values.

Further classificiation, within areas, by means of synoptic type, could lead to further insight into data retrieval, since the models can be used for instance to indicate rain, high water vapour content etc. This classification would be aided by use of additional material such as satellite photographs and manual analyses (i.e. with fronts identified).

5. THE POTENTIAL OF THIS APPROACH AND POSSIBLE LIMITATIONS

The principle advantages in using models for the purpose of validation can be listed as follows:

(a) An extension of temporal and areal domains, away from co-located surface measurements, allows the use of much more satellite data, perhaps ensuring the examination of more extreme environmental conditions.

(b) Well established models will already have been extensively validated, and much of the required processing software for the comparison task will already exist. In the case of wind models it will be possible to categorise model performance in terms of geographic area and (if required) synoptic type.

(c) Models are presently a highly acceptable means of obtaining information on environmental conditions. During the intervening years to satellite launch it can be expected that model performance will further improve due to better physics/numerics and more powerful computers.

(d) The outlined approach, if successful, will lead naturally to the necessary impact studies, data assimilation, and the prospect of interactive retrieval systems.

(e) Given sufficient information on data location, the use of models is independent of orbit configuration.

Other, perhaps more speculative, advantages include the chance to assess variations in the performance of different surface instruments (by means of comparison of model to instrument error distributions); the aiding of dedicated network design (by using past modelling results to indicate likely areal & temporal variability); and the indication of remote weather conditions that might affect performance of retrieval algorithms.

A few possible limitations can be readily identified:

(f) The lack of knowledge of the spatial variation in performance of wave models, particularly on a global scale, due to the very poor surface measuring network at present. This could be partially remedied by a concerted attempt to improve the network.

(g) Some duplication of effort will be necessary (i.e. at least two models in each comparison campaign) in order to remove possible model biases.

(h) Viable comparison techniques and analyses need to be defined, and the relevant software written before time of launch.

6. RECOMMENDATIONS FOR PROCEDURE

The recommended actions can be easily divided into pre- and post-launch activities.

Pre-launch:

(1) A pre-assessment of the viability of the approach, using data from GEOSAT when that becomes available. Duration 6 months.

(2) Based on the above study, the analysis of comparison data should be designed, incorporating both point-to-point and areal/temporal averaging techniques. Duration 3 months.

(3) Co-ordinating bodies such as WMO should be approached in order to stimulate the development of real-time reporting surface wave measurement networks.

(4) Studies of the performance of global and regional, wave and wind, models should begin, in order to identify characteristic performance in well defined areas. Based on this work representative areas should be chosen for study after launch. The assessment should be carried out in the 6 - 12 months prior to launch.

Post-launch:

(5) Validation of ERS-1 wind and wave data in chosen areas, using chosen models, during commissioning phase.

(6) Extension into operational phase, in order to monitor effects of engineering algorithm or retrieval algorithm changes.

(7) Extension to data assimilation studies and/or multi-variate retrieval methods.

REPORT OF WORKING GROUP 2

THE USE OF AVAILABLE ENVIRONMENTAL DATA IN THE STATISTICAL APPROACH TO CALIBRATION AND VALIDATION

P K Taylor *(Chairman)*
F Monaldo
P Challenor
A Laing
J-P Dumont
C T Swift
M H Freilich
J Louet
J Demurger
J-P Malarde

1. INTRODUCTION

1.1 Terms of Reference

To consider, for calibration and validation by statistical techniques, the use of:

a) World Weather Watch data from ships of opportunity and buoys.
b) Other satellite data sets such as that from the SSM/I on the DMSPand NROSS satellites.
c) Statistical techniques applied to ERS-1 data itself.

To assess the potential and limitations of the statistical approach for the commissioning phase and on the longer term, whether the method should be applied on a global basis or at specific sites, and to recommend procedures and the planning required.

1.2 Calibration and Validation

The Working Group adopted the following definitions:

Calibration requires accuracy assessments which can be related to the method of operation of the satellite sensor, for example detection of variations in performance across a satellite swath. Data for calibration should be of high accuracy on a point-by-point basis and sufficiently comprehensive to allow generation of a model function.

Validation is the comparison of geophysical data from the satellite against other geophysical data. It must be performed to a level of accuracy similar to that required for calibration. Validation covers a wide range of geophysical conditions although a limited range of system dynamics.

The statistical approach involves the use of a large number of satellite and in-situ data. These may be compared by using satellite in-situ data pairs to form a regression and using that regression as a reference for the satellite data. This will be referred to as "paired analysis". Alternatively the statistical characteristics of each data set may be calculated and these compared ("binned analysis").

The environmental data sources considered by this Working Group are such that they are not suitable for calibration, but are an important source of validation data. The statistical approach must, therefore, be considered a means of validation of satellite data.

1.3 Report Structure

The various data sources (in-situ wind and wave data, other satellites, and ERS-1 itself) are considered in section 2. The details of the statistical approach are defined in section 3.

Limitations due to sampling induced errors are considered and a simulation experiment proposed. The conclusions and recommendations of the Working Group are summarised in section 4.

2.1 In-situ Wind Data

In-situ sources of available environmental wind data over the ocean are the Voluntary Observing Ships (VOS), the off-shore data buoys and other platforms operated by certain countries.

VOS Ships

The quality of VOS data has been discussed at this workshop by Taylor and Wilkerson (this volume). There are many deficiencies in the individual data reports. However, most of the errors are random and the means of many observations agree, or show a definable bias, when compared to fixed platforms. The ships observe nominally at 6-hourly intervals and by no means all these observations reach the GTS (Global Telecommunications System). Thus direct coincidences between satellite data and ship data are few (Offiler, this volume).
For these reasons the VOS data are not suited to the point-by-point statistical approach. Nevertheless, the large number of VOS observations routinely available allows the data to be used by comparing the statistical characteristics with satellite data ("binned analysis"). Such a validation technique requires relatively little investment, either for data collection or analysis. It is therefore likely to be cost effective.

For statistical significance, a large number of

Proceedings of a Workshop on ERS-1 Wind and Wave Calibration, Schliersee, FRG, 2–6 June, 1986 (ESA SP-262, Sept. 1986)

VOS reports (probably over 100) will be required to perform each validation. The concentration of the VOS in shipping lanes results in a sufficient density of observations from certain regions of most oceans. The validation should be performed in all sufficiently sampled areas taking care that the geographical distribution of satellite and in-situ data is compatible. Validation by this method in both tropical and southern hemisphere regions seems feasible.

The VOS data are either available within 24 hours of observation on the GTS, or after a delay of typically 6 months to 4 years, from ship log-books. The latter source is more accurate and complete, however, the delay is not considered acceptable for satellite validation. GTS data are subject to transmission errors and duplication of reports and careful quality control is necessary. This is best done by obtaining the data from a forecasting centre which has already applied suitable controls. The data would then be made available for validation purposes through one or more PAF(s) (Processing and Archiving Facility). Typically there are 4000 observations per day with at least 11 variables needing to be stored for each observation. It will be necessary for negotiations to obtain these data to commence as soon as possible.

Various measures are possible to increase the quality and quantity of VOS data and these should be encouraged. However, a quantitative assessment of the likely impact of such improvements is urgently required. This would be by an observing system simulation exercise (section 3.4). Following such assessment the degree of action (if any) to be undertaken within the ERS-1 programme could be objectively determined. The simulation exercise would also determine over what areas adequate VOS data will be available, and the degree to which the various climatic regions are presented. Although it is unlikely that all climate types will be covered, the range will still be greater than any other validation technique. This emphasises the importance of including these data in the ERS-1 validation.

Other Platforms

Several nations maintain instrumented meteorological buoys and lightships. In addition, off-shore structures (such as oil platforms) are often instrumented to provide similar measurements. Typical met. buoys observe wind velocity, SST, air temperature, humidity and some wave data.

The U.S. National Data Buoy Office (NDBO) operates the most extensive buoy network (April, 1986, Bull. of the AMS).
The buoys typically report measurements once every one or three hours. In the U.S., buoy instruments are calibrated prior to deployment, and consistency/engineering checks are performed on the operational data by NDBO.

The data from these buoys are thus considered to be of reasonably high quality, with rms instrument accuracy estimated to be (the greater of) 1 m/s or 10% in speed and 10° in direction. The large quantity of auxiliary (non-wind) data allows accurate calculation of neutral stability winds from the measured wind. The buoys report, typically, at hourly intervals. Estimates suggest that an acceptable number of near coincidences between satellite and in-situ data will occur during the three month commissioning phase. Thus buoys are an important source of wind data for statistical comparison using the "paired analysis" method.

In addition to NDEO, Europe, Japan and Australia have a significant number of buoys. The utility of a particular buoy network for validation will depend to some extent on the phase of the ERS-1 orbit. Since buoy data will be important for validation during the commissioning period, this should be considered in choosing the orbit phase. For more discussion on the availablility of data buoys and other platforms see the report of Working Group 3.

Drawbacks of the operational met. buoys involve their locations, sampling periods, and data availability. Many of the buoys are in close proximity to land. Thus, satellite data nearly co-located with buoy measurements must be carefully checked to avoid those satellite measurements contaminated by land. The short averaging times of some measurements (8.5 min., once/reporting period) lead to incompatibilities between measured velocities and the synoptic wind characteristic of the satellite measurements. This incompatibility appears as an additional random "error" source for the buoy measurement. A model due to Pierson (1983; Seasat Special Issue # 2, J. Geophys. Res.) can be used to estimate the magnitude of these errors. Efforts are underway in the U.S. to upgrade the systems so that they can provide nearly continuous averages of wind velocity (J. Wilkerson, personal communication, 1986). If successful, this upgrade could greatly decrease the magnitude of the satellite-buoy incompatibility. At the present time, buoy data is not available over the GTS. Special arrangements with the appropriate national agencies must be made in order to insure timely receipt of buoy data for ERS-1 validation activities, especially in the commissioning phase.

2.2 In-situ Wave Data

In-situ wave data for validation is of two distinct types. The first and most abundant is the visual data made from ships of opportunity. Elements reported are the wind-wave height and period, and swell height, period and direction for any number of observable features.
The data is available in real time though the GTS.

The other type is from measurements made by the buoy (and other fixed measuring device) networks. Full spectra or integral parameters may be available.

The quality problem inherent in the visual data precludes its use except in a gross statistical sense. Assessments of this data (see Hogben & Lumb 1967, Jardine 1979, Laing 1985, Wilkerson (this volume))indicate that observed periods are dubious, directions very scattered, and heights (i.e. combined height of wind, waves and swell) perhaps useful if used in large enough ensembles. Observing and reporting difficulties indicate that before use these data should be subjected to an editing process to remove or possibly correct (if the effort is warranted) gross errors. This should be done in conjunction with the wind data so that consistency checks can be applied (e.g. WMO 1981).

Although less extensive than for wind data, coverage from visual observations is quite good in the northern hemisphere, but in the critical southern hemisphere it is still sparse. Improved data quantity in these regions may be achieved by stimulating a more conscientious approach to reporting over the GTS through the WMO Wave Programme. Substantial impact on the coverage, however, is not expected from such conventional sources. Improvements in data quality are also a priority of the WMO Wave Programme and should be encouraged. The impact of such an effort may be assessed by a simulation experiment (section 3.4).

The measured data (mostly from buoys) is of much better quality. However, quality checks on these data are necessary, particularly on data from small networks or individual operators. Buoy wave data are not presently available on the GTS. Private arrangements in existence could be extended so that the data are available for validation. A more desirable approach is for a formal initiative through WMO to ensure GTS transmission. This is feasible for the routinely calculated wave parameters (such as significant wave height) which are required for validation. Full wave spectra comparisons with ERS-1 data would be left to subsequent detailed investigations.

Involvement of WMO through their Wave Programme should be made at an early opportunity if this rather long process is to bear any results of use to the ERS-1 programme.

2.3 Validation using data from other satellites

Satellite data to be used for validation must come from sensors which have been fully calibrated and validated before the launch of ERS-1. Suitable instruments will be the SSM/I on DMSP and the Geosat Altimeter (if still working). Except for the SSM/I, NROSS sensors probably will only be validated during or after the ERS-1 mission and must therefore be excluded. Also excluded are cloud motion winds from geostationary satellites. Although these might theoretically be used for ERS-1 validation, the relationship between the cloud motion and the surface wind is not sufficiently well defined for such data to be of use.

The Special Sensor Microwave/Imager (SSM/I) is a seven channel imaging microwave radiometer system that is planned to be launched in 1987 as a payload on the U.S. Defense Meteorological Satellite Program (DMSP).
The satellite is in a near polar, sun synchronous orbit. Preparations for the post launch verification activity (at the University of Massachusetts) include an investigation of the number of coincident SSM/I and buoy measurements needed to specify a confidence level on the measurement of windspeed by the SSM/I. An example of the spatial and temporal frequency of expected coincident SSM/I and buoy hits are shown in figures 8 and 9 of the paper by Swift and Mognard (this conference proceedings).

Assuming that SSM/I is launched before June 1987 (the specific launch date is undefined at this time), an operational satellite derived windspeed product will be available before the end of 1988. Since the data will have unlimited distribution, a wide swath windspeed product will be available as an inexpensive resource for ERS-1 windspeed validation. Since the NROSS SSM/I instrument will be similar, this also could be used for ERS-1 validation. The assimilation of radiometer derived winds into the ERS-1 data base would not only provide redundant measurements, but also a more accurate measurement under high windspeed conditions where the active sensors begin to lose sensitivity.

2.4 Validation Using ERS-1 Data Self-Consistency

Perhaps the first and most straightforward validation procedure for ERS-1 geophysical parameter retrievals are checks for internal data consistency and reasonableness. The checks can be divided into two broad categories: single parameter and cross parameter checks.

Single parameter comparisons involve examination of geophysical parameter probability density distributions to determine if parameter mean and variance fall within expected limits and if preferential values are being selected. For example, point-by-point comparisons of Seasat altimeter winds and buoy winds had shown agreement to within a quite reasonable 2 m/s (Brown, 1979). However, clear problems in the radar cross section to wind speed algorithm became apparent when the Seasat altimeter wind speed distribution was shown to be bi-modal (Chelton and McCabe, 1985).

In addition, ERS-1 geophysical parameter retrievals can be cross compared for reasonableness. For example, comparisons of the wind speed distributions obtained from the scatterometer for different swath positions should be uncorrelated with swath position. Another example would be peak wavenumber and directions from the ERS-1 SAR. A correlation between the significant wave height measured by the altimeter and the azimuth component of the peak wavenumber could reveal the limits in detectability of azimuth traveling waves as a function of sea state.

In short, ERS-1 geophysical parameters can, and ought to be checked against one another as a first test of the data consistency. One test not recommended however is detailed comparison of geophysical parameters against climate. This is because the interannual variability is likely to be of similar order or greater than the likely sensor errors.

3. ANALYSIS TECHNIQUES

It has been noted that two basic forms of analysis can be applied to joint satellite/surface data sets: paired analysis, and binned analysis. Due to the different coverages, sampling, and accuracies of the buoy and ship data, paired analysis appears to be most appropriate for satellite-buoy comparisons, while binned techniques are appropriate for satellite-ship analyses.
This section will consider each analysis technique in more detail.

3.1 Paired Analysis

Paired analysis is based on the fact that nearly co-located (in space and time) buoy and satellite observations should each be sampling nearly the same wind or wave conditions.

This method may be described as the 'classical' calibration technique, as would be used, for example, in a laboratory. Such calibrations are often performed by means of regression. However, this is not strictly correct. In a regression a random variable (y, say) is compared with an 'error free' variable, x, so as to minimise the error when predicting a value of y, $\hat{y}$, from a new, given value of x, $\hat{x}$. In a calibration or validation, however, we are interested in predicting a value of x from a measured $\hat{y}$ and minimising the resulting error in x.

This leads to a different statistical procedure. A review, and discussion, of the statistics of calibration is given by Brown (1982).
In the case of ERS-1 the statistics are further complicated by the fact that x is not error-free, but is itself a random variable (Freilich, this volume). Statical calibration under these circumstances is discussed by Theobald & Mallinson (1978) and it is recommended that procedures, based on those given in this reference, should be used.

Standard analysis of the data (including checks on the quality of the fit and searches for dependencies on other geophysical variables) can be carried out by examining the dependencies of residuals between the y_i and the regression line on variables such as wind speed, SST, wave conditions, stability, etc.).

Differences in (corrected) regression coefficients can be expected as functions of the spatial and/or temporal window sizes used to co-locate the data. However, the sensitivity of the final results to window size can be determined a posteriori, by re-doing the analysis with different size windows.

The relatively large ($\gg$50) number of buoys and platforms, their wide geographical distribution, and their frequent sampling will allow for a large number of paired observations spanning a wide range of conditions. Comparisons between buoys and Seasat scatterometer suggest that several thousand co-located pairs should be obtained during the commissioning phase of ERS-1.

3.2 Binned Analysis

In binned analysis techniques, satellite-surface observation pairs are not co-located within small spatial and temporal windows. Rather, various bulk statistics (including the shapes of the statistical distributions or histograms) from each data set are compared.
A different set of statistical techniques is therefore needed.

One method would be to compare measures of location, such as the mean or median, or measures of scale, such as the standard deviation or inter-quartile range. The median and inter-quartile range may be preferable as data from the VOS ships might contain outliers which have a disproportionately large effect on means and variances. However, such tests would not give information on how alike the two distributions were in their tails, where most interest would probably lie. To compare two distributions in their entirety, either a rank method (such as the Mann-Witney test) or a modified 'goodness-of-fit' test (such as a chi-square or a Kolmogorov-Smirnov test) would be needed. In any binned analysis a problem arises as to the number of independent data points in either the satellite or surface data set. All these statistical tests require independent data and some modification, either to the tests or the number of data points, would be needed to deal with the non-independence of data within either set that are close in space and time.

A further problem is caused by the need to calibrate wind velocity, a vector rather than a scalar quantity. All the statistical tests so far mentioned (both in the paired and binned analyses) have assumed scalar data. If wind velocities are considered as complex numbers it is relatively easy to generalise the regression based techniques used in the paired analysis. However, some of the methods described for the binned analysis cannot be generalised in this way. In particular, rank methods and those requiring ranking (e.g. medians and inter-quartile ranges) are inappropriate.

3.3 Limitations due to Sampling Induced Errors

For time periods of weeks and longer, satellite scatterometer data will uniformly cover any geographical region. However, ship data does not necessarily have this property. (In fact over large portions of the world ocean, virtually all shipping follows well-defined lanes). Thus comparisons using binned data will need to be limited to geographic areas where the sampling is consistent between ERS-1 and ships.

More generally, the problem arises when estimating the spatial/temporal mean wind or wave height in a region based on satellite observations. As the environmental parameters in the region are variable in both space and time, and the satellite will sample irregularly within the region, the sample mean will not be identical to the "true" mean. The magnitude of variability between the sample and true means is a function of the spectrum of the environmental variability and the exact sampling of the satellite sensor.

Simulations of the NSCAT scatterometer sampling, and atmospheric variability derived from historical data, indicate that sampling errors are large at all latitudes for 2° x 2° x n-day averages if n $\leq$ 10 (Chelton and Freilich, 1985, Sampling Errors in Altimeter and Scatterometer Data, U.S. WOCE Technical Report # 1; Freilich and Chelton, 1986, Sampling Characteristics of Satellite Scatterometers with Application to Oceanography, in preparation). The errors fall off rapidly with increasing n, and for n $>$ 30 days, rms errors in sample mean zonal component speeds are $<$ 0.2 m/s in equatorial regions, and $<$ 0.3 m/s in mid-latitudes. Thus using monthly data sets validation using statistical techniques will be possible.

3.4 Global Validation Simulation Experiment

Several aspects of the design of "binned analysis" validation can be examined through pre-launch simulation exercises. Among the questions to be addressed are:

a) Choice of regions over which statistics are compared;
b) Quantitative benefits of increased size and/or accuracy of conventional data sets;
c) Choice and sensitivity of statistics to be calculated and compared.

The experiment could be conducted using existing data. One suggestion for the method is as follows. The locations and times (and, preferably, method of transmission) of ship reports for a 3-6 month period are required, as well as frequent, high-resolution operational estimates of surface wind velocity and for wave conditions for a similar length of time. Note that the wind data and ship reports need not really be from the same time for the purpose of this experiment.

Ship reports are simulated by interpolating the wind/wave analyses to the known temporal and spatial locations of the ships. These simulated "perfect" reports can then be degraded by the addition of noise with known characteristics. Similarly, simulated satellite observations can be calculated by interpolating the wind/wave analyses to satellite measurement times and locations. The model from which the "perfect" reports are derived will have filtered out atmospheric variability on meso- and sub-meso-scales. However, estimates of this effect can be made and corrections applied in the analysis.

The choice of regions is influenced by interactions between the coverages of the ship and satellite observations, and the variabilities of the wind/wave fields. Regions of suitable ship coverage can be identified by comparing sample statistics of "perfect" ship and satellite measurements. (Suitable regions are those for which most or all of the sample statistic comparisons are nearly identical). The variability of ship coverage will lead to choices of different-sized regions in different geographical locations.

Several simulations can be run with varying types and levels of noise used to degrade the ship measurements. Similarly, increases in the number of ship reports can be examined by including "logbook reports" in addition to those observations reported on GTS. The sensitivity of ship-satellite comparison results to the quantity and quality of ship data can then be quantitatively assessed. These simulations could identify specific regions where small increases in the quantity or quality of timely ship reports could increase the precision or significance of the comparison results. The benefits of re-analysis after logbook reports become available can be investigated.

While the various binned analysis statistics (section 3.2) should be computed and compared in all regions, differing wind characteristics could result in different statistics being most illuminating in different regions. Simulations with several deliberately introduced satellite errors could be used to identify those comparisons/regions that are both sensitive and reliable.

Finally, the simulation experiments will allow for pre-launch development and testing of the analysis procedures and algorithms to be used for validation of ERS-1 measurements.

4. CONCLUSIONS & RECOMMENDATIONS

4.1 Available environmental data should be used for validation of ERS-1 measurements because it covers a wider range of geophysical conditions than any other technique. The resources required for such validation are modest.

4.2 Available environmental data is not well suited for calibration purposes because it does not necessarily provide information which covers the full operating characteristics of the instrument (i.e. for scatterometry, the full range of incidence angles).

4.3 The analysis techniques adopted must take into account the quality of the available data both in terms of distribution and accuracy. Preliminary studies have demonstrated quantitatively that two classes of statistical technique will be feasible using particular data sets. These are the "paired analysis" and "binned analysis" techniques.

4.4 Paired analysis requires near coincidence of ERS-1 satellite and in-situ data. Suitable validation data are provided by buoys and similar fixed platforms which report frequently. Enough data are available for meaningful validation during the commissioning phase, however, the actual number will vary depending on the phase of the ERS-1 orbit.

4.5 Binned analysis does not require co-location of ERS-1 and in-situ data pairs. It is appropriate for use with ship observations which are available at intervals of six hours or more from any one platform. The quality of these data are such that only limited validation will be possible during the commissioning phase. However, because of the large range of geophysical conditions sampled by these data, they must be included in the longer term validation exercise.

4.6 Data from other satellites should only be used for validation if it is obtained from sensors which have already been fully calibrated and validated. Potentially useful data will be available from the SSM/I on DMSP (and later NROSS) and from Geosat Altimeter (if still working). Both paired and binned analysis techniques should be used as appropriate.

Action on the following recommendations should commence as soon as possible:

4.7 The statistical characteristics of each in-situ data set must have been determined prior to its use in validation. In particular, any systematic biases must have been detected and understood so that adequate correction can be made.

4.8 Adequate arrangements must be made before the ERS-1 launch to ensure that in-situ data will be rapidly available to the validation teams (within 2 weeks of observation is thought to be adequate).

4.9 To determine the extent and characteristics of the data required for validation (and hence minimise the implementation costs) it is recommended that a suitable simulation exercise be undertaken. Such simulations would also determine whether direct measures to improve the quality or availability of in-situ data would be cost-effective. The detailed validation procedures deployed and tested during the exercise would then be available for implementation prior to the commissioning phase.

REFERENCES

Hogben, N., Lumb. T.E. 1967: "Ocean Wave Statistics"
Her Majesty's Stationary Office, 263 pp

Jardine, T.P. 1979: "The reliability of visually observed wave heights". Coastal Engineering, 3, 33-38

Laing, A.K., 1985: "An assessment of wave observations from ships in Southern oceans". JCAM 24(5) 481-494

WMO 1981: Commission for Marine Meteorology (VIII), Hamburg,
Final Report, Recommendation 8, and CMM/VIII/Doc. 5, Appendix D

Chelton, D. and McCabe, P.J., 1985: "A review of satellite altimeter measurement of sea surface wind speed with a proposed new algorithm, J. Geophys. Res., 90, CS 4707-4720

Brown, P.J. 1982. Multivariate Calibration
J. Roy. Statist. Soc. B, 44(3), 287/321

Freilich, M.H. 1986. Satellite Scatterometer Comparisons with Surface Measurements: Techniques and Seasat Results.
This volume.

Theobald, C.M. and Mallinson, J.R., 1978. Comparative Calibration, Linear Structural Relationships and Congeneric Measurements.
Biometrics, 34, 39-45.

REPORT OF WORKING GROUP 3

THE COORDINATION OF EXISTING RESEARCH PLATFORMS – THE IDENTIFICATION OF SPECIAL OBSERVING PERIODS FOR ERS-1 RELATED MEASUREMENTS BY RESEARCH PLATFORMS ENGAGED IN OTHER TASKS

N C Flemming *(Chairman)*
J Wilkerson
S A Hsu
P Queffeulou
S Zecchetto
D Offiler
I Barton
C R Francis
P Smith
A Kjelaas
W Wijmans

2. INTRODUCTION

The following types of research platform were considered: tide gauges, moored buoys, research ships, oil rigs, drifting buoys, research towers or platforms, research aircraft, military aircraft, lightships, weatherships, ground wave HF radar, skywave radar and microwave radar.

It is assumed that the deployment of instruments and choice of cruise tracks is not influenced by the requirements of ERS-1. It is probable that we can influence the rate of observation, data recording, precision of calibration, and rate of transmission of data from the relevant platforms during the 3-month calibration phase. It is also important that all procedures and techniques are agreed well in advance so that experimental runs can be carried out about 1 year before launch.

Examples were cited of calibration exercises for SEASAT and GEOSAT. Inorder to allow for final utilisation of the data it is assumed that about 60 days will be available for data acquisition for ERS-1. During this time data from relevant platforms must be transmitted to the ERS-1 comparison/calibration team within a few hours to a few days. Maximum acceptable delay is 14 days. Data which are going to be assimilated into numerical models would have to be transmitted in real time.

3. INVENTORY OF PLATFORMS

Some inventories of platforms and sensor locations already exist. RAL, England, are undertaking an exercise to collate data on platform positions, ships, campaigns, and institutes. IOC and IODE publish global lists of some types of platforms, and mational cruise plans are published by numerous states, and collated by IOC. It was agreed that N.C. Flemming would provide copies of published inventories to David Offiler at the UK Met. Office.

Action: Flemming

As a rough estimate of numbers of platforms, the following figures were compiled:

	Global Estimate
Wave sensors, non-directional and directional	200
Moored meteorological buoys	150
Drifting buoys, (SST and Barometric Pressure)	?
Microwave radar	2-5
Recording tide gauge stations	740
Airborne sensors, research aircraft	10
Ground wave HF radar	20
Skywave radar	2-5
Weather ships ... possibly defunct as data sources	1-2
Light ships ......probably defunct as data sources	0
Towers and oil rigs, approximate	50
Research ships, approximate	200
Military aircraft making met. measurements, guess	5

Notes on the above list:

a) A catalogue of wave sensors can be provided by the Responsible National Oceanographic Data Centre of IOC.
b) A catalogue of tide gauge stations has been published by IOC.
c) USA, Canada, Britain, France, and Germany have made presentations at this meeting on meteorological flight facilities. There are probably other groups who could support if required. (Annex 1)
d) Ground wave radar experiments measuring waves and currents have been conducted in USA, Australia, UK, France, Norway and Italy. Equipments have been installed on some commercial oil rigs. Microwave radar equipment has been installed on some Norwegian oil rigs. (See also Annex 2)
e) Skywave radar has been used experimentally in UK and USA, but is almost operational in Australia. So far wind direction only has been published in a grid of about 50 km. Wind speed accuracy may not be sufficient to serve as a calibration data set for ERS-1, but associated in-situ validation data may also be available.
f) Commercial oil platforms off-shore in most countries provide some met. and wave data to the national meteorological service on line. Wind data and sea surface temperature are most commonly transmitted; measured wave data are

less common, and are sometimes classified as commercially confidential.

g) Research ship cruise plans are usually published at national level 1 year in advance, although actual cruise out-turn is somewhat different. The world list of research ships is available from the World Data Centre (Oceanography) A, in annual published form. UK NODC will try to get a world list of cruises for 1984 or 1985, so as to compile a catalogue of total track miles sailed by research ships, and the sea areas most densely studied.
   Action: Flemming
   The USA can provide an annual forecast list of planned cruises by US institutes, universities, and military research vessels, known as the UNOLS inventory.
   Action: Wilkerson
   IODE records all past cruises through ROSCOP forms, and computerised inventories of these forms have been compiled at some data centres. It should be possible to search these inventories to produce a catalogue of past ship time per Marsden square.
   Action: Flemming
h) Norway suggests that low level meteorological data from P3 military aircraft could be available. Delegates from other countries were uncertain as to whether data could be obtained from military sources. Unclassified data on meteorological data near hurricanes are available from US military sources in the hurricane season.
i) The use of FFT analysis of conventional ships' radar images to extract wave spectra was discussed. This analysis cannot produce Hs. It is also not suitable for on-line processing on board ships in real time, which would be required for ERS-1 calibration.
j) US (NOAA) have designed hurricane meteorological buoys which are air dropped into the path of a hurricane, and subsequently retrieved. The data are in the public domain.

It was agreed that Delegates from all ERS-1 participating states would be requested to compile national lists of routine research and operational data platforms which they consider could most usefully and reliably provide data in near real time, or via the GTS. The co-ordinates of platforms should be provided with an accuracy of 1 km, or 0.01 degrees of arc.
Action: All

The volume of data produced by all the sensors listed above, and the problems of transmission, quality control, and compatibility of data sets, result in the necessity to be selective. Although all the data are potentially interesting given sufficient quality control- only a subset will be of sufficient value to warrant detailed attention by the comparison/validation team.

All research ship cruise data should be treated as potentially relevant, and no ship or geographical area should be ruled out in advance. Priorities can be established nearer the commissioning phase, if it is apparent that certain ships are going to be in key areas.

The phase of orbits during the commissioning phase should be published as early as possible in 1986 or 1987, so that the oceanographic community can become thoroughly familiar with the orbit pattern in the vicinity of major institutions, data gathering networks, or cruise tracks.
Action: ESA

Conventional oceanographic and met. data should be obtained from as wide a range of environmental conditions as possible. A special effort should be made to obtain data from observation platforms in the following areas:

a) Polar seas (Norway, Canada, Denmark/Greenland, Australia, USA)
b) Tropical seas (USA/Hawaii, Guam, Australian SAVE project, El Nino Projects, EPOCS, TOGA). (Annex 3)
c) Mediterranean Area (Italy). (Annex 4)
d) Gulf of Alaska and Gulf of Mexico (USA).

Research and operational data from the northern mid-latitudes will be available in quantity, and there is no special need to emphasise the data gathering. Nevertheless, special attention should be paid to the routes of fast data transmission from all areas. The North Sea is a special case since it is geophysically unsuitable for (generally applicable) calibration exercises, and yet there will be a great deal of interest in trying to use remote sensed data in the North Sea during the Operational Phase. (See Annex 5)

In-situ data platforms should not be closer than 100 km to land for calibration of the scatterometer, and not closer than 50-20 km for altimeter data channels.

Major international oceanographic projects, such as TOGA, GLOSS, EPOCS, POEM and WOCE will result in greatly increased rates of data gathering, and improved methods of data transmission during the next 5 years. ESA should maintain close contact with the scientific committees of these projects, and with CCCO and IOC to maximise the chance that data gathering systems will support the calibration exercise.
Action: ESA

UK Met. Office agreed to run simulated ERS-1 orbits with various phases against maps of known sensor platform distribution, so as to compute the numbers of potential "hits" per day.
Action: Offiler

Criteria for elimination of unsuitable platforms as above. Criteria for a "hit" to be within 100 km and 2 hours of overflight for scatterometer; 50 km and 1 hour for radar altimeter. Later simulations can be run using different "hit" criteria for different regions and environmental conditions, or different orbit repeat times or phase.

The previous sections indicate that there are about 1200 research data platforms world wide, including some high quality operational platforms providing data for oil operations and meteorological services, which can potentially provide data of suitable quality for calibration. This large data set is potentially available for monitoring before and after the commissioning phase. Instrument types are changing, data transmission rates, and data storage capacities are continually increasing. Through contacts with the major oceanographic research programmes, and with individual institutes, ERS-1 scientists should seek to influence data collecting methods towards more closely spaced temporal sampling strategies.

4. HARMONISATION OF FORMATS AND DATA

Since the platforms under discussion are not dedicated to ERS-1 support, the data formats will be variable, fixed in advance by the operators, and not necessarily compatible. The objective for ERS-1 should be to ensure that data are converted into a common compatible format before delivery to the comparison/calibration team.

In addition to individual formats preferred by data originators, some large programmes will have already agreed upon standard formats, and ERS-1 cannot expect to ask these programmes to alter their formats.

Data will reach the comparison/validation team by three different routes: real-time data of low volume can be transmitted via the GTS, provided that suitable codes and formats exist; near real-time data (days to weeks) can be transmitted either electronically via PSS or other networks; or via mailed recording media such as tape or optical disk. GTS already accepts XBT and sea level data in delayed mode, and codes and formats are being developed for Hs-Tz wave data statistics and spectral statistics. For non-GTS transmission, IODE has developed the GF3 data format (Annex 6), which is suitable for bulk data sets in non-real time.

Research oceanographic data at present is transmitted through the IGOSS programme in real time using GTS. Non-real time data are transmitted in the originators' format (or sometimes GF3) to National Oceanographic Data Centres, which exist in about 35 countries. NODCs apply quality control to incoming data, and provide subsequent exchange facilities with other data centres, or with the World Data Centres for Oceanography. The official format for all data exchanges between NODCs is GF3. It is logical that, in order to achieve a standard format for incoming oceanographic data, the ERS-1 comparison/validation team should use GF3. Manuals on GF3 have been published, together with training and instructional materials, demonstration tapes, and software to assist in reading GF3 tapes, useable on most mainframe computers. Information on GF3 will be provided to ESA.

Action: Flemming

IGOSS oceanographic data are received at designated NODCs and SOCs for archiving. Thus teams already exist who are familiar with both GTS codes and archival and exchange formats, such as GF3. The experience of these groups should be used where possible.

Various oceanographic parameters, including drifting buoy data, are being transmitted from various European platforms to Darmstadt, via Meteosat, and hence into the GTS. It follows that GTS codes already exist for a range of oceanographic parameters. These should be checked.

Action: ESA

5. DATA BANKING AND QUALITY CONTROL

Primary quality control of oceanographic research data is conducted by the data originators, and by the regional or national NODCs upon receipt of data. Data transmitted via GTS will only receive the orginators' quality control. Most NODCs apply standard quality control procedures, and these should be collated and provided in summary form for the ERS-1 comparison/validation team. Principle NODCs are requested to provide this information.

Action: National Representatives

Data documentation must be provided fully to the NODCs, including type and resolution of sensors, sampling rate, averaging period, scalar or vector average height of anemometer, sea surface and air temperature, surface barometric pressure exposure or sheltering of wave sensors, types of mooring, water depth at measuring location etc. Although this information is vital in order to ensure that the data are of adequate quality, it is not necessary to burden the ERS-1 comparison/ validation team with so much text documentation with every record. A summary of quality control and documentation are provided in the GF3 format as tape or file header information, and these should be checked by a data acquisition group before transmission to the comparison/validation team. The minimum information transmitted with each record is an identifier of origin so that any data can be checked back through the system if there are queries.

In general, NODC data management practice is not to alter values. Data may be screened, flagged, marked as of high or low quality, but values are not altered, improved, smoothed, or gap-filled. The correction of anemometer readings for heights is a special case. It was agreed that wind data should be presented to the comparison/validation team corrected to 10 m height and neutral stability. NODCs are not familiar with this procedure, and if it were done by national Met. Services, there would have to be an agreed standard algorithm.

It was agreed that a small team would be needed, provisionally entitled "Intermediate Oceanographic Data Collection Centre" to collate data from national Met. Services and NODCs, screen it, and provide it to the comparison/validation team with a minimum of site-specific information to avoid overloading the system.

The tasks of this group would be as follows:

(i) Active chasing of data sources, and collation of data sources and documentation.
(ii) Conversion of data into a common format if not already in GF3, and extraction of subsets of the data for use by the comparison/validation team.
(iii) Conversion of the wind subset to 10 m and neutral stability values.
(iv) Screening of the quality control information, and gross checks on data values.
(v) Addition of source code to each record passed to the comparison/validation team, and addition of a quality assessment label.

Where possible, information on the standard deviation of wind data should be made available, so that comparisons can be made taking this factor into account.

The data transmission and quality control procedures should be rehearsed one year prior to launch.

6. POTENTIAL SIZE OF THE DATA SET

The entire data set from over 1000 sensors will be very large, and most of it will be retained in archival centres, either Meteorological Services or NODCs. Subsets will be extracted and transferred rapidly to the Intermediate Oceanographic Data Collection Centre, from which a smaller subset should provide a number of direct "hits", with co-location in time and space of in-situ and remote sensed data measurements. It is important to assess the total number of probable "hits" during the commissioning phase, since this determines the value of trying to utilise routine research data sources. The probable number of "hits" also determines the volume of data to be processed by the ERS-1 teams, and hence the effort available to ensure high quality for each comparison.

A simulation by the UK Met. Office for the scatterometer, using reported marine met. data, acceptable co-location to within 100 km and 2 hours, excluding in-situ data within 50 km of the coast, produced 10 "hits" in one day. The radar altimeter can be used closer to the coast, making more in-situ platforms relevant, but the footprint is smaller, making co-location less likely. The number of "hits" for the altimeter should be of the same order of magnitude or higher than the scatterometer, since data of value may be obtained for both wave data and sea-level measurements. If we assume that the total number of "hits" for all sensors and instruments is 20 per day for 60 days, this produces a total number of paired data points of 1200.

Simulated orbits and identification of probable "hit" sites would appear to indicate that of the order of 20 sites can be identified well in advance from which data will be requested very rapidly at predictable times. (This excludes ship data). It will therefore be possible for the "Intermediate Oceanographic Data Collection Centre" to establish personal contact with these data originators, and ensure that data are submitted rapidly. It is recommended that all wind/wave data from the selected sources during the commissioning phase should be transmitted to the "Intermediate Oceanographic Data Collection Centre" with appropriate documentation.

7. TYPES OF MEASUREMENT

Since the in-situ sites of most probable value can be identified in advance, it is important to ensure that these instruments are not out of action during the commissioning phase. Contact should be maintained with operating agencies to check maintenance schedules, replacement dates, etc. Whenever possible the operating agencies should be requested to operate instruments at a high data rate or even continuous measurement, during the commissioning phase. This would greatly increase the chances of "hits".

It is anticipated that 90% of wave data will be non-directional. Wave data sampling is usually based on a 20-minute sample every 3 hours, though this has now been increased to 20 minutes every hour for some US buoys, and 33 minutes every hour for some French buoys. HF ground wave radar systems are usually operated for 30 minutes every hour, and microwave radar 20 minutes every hours. All Delegates are requested to send information on sampling rates to David Offiler for inclusion in the simulation of potential "hits".
Action: All

Wind data are usually sampled with one 10 minute average every hour. An essential feature of the required documentation is anemometer height. Ships and oil rigs usually have the anemometer mounted 20-60 m above sea level. The larger US buoys mostly have mountings at 10 m; the UK large data buoys are approximately 8-10 m; most other buoys are only 3-5 m (Norway, UK, Australia). All Delegates are requested to send information on buoy mast anemometer heights to David Offiler for inclusion in the inventory of in-situ platforms. Where possible research ships shall be encouraged to obtain quality wind data, and contribute data in real time. The ideal wind data would consist of a continuous record of one minute averages, but a compromise of 5 x 10 minutes averages per hour would be extremely useful.

8. ASSESSMENT OF FEASIBILITY AND USEFULNESS

The probable number of "hits" makes the use of the routine research oceanographic data an attractive programme. The previous discussion indicates that it is feasible, provided that there is plenty of advance preparation, rehearsal of transmission and quality control procedures, and familiarisation with formats. As a management aid, it would be useful to draw up a general matrix showing instrument/platform types, numbers of sensors, relevance of data types, accuracy, regional and environmental relevance, chances of a "hit" etc.

ANNEX I

1. NORDA conducts a major ship or a ship/aircraft experiment each year. Experiments are planned 2-3 years in advance, with funding approval usually 1-1½ years in advance. Most of these exercises have occured near strategic straits. Most recently NORDA has been investigating oceanographic conditions in the Alboran Sea, east of Gibraltar. These experiments seek to determine the density structures and associated hydro-dynamics related to eddies and boundary currents, such as the Gulf Stream. Measurements include traditional XBT, AXBT and CTD data collection.

2. The Naval Oceanographic Office employs (3) research aircraft for the purpose of routinely conducting oceanographic surveys. While the wind direction and speed data collected by these aircraft are suspect, the wave information is quite useful (as obtained by laser altimeter). The wave number spectra could be very useful.

ANNEX 2

HF Radar Studies

(a) COSRAD coastal radar which gives sea state out to 30 km from the shore will be operated from the Queensland coast for an extended period after ERS-1 launch. Accuracies are: wind velocity ± 3 m sec^{-1} and ± 10°, wave height ± 0.15 m and surface current 0.02 m sec^{-1}. The radar will be located to give a maximum number of coincidences with ERS-1.

data. A buoy giving supporting in-situ measurements will be deployed in the study area. Experiments on microwave scattering of long sea waves are planned.

(b) Data from JINDALEE skywave radar will be compared with ERS-1 wind wave measurements throughout the lifetime of the satellite. The radar has a coverage of 10^6 km^2 in the oceans between Australia and Indonesia. In-situ measurements will be made for further validation.

ANNEX 3

SAVE

Validation of the ATSR product in tropical waters to the North-East of Australia. SAVE will include aircraft and several vessels measuring SST and various meteorological parameters during the 3-month commissioning phase of ERS-1. Two or three concentrated periods of two weeks each are envisaged. Buoys may be deployed in the deep ocean and various platforms on The Barrier Reef will be instrumented. These measurements may be part of a programme studying the heat budget of tropical oceans.

Tropical Campaigns as part of TOGA

These include modelling of SST variations North of Australia; careful instrumentation of ships of opportunity to give data in the tropical West Pacific, and ENSO studies.

Wind/Wave Validation in Tropical Areas

In the past, validation of satellite products in tropical areas has proved most difficult due to the lack of ground truth data at low latitudes. There are several reasons for this, including:

(i) Drifting buoys deployed in tropical areas tend to quickly migrate to middle latitudes.

(ii) The lack of general shipping lanes crossing the equator.

(iii) The lack of developed countries interested in oceanography that are located in the tropics.

(iv) The increased cost of oceanographic campaigns that require the transit of aircraft and ships, that are based at middle and high latitudes, to the tropics.

This lack of good tropical data in the past has severely hindered the validation of operational SST measurements from satellites i.e. the algorithms have been most thoroughly validated from 0-25°C, but not so well above 25°C sea surface temperature. Therefore every effort should be made to ensure that sufficient in-situ data are available to ensure a useful validation of ERS-1 wind/wave products in tropical areas.

ANNEX 4

The Existing Geophysical In-Situ Data Network on the Italian Waters

Up to now (1986) there are three different sources collecting in-situ data off-shore the Italian coasts. Their position along with the nominal three days repeat orbits and scatterometer swaths is shown in Fig. 1. They are:

. ENI (National Oil Company) platform network on Adriatic Sea and Sicily Channel. Some of these towers (4-5) are provided with meteorological stations (wind speed and direction, air temperature, humidity) and with wave ganges to get directional and power sea height spectrum.

. ENEL (National Electric Company) has a series of non-directional buoys and one directional close to Italian coasts. On land, just on face to each buoy, there is a meteorological station.

. Some of research institutes and universities operate wave and/or meteo ganges. The main facilities are:

- the C.N.R research tower off the Venice coast (meteo/ocean parameters).
- the C.N.R. meteo buoy off Genova.
- the University of Genova automatic move gange close to Genova coast
- the University of Torino mobile radar systems

Up to now data are collected separately by each courier. Nevertheless, due to the companies' interest, there should be no problem in reaching an agreement to publish data.

Furthermore a global on-line data acquisition can be foreseen, due to the relative inexpensiveness of this, and other ENI towers can be provided with meto/ocean instruments according to the satellite ground tracks and the sensor to be validated.

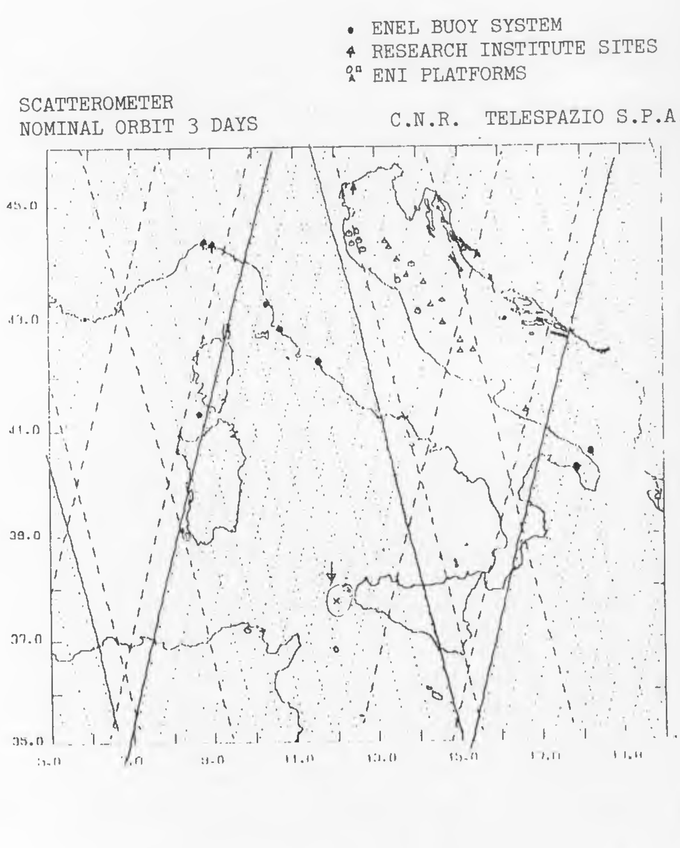

ANNEX 5

Because of the high degree of interest for various reasons of its neighbouring countries, the North Sea has been highly instrumented, making it attractive for ERS-1 calibration and validation campaigns. Instruments mounted on fixed platforms on strategically selected locations in the Dutch, German, UK and Norwegian areas, provide for wind, waves, air/sea temperature, barometric pressure, tide measurements available in quasi-real time.

However, the North Sea is also considered a special case because of:

- the difficulty to use ERS-1 measurements due to land proximity
- its semi-enclosed nature and shallow depth giving rise to special bottom-sea-air-interaction rules.

For the local scientific community this makes it all the more interesting and necessary to derive a calibration data set, particularly applicable for the ERS-1 measurements to the North Sea.

ANNEX 6

The GF-3 format is fully described in "The IOC General Magnetic Tape Format for the International Exchange of Oceanographic Data, Part 3: Introductory Guide to GF-3", published by Intergovernmental Oceanographic Commission. A descriptive introduction from this guide is reproduced below.

GF-3 is a general purpose format scheme which has been developed for use in the exchange of data within the environmental data. It is a highly flexible, self-documenting magnetic tape system designed primarily for numerical data. It is not, however, restricted to numerical data, as the variety of structures available permit the inclusion of textual information in several ways. The scheme was developed to facilitate the exchange and dissemination of many types of oceanographic data, ranging from the most simple cases to complex multidisciplinary datasets. For certain types of data such as project datasets, however, GF-3 could be the most logical archival format.
GF-3 is not recommended as a real time telecommunications format. It was not designed to be efficient for such a carrier.

The GF-3 format system was developed to meet a number of specifications.

1. The format was to consist of rather simple structures so that it could be used by single scientific users and small institutions, as well as large data centers.
2. The format was to be largely self-documenting through the provision of "plain language comment" capabilities at all levels of the structure and through inclusion of formatting information and character coding information on the tape.
3. The format was to be capable of being processed automatically by the user or data centre receiving tape.
4. The structures of the format were to be capable of transmitting complex multi-disciplinary datasets, as well as the most simple sets.
5. The format was to be a magnetic tape format for the exchange of data and in many cases was to be suitable for archiving of these data.

GF-3 has been designed to facilitate automatic processing. The self-documenting aspect of the system is one of its more useful and elegant features. To the user receiving a GF-3 tape, this means that foreknowledge of the detailed formatting is not required. All the necessary information to interpret and understand the contents of the tape is included on the tape in fixed positions in the various record structures. Only the recording density and the fact that the tape is in the GF-3 format need to be known in advance.
The flexibility of the format results from the variety and number of possible usages and combinations of the GF-3 record types. This makes it possible to include, within the format scheme, structures from the very simple to those which can contain multidisciplinary data with several levels of hierarchy. It has been found possible to encode in GF-3 physical, chemical, biological, geological, meteorological, and geophysical data.

CONCLUSIONS AND RECOMMENDATIONS

Conclusions

The use of high quality research and operational met-ocean data for ERS-1 calibration and validation is feasible. The data can be obtained using largely existing data handling procedures and organisations, with special attention to speed of delivery and quality control.

The approach is a low cost, low risk, and robust method, which should produce consistent data volumes independent of orbit changes or changes in launch date.

These data should provide of the order of 1000 paired values of in-situ and ERS-1 values within a 60-day period, and should be used. The location of the in-situ data sites cannot be planned to cover all environmental extremes.

The Working Group has identified a necessary function which has to be performed between the existing data sources and the ERS-1 calibration/validation team. This function consists of:

(i) Chasing data sources and ensuring transmission of data and documentation in time.
(ii) Conversion of data into a common format if not already in GF3, and extracting subsets of the data for use by the calibration/validation team.
(iii) Conversion of the wind subset to 10 m anemometer height and neutral stability values.
(iv) Screening of the quality control information, and gross checks on data values.

Recommendations

Data from existing research platforms and high quality operational platforms should be used in the calibration of ERS-1.
In-situ management of the met-ocean data requires a management and data processing function before the data are passed to the calibration/validation team, and the Working Group recommend that this

work should be carried out. The work involves maintenance of standard formats, quality control procedures, ensuring timely delivery and documentation of data for the calibration/ validation team.

Catalogues should be established of research platforms and ships and ship-cruise plans, including details of the platforms such as data channels recorded, sampling intervals, averaging periods, accuracy, quality control procedures, and means of transmitting data.

A quality control standard is needed. Initially a survey should be conductged of the present best practices in quality control of met-ocean data, and the results of this survey should be used to improve the quality control, if necessary, of source data platforms. Documentation on quality control procedures should be made available to the calibration/validation team.

The phase of the orbit of ERS-1 should be published as early as possible, preferably in 1986-87, so that in-situ data sites can be predicted.

Contact should be established with the most probable data sources two years in advance of launch, and there should be a complete rehearsal of data delivery procedures one year in advance of launch.

Data originators should be encouraged to use the standard systems of data transmissions, including the GTS, IGOSS procedures, and the assistance of NODCs to convert data to GF3 format, either for transmission by electronic means, or by mailed tapes or disks.

Close co-operation should be maintained with the scientific plans and procedures developed for the major internal oceanographic projects such as WOCE, TOGA, EPOCS, etc., since these groups share common interests in improving the coverage of data gathering sites, and increasing the speed of delivery of data products.

LIST OF ACRONYMS

CCCO	Committee for Climatic Change in the Ocean
EPOCS	Equatorial Pacific Oceanographic Survey
GF3	General Format -3, standard international format for oceanographic data exchange between data centres
GLOSS	Global Sea Level System
GTS	Global Telecommunication Service
IGOSS	International Global Oceanographic Service System
IOC	Intergovernmental Oceanographic Commission
IODE	International Oceanographic Data Exchange
NOAA	National Oceanographic and Atmospheric Administration
NODC	National Oceanographic Data Centre
NORDA	Navy Oceanographic Research and Development Agency
POEM	Physical Oceanography of the Eastern Mediterranean
RAL	Rutherford Appleton Laboratory
ROSCOP	Report of Oceanographic Scientific Observing Project
SAVE	Satellite Validation on Experiment (Australia)
TOGA	Tropical Ocean Global Atmosphere (Programme)
UNOLS	University Oceanographic Laboratories
WOCE	World Ocean Global Atmosphere (Programme)

REPORT OF WORKING GROUP 4

FEASIBILITY OF A DEDICATED, FLEXIBLE, MOBILE CALIBRATION TASK-FORCE

A Cavanie *(Chairman)*
R J Powell
E Attema
R Bernard
R Ezraty
H Finkenzeller
N G Freeman
L Krul
V Wismann
M Srokosz
W Oost

1. OBJECTIVES OF THE TASK FORCE

In-situ and remote measurements and processing necessary for verification and initial post-launch tuning of F.D. products (significant waveheight and windspeed from the altimeter, wind vectors from the scatterometer, AMI wave mode spectrum).

A wave mode verification campaign, within the same period, on the Western side of the N. Atlantic is being planned by U.S./Canadian investigators.

2. TIME LIMITS

Measurements to be made during the three-month commissioning phase; comparison with ERS-1 data to be completed one month later.

3. GEOGRAPHICAL LOCATION

Two sites, one in the Northern hemisphere (about 56°N and 15 to 24°W, to take advantage of cross-over points), the other in the Southern hemisphere (west of New Zealand or Chile or Australia and south of 45°S) are to be pre-selected. One will be maintained as a function of launch date. In the case of a Northern hemisphere Summer launch it will be necessary to operate in the Southern hemisphere to ensure a sufficient range of geophysical conditions.

Sea surface temperature effects must also be considered; this suggests that a third, warm water, site would be advantageous.

The areas chosen should be devoid of strong gradients in currents or sea surface temperature.

Some instrumentation will gather data more efficiently if deployed to take into account the satellite cross-over points. Ideally for the Northern hemisphere site phasing of the ERS-1 orbit should be such that a cross-over point exists approximately at 56°N and 15°W.

4. WHAT IS REQUIRED

Instrumented ships, buoys and aircraft are the main source of data recommended, although other instrumentation (sky-wave radars and other satellites) may prove useful in data selection and analysis.

These platforms should carry out the following tasks:

- Ships:
  - Put out, tend and retrieve buoy networks
  - Cross-calibrate the buoys
  - Measure T_a, T_s, humidity, wind vector, cloud cover, precipitation.
  - Receive data from radio transmitting waverider or pitch and roll buoys.
  - Inform airplanes of local conditions
- Buoys:
  - Measure wind speed and direction
  - Measure heave spectrum
  - Pitch and roll directional spectrum information (VHF transmission to ship). (All other data is to be transmitted via satellite).
- Aircraft :
  - Radar Altimeter, $H^1/_3$
  - Directional wave spectra (ROWS, SCR, SLAR)
  - Navigation - extracted winds at altitudes of 30 and 100 meters.
  - Scatterometer winds
  - Sea surface temperature
  - Air temperature

5. WHAT IS AVAILABLE

- Research ship time: 1 month (France) possibly 3 months (The Netherlands)
- Chartered: Ship: Possible.
- Buoys: 7 ARGOS Waveriders, 1 pitch and roll (France) tested proto-type ARGOS wind buoy - France - (7 to be purchased).
- Aircraft :
  - . Possible French, German and English Meteorologicalairplanes to measure navigation winds.
  - . NASA instrumented aircraft to be sought by ESA

- P3 with ROWS, Laser Profilometer, SCR
- DC8
- C130

However, these aircrafts may be committed to the Western Atlantic Campaign.

. Other specialised aircrafts are available for charter.

- Aircraft /: Instrumentation
  . French, Dutch, U.K., German, C-Band Scatterometers
  . U.K. rader altimeter and ROWS

6. IDENTIFICATION OF CONSTRAINTS

Finances

- Wind buoy with mooring 40.000 $ (7 required)
- Chartered ship 3 to 8.000 $/day
- Chartered aircraft 200 to 800.000 $ for a 90-day campaign
- Operational overhead will be much larger for a Southern hemisphere than for a Northern hemisphere campaign involving European groups.

Scheduling (Lead Time)

Two weeks using a chartered fishing vessel. In contrast, research vessels have a required schedule fixed one to two years in advance. Aircraft should be scheduled on a preliminary basis one to two years ahead, and a firm commitment should be made six months in advance.

Logistics

To be determined.

Availability of In-Situ Data

Two weeks after measurements.

Optimum Locations

56 to 60 N or S for buoy networks (satellite coverage)

- West of Scotland, 56 N and 15 to 24 W (climatology, logistics)
- West of Chile, New Zealand, Australia (climatology, possible collaboration).
- These sites are proposed recognizing that a SAR-oriented calibration experiment is planned for ERS-1 in the Labrador Sea.

Base of Operation

To be determined.

Collaboration

- To be sought with all institutes having a potential to contribute to the calibration effort. Special effort should be made to establish collaboration with institutes in the Southern hemisphere (Australia, New Zealand, South Africa, South America).
- ESA should urge COST-43 to upgrade its buoys to measure winds at the time of ERS-1 launch, as a complement to our effort.
- Close links have to be developed with the US/Canada group carrying out the Western Atlantic campaign, both with planning and data interpretation.

7. ASSESSMENT OF FEASIBILITY AND USEFULNESS

- All key instrumentation proposed will have been tested and used in a pre-launch experiment. Most instruments exist and have been used previously. Also data gathering and processing procedures required to meet the schedule must be tested.
- The number of measurements made over the three-month period are evaluated in the following table:

	Buoy Winds	Ship Winds	Aircraft Scat. Winds	Aircraft Nav. Winds
Scat. Winds	420	60	600	600
+ Labrador Sea			200	
Alt. Winds	120			
Stand Deviation	± .8 m/s	± .8 m/s	± 1.5 m/s	± 1.5 m/s

- Directional buoy measurements coincident with scatterometer meas. : 60
  Argos waveride buoy measurements coincident with AMI wave mode meas.: 360
  ROWS measurements coincident with AMI wave mode: 50
- In order to demonstrate that the amounts and types of data acquired will be sufficient, simulations of the use of this data as well as that from existing platforms will be necessary and are strongly recommended. Such an analysis should consider the use of data from all campaigns envisaged.
- Awaiting these simulations, we presently believe that the campaigns, as proposed, will meet the requirements of algorithm verification and initial post-launch tuning of F.D. products.

REPORT OF WORKING GROUP 5

THE IMAGE SPECTRUM/WAVE SPECTRUM PROBLEM: REQUIRED MEASUREMENTS

R C Beal *(Chairman)*
W Rosenthal
R Cordey
J-P Guignard
E Oriol
P Piau
P Trivero
I A Ward
L A Maron
J Perbos
A R Birks
S Bruzzi
C Cappa

1. INTRODUCTION

The European ERS-1, to be launched in 1990, will offer the first opportunity since the American SEASAT in 1978 to collect estimates of directional wave spectra over global scales. The collection of this data will be an important step in wave model validation and may also yield information on global directional wave climatology, particularly if the satellite operates over several seasons. SEASAT was able to operate only during the Northern summer, collecting imagery only in the vicinity of four Northern Hemisphere ground stations. Although three or four hurricanes were sampled during the life of the satellite, there was no opportunity to attempt tracking of major winter storms in the North Atlantic.

Notwithstanding the brief but important American SIR-B mission in 1984, ERS-1 will offer wave modelers a new opportunity to assess the value of SAR-estimated wave spectra for updating and improving wave forecasts. There are several reasons for the growing interest in the application of global wave spectra. Not only are the measurements potentially valuable for model validation, but they may also be important for correcting scatterometer wind estimates. In other words, ignorance of an initial estimate of the wave field may create a bias in the wind field estimate, in turn rendering the model-derived wave fields considerably less reliable.

Although the sparsely-sampled ERS-1 Wave Spectra mode is designed to operate in conjunction with its scatterometer, validation and calibration exercises normally will be conducted with the full SAR imaging mode. In general, the full imaging mode is required whenever high intensity field validation measurements are collected, since a much larger number of independent spectral estimates can be collected during a single overpass.

Typically, one may collect as many as ten useful independent spectral estimates from an aircraft under-flight within an hour of the overpass. Moreover, spatial averaging of the full SAR mode over large areas (say 50 km on a side) can result in spectral density uncertainties, an order of magnitude less than might be present for a single spectral estimate in the wave mode. It is important therefore to give high priority to operating in the full SAR image mode whenever high intensity calibration and validation of the wave spectra occurs, even at the expense of omitting simultaneous scatterometer estimates of the wind field.

2. PRESENT STATUS OF RESEARCH

2.1 SAR Modulation Mechanisms

The modulation transfer function M that relates the SAR image spectrum to the wave spectrum can be modelled as a linear combination of three modulation transfer functions M_h, M_t and M_v corresponding to three modulation mechanisms. The first two, hydrodynamic modulation (due to small wave spectral modulation by larger scale waves), M_h, and tilt modulation (due to modulation of the angle with which the small-scale waves are presented to the radar), M_t, are both a maximum for range-travelling waves and fall-off with increasing azimuthal angle. The tilt-modulation mechanism is thought to be well-understood, but there are still some uncertainties about the nature of the fall-off of M_h, especially in situations of cross-winds where air-sea interactions modify the purely hydrodynamic effects on the spatial distribution of the small-scale waves.

The velocity-bunching mechanism (M_v) is an imaging mechanism unique to the synthetic aperture radar and is most effective for azimuthally propagating waves, with a minimum for range-travelling waves. However, this imaging mechanism remains linear only as long as the azimuthal shift Δx imposed by the radial component of the long wave orbital velocity remains much less than the long wave wavelength λ. This has the effect of imposing a minimum azimuthal wavelength that can be retrieved from the image-spectrum by applying a linear form of M_v and causes, in part, distortion of the derived two-dimensional wave-spectrum.

Another cause of this loss of resolution is thought to be the defocusing in the azimuthal-direction caused by the range component of the orbital acceleration of the long-waves, although some schools of thought attribute this to be the effects of the phase-velocity of the long waves, or the presence of waves with different

Proceedings of a Workshop on ERS-1 Wind and Wave Calibration, Schliersee, FRG, 2–6 June, 1986 (ESA SP-262, Sept. 1986)

phase-velocities, and the consequences of this for a system with a finite integration time.

Although there is dispute as to the causes of this spectral distortion in the azimuthal direction, there is no doubt that it exists. Thus, future work should be directed towards determining its dependence on sea-state and wind-conditions, and in developing methods for applying optimum corrections.

2.2 Automatic Techniques for Correction

A series of operations must be carried out on a raw SAR power spectrum before useful estimates of ocean wave parameters can be extracted.

The spectrum is attenuated at high frequencies by the finite resolution of the system and also contains an undesirable component due to speckle noise in the image. Removal of these two effects is cheap in terms of computer time and can, in principal, be carried out automatically.

Correction for finite resolution involves dividing the power spectrum by an appropriate transfer function which can be derived from the image point-spread function. Where this is unknown, a useful alternative is to fit the fall-off frequency of the speckle component, which is usually the dominant component of the image spectrum, and then to divide the whole spectrum by that fitted function.

Separation of signal and speckle components of the spectrum is achieved by a simple thresholding technique since the mean speckle component is now a uniform (white) background. Smoothing of the spectrum before thresholding allows better discrimination between the two components, each of which is noisy. The appropriate thresholding level to use can be derived automatically from the mean image intensity.

The spectrum at this point is that of a SAR image of ocean waves. The relationship between this and the ocean wave spectrum is, if imaging is a linear process, simply via a modulation transfer function (MTF) and inversion is a straightforward division by this (subject to some long-wave cut-off to avoid singularities introduced by the use of current MTFs near zero wavenumber). Such MTFs would, if imaging were independent of environmental parameters, require as inputs only known radar parameters (R/V, incidence angle). Calibration of the output spectra to absolute intensities (meters^4) is currently carried out by dividing through by the square of the mean backscattered intensity, since linear imaging theories predict that wave images are a modulation of that mean intensity. Techniques are not yet available for the recovery of information in cases where imaging is a non-linear process. Further investigations of what information can be recovered and methods for doing so quickly are clearly required.

2.3 Refinement of the Azimuth Transfer Function

In order to produce an acceptable wave mode product there are two, not necessarily exclusive, paths that could be taken to resolve the problem of the azimuth transfer function.

The first is a purely pragmatic/empirical approach to provide a correction procedure for the non-linear imaging situation. This would involve investigations using an airborne SAR with other sea-truth experiments to measure the fall-off of M_v with waveheight, or range-travelling component of waveheight, windspeed, or radar backscatter sigma-nought. Derived curves could be used to correct spectra which are only weakly non-linear, e.g. $\Delta x/\lambda \leqslant 0.5$, although such a technique has yet to be tested.

The second is a more fundamental approach involving experiments (SLAR or tower-based scatterometers) to measure M_h and M_t, under different sea and wind conditions, accompanied by theoretical investigations of:

a) the exact conditions for and nature of non-linear imaging with a view to forumulating a theory for the exact reconstruction of a non-linearly imaged spectrum, and

b) incorporation of non-Bragg scattering mechanisms (such as specular scattering and wedge diffraction) into current imaging theories, as these may be important for high sea-state or high wind conditions, and possibly produce a different form for the modulation transfer function.

Without an improvement in our understanding of the behaviour of the azimuth transfer function, we can consider only the range-travelling component of the wave spectrum as a reliable product under all sea-states and wind conditions. By following the empirical path, we may well be able to grade two dimensional spectra with quality flags assessed from studies of non-linearity effects on the two-dimensional spectrum as a function of range travelling component wave-height, sigma-nought and wind vector (all of which can be measured by ERS-1) simultaneous with or close to the wave-mode samples.

With a more complete understanding, afforded by further experimental research, we should hope to achieve confidence in an extended, but precisely limited, range of two-dimensional spectral.

2.4 Numerical Modelling

Further understanding of non-linear imaging can be gained by means of numerical simulations of SAR image spectra. For example, Alpers and his co-workers have investigated the imaging, based on current velocity-bunching ideas, of azimuthally-travelling waves, and have simulated one-dimensional spectra for a variety of sea states. They have extended their work to full two-dimensional simulations of actual datasets from the North Sea SIR-B experiment and these demonstrate the way in which azimuthal fall-off may occur and how SAR wave spectra can be rotated with respect to the actual spectra.

Such modelling is important in attempting to compare SAR and sea measurements when imaging is non-linear. From a measured two-dimensional wave spectrum, the numerical model can predict the theoretical SAR-spectrum. The comparison of the theoretical with the actual SAR-spectrum will improve our knowledge of the underlying mapping mechanism.

In particular, modelling will be of use, if and when we have confidence in the velocity-bunching imaging mechanism, in helping to identify situations in which we can hope to recover information on the azimuthal wave spectrum.

Once the non-linear mapping mechanism has been verified, the inverse transformation from the SAR-spectrum to the surface wave spectrum by numerical techniques has to be developed.

3. INTERIM PLANS FOR RESOLVING MAJOR ISSUES

3.1 Background

Significant progress in understanding SAR imaging mechanisms has occurred in the last few years, due in a large part to the calibrated data sets from the SEASAT (1978) and SIR-B (1984) analyses. It is now fairly clearly established that the motion of the Bragg scatterers on the surface of the ocean produces significant degradation of the SAR spectrum in the azimuth direction, as discussed above. However, several details of the azimuth degradation are not yet well understood, partly because the existing data has not yet been fully analysed, and partly because auxiliary comparisons with the associated environmental monitoring have been incomplete. Therefore, it seems prudent 1) to complete the analysis and interpretation of existing data, particularly the recent SIR-B and PROMESS data sets, and 2) to plan and execute one or two well-controlled field experiments specifically designed to resolve our existing uncertainties in the details of the azimuth transfer function.

3.2 SIR-B Data Set

The shuttle imaging radar, SIR-B, flew in October 1984. Horizontally-polarised L-band imagery was obtained at a 4-look resolution of about 30 meters with an R/V ratio of between 35 and 50 seconds.

The SIR-B mission produced at least three sets of wave data for which independent estimates of the directional spectrum are available. Two of these sets are supplemented by European buoy measurements; the other by a number of American aircraft measurements, including an SCR (Surface Contour Radar), a ROWS (Radar Ocean Wave Spectrometer), a laser altimeter, and a nadir-looking altimeter. Early results have already been reported, and we can expect more comprehensive results to emerge in the literature over the next two years or so. The SIR-B data (both European and American) occasionally show the effects of motion in the azimuth direction, either in the form of an apparent rotation of the dominant waves into the range direction, or in the more severe cases, obliteration of energy at the higher wave numbers. The problem is definitely more severe in higher seas, and is further aggrevated by increasing the satellite altitude.

The SIR-B experiment in the NE Atlantic, involving RAE, Farnborough (UK) and the Marconi Research Centre included measurement of sea state with directional and non-directional wavebuoys. Significant waveheights of less than 2.7 meters and dominant swell wavelengths of 200 meters were expected to result in SIR-B imagery <u>not</u> being significantly degraded by non-linear imaging. Two SIR-B data sets, obtained when waves were travelling close to range and azimuth directions respectively, were corrected with a theoretical linear MTF and compared quantitatively with the in-situ measurements.

The results suggest that, under the conditions of that experiment, our understanding of the MTF for range-travelling waves with scattering from HH polarisation is not enormously in error (buoys and SAR estimated values of H_s within 35% of each other). Our knowledge of the imaging mechanism for azimuth-travelling waves is however incomplete in that SAR spectral intensities were an order of magnitude weaker than expected from a linear velocity-bunching model.

3.3 PROMESS Data Analysis

The PROMESS data set, resulting from a comprehensive aircraft SAR campaign, is allowing study of the SAR modulation transfer function with R/V = 50 s and low-to-very-high sea states. A comparison is being made of the imaging mechanisms in C and X-band as they were recorded simultaneously in VV polarisation.

The problem of imaging of azimuth-travelling waves is emphasised as each measurement consists of crossing passes with different azimuth directions.

The use of four scatterometers allows one to know very accurately the level and angular variation of the backscattering coefficient at the time the SAR was flown. The air-sea stability was also measured.

So we may hope for new results this year about the SAR imaging of very high sea states, and of complicated seas with as much as three wave systems present at the same time.

From all of these experiments, however, several questions still remain. For example:

1) What is the exact dependence of the azimuth fall-off on sea state?

2) Since the smear is aggrevated by a broad velocity distribution of the small-scale (subresolution element) scatterers, should not the fall-off depend also on local windspeed and perhaps processed resolution?

3) Does the SAR modulation depend significantly on the local environment (wind, air-sea temperature difference, as well as sea state)?

4) Is range-to-velocity ratio (R/V) the dominant governing parameter to describe azimuth fall-off, or is there any significant contribution from the finite integration time?

Future investigations and analyses should be directed towards resolving these questions.

3.4 The Labrador Sea 1987 Extreme Waves Experiment

The Labrador Sea experiment will be an attempt to extend the results of the American SIR-B experiment off the coast of Chile into a region of high and actively developing waves.

Although the American SIR-B experiment off Chile was limited to sea states under 4.5 m, several important conclusions have already emerged:

1) The wave forecast model correctly predicted the mean directional energy properties of the wave field over the five-day period. However, there were substantial errors in wave height, wave length, and wave direction on a daily time scale.

2) The SAR spectra closely resembled surface slope spectra within a limited wave number range, and within this range, agreed closely with aircraft estimates of wave length, direction, and spectral width.

3) Although the SAR accurately detected and tracked long azimuth travelling waves, on at least two days out of the five, some distortion was introduced. On one of those days (the lowest sea state of the entire experiment) substantial azimuth energy was filtered out by the SAR azimuth fall-off. The exact character of this fall-off has yet to be resolved.

Further detailed comparisons are now underway for the entire five-day data set, and are expected to be essentially completed by the end of 1986. There were three serious limitations to the SIR-B data set, all of which will be addressed in the Labrador Sea Experiment:

1) Ocean wave heights greater than 4.5 m were not observed. In the Labrador Sea Experiment, there will be at least a 50% chance of observing wave fields between 6 and 8 meters.

2) In situ wave measurements were not performed. In the Labrador Sea Experiment, there will be various surface wind and wave measurements performed from ships and ship-deployed buoys.

3) The SAR operating frequency was limited to L-band, whereas many future orbiting SARs (SIR-C, ERS-1 and the proposed Spectrasat) will use C-band.

Addressing the three limitations encountered in the SIR-B experiment, the major components of the proposed Labrador Sea Extreme Waves Experiment are directed toward:

1) Including comprehensive measurements of in situ spectra from buoys, surface wind speed and direction, and both air and sea temperatures.

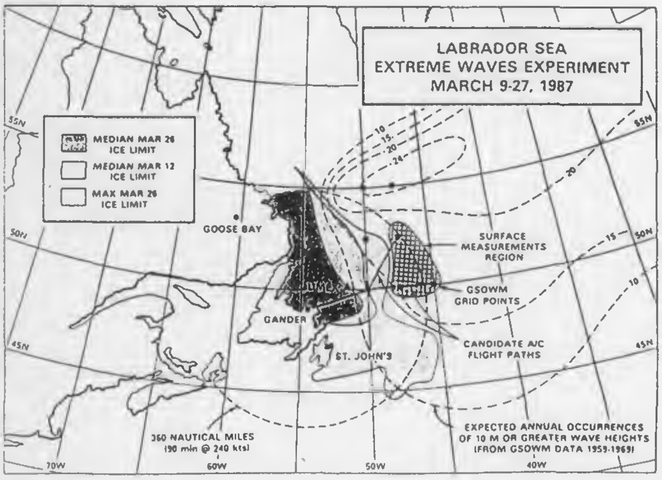

Figure 1: Labrador Sea Extreme Waves Experiment

2) Capturing one or more extreme wave events, for which there is at least a 50% chance of experiencing wave heights of twice the winter North Atlantic average.

3) Evaluating the wave monitoring capability of a calibrated C-band SAR at incidence angles from 15° to 30°, and range-to-velocity ratios from 30 to 150.

The experiment site is depicted in Figure 1, along with contours of the regional wave climatology and expected locations of the ice pack during late March. The expected rapid retreat of the ice pack indicates some of the dynamics occurring here during late March. The experiment site and timing are both chosen to maximise the probability of capturing not only the extreme wave events, but also their influence on the local ice decay rates.

The major anticipated results are a comprehensive comparison of extreme wave directional spectra or height as measured or estimated by

a) an airborne C-band SAR operating at various R/V ratios and incidence angles;

b) an airborne surface contour radar (SCR);

c) an airborne radar ocean wave spectrometer (ROWS);

d) various in situ buoys, both directional and non-directional;

e) various wave models, including the US Navy Global Spectral Ocean Wave Model (GSOWM), and a regional Canadian model.

3.5 UK X-band SAR Imaging Experiment

In Autumn 1986, the UK will be carrying out an airborne SAR (X-band) sea-imaging campaign in conjunction with a SLR, wavebuoys, current, and wind-measurements, HF coastal radar, surface roughness photography, and a helicopter-borne scatterometer. Some of the objectives of this campaign that will have an impact on our understanding of the azimuth transfer function are:

a) The measurement of the dependence of the directional spectrum and the associated speckle statistics on incidence-angle.

b) The measurement of the dependence of the azimuthal degradation of the directional spectrum on wave-height, wind-vector, wave-spectrum, scattering mechanism and surface currents.

c) Investigation of the directional distribution of the small scale surface roughness with respect to wind-direction and its dependence on wind-speed.

There may also be a need to build a European airborne C-band SAR to:

a) enable further campaigns aimed at answering the questions concerning the dependence of M on R/V, ϕ, θ and wind-vector;

b) provide a data base for the empirical approach to providing a useful wave-mode product, and

c) gain experience using ROWS, SAR, and wavebuoys together for calibration exercises to improve coordination, data formats, and rapid input of well-understood calibration data into the algorithms.

3.6 General Goals of Future Experiments

It is the concensus of the working group that we may hope to reach an understanding of the problem of dynamic effects in the SAR imaging of waves before the ERS-1 launch. However, we may not even then completely understand the MTF.

The main purpose of all the planned experiments in North America and Europe is to deal with this problem. Even if some experimenters work from differing hypotheses, there is general agreement about the kind of experiment to perform.

An important element is to obtain a variation of the R/V ratio. It seems practical to obtain this variation with the use of an airborne SAR at different altitudes. Some remarks have shown that we have to keep in mind that there are other parameters which may be relevant to the linear dynamic effect, for example, the incidence angle and the integration time. The incidence angle is easily kept constant, but the possible confusion from the varying integration time can be avoided only with considerable care.

Another idea is to use at the same time a SAR and a high resolution SLAR. The working group recommends that such an experiment is organised by ESA, coordinating a well-controlled European experiment, including acquisition of reliable surface data.

4. DISCUSSION OF FAST DELIVERY WAVE MODE PRODUCTS

The new data on ocean sea state will be used by meteorological offices that are not yet familiar with the new type of information. So far, the sea state has been reported by ships giving mainly visual sea state parameters (height, period) for several wave systems (WMO handbook). It is recommended to prepare three levels of wave mode products. Neglecting yet unknown constraints posed to the amount of data for instance by data transmission speed, we subsequently list possible products in the order of degraded content of information.

The SAR wave mode provides a two-dimensional symmetric image-spectrum $I(K_1,K_2)$ in wave number space K_1,K_2 (512 x 512 wave number bands). The user needs the wave spectrum $E(K_1,K_2)$ which is connected to $I(K_1,K_2)$ by a not yet fully known azimuth and range MTF correction.

Level 1: FD image spectrum product:

The full image spectrum $I(K_1,K_2)$ in Cartesian coordinates. It is anticipated that for several larger meteorological offices, it would be of high interest to extract the wave information from the image spectrum and to develop experience for approximation of the MTF correction.

Level 2: FD image spectrum data reduction

In case the delivered data size must be reduced a product similar to the conventional ship observation is proposed:

After suitable spectral smoothing, the peaks of $I(K_1,K_2)$ (up to three) should be described by amplitude, half-width extension, and peak position K_{1p}, K_{2p}). In addition, the spectral noise level should be given (derived from spectral regions without wave information). K_{1p},K_{2p} should be expressed by the peak period T_p and peak direction Θ_p, since these are the parameters presently used in ship observations. The directions should refer to north-oriented axes, rather than spacecraft-oriented axes.

Level 3: FD Wave Spectrum Product

As soon as an acceptable MTF correction can be applied, the parameters described above (Level 2) should be delivered for the derived wave spectrum, so that the delivered spectra may be considered first-order estimates of either slope or height spectra. However, this final step will be useful only if complete annotation accompanies the estimates, so that the MTF *assumptions*, and evolution of the assumptions, can be fully reconstructed by the user and even removed, if desired.

Thus, several versions, or "levels", of spectral estimates should be supplied to the modelers, but the final (and potentially most useful) version should be supplied only if complete and continuous quality control can be insured, and if future changes to improve the estimates are clearly documented in the data annotations.

5. A STRATEGY FOR ERS-1 CALIBRATION AND VALIDATION

5.1 Space and Time Constraints

Even though the complete validation of all instruments is desirable by the end of three months from launch, there was common agreement that algorithm development in the SAR spectrum-to-wave spectrum will continue well past the initial validation phase. Nevertheless, the main objective of the calibration/validation phase should be to establish the initial parametric form of the algorithm, particularly including the verification of an azimuthal transfer function.

To accomplish a credible test of the azimuth algorithms, it is necessary to:

1) capture at least one, and preferably several, extreme events containing unusually high wind and wave conditions;

2) apply all resources at our disposal during the actual passage of the events through the chosen measurement area, so that statistically reliable estimates of the spectrum may be made, and

3) insure that top priority is given to activating the full SAR image mode at every possible overpass of the calibration/validation sites, especially when aircraft underflights are planned.

Since the full two-dimensional wave energy spectrum is a very difficult measurement to make with any precision and confidence, even with the most advanced in situ or aircraft techniques, we cannot practically expect to conduct a continuous comprehensive campaign of calibration throughout the entire period. Rather, we recommend a balance of a long, low intensity period mixed with short, high intensity periods. The low intensity period, mainly relying on moored directional buoy comparisons and perhaps tower measurements at fixed locations (locations to be determined, but not necessarily centralised) would require the implementation of the AMI wave mode at preplanned intervals. The high intensity periods, on the other hand, would incorporate both ship-deployed buoys and aircraft estimates of the directional spectrum. These high intensity periods would typically last for three-week intervals, for which times all necessary resources would be reserved and fully committed several months in advance.

5.2 The Search for a Primary Standard

Of all the techniques currently available for measuring or estimating the full directional spectrum, very few can be considered of sufficient quality to be useful in SAR validation. Most yield either a reduced form of the spectrum, or an indirect and poorly understood estimate of it. For every technique, an estimate of the instrument transfer function must be implicitly applied to derive absolute energy spectra.

In non-directional buoys, this transfer function is quite well known and accepted. However, in directional buoys, directional ambiguities can often occur for complicated spectra, since the buoy can yield only one estimate of mean direction at every wave frequency, and cannot respond to the higher angular moments of the spectrum. In situ arrays of wave staffs can theoretically overcome this problem, but the practical implementation of sufficiently dense arrays in field conditions has never been demonstrated. Consequently, no currently available in situ technique for estimating the full (as opposed to "reduced") spectrum can be considered a satisfactory primary standard.

5.2.1 Development in the US. Over the past decade, NASA has been developing two aircraft-mounted radar techniques for monitoring the directional wave field, and has recently been able to demonstrate remarkable consistency of wave number spectral estimates, both between the two techniques, and between each technique and existing directional buoys. The two techniques, already discussed earlier, are:

1) the surface contour radar (SCR), and

2) the radar ocean wave spectrometer (ROWS).

Of the two, the SCR must be considered the more primary, since it obtains a direct three-dimensional surface height map using no more complicated a concept than direct ranging with a narrow beam raster scanning radar. The ROWS, however, must rely on a surface-backscatter-to-surface-slope transformation, a step which must be verified by comparison with the SCR.

Both instruments are currently mounted on the same aircraft, (a NASA P-3), and have been intercompared several times over the last few years, most recently in 1984, in a series of flights off the coast of Chile under the SIR-B. Although even these instruments have certain ambiguities in their transfer functions, they are presently considered as close to a primary calibration facility as exists anywhere in the world for estimating the full two-dimensional spectra.

Consequently, we strongly recommend that the high intensity period of calibration for the ERS-1 SAR spectra employ this facility (or the equivalent) as its centre-piece.

5.2.2 Development in Europe. A ROWS system is currently under development in the UK at RAL. This development should be encouraged by ESA as it would be of great interest for a high intensity site in Europe.

At GKSS-Foreschungszentrum, Geesthact, FR Germany, a modified nautical radar has been developed to measure the three-dimensional and two-dimensional wave spectrum (Young et al. I, 1985, Atanassov et al., 1985, Young et al. II, 1985).

The instrument provides the asymmetric two-dimensional spectrum which is free of the 180° ambiguity for the travel direction of waves. Due to the use of three-dimensional spectra it has a signal to noise level that so far has only been reached for one-dimensional spectra by wave buoys. A similar instrument is under development at TNO in the Netherlands. The first results from there are expected at the end of 1986 (Hoogeboom et al.). The nautical radar is best used from fixed platforms (oil rigs, etc.).

The MIROS system has been developed by A/S Informasjons Kontroll in Norway (MIROS development program). It is operational since 1983 and is installed on platforms in the northern North Sea. This radar uses the Dopplershift of the orbital velocity of waves to produce the two-dimensional spectrum. It is at present capable of measuring frequential wave energy spectra in directional intervals of 30°. The angular resolution will be refined to 10° in the future. The MIROS program is funded by governmental and industrial sponsors in Norway and the intention is to build up a net of MIROS-stations on offshore-platforms to provide better wave forecasts.

The tower radars are easy to maintain and relatively cheap in operation. Once installed, they can be operated in all weather situations day and night quasi continuously over a principally unlimited time period. Measurements can be repeated at the same location during later phases of the satellite mission.

5.3 NASA Constraints on Location of High Intensity Site

The recommended use of the NASA airborne system (SCR and ROWS) places constraints on the preferred choice of the high intensity sites, since the current version of the instrument is considered only experimental, expensive and possibly not sufficiently reliable to transport to locations remote from the US East Coast. In view of this tenuous situation for such a vital international resource, it is strongly recommended that ESA express its interest to NASA for the maintenance and up-grading of the facility prior to the ERS-1 launch. For example, remounting the instruments on an aircraft with longer endurance would greatly increase their flexibility (present endurance is only about five hours).

Nevertheless, the presence of this facility on the US East Coast strongly argues for a primary wave measurement site in the north-west Atlantic. considering the wave climatology of the North Atlantic, and the need for proximity to acceptable aircraft bases, the region just to the north-east of St. John's, Newfoundland (around 52.5N, 47.5W) is quite attractive. Not so coincidentally, this location is also the most likely location of a planned 1987 Labrador Sea Extreme Waves Experiment, in which several European countries are planning to participate.

5.4 Strategy for a Calibration Experiment in Europe

The tower-based instruments, described above, suggest locating a possible European high/low intensity site in a region of the north-east Atlantic or northern North Sea, where tower facilities are available and maintenance for these instruments is easy. If a high intensity site is to be located within Europe, the RAL ROWS system should be developed to become an essential component of this site operation.

1. During the high intensity period, the two-dimensional wave spectrum would be measured with the nautical radar and the MIROS-radar quasi continuously (measurements continued between the overflights would ensure the proper performance of the instruments). The output would be the asymmetric two-dimensional spectrum.

2. With a scatterometer of small footprint the Modulation Transfer Function (MTF) would be measured from the tower during the satellite overflights. This is necessary since the MTF is dependent on environmental parameters and cannot yet be predicted uniquely (Feindt, Wright et al.).

3. With the MTF from 2. and the asymmetric two-dimensional spectrum from 1. the theoretical SAR spectrum would be predicted by linear and non-linear numerical modelling.

4. The measured SAR spectrum would be compared with the theoretical SAR spectrum to improve the numerical models under 3.

In cooperation with the oil industry, a deep water platform facility along the Norwegian cost-line should be selected for a tower-based experiment.

Core-equipment: The sensors necessary for the strategy of Section 5.4 are Modified Nautical Radar (presently available at GKSS Research Centre, FRG, TNO, The Netherlands; MIROS Radar (presently available at Informasjons Kontroll, Norway); Scatterometer (presently available from Bremen University, F.R. Germany, Naval Research Laboratory, USA); Directional Sensitive Buoy (presently available at several European institutes); Meteorological and Oceanographic Sensors to Monitor Local Environment Parameters.

Time: 3 weeks between 15 November to 15 April.

Lengths of satellite swath: 200 km centered around the platform.

6. SUMMARY RECOMMENDATIONS

The following summarises the major recommendations of the group to execute a meaningful calibration and validation of the ERS-1 SAR wave mode:

1. Perform the majority of high intensity full wave measurements at the Labrador Sea site, using the full complement of buoy, aircraft, and ERS-1 SAR imagery that can be applied during a three-week period, preferably occurring during the second month after launch. Choose the three-week period to coincide with a likely passage of at least one extreme event, apparently ruling out the May through August interval. Delay the validation/calibration interval until the northern autumn (15 September or later) if the ERS-1 launch occurs after 15 March, since transporting the instruments to perform high intensity measurements to the southern hemisphere does not appear practical.

2. Conduct a parallel low level, but long duration, validation phase off the European north-west coast, at locations to be determined by the availability of buoys and towers with associated instrumentation, and possibily also coincident with the primary wind validation location. This would permit a decentralised coverage from individual buoys in place along the Western European coast from Spain to Norway.

3. Consider, as an adjunct to the calibration phase, the use of both tower-based radars and aircraft-mounted C-band SAR's. Although neither can be considered primary standards for the estimate of directional wave spectra, each can provide useful insight into the SAR imaging mechanisms. With carefully controlled experiments, each can add significantly to our knowledge of the environmental dependence of the SAR modulation transfer function.

4. Include high quality measurements of both the surface windfield and the air and sea temperatures at all high and low intensity sites wherever a spectral comparison of any kind is made.

5. Further examine the possibility of a single European site, as a way of coordinating aircraft, buoy, and/or tower-based measurements. Such an arrangement, even though not necessarily containing all of the capability of the Labrador Sea site for full two-dimensional wave estimates, nevertheless could be extremely valuable as a focal point of European activities and intercomparisons over the entire life of ERS-1.

6. Establish a format for the fast-delivery SAR spectra product which is most compatible with the wave modellers who are planning data assimilation exercises.

7. REFERENCES

1 Alpers, W, "Monte-Carlo-simulations for studying the relationship between ocean wave and synthetic aperture radar image spectra", J. Geophys. Res., 88, No. C3, 1745-1759, 1983.

2 Atanossov, V, Rosenthal, W, Ziemer, F, "Removal of ambiguity of two-dimensional power spectra obtained by processing ship radar images of ocean waves", J. Geophys. Res., 90, No. C1, 1061-1067, 1985.

3 Beal, R C, Gerling, T W, Irvine, D E, Monaldo, F M, Tilley, D G, "Spatial variations of ocean wave directional spectral from the SEASAT synthetic aperture radar", J. Geophys. Res., 91, No. C2, 2433-2449, 15 February 1986.

4 Beal, R C, Monaldo, F M, Tilley, D G, Irvine, D E, Walsh, E J, Jackson, F C, Hancock III, D W, Hines, D E, Swift, R N, Gonzalez, F I, Lyzenga, D R, Zambreskey, L R, "A comparison of SIR-B directional ocean wave spectra with aircraft scanning radar spectra and global spectral ocean wave model predictions", Science, 20 June 1986.

5 Feindt, F, "Radar Rückstreuexperimente am Wind-Wellen-Kanal bei sauberer filmbedeckter Wasseroberflche im x-band (9.8 GHz)", Hamburger Geophysikalische Einzelschriften, GML Wittenborn Sohne, 2000 Hamburg 13.

6 Ford, J P, Cimino, J B, Holt, B, Ruzek, M R, "Shuttle imaging radar views the earth from Challenger: The SIR-B experiment", JPL Publication 86-10, 15 March 1986.

7 Fu, L L, Holt, B, "SEASAT views oceans and sea ice with synthetic aperture radar", JPL Publication 81-120, 15 February 1982.

8 Hasselmann, K, Raney, R K, Plant, W J, Alpers, W, Shuchman, R A, Lyzenga, D R, Rufenach, C L, "Theory of synthetic aperture radar ocean imaging: A MARSEN view", J. Geophys. Res., 90, No. C3, 4659-4686.

9 Hoogeboom, P, Kleyweg, J C M, van Halsema, D, "Seawave measurements using a ship radar", IGARSS 86, 10 Sept. 1986.

10 Jackson, F C, Walton, W T, Peng, C Y, "A comparison of in situ and airborne radar observations of ocean wave directionality", J. Geophys. Res., 90, No. C1, 1005-1018, 1985.

11 Rosenthal, W, "Remarks on the use of wave scatterometer data in conjunction with the wind scatterometer", Proc. of a conference on the use of satellite data in climate models, Alpbach, Austria, 10-12 June, 1985 (ESA SP-244, Sept 1985).

12 Walsh, E J, Hancock III, D W, Hines, D E, Swoft, R N, Scott, J F, "Directional wave spectra measured with the surface contour radar", J. Phys. Oceanogr., 15, 566-592, 1985.

13 World Meteorological Organisation: Handbook on Wave Analysis and Forecasting, WMO-No. 446, 1976.

14 Wright, J W, Plant, W J, Keller, W C, Jones, W L (1980), "Ocean wave-radar modulation transfer functions from the West Coast Experiment", J. Geophys. Res, 85, 4957-4966.

15 Young, I R, Rosenthal, W, Ziemer, F, "A three-dimensional analysis of marine radar images of the determination of ocean wave directionality and surface currents", J. Geophys. Res., 90, No. C1, 1049-1059, 1985.

16 Young, I R, Rosenthal, W, Ziemer, F, "Marine Radar Measurements of Waves and Currents During Turning Winds, Deutsch. Hydr. Zeitschr., 38, 23-38, 1985.

REPORT OF WORKING GROUP 6

THE FEASIBILITY OF AN ERS-1 ORIENTED, BUT SCIENTIFICALLY AUTONOMOUS, INTERNATIONAL EXPERIMENT CAMPAIGN

K Hasselmann *(Chairman)*
T H Guymer
D R Johnson
T Kaneshige
M P Lefebvre
C Rapley
E Mollo-Christensen
P Lecomte
J J Conde
E Svendson
A Liferman

1. TERMS OF REFERENCE

The main task of the Working Group was to investigate the feasibility of making use of international experimental field programmes dependent on ERS-1 to obtain useful in-situ data or other support for the validation and calibration of the ERS-1 instruments. Since this hinges critically on the way in which the interaction between the ERS-1 programme and large-scale international scientific field programmes is developed, the Working Group placed this question in the focus of its discussion.

2. EXISTING PROGRAMMES

The ERS-1 flight will coincide with a number of important scientific research programs addressing problems of global dynamics, weather and climate.

The WG considers it an important matter to coordinate the research activities connected with ERS-1 with other ongoing research.
The World Climate Research Programme (WCRP) with its several components can contribute significantly to the calibration and validation of ERS-1; principal among these are WOCE and TOGA. Other experimental programmes being planned include SATLANT, SAVE, WAM, COST43 and several Arctic and Antarctic programmes.

At this time the ensemble of large-scale international scientific programmes which could make useful contributions to ERS-1 instrument validation and calibration is so large and encompasses such a broad range of activities that the Working Group did not see a need to propose any additional new autonomous scientific programmes.

This report will address the question of establishing the requiredscientific and technical interfaces with these existing programmes to ensure mutual benefits in data validation, sensor performance assessment and enrichment of scientific research programmes by collaboration and data exchange.

3. INTERFACING WITH OTHER PROGRAMMES

The WG recognises the need to establish interfaces and liaison with research programmes not directly related to ERS-1, with agencies and institutions in countries that launch and operate Earth-observing satellites, and with international organisations and projects. While many of the needed links do exist, it will benefit the scientific efforts related to ERS-1 to identify existing links and to establish new links as needed.

Specific satellite systems and projects that need to be considered are the following:

- ERS-1
- NROSS
- MOS-2
- EOS and other polar platforms
- ARGOS
- TOPEX-POSEIDON
- DMSP
- SIR-C

In the process of setting up such liaison programmes, the WG suggests that the guiding principle be to establish direct contact between active research groups and between teams engaged in system validation, data interpretation and data communication; the WG also suggests that the charge to the liaison links be broad and that the ultimate purpose continuously be kept in mind, namely the furthering of understanding of the global system and the operational needs of forecasting and assessment.

In order to establish effective links to strengthen the ERS-1 instrument validation and calibration programme, the role of this particular activity within the framework of the overall ERS-1 programme and the parallel international scientific programmes must be kept clearly in mind.

It is an essential characteristic of the contribution of scientific programmes to the ERS-1 instrument calibration and validation that this is a spin-off contribution which cannot be separated from the overall scientific programme planning.

The relation between ERS-1 instrument calibration and validation, similar activities for other satellites (N-ROSS, TOPEX/POSEIDON, MOS-2), the various scientific field programmes, other sources of data such as the World Weather Watch and IGOSS, and data assimilation and modelling activities, is indicated in fig. 6.1. The interfaces and

Proceedings of a Workshop on ERS-1 Wind and Wave Calibration, Schliersee, FRG, 2–6 June, 1986 (ESA SP-262, Sept. 1986)

comunication links between the different sub-systems of this end-to-end system need to be carefully planned if a mutually beneficial cross-interaction between the ERS-1 programme and the various international scientific programmes - all of which have their own complex internal organisational structures - is to develop fruitfully.

We discuss organisational mechanisms to achieve the necessary communication links and the scientific and technical questions to be addressed in the coordination of the various component activities shown in fig. 6.1 in the next section.

As background for this discussion it is useful to first give a brief review of the activities involved in the different components of the end-to-end system (paragraph numbers below cross-refer to the boxes in fig. 6.1).

1. For TOGA and WOCE the data from satellite are regarded as a central part of the observational system. Satellite data will be used, in particular, for:

   - sea surface topography (altimeter from TOPEX/POSEIDON ERS-1, MOS-2(?) Geosat will also be considered if data are available in the extended mission).

   - wind forcing (scatterometer, wind velocities and altimeter wind speeds from - NSCATT (NROSS) - ERS-1 - MOS-2

   In both of these experiments in-situ measurements will be implemented in two ways:

   a) as part of the extensive observational network designed to provide the basic oceanic data sets of the experiments to constrain the modes (direct scientific objectives)
   b) as part of the process of calibration and validation of the satellite data. The objectives of these measurements are identical to the long-term calibration and validation activity of the ERS-1 programme.

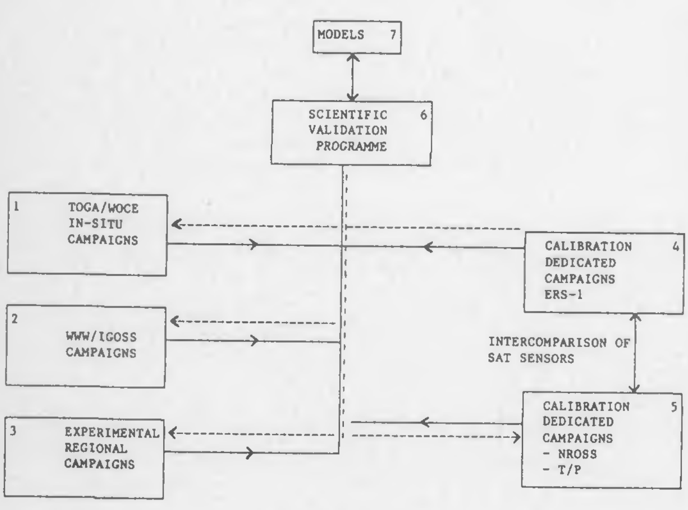

FIG. 6.1

2. Both WOCE and TOGA will lean heavily on the ongoing data collection provided by the WWW and IGOSS. These data will also be useful in conjunction with the continual comprehensive data assimilation operation planned for WOCE and TOGA (and required also for various other applications of ERS-1 data, for example, for real time weather and wave forecasting) to validate and calibrate ERS-1 data.

3. Besides WOCE and TOGA there are other campaigns planned to collect in-situ data, generally in regional areas. On the average there is a lag of 2-3 years between the proposal and/or decision and the implementation of such experiments. Thus it will still be possible for the ERS-1 programme planning to impact on these campaign plans.

4/5 The various satellite projects will carry out calibration activities during commissioning phases (a few months)

   - to assess the accuracy of the instruments (within given specifications)

   - to give a preliminary evaluation of geophysical parameters.

   However, because of the limited time frame, this calibration can have only limited objectives and cannot guarantee the value of the geophysical parameters e.g. in various conditions of sea state.

   An important feature of the calibration and validation activities during the commissioning phase is that they will need to be synchronised with the launch date. Since this cannot be precisely determined in advance, this implies that the programme will need to be very flexible. This requirement will generally be in conflict with the field programme and data collection activities of the components 1, 2 and 3. Nevertheless, the value of the calibration and validation campaigns during the commissioning phase to the scientfic programmes, and the possibility of augmenting these activities through supplementary in-situ measurements from the scientific field programmes, should be investigated.

6. The scientific validation programme represents the central activity of all scientific programmes. It is concerned with the application of models (component 7 of fig. 6.1) to the data coming in from all component streams 1-5, to test the physical concepts which are the object of the scientific programmes.

   A basic output of the validation programme will be complete reconstruction of all geophysical fields for which sufficiently dense data coverage is available. This includes particularly thesea surface properties measured by satellites. A continuous data assimilation system of this form, in which the satellite data are combined with all other available data sources, provides an excellent long-term instrument calibration and validation tool. Thus in the planning of the calibration/validation programme, attention should be given to this aspect, as well as to the standard in-situ intercomparison techniques.

Time Scale

Both TOGA and WOCE are long term programmes and are expected to span the full life time of the oceanographic satellites.
TOGA has already started and will certainly still be operational during the lifetime of ERS-1. Significant deployment of in-situ measurements is planned but will be limited primarily to tropical areas.

The current planning for WOCE is to start the experiment in the early 90's. The time scale is based upon the expected launch time of NROSS (NSCAT), TOPEX/POSEIDON and ERS-1. The possible shift in the launch of ERS-1 (end of 89) relative to the launch of the other satellites (mid 91) will have disadvantages.

The timing of most of the other campaigns is also matched to the operation periods of the satellites. However, any advantage gained by extending the total period of satellite coverage, may be partially off-set by reducing the common operation period.

4. ORGANISATIONAL ASPECTS

In setting up both the inter-governmental and working level interactions between ESA and the international campaigns, the following approach, illustrated in figure 6.2, should be followed:

1. The ERS-1 Science and Applications Working Team (ESAWT), whose membership will be determined primarily by the response to the ERS-1 Announcement of Opportunity, shall provide inputs to ESA for the establishment of agreements with the organisations responsible for major international scientific experiments and campaigns of interest to the ERS-1 mission.

2. The ESA ERS-1 team, with the assistance of the ESAWT, shall maintain close links with the Scientific Steering Groups (SSG's) of the various major international campaign organisations. The working group underlined the convenience of overlapping membership between the ESAWT and SSG's.

3. ESA, with the support of the ESAWT, shall set up ad hoc task groups of limited lifetime to address specific issues such as the initial planning arrangements for bilateral or multilateral data exchange, for data processing and interpretation, the deployment of in situ measurement equipments etc.

4. ESA shall ensure that direct scientific and technical links are made at working level in order that the recommendations of the ESAWT, endorsed by the ERS-1 programme, are fully implemented in practice.

The inter-relationship between ESA and the parent organisation(s) responsible for the campaign(s) as well as the proposed procedures by which campaign data should be collected is as follows:

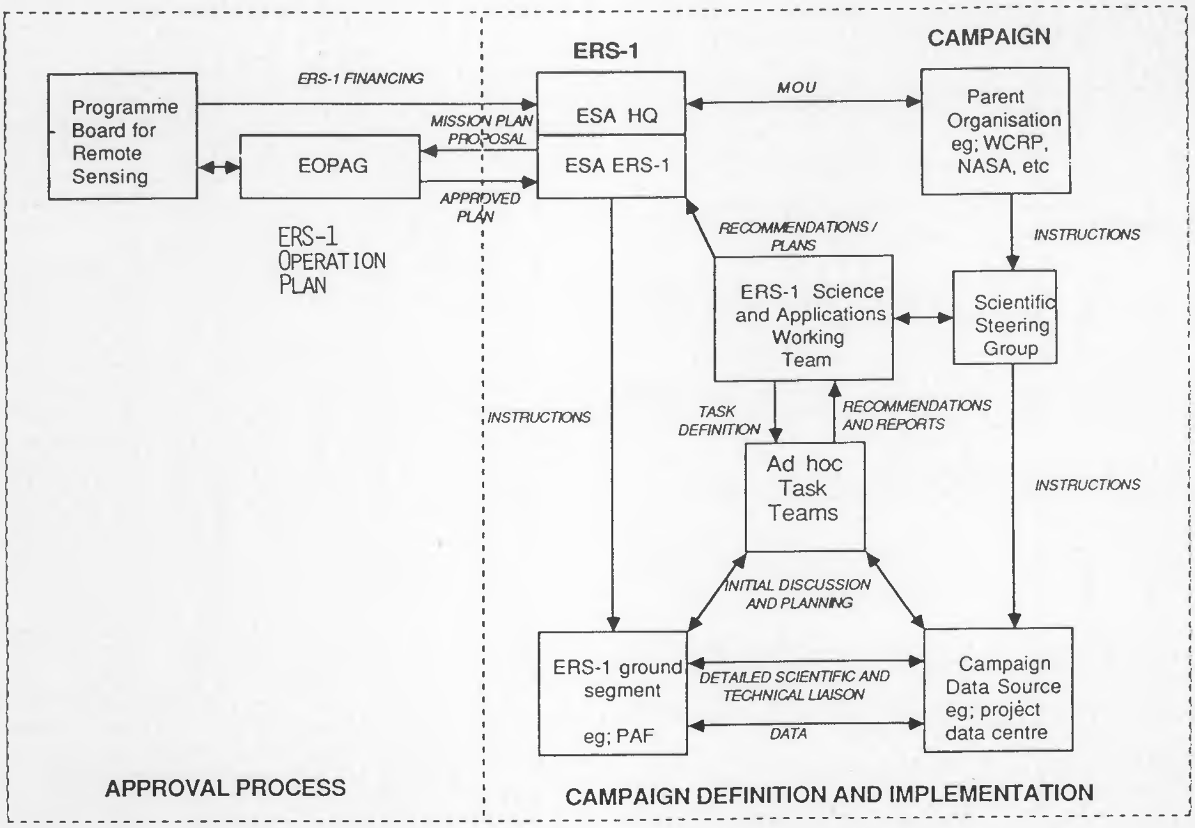

Figure 6.2: Organisation chart for ERS-1 international campaign data acquisition

a) The ESAWT shall assist ESA in the formulation of a plan for interaction with a given appropriate international campaign based on the results of discussions with the Scientific Steering Group of that particular international campaign and on a report of an ad hoc group which will have carried out a preliminary assessment of the detailed technical issues at working level (i.e. discussions with potential providers and receivers of data).
b) Following the analysis of technical, operational and financial implications, ESA shall enter into a dialogue with the parent organisation of the campaign, maintaining discussion with the ESAWT, and culminating in the signing of an Agreement/Memorandum of Understanding (MOU).
c) At the working level, scientific and technical liaison will take place between the teams collecting or generating the campaign data and the ESA teams and associated entities (e.g. ERS-1 PAF's) whose task is to assimilate the data for the purpose of ERS-1 sensor calibration and data validation.

The organizational structure for these activities is shown in Fig. 6.2. Note that the responsibility for the final decisions concerning the ERS-1 mission lies with the Remote Sensing Programme Board (PB-RS), the ESA delegate body responsible for Earth Observation matters, assisted by the ERS-1 Operation Plan Advisory Group (EOPAG) for those aspects related to the mission operation plan.

5. COORDINATION TASKS

A number of problems affecting the coordination of the ERS-1 calibration/validation programme and the scientific field programmes will need to be addressed by the various inter-acting groups described in fig. 6.2.
In particular, the Working Group expressed its concern that existing planned campaigns may be limited in scope and may not address all of the necessary requirements for calibration and validation. Therefore, the following were identified as possible gaps, which should be taken into account:

5.1 The identification of measurements (wind and waves) planned for WOCE, TOGA and other campaigns.

Such measurements can be used:
- to validate ERS-1 instruments
- to help to cross-calibration of ERS-1 instruments and other satellites NSCAT/NROSS, TOPEX/POSEIDON, GEOSAT

A detailed discussion is needed with respect to the
- type of measurement (sensors, platforms)
- accuracy of measurements
- sampling problems
- areas of specific interest

5.2 Plans for other satellites

This will enable the optimal use of the specific validation and calibration campaigns of ERS-1, and other satellites, in the design of the planned scientific campaigns during the 1990 - 1995 period.

5.3 Sampling of high winds and waveheights by in-situ measurements

Major oceanographic and atmospheric processes of scientific and operational interest are associated with extreme wind and wave situations. This means that the full dynamic range of the satellite instruments must be evaluated, implying in-situ observations to be taken in areas and at times when extreme weather is most likely to occur. On the large scale, this is between 40 - 60° N during winter and throughout the year in some parts of the Southern Ocean.

There are some technical problems to be overcome with the in-situ measurement of extreme wind and wave conditions. Airborne measurements may be assistance.

5.4 Coverage of a broad SST Range

There is some evidence that radar backscatter depends not only on surface roughness but also on sea surface temperature (Freilich, these proceedings). Such behaviour should be taken into account in the calibration and validation of both scatterometer and altimeter winds and for this comparison data sets should be obtained at a variety of SST's. Within the high wind speed regions of mid-latitudes there is rather little variation in SST. In order to obtain measurements covering a reasonable range of wind and wave conditions at high SST the western portion of the Trade winds should be considered e.g. Caribbean where temperatures exceed 25°C.

5.5 Inclusion of Frontal Regions

Atmospheric and oceanic fronts are of interest in air-sea interaction because they are often associated with significant fluxes and they induce vertical motion coupling boundary layer processes with the free atmosphere and ocean. It is therefore important that wind and wave parameters should be accurately retrieved in such regions and the calibration/validation should incorporate possible effects of rapidly changing thermo/dynamic stability (i.e. air-sea temperature difference) and sea-state.

5.6 Inclusion of adequate wave spectra variability

The discussion under 5.3 also holds for obtaining waveheight measurements which span a wide range. However, the same locations may not provide an adequate variation of wavelength and direction. In-situ data should be gathered over a range of conditions varying from those dominated by long swell to a wind generated sea. This may necessitate the use of open ocean and coastal sites with limited fetch and depth. Wind retrieval algorithms may differ for the two cases, however, we must remember the limit of near coastal scatterometer wind retrievals due to the large footprint. It is also known that SAR imaging of ocean waves depends on the orientation of wave direction with respect to the radar look angle. Therefore calibration/validation should encompass the whole range of this parameter.

5.7 Establishment of continuously monitoring stations

After the initial calibration/validation period there will be need for continuous in-situ data to check possible drift or minor failures in the satellite instrument performance. This can be obtained in near real time from platforms of opportunity such as buoys, research vessels, weather ships and oil rigs. In addition, if the satellite retrievals are interactively used in operational atmospheric and wave models, any "bad" data will soon be discovered.

5.8 Measurements near the ice edge

Wind and waves are extremely important in determining marginal ice zone (MIZ) processes, and the MIZ is a generation area for polar lows. Since this is the area where, in general, the coldest surface water is found, some calibration points should be obtained here to check the SST sensitivity (see 5.4) of the satellite retrievals near 0°C. As mentioned in 5.6), due to the large footprint of the scatterometer the wind velocity retrievals are limited to a certain distance from the ice edge and must, therefore, be coupled with an atmospheric model. Another important limitation in these areas is the sometimes sudden formation of a very thin layer of grease ice over large areas, having similar effect as oil or micro-organisms by the dampening of capillary and small gravity waves.

5.9 The Establishment of combined data sets for real-time operational forecasting

Most of the planned large-scale international experimental programmes are directed towards problems of climate or long-term ocean dynamics. To our knowledge there exist at present no specific scientific programmes designed to exploit the data provided by ocean satellites, and in particular by ERS-1, for real-time forecasting operations (although some centres, such as ECMWF, are making efforts to investigate how these data can be included in their future operations). Such programmes could provide a valuable feedback into the validation problem.

The assimilation of oceanographic satellite data poses a number of non-trivial scientific questions which will need to be addressed by a concerted collaborative effort of the scientific community and operational forecast centres.

There is a strong interest of the climate community and other researchers concerned with long time scale processes that these questions are resolved and ocean satellite data are routinely assimilated and used by operational forecasting centres. For it is only through such an operational real-time activity approval that continuous gridded data can be generated for other research applications. In addition to these considerations, however, it should be recognised that ocean satellites will also open up unique new opportunities in the field of real-time forecasting itself.

The scientific community should attempt to develop the methodology to make use of these new forecasting possibilities in collaboration with forecasting centres. These concern, for example, the prediction of sea ice, wind fields and surface waves in the marginal ice zones, the interaction of currents and waves in frontal zones or the possibilities of extended range weather forecasting using coupled atmosphere/ocean models. A closer analysis of these problems could well lead to the definition of additional experimental programmes designed to augment the ocean satellite data with data from conventional instruments, which could then also provide useful data for instrument validation.

5.10 Investigation of the space time variability and its implications for calibration/ validation

Satellites and in-situ instruments provide very different views of the sea-surface, one giving a spatial average over footprints as large as a few thousands of km^2, the other time series at single locations. The space time variability inherent in wind and wave fields will affect the choice of appropriate averaging of both the in-situ and the satellite data. It will also help determine the weighting to be applied to data from platforms that are not coincident with ERS-1 sensor footprints. Aircraft offer the possibility of relating the two types of measurements. The study of such variability is of scientific interest and emphasis should be placed on this aspect in the design of any ERS-1 oriented experiment. For example, wind and wave instruments on ships, buoys and aircraft could be deployed in arrays spanning scales of kilometres to tens of kilometres. It is important that all surface-based and aircraft sensors be carefully inter-calibrated and such activities should form part of any experiment plan.

6. RECOMMENDATIONS

In addition to the organisational recommendations in 4 the following, more general, points emerged.

(i) The Group endorses the recommendation that the positioning of the 3-day repeat ground tracks should be decided soon as it could influence the location of scientific measurement programmes.

(ii) We note the uncertainty in data reception on three of the ERS-1 orbit tracks during the commissioning phase. In view of the requirement for global satellite date in many of the planned scientific programmes and that these orbits include critical regions such as the Drake Passage and the Southern Ocean near South Africa, we recommend that every effort be made to ensure that global coverage is possible.

(iii) We recommend that calibration of the AMI wind and wave modes using scientific programmes in coastal regions should be made possible through appropriate harmonisation with the operation of the SAR imaging mode.

(iv) We recommend that ESA should bring the general requirements noted in sections 5.1 - 5.10 to the Scientific Steering Groups of relevant experiments.

List of Participants

Attema, Evert,
ORM/ESTEC,
Keplerlaan 1 - Postbus 299,
2200 AG Noordwijk,
THE NETHERLANDS.

Barton, Ian,
CSIRO,
Private Bag No. 1,
MORDIALLOC,
Victoria 3195,
AUSTRALIA.

Beal, Robert C.,
Johns Hopkins University,
Applied Physics Laboratory,
Johns Hopkins Road,
LAUREL, Maryland,
U. S. A.

Bernard, Rene,
CRPE,
38-40 rue du General Leclerc,
92131 Issy les Moulineaux,
FRANCE.

Birks, Andrew Robert,
Rutherford Appleton Laboratory,
Chilton, Didcot,
OX11 OQX, Oxon,
UK.

Bruzzi, Stefano,
EOM/OY, ESA HQ.,
8010 Rue Mario Nikis,
75738 Paris, Cedex 15,
FRANCE.

Callahan, Philip S.,
Jet Propulsion Laboratory,
4800 Oak Grove Drive,
PASADENA, T1206D,
CA 91109,
U.S.A.

Cavanie, Alain,
CREO,
Antenna CREO,
Centre IFREMER,
BP337, Brest 29273 CEDEX,
FRANCE.

Challenor, Peter,
IOS,
Brook Road,
Wormley, Godalming,
Surrey GU8 5UB,
U.K.

Conde, Juan Jose,
Ministerio Obras Publicas
Yurbanismo,
Paseo Castellana 67,
Madrid 28046,
SPAIN.

Cordey, Ralph,
Marconi Research Centre,
West Hanningfield Road,
Great Baddow, Chelmsford,
Essex, U.K.

Demurger, Joelle
Antenne CREO,
IFREMER,
BP 337,
29273 Brest Cedex,
FRANCE.

Duchossois, Guy,
EOM/OY, ESA HQ,
8-10 Mario-Nikis,
75738 Paris Cedex 15,
FRANCE.

Dumont, Jean-Paul,
GDTA (CNES),
18 avenue Edouard Belin,
31000 Toulouse,
FRANCE.

Ezraty, Robert,
IFREMER,
BP 337,
29273 Brest Cedex,
FRANCE.

Fea, Maurizio,
ESA-Earthnet,
via Galileo Galilei,
Casella postale 64,
00044 Frascati, (Roma),
ITALY.

Finkenzeller, Heinz,
DFVLR,
Oberpfaffenhofen,
Flugplatz,
D-8031 Wessling,
GERMANY.

Flemming, Nicholas,
IOS,
Wormley, Godalming,
Surrey, U.K.

Francis, C. Richard,
ORM/ESTEC,
Postbus 299,
2200 AG Noordwijk,
THE NETHERLANDS.

Francis, Peter,
Meteorological Office (Met.0 2b),
London Road,
Bracknell RG12 2SZ
UK.

Frassetto, Roberto,
ISDGM-CNR,
1364 San Polo,
30125 Venice,
ITALY.

Freeman, Nelson G. S.,
RADARSAT Project Office,
110 O'Connor St.,
Suite 200,
KIP 5M9 Ottawa, Ontario,
CANADA.

Freilich, Michael H.,
Jet Propulsion Laboratory,
4800 Oak Grove Drive,
169-236 Pasadena, CA,
U. S. A.

Graf, Georg,
ORP/ESTEC,
Postbus 299,
2200 AG Noordwijk,
THE NETHERLANDS.

Guddal, Johannes,
The Norwegian Meteorological Inst.,
Div. Western Norway,
Allegate 70,
5000 Bergen,
NORWAY.

Guignard, Jean-Pierre,
ORM/ESTEC,
Postbus 299,
2200 AG Noordwijk,
THE NETHERLANDS.

Guymer, Trevor,
Institute of Oceanographic Sciences,
Wormley, Godalming,
GU8 5UB Surrey,
UK.

Hasselmann, Klaus,
Max Planck Institute of Meteorology,
Bundestr. 55,
D2000 HAMBURG 13,
GERMANY.

Hsu, S. A.,
Coastal Studies Institute,
Louisiana State University,
70803 Baton Rouge,
U.S.A.

Hunt, James,
IP/ESTEC,
2200 AG Noordwijk,
THE NETHERLANDS.

Johnson, D. R.,
Norda,
NSTL,
MS35929k,
U.S.A.

Kaneshige, Thomas,
World Meteorological Organisation,
C.P. No. 5,
CH-1211, Geneva,
SWITZERLAND.

Kjelaas, Anton,
Saga Petroleum,
P.O. Box 9,
N-1322 HØVIK,
NORWAY.

Koch, Wolfgang,
GKSS Forschungszentrum,
Max Planck Str.,
2054 Geesthacht,
WEST GERMANY.

Krul, Leo,
Delft University of Technology,
PO Box 5031,
2600-GA Delft,
THE NETHERLANDS.

Laing, Andrew,
New Zealand Meteorological Service,
P O Box 722,
Wellington,
NEW ZELAND.

Landman, Margareet,
OR/ESTEC,
Postbus 299,
2200 AG Noordwijk,
THE NETHERLANDS.

Lecomte, Pascal,
IFREMER/CREO,
BP 337,
29273 Brest Cedex,
FRANCE.

Lefebvre, Michel P.,
GRGS,
18 Av. Edouard Belin,
31055 Toulouse Cedex,
FRANCE.

Lifernann, Anne,
CNES/GRGS,
18 Av. Edouard Belin,
31055 Toulouse Cedex,
FRANCE.

Louet, Jacques,
ORM/ESTEC,
Postbus 299,
2200 AG Noordwijk,
THE NETHERLANDS.

de Luis, Josie Enrique,
Programa de Clima Naritimo,
Direccion General de Puertos,
Mopu, Paseo de la Castellana 16,
28046, Madrid,
SPAIN.

Malarde, Jean-Pierre,
GDTA,
18 av., Edouard Belin,
31055, Toulouse,
FRANCE.

Maron Loureiro, Adolfo,
Programa de Clima Maritimo,
Ministerio de Obras Pubucas,
Paseo de la Castellana 16-5°,
28046 Madrid,
SPAIN.

Mollo-Christensen, Erik,
NASA/Goddard Space Flight Center,
670 Greenbelt,
MD 20771,
U S A.

Frank, Monaldo,
Johns Hopkins University
Applied Physics Laboratory,
Johns Hopkins Road,
23-348 Laurel,
Maryland,
U S A.

Offiler, David,
Meteorological Office,
London Road,
Bracknell,
RG12, 2SZ, U.K.

Oost, Wiebe,
Royal Netherlands Meteorological Inst.,
Postbus 201,
3730 AE Bilthoven,
THE NETHERLANDS.

Oriol, Evangelina,
ESA/ESRIN,
via Galileo Galilei,
Casella Postale 64,
00044 Frascati,
ITALY.

Perbos, Jacqueline,
CNES,
18 Ave., Edouared Belin,
31400 Toulouse Cedex,
FRANCE.

Piau, Pascal,
IFP,
BP 311,
92506 Rueil Malmaison,
FRANCE.

Powell, Redvers John,
Rutherford Appleton Laboratory,
Chilton, Didcot,
Oxon. OX11 OQX,
U.K.

Qefffeulou, Pierre,
Centre Oceanographique de Bretagne,
Antenne CNEXO,
BP 337,
29273 Brest,
FRANCE.

Raiff, J.,
KNMI,
PO Box 210,
3730 AE de Bilt,
3730 AE THE NETHERLANDS.

Rapley, Chris,
University College London,
Mullard Space Science Lab.,
Holmbury St. Mary,
Dorking,
RH5 6NT, Surrey,
ENGLAND.

Ratier, Alain,
Direction de la Météorotogie Nationale,
avenue Rapp,
Paris,
FRANCE.

Rosenthal, Wolfgang,
GKSS-Fouschungzentrum Geestkacht,
Max-PlanckStr.,
2054 Geesthact,
WEST GERMANY.

Smith, Peter,
Naval Ocean Research &
Development Activity (NORDA),
NSTL Station, MS,
U.S.A.

Srokosz, Meric,
Institute of Oceanographic Science,
Brook Road,
Wormley,
GU8-5UB Godalming,
ENGLAND.

Stum, Jacques,
GDTA,
18 ave., Edourard Belin,
Toulouse,
FRANCE.

Svendsen, Einar,
Nansen Ocean & Remote Sensing Center,
Eduard Griegsvei 3A,
N-5037 Solheimsvik,
Bergen,
NORWAY.

Swift, Calvin T.,
University of Massachusets,
Dept. of Electrical and Computer Engineering,
Amherst,
MA 01003, U. S. A.

Taylor, Peter K.,
Institute of Oceanographic Sciences,
Wormely, Godalming,
GU8 5UG Surrey,
U.K.

Trivero, Paolo,
CNR,
Cso Fiume 4,
10133, Turin,
ITALY.

de Voogt, Willem J. P.,
Delft Hydraulics Laboratory,
P.O. Box 152,
8300 AD Emmeloord,
THER THETHERLANDS.

Ward, Dr. Ian A.,
Marconi Research Centre,
Great Baddow,
Chelmsford,
Essex,

Wilkerson, John,
NOAA/NESDIS,
5001 Silver Hill Road,
Suitland,
RM-300 Maryland,
U.S.A.

Wijmans, Willem,
ESA/Earthnet,
via Galileo Galilei,
00044 Frascati,
ITALY.

Wismann, Volkmar,
University Bremen,
NW1 S320 University of Bremen,
2800 BREMEN 33,
WEST GERMANY.

Zecchetto, Stefano,
ISDGM-CMR (Telespazio),
1364 S-Polo,
Venice,
ITALY.